



A University of Sussex DPhil thesis

Available online via Sussex Research Online:

<http://sro.sussex.ac.uk/>

This thesis is protected by copyright which belongs to the author.

This thesis cannot be reproduced or quoted extensively from without first obtaining permission in writing from the Author

The content must not be changed in any way or sold commercially in any format or medium without the formal permission of the Author

When referring to this work, full bibliographic details including the author, title, awarding institution and date of the thesis must be given

Please visit Sussex Research Online for more information and further details

Ultrastructure-function properties of recycling synaptic vesicles in acute hippocampal slices

Freya Crawford

Submitted for the degree of Doctor of Philosophy

University of Sussex

September 2014

Declaration

The work in this thesis is my own, except where references to the work of others are acknowledged. This thesis has not and will not be submitted in whole or in part to this or any other university as part of a degree.

Signature:

Freya Crawford

Acknowledgements

Thank you to the BBSRC for providing the funding for my PhD scholarship.

There aren't words to express my gratitude for the help and support of my supervisor, Kevin Staras, during my PhD, and my appreciation for his phenomenal efforts on my behalf. Thanks also to my secondary supervisor, Louise Serpell, for her sympathetic ear and advice.

I am grateful to Arjuna Ratnayaka and Milena Wagner for their assistance with tissue culture, and for lending me coverslips from time to time! Also thank you to Milena for her assistance in the calcium imaging. The endless patience of Julian Thorpe in assisting with processing for electron microscopy, particularly through the preparation of ultrathin section, is greatly appreciated. Special thanks to Vincenzo Marra for knowing everything in the world, and for trying to teach me as much of it as he could.

I was fortunate enough to have marvellous colleagues during my PhD, so thank you to Lenzie, Terri, and most especially Mikey, for the journal clubs, the nights in the pub, letting me cry on your shoulders, rant at you, and for making my time at Sussex enjoyable.

Finally, thank you to my parents for their understanding, and thank you to Rob, for everything.

University of Sussex

Freya Crawford

Ultrastructure-function properties of recycling synaptic vesicles in acute hippocampal slices

Abstract

Synaptic vesicles are the substrate of neurotransmission in most nerve terminals in the central nervous system. These small membrane spheres fuse with the synaptic membrane in an activity-dependent manner and release neurotransmitter into the synaptic cleft. Subsequently, vesicles are reclaimed through endocytosis prior to reuse. This recycling process is key to supporting ongoing signalling in the brain.

While substantial effort has gone into defining basic characteristics of vesicle recycling, for example elucidating the timing of vesicle turnover, key questions remain unanswered. An important area with significant knowledge deficits relates to the relationship between vesicle function and ultrastructural organisation in the terminal. The aim of this thesis is to address this issue, exploiting new methodologies which provide novel insights into function-structure relationships of vesicle populations in acute brain slices. Specifically, this study considers organisational principles of three defined vesicle pools as well as examining the impact of an established plasticity protocol on pool properties.

The first results chapter, Chapter 3, outlines and validates the novel protocol used for fluorescently labelling functional recycling vesicle populations in acute rat brain slices using the vesicle-labelling dye FM1-43 and new antibody based probes (syt1-Oyster, CypHer5E). Reporter-labelling and release properties are compared to similar approaches using cultured neurons. We conclude that this approach provides a more physiologically relevant method to study the functional properties of cells than used previously in cultured neurons.

Chapter 4 outlines experiments utilising the capability of FM 1-43 to be photoconverted to an electron-dense form to allow a defined vesicle population, the readily releasable

pool (RRP), to be characterised ultrastructurally. The RRP is arguably the most significant pool class, released first in response to an activity train. Functional assays and time-stamped electron microscopy are used to define basic properties of this pool, including its size, functional release kinetics, and temporal organisation. Specifically, the results demonstrate that retrieved vesicles are close to the active zone after stimulation, but mixed randomly in the terminal volume over 20 min. These findings address fundamental questions about vesicle reuse, the composition of future vesicle pools, and thus the mechanism of ongoing signalling in the brain.

The same approach was used in Chapter 5 to examine the influence of Long Term Depression (LTD) on pool function and ultrastructure. LTD was induced in presynaptic terminals in CA1 via Schaffer collateral activation, and the following effects were observed: 1) a change in release kinetics; 2) a reduction in the total recycling pool size; and 3) no change in the composition of the docked pool. These findings demonstrate that there is a presynaptic component to LTD and that vesicle recruitment into the recycling pool appears to be an important possible substrate. However, the results suggest that such changes appear to be selective for specific pool subsets. Overall, work in this chapter offers new insights into fundamental principles supporting synaptic plasticity.

Chapter 6 expands on previous studies which have demonstrated that recycling vesicles are constitutively shared between neighbours. This sharing of a 'superpool' of vesicles has implications for the ability of synapses to adapt to changes in input weighting. In this chapter, the methods outlined above, as well as a new 3D EM technology, are used to define the size, positional organisation, and clustering properties of this pool in native hippocampal slice system. The findings in this chapter reveal that extrasynaptic vesicles appear to show a greater degree of motility than vesicles which remain in the intrasynaptic cluster, perhaps implying differential interactions with structural proteins in the synapse. Characterising the superpool is increasingly relevant, as it is now implicated in models of plasticity and disease.

Taken together, these results show that the ultrastructural arrangement of recycling vesicles is highly activity-dependent, and that the cytoarchitecture plays a large role in determining the functionality of individual vesicles and synapses.

Chapters

| | | |
|---|--|-----|
| 1 | Introduction | 18 |
| 2 | Materials and methods | 56 |
| 3 | Fundamental properties of presynaptic terminals in culture and acute slice | 79 |
| 4 | Characterising release ready vesicles in acute slice preparation..... | 122 |
| 5 | The effect of long-term plasticity on ultrastructure and function of recycling vesicle pools | 155 |
| 6 | Recycling vesicles at extrasynaptic locations in hippocampal slice | 184 |
| 7 | General discussion | 222 |

Table of Contents

| | |
|--|----|
| Declaration | 2 |
| Acknowledgements..... | 3 |
| Abstract | 4 |
| Abbreviations..... | 15 |
| Metric prefixes | 17 |
| 1.1 History of synaptic transmission..... | 19 |
| 1.1.1 The neuron doctrine versus reticular theory..... | 19 |
| 1.1.2 Chemical transmission at synapses..... | 19 |
| 1.1.3 Quantal theory and synaptic vesicles | 21 |
| 1.2 Chemical synapses in the central nervous system..... | 22 |
| 1.2.1 Synapse anatomy..... | 22 |
| 1.2.2 Presynaptic terminal..... | 22 |
| 1.2.3 Postsynaptic region | 24 |
| 1.3 Synaptic vesicle recycling | 25 |
| 1.3.1 Exocytosis | 27 |
| 1.3.2 Endocytosis..... | 29 |
| 1.3.3 Calcium in synaptic vesicle recycling..... | 33 |
| 1.4 Synaptic vesicle pools in hippocampal terminals..... | 34 |
| 1.4.1 The spontaneous pool..... | 35 |
| 1.4.2 The recycling pool and resting pool | 35 |
| 1.4.3 The readily releasable pool | 36 |
| 1.4.4 The superpool | 37 |
| 1.5 Long-term plasticity in the hippocampus | 38 |
| 1.5.1 Long-term potentiation in hippocampal synapses | 39 |
| 1.5.1.1 Postsynaptic factors in LTP..... | 40 |
| 1.5.1.2 Presynaptic factors in LTP | 40 |
| 1.5.2 Long-term depression in hippocampal synapses..... | 40 |
| 1.5.2.1 Postsynaptic factors in LTD | 41 |

| | |
|--|----|
| 1.5.2.2 Presynaptic factors in LTD | 43 |
| 1.5.3 Linking pre- and postsynaptic plasticity | 45 |
| 1.5.4 Calcium stores and long-term plasticity | 46 |
| 1.6 Methods of studying synaptic terminals..... | 47 |
| 1.6.1 Electrophysiological measurement of synaptic properties..... | 47 |
| 1.6.2 Imaging synapses | 47 |
| 1.6.2.1 Fluorescent probes for studying synaptic function..... | 48 |
| 1.6.2.2 FM 1-43 and the FM dyes | 49 |
| 1.7 Emerging techniques | 51 |
| 1.7.1 Qdots as biomarkers | 51 |
| 1.7.2 Super-resolution microscopy | 51 |
| 1.7.3 FIBSEM..... | 53 |
| 1.8 Conclusions and aims..... | 54 |
| 2.1 Animal handling | 56 |
| 2.2 FM dye loading in hippocampal neuronal cultures | 56 |
| 2.2.1 Chemicals / reagents / products for culturing..... | 56 |
| Table 2.1 | 56 |
| 2.2.2 Solutions and buffers..... | 57 |
| Table 2.2..... | 57 |
| 2.2.3 Dissection..... | 57 |
| 2.2.4 Astrocytic feeder layer..... | 58 |
| 2.2.5 Hippocampal neuronal culture | 59 |
| 2.3 Optical probe labelling of hippocampal cultures | 61 |
| Table 2.3..... | 61 |
| Table 2.4..... | 61 |
| 2.3.1 Electrical stimulation of hippocampal neuronal cultures..... | 61 |
| 2.3.2 Imaging functional properties of cultured synapses | 62 |
| 2.3.3 Calibration of stimulation chamber for hippocampal neuronal cultures | 62 |
| 2.4 Labelling functional synapses in hippocampal slices..... | 64 |
| Table 2.5..... | 64 |
| Table 2.6..... | 64 |
| 2.4.1 Preparing hippocampal slices..... | 65 |
| 2.4.2 Experimental set-up | 66 |

| | |
|---|----|
| 2.4.2.1 Imaging system..... | 66 |
| 2.4.2.2 Electrophysiology rig..... | 67 |
| 2.4.3 Stimulating Schaffer collaterals in hippocampal slices..... | 67 |
| 2.4.3.1 Electrophysiology trace analysis..... | 68 |
| 2.4.4 FM dye labelling in hippocampal slices..... | 69 |
| 2.4.5 Measuring fluorescence levels of native terminals..... | 69 |
| 2.4.5.1 Determining calcium dependence of experiments..... | 70 |
| 2.4.6 Analysing fluorescence data..... | 70 |
| 2.5 Ultrastructural studies of recycling vesicles..... | 70 |
| Table 2.7..... | 70 |
| Table 2.8..... | 71 |
| 2.5.1 Calibrating microwave for rapid fixation..... | 72 |
| 2.5.2 Microwave enhanced fixation..... | 72 |
| 2.5.3 Photoconversion of DAB..... | 72 |
| 2.5.4 Preparation for conventional electron microscopy..... | 73 |
| 2.5.5 Ultrathin serial sections..... | 74 |
| 2.5.6 Image acquisition..... | 74 |
| 2.5.7 Analysis..... | 74 |
| 2.5.7.1 Density maps in MATLAB..... | 74 |
| 2.6 Preparation of samples for FIBSEM electron microscopy..... | 76 |
| Table 2.9..... | 76 |
| Table 2.10..... | 76 |
| 2.6.1 Analysis..... | 78 |
| 2.7 Statistics..... | 78 |
| 2.8 Collaborators..... | 78 |
| 3.1 Introduction..... | 79 |
| 3.2 Fluorescence readout of recycling vesicle properties in cultured hippocampal neurons..... | 81 |
| 3.2.1 Establishing dissociated hippocampal cultures..... | 81 |
| 3.2.2 Establishing conditions for effective synaptic activation..... | 83 |
| 3.2.3 FM dye labelling of hippocampal synapses in culture..... | 86 |
| 3.2.4 Assaying ongoing synaptic function using FM 1-43 dye destaining..... | 88 |
| 3.2.5 Alternative acutely-applied reporter for monitoring vesicle recycling..... | 90 |

| | |
|--|-----|
| 3.2.6 Acute probes for optical measurement endocytosis timings in cultured neurons | 93 |
| 3.3 Developing FM-dye-labelling in the native slice system | 96 |
| 3.3.1 Generating synaptic activation in hippocampal slice preparations, and basic calibration..... | 97 |
| 3.3.2 Confirming calcium dependence of hippocampal responses | 100 |
| 3.3.3 Fluorescent labelling of hippocampal slices in acute slice preparation..... | 102 |
| 3.3.4 Challenges of background dye elimination | 105 |
| 3.3.5 Assay of function in native hippocampal terminals..... | 108 |
| 3.3.6 Frequency dependent recycling in native terminals | 110 |
| 3.3.7 Alternative methods of viewing synaptic function in hippocampal slice | 111 |
| 3.4 Discussion | 117 |
| 3.4.1 FM dye labelling and release from hippocampal neurons | 117 |
| 3.4.2 Immunological methods for studying functional properties in hippocampal slice | 118 |
| 3.4.3 Future development for methods of studying vesicle properties in slice..... | 120 |
| 3.5 Acknowledgements..... | 121 |
| 4.1 Introduction..... | 122 |
| 4.2 Ultrastructural properties of RRP vesicles in the hippocampal slice system | 125 |
| 4.2.1 Establishing a robust method of labelling the RRP in native tissue..... | 125 |
| 4.2.2 Development of a procedure for photoconversion of the RRP | 127 |
| 4.2.3 Characteristics of photoconverted vesicles..... | 129 |
| 4.2.4 RRP vesicles as a fraction of the total pool..... | 133 |
| 4.2.5 Arrangement of readily releasable vesicles following reuptake | 136 |
| 4.2.6 RRP vesicles and the docked pool | 139 |
| 4.3 Functional properties of RRP vesicles in the acute hippocampal slice preparation | 143 |
| 4.3.1 Rate of fluorescence depletion in RRP labelled synapses | 143 |
| 4.3.2 Using fluorescence based assays of function for short time scales | 146 |
| 4.4 Discussion | 149 |
| 4.4.1 Labelling the RRP in the hippocampal acute slice preparation | 149 |
| 4.4.2 Distribution of RRP vesicles following recycling..... | 150 |
| 4.4.3 RRP vesicle re-entry around the active zone..... | 152 |
| 4.4.4 Functional properties of RRP vesicles on reuse | 153 |

| | |
|--|-----|
| 5.1 Introduction..... | 155 |
| 5.2 Functional labelling of recycling vesicles in hippocampal slices with LTD induced | 157 |
| 5.2.1 Protocol of LTD in Schaffer collateral synapses | 157 |
| 5.2.2 Electrophysiological evidence for LTD induction..... | 159 |
| 5.2.3 Anomalies of LTD induction..... | 162 |
| 5.2.4 Labelling synapses with FM 1-43 for fluorescence imaging | 165 |
| 5.2.5 Functional properties of synaptic vesicle pools in LTD synapses..... | 167 |
| 5.2.6 Ultrastructural properties of the total recycling pool in LTD synapses..... | 168 |
| 5.2.7 Properties of the docked pool in LTD synapses..... | 175 |
| 5.3 Discussion | 179 |
| 5.3.1 Functional properties of LTD synapses | 179 |
| 5.3.2 Relating ultrastructure and function in LTD synapses..... | 180 |
| 5.3.3 Linking pre- and postsynaptic factors of LTD..... | 182 |
| 6.1 Introduction..... | 184 |
| 6.2 Fluorescence imaging of extrasynaptic vesicles..... | 186 |
| 6.2.1 FM dye imaging mobile vesicles in cultured neurons..... | 186 |
| 6.2.2 Using FM 1-43 to observe mobile vesicles in acute hippocampal slice preparations | 187 |
| 6.2.3 Using antibodies to observe extrasynaptic functional vesicles | 189 |
| 6.3 Ultrastructural studies of extrasynaptic functional vesicles..... | 192 |
| 6.3.1 Using conventional electron microscopy to study functional extrasynaptic vesicles | 192 |
| 6.3.2 Properties of extrasynaptic recycling vesicle populations | 195 |
| 6.4 Using Focused Ion Beam Scanning Electron Microscopy to study extrasynaptic vesicles..... | 205 |
| 6.4.1 Identifying recycling vesicles in FIBSEM images | 209 |
| 6.4.2 Investigating distribution of recycling vesicles using FIBSEM | 212 |
| 6.5 Discussion | 218 |
| 6.6 Acknowledgements..... | 221 |
| 7.1 Functional studies in the acute hippocampal slice preparation..... | 222 |
| 7.1.1 A method for studying function in slice | 222 |
| 7.1.2 Physiological temperature and functionality..... | 223 |
| 7.1.3 Ultrastructural properties of synaptic vesicles in hippocampal slice | 224 |
| 7.2 Synaptic vesicle pools and the fate of retrieved vesicles..... | 224 |

| | |
|---|-----|
| 7.3 Plasticity-induced changes in synaptic properties | 227 |
| 7.3.1 Recycling pool scaling in response to plasticity protocols | 227 |
| 7.3.2 Docking sites as a mechanism of synaptic plasticity | 227 |
| 7.4 Activity-dependent arrangement of recycling vesicles within terminals..... | 229 |
| 7.5 Evidence for a preferentially-accessed pool of vesicles near the active zone..... | 230 |
| 7.6 Activity-dependent properties of the superpool | 232 |
| 7.7 Conclusions and future work..... | 233 |

Table of Figures

| | |
|---|-----|
| Figure 1.1 An example electron micrograph of a synapse..... | 25 |
| Figure 1.2 Summary of exocytosis and endocytosis in synapses..... | 27 |
| Figure 1.3 Proteins associated with synaptic vesicle exocytosis | 29 |
| Figure 1.4 Clathrin-mediated endocytosis..... | 30 |
| Figure 1.5 Proteins associated with endocytosis in synaptic terminals | 32 |
| Figure 1.6 Synaptic vesicle pools in hippocampal neurons | 35 |
| Figure 1.7 Postsynaptic pathways in LTD induction | 43 |
| Figure 1.8 Summary of factors affecting presynaptic expression of LTD | 45 |
| Figure 1.9 FM dye structure and mechanism of action | 50 |
| Figure 2.1 Dissection and preparation of rat brain for slicing | 58 |
| Figure 2.2 Brightfield images of hippocampal neuronal cultures..... | 60 |
| Figure 2.3 Method for labelling neuronal cultures with FM dye | 62 |
| Figure 2.4 Preparing hippocampal slices for FM dye loading | 65 |
| Figure 2.5 Producing a field excitatory postsynaptic potential in CA1 of a hippocampal slice ... | 67 |
| Figure 2.6 Producing density plots using MATLAB | 75 |
| Figure 3.1 Culture and stimulation of hippocampal neurons..... | 82 |
| Figure 3.2 Calibrating tissue culture stimulation chamber)..... | 86 |
| Figure 3.3 Activity dependent labelling of cultured neurons with styryl dye..... | 87 |
| Figure 3.4 Visual assay of synaptic recycling in hippocampal cultures..... | 90 |
| Figure 3.5 Using syt1Oyster550 antibodies to provide readouts of synaptic function | 92 |
| Figure 3.6 Obtaining an optical readout of endocytosis in cultured neurons using an acutely applied probe..... | 95 |
| Figure 3.7 Establishing a robust synaptic response from the hippocampal slice system and basic calibration of stimulus | 100 |
| Figure 3.8 Measured fEPSP is calcium dependent..... | 101 |
| Figure 3.9 FM dye labelling of functional synapses in hippocampal slices..... | 104 |
| Figure 3.10 Using an FM-dye chelator to improve signal to noise ratio..... | 107 |
| Figure 3.11 Visual assay of synaptic function in hippocampal slices using FM 1-43 | 109 |
| Figure 3.12 Release of FM 1-43 in native hippocampal terminals is frequency dependent | 111 |
| Figure 3.13 An alternate method of viewing functional synapses in the hippocampal slice system | 113 |
| Figure 3.14 Observing endocytosis in the hippocampal slice system..... | 116 |
| Figure 4.1 Possible routes of vesicle re-entry and reuse | 124 |
| Figure 4.2 Lower levels of fluorescence labelling of RRP compared to TRP | 127 |
| Figure 4.3 Photoconversion of DAB labelled functional vesicles at an ultrastructural level | 129 |
| Figure 4.4 Photoconverted vesicles are readily identifiable under the electron microscope... | 131 |
| Figure 4.5 Black vesicles are specific to FM dye loading and photoconversion | 133 |
| Figure 4.6 Recycling pool fraction is stable over time and is not related to synapse size..... | 136 |

| | |
|---|-----|
| Figure 4.7 Recycling vesicles are positioned towards the back of the cluster over time | 137 |
| Figure 4.8 Clustering of recycling vesicles at multiple time points..... | 139 |
| Figure 4.9 Recycling vesicles are more common at docking sites at shorter times following stimulation | 140 |
| Figure 4.10 Recycling vesicle positioning at docking sites at three different time points..... | 143 |
| Figure 4.11 Functional activity of RRP vesicles in native tissue | 145 |
| Figure 4.12 BPB quenches FM 1-43 fluorescence..... | 148 |
| Figure 4.13 Rate of fluorescence loss at 1 min vs 20 min after stimulation..... | 149 |
| Figure 5.1 Location of a tissue response for plasticity induction | 159 |
| Figure 5.2 Low frequency stimulation alters parameters of the tissue response. | 161 |
| Figure 5.3 Short-term plasticity induction in Schaffer collateral synapses | 163 |
| Figure 5.4 Induction of LTP using 3 Hz / 5 min protocol | 164 |
| Figure 5.5 CNQX and AP5 effectively eliminate the post synaptic response..... | 166 |
| Figure 5.6 Activity dependent fluorescence loss in LTD synapses..... | 168 |
| Figure 5.7 Visualising the total recycling pool in LTD synapses | 170 |
| Figure 5.8 Recycling fraction of LTD versus control synapses | 171 |
| Figure 5.9 Density maps of synaptic vesicles within LTD and control terminals | 173 |
| Figure 5.10 Distance from active zone of vesicles in control and LTD synapses | 174 |
| Figure 5.11 Recycling fractions in the docked pool in LTD and control synapses | 176 |
| Figure 5.12 Location of recycling vesicles within the docked pool..... | 178 |
| Figure 6.1 Lateral movement of FM 1-43 labelled vesicles in cultured neurons..... | 187 |
| Figure 6.2 Lateral movement of FM 1-43 labelled vesicles in native tissue | 189 |
| Figure 6.3 Using syOyster550 to label mobile vesicles | 191 |
| Figure 6.4 Producing 3D reconstructions of processes containing recycling vesicles | 194 |
| Figure 6.5 Identifying and quantifying intrasynaptic and extrasynaptic vesicles in native tissue | 198 |
| Figure 6.6 Distribution of intra- and extrasynaptic vesicles relative to the active zone | 201 |
| Figure 6.7 Vesicle density within synapses and processes | 202 |
| Figure 6.8 Clustering analysis of synaptic vesicles..... | 204 |
| Figure 6.9 FIBSEM images are suitable for tracing synapses over large distances..... | 207 |
| Figure 6.10 Identifying recycling vesicles in FIBSEM sections | 211 |
| Figure 6.11 Extracting distance data from FIBSEM images | 214 |
| Figure 6.12 Recycling vesicle distribution relative to the active zone within synapses and processes..... | 214 |
| Figure 6.13 Intrasynaptic and extrasynaptic vesicle distribution | 216 |
| Figure 7.1 Cartoon of RRP vesicle positioning on re-entry into the synapse..... | 226 |
| Figure 7.2 Hypothesis of docking sites as a mechanism of synaptic vesicle recycling | 228 |
| Figure 7.3 Hypothesis of activity dependent preferential positioning of recycling vesicles at active zones..... | 230 |

Abbreviations

| | |
|---------|---|
| °C | degrees Celcius |
| ACSF | artificial cerebrospinal fluid |
| ADP | adenosine di-phosphate |
| AMPA | α -amino-3-hydroxy-5-methyl-4-isoxazolepropionic acid |
| AMPA R | AMPA receptor |
| ANOVA | analysis of variance |
| AP | action potential |
| AP-5 | (2R)-amino-5-phosphonopentanoate |
| ara-C | cytosine arabinoside |
| ATP | adenosine tri-phosphate |
| BAPTA | 1,2-bis(o-aminophenoxy)ethane-N,N,N',N'-tetraacetic acid |
| BDNF | brain derived neurotrophic factor |
| BME | basal medium Eagle |
| BPB | bromophenol blue |
| CA1 | cornu ammonis 1 |
| CA2 | cornu ammonis 1 |
| CA3 | cornu ammonis 3 |
| CaMKII | calcium/calmodulin dependent kinase 2 |
| cAMP | cyclic adenosine monophosphate |
| CAST | cytomatrix at the active-zone associated structural protein |
| CCD | charge coupled device |
| cdk5 | cyclin dependent kinase 5 |
| cDNA | complementary DNA |
| CNQX | 6-cyano-7-nitroquinoxaline-2,3-dione |
| Cy | cyanine |
| d | day |
| DAB | 3,3'-diaminobenzidine |
| DIC | differential interference contrast |
| DIV | days <i>in vitro</i> |
| DNA | deoxyribonucleic acid |
| EBS | extracellular bath solution |
| EDTA | ethylenediaminetetraacetic |
| EM | electron microscope/microscopy |
| F-BAR | F-bin-amphiphysin-Rvs |
| FCS | foetal calf serum |
| fEPSP | field excitatory postsynaptic potential |
| FIBSEM | focused ion beam scanning electron microscopy |
| FM 1-43 | N-(3-triethylammoniumpropyl)-4-(4-(dibutylamino) styryl) pyridinium dibromide |
| fps | frames per second |
| FRAP | fluorescence recovery after photobleaching |
| GABA | γ -aminobutyric acid |

| | |
|----------|--|
| GPCR | G-protein coupled receptor |
| h | hour |
| HBSS | Hank's balanced salt solution |
| HEPES | 4-(2-hydroxyethyl)-1-piperazineethanesulfonic acid |
| HRP | horseradish peroxidase |
| Hz | Hertz |
| IP3 | inositol (1,4,5)-trisphosphate |
| l | litre |
| LTD | long term depression |
| LTP | long term potentiation |
| m | metre |
| M | moles/litre |
| mGluR1 | metabotropic glutamate receptor 1 |
| min | minute |
| NA | numerical aperture |
| NMDA | N-methyl-D-aspartate |
| NMDAR | NMDA receptor |
| NMJ | neuromuscular junction |
| NO | nitric oxide |
| NSF | N-ethylmaleimide-sensitive factor |
| OGB | Oregon green BAPTA |
| p | post-natal |
| PALM | photoactivated localisation microscopy |
| PBS | phosphate buffered saline |
| PDL | poly-D-Lysine |
| PMT | photomultiplier tube |
| psi | pounds per square inch |
| Qdots | Quantum dots |
| RRP | readily releasable pool |
| s | second |
| SEM | scanning electron microscopy |
| SNAP | soluble NSF attachment protein |
| SNARE | SNAP receptor |
| STED | stimulated emission depletion |
| STORM | stochastic optical reconstruction microscopy |
| TEM | transmission electron microscopy |
| TRP | total recycling pool |
| TTX | tetrodotoxin |
| V | volts |
| VDCC | voltage dependent calcium channel |
| VGAT | vesicular GABA transporter |
| VGluT | vesicular glutamate transmitter |
| W | watt |
| Ω | ohm |

Metric prefixes

| | | |
|-------|--------|-----------|
| n | nano- | 10^{-9} |
| μ | micro- | 10^{-6} |
| m | milli- | 10^{-3} |
| c | centi- | 10^{-2} |
| k | kilo- | 10^3 |
| M | mega- | 10^6 |
| G | giga- | 10^9 |

Chapter 1: Introduction

A key role of brain operation is to receive, interpret, and store input from the external environment and use it to formulate, coordinate, and deliver appropriate responses. Transfer of information between the nervous system building blocks – or neurons – is a critical aspect of this function. Such information transmission occurs at specialised connection sites called ‘synapses’. These remarkable nanoscale machines propagate information between cells, but can also modulate those signals with changing operational demands. The fundamental mechanisms of synaptic transmission and modulation are therefore of central interest in modern neuroscience.

There are two types of synapse in the mammalian central nervous system: the electrical synapse, and the chemical synapse (Cowan et al., 2001). In electrical synapses, a signal is transferred via direct ion movement through gap junctions in the membrane. These synapses provide fast, synchronous transmission, but provide limited modulation (although see Landisman and Connors (2005)). Chemical synapses are responsible for the majority of neuronal communication in mammals (Cowan et al., 2001).

Though slower in conveying signals than electrical junctions, chemical synapses can readily scale and modulate their response to input (de Jong and Verhage, 2009). The action potential is largely binary, with frequency increase being the primary method of encoding a greater signal intensity (Dittman et al., 2000). The chemical synapse therefore provides the principal means of filtering information in a network. Responses such as increasing the weighting of a high intensity stimulus, or decreasing the response to a sustained stimulus, occur at a synaptic level (Dobrunz and Stevens, 1999). As such, studying the mechanisms underlying synaptic responses, particularly and their mechanisms of modulation, is of fundamental importance. The objective of this study is to address key aspects of these processes in central mammalian chemical synapses.

1.1 History of synaptic transmission

1.1.1 The neuron doctrine versus reticular theory

Cells in brain tissue are fragile, complex, and densely packed. These properties still pose difficulties today, but made comprehensive study of the central nervous system nearly impossible for early researchers. Early histologists posited that the dendrites of neurons formed a continuous network with processes fused to one another to allow communication. In 1873, Camillo Golgi's silver nitrate and potassium dichromate reaction solved the problem of density, producing dark black staining in 1-5% of cells in brain tissue (Mazzarello, 1999). Having studied cells stained with his technique, Golgi developed a new theory that dendrites were trophic cells, and that axons formed the networks described by his colleagues (Raviola and Mazzarello, 2011). This 'reticular theory' was generally accepted at the time.

By the late 1880s, however, a growing number of researchers began to doubt reticular theory. Wilhelm His made observations of the spinal cord during development and identified neuronal precursor cells, which were discrete and distinct; he saw that, later in development, processes grew out from these cells, but were free ending (Cowan and Kandel, 2001). August Forel's observed that what we now call 'retrograde degeneration', following the severing of a process, only affected those specific cells, and did not have a wider effect on the network (Cowan and Kandel, 2001). Following refinements to Golgi's technique, Santiago Ramon y Cajal was able to make detailed histological studies of many morphologically different cells within the brain. He observed that axons were free-ending, and that each neuron was completely autonomous. Through observations of structures like the retina and the olfactory bulb, Cajal also deduced that information transfer between neurons was directional (Lopez-Munoz et al., 2006). Cajal's histological studies would later provide the most compelling evidence for the neuron doctrine.

1.1.2 Chemical transmission at synapses

Nearly 100 years before Cajal's studies, Luigi Galvani demonstrated that applying electricity to a nerve could cause a frog's leg to move. From the late 18th to late 19th century, huge progress was made in understanding how transmission of the electrical signal occurred, with the concepts of the endplate, the action potential, and the neuromuscular delay all raised experimentally. There was now increasing certainty that

the point of contact between a neuron and another tissue must be the site at which the electrical signal from the axon became a response from its target (Bennett, 1999).

In 1897, Charles Sherrington, already noted for his work on the cerebellum and reflex arcs, stated that the nexus between neurons must have a surface of separation and distinct physical features, and would probably be a site of chemical transduction of the signal (Pearce, 2004). To describe this connection point, he coined the term 'synapse', from the Greek for "to clasp"; he rejected the alternative 'junction', feeling it suggested physical union and that the connection was a passive one (Tansey, 1997).

The next step in examining the mechanisms behind signal transduction at these synapses involved exploration of the idea that transmission may be mediated by chemicals. Around 1900, John Newport Langley found that the application of adrenaline to tissues caused effects similar to those caused by sympathetic nervous stimulation. He also found that the application of adrenaline to tissues on which the nerves had been cut and allowed to degenerate still caused an effect (Valenstein, 2002). In 1905 and 1906, Langley published papers containing observations which would prove central to our understanding of neurotransmission today (Langley, 1905, Langley, 1906). He deduced that not only were there substances which caused tissues to produce a response, but there must also be 'receptive substances' which set this response into action (Cowan and Kandel, 2001). Further work followed by such luminaries as Henry Hallett Dale, who isolated acetylcholine and suggested it as the basis of parasympathetic neurotransmission in 1914, and Otto Loewi, who performed classic experiments with frog hearts in 1921 and conclusively demonstrated that there was a chemical basis for control of the heart (Raju, 1999).

Other neurotransmitters were discovered over the course of the next century, of which GABA (γ -aminobutyric acid) and glutamate are key for the central nervous system. In 1950, several groups identified that GABA was present in brain tissue at much higher levels than in other tissues or bodily fluids (Awapara et al., 1950, Roberts and Frankel, 1950, Udenfriend, 1950). A large number of studies attempted to apply this amino acid onto brain tissue in order to determine its role (Krnjevic, 2004), including one which showed that it depressed spikes from motor neurons (Curtis et al., 1959b), and it was finally determined to be an inhibitory neurotransmitter (Krnjevic and Phillis, 1963).

L-glutamate is the most abundant intracellular amino acid, and is present in every cell in the body. It has important roles in the synthesis of other amino acids, including GABA, and in metabolic processes of the cell, such as the Krebs cycle (Newsholme et al., 2003). Because of this, there was a long period in which there was some debate as to whether or not glutamate was a neurotransmitter. Glutamate was isolated in brain tissue in 1949, but the levels found there were not significantly different to those in other tissues in the body (Krebs et al., 1949).

In 1954 it was observed that injecting sodium glutamate via a capillary into the grey matter of a variety of organisms caused them to have convulsions. This led to the conclusion that glutamate must have a direct physiological action on the central nervous system (Hayashi, 1954). The direct effect of glutamate on the central nervous system was later proved when it was shown to cause spiking in interneurons from the cat spinal cord (Curtis et al., 1959a). However, the ubiquity of glutamate and the sheer number of pathways in which it seemed to be involved led to its not meeting the criteria for many definitions of a neurotransmitter (Watkins, 2000).

Major categories of glutamate receptor were identified over the next two decades, including NMDA receptors (Curtis and Watkins, 1963), kainate receptors (Johnston et al., 1969), and AMPA receptors (Honore et al., 1982), and consequently antagonists for these could be located. These discoveries overcame much of the resistance to categorising glutamate as a neurotransmitter, a status which is now accepted (Watkins and Jane, 2006).

1.1.3 Quantal theory and synaptic vesicles

In 1951, Paul Fatt and Bernard Katz noted that acetylcholine produced a separate effect on the endplate compared to the muscle fibre (Fatt and Katz, 1951). Recording these endplate potentials allowed for a sensitive method of measuring acetylcholine release at the synapses. Whilst conducting this research, Fatt and Katz observed spontaneously generated miniature endplate potentials, too small to generate a response from the muscle fibre. When the amplitude of these miniature endplate potentials was measured, it was found that they were all in multiples of a basal unit. The authors deduced that this was due to there being 'discrete unitary discharge' of neurotransmitter (Fatt and Katz, 1952).

Following the development of the scanning electron microscope, synapses at an ultrastructural level became amenable to analysis. During these studies, one of the key features of nerve terminals was found to be a group of membrane spheres, 40-60 nm in diameter (Palay and Palade, 1955, De Robertis and Bennett, 1954). These two discoveries were quickly combined, with Palay (1956) hypothesising these to be the vehicles required for delivering the quantal release of neurotransmitter that Fatt and Katz (1952) deduced. This idea that the synaptic vesicles were the mechanism of delivery of neurotransmitter, termed the 'vesicular hypothesis of neurotransmission', was reinforced when acetylcholine was found to be stored in synaptic vesicles (Whittaker, 1968). The vesicular hypothesis is now generally accepted as the mechanism of transmission at chemical synapses.

1.2 Chemical synapses in the central nervous system

1.2.1 Synapse anatomy

The synapse is composed of a presynaptic compartment and a postsynaptic compartment, separated by a ~20 nm gap, roughly the thickness of a double membrane layer (De Robertis and Bennett, 1954), and held in opposition by a wide variety of adhesion molecules (Sudhof, 2012). Each compartment has specific morphological and molecular features which help them carry out the functions of synapses.

1.2.2 Presynaptic terminal

Presynaptic terminals can chiefly be identified by the synaptic vesicles. These are membrane spheres around 30-50 nm in diameter (De Robertis and Bennett, 1955, Palay and Palade, 1955) (highlighted in pink in Fig.1.1). These are posited to be the mechanism for the quantal release of neurotransmitter described by Fatt and Katz (Fatt and Katz, 1952).

The majority of the vesicles are held together in a cluster. Clusters of synaptic vesicles in the hippocampus typically contain something of the order of 100-200 vesicles (Harris and Sultan, 1995). The protein synapsin is partially responsible for this clustering of vesicles, and its absence causes both a decrease in the cohesion of the cluster and a decrease in the release properties of the synapse (Orenbuch et al., 2012). Synapsin probably links synaptic vesicles to the actin filaments or other cytoskeletal elements that are attached to the plasma membrane (Doussau and Augustine, 2000). The synaptic

vesicles themselves are uniform in appearance, but feature a large number of proteins specifically designed to aid neurotransmitter release.

The protein content of synaptic vesicles has been well catalogued thanks to the groundbreaking article by Takamori et al. (2006). They harvested large quantities of synaptic vesicles from within terminals then identified and quantified the proteins found. They found 34 different proteins which were co-purified with synaptic vesicles, suggesting that synaptic vesicles were more densely covered in proteins than previously suspected. Synaptophysin and the synaptobrevins were the most common molecules on the surface of synaptic vesicles. A month later, a similar study was released, detailing even larger numbers of proteins on synaptic vesicles (Burre et al., 2006).

Synaptic vesicles have only a single proton pump for reacidification, though this structure is sufficiently large as to make up 10% of the vesicle protein. It appears as a 'knob like' protrusion on the surface of the vesicle (Stadler and Tsukita, 1984). They also contain Rab 5 and Vtib, which are proteins associated with endosomal fusion, indicating that vesicles have the capability to undergo bulk endocytosis (Sudhof, 2006).

The study by Takamori et al. (2006) was unable to separate glutamatergic excitatory vesicles from GABA-ergic inhibitory vesicles, so although the VGLuT proteins were identified, alongside VGAT proteins from the purified synaptic vesicles, the composition of these on each vesicle could not be determined. GABA-ergic and glutamatergic synaptic vesicles have been observed to have different structural appearances (Gray, 1959), but their protein content is highly similar (Boyken et al., 2013).

Quantification of proteins at a single vesicle level demonstrated that the protein content of a vesicle has a high degree of uniformity (Mutch et al., 2011), leading the authors to suppose that this was due to synaptic vesicles retaining their identity on recycling, despite several studies indicating that vesicles do not retain individual proteins (Hua et al., 2011, Fernandez-Alfonso et al., 2006). The protein content of synaptic vesicles is believed to be regulated by the stonin proteins, sorting copies of proteins from a common vesicle, ensuring vesicle uniformity, but not maintaining individual vesicle identity (Kononenko et al., 2013).

Another key feature of the synapse is the active zone (shown in green in Fig.1.1). This is a specialised region of the plasma membrane characterised by synaptic vesicles

positioned in contact with the membrane, arranged in a grid-like formation (Couteaux and Pecot-Dechavassine, 1970, Harris and Weinberg, 2012). This region of the synaptic membrane is the location of neurotransmitter release, and contains most of the machinery to allow this to occur.

In addition to the electron-lucent synaptic vesicles containing neurotransmitter, there are also large, dense core vesicles. These vesicles, 70-200 nm in diameter, are larger than the rest of the vesicle cluster, and feature an electron dense core, appearing black under the electron microscope. These release peptide neurotransmitters into the synaptic cleft. These vesicles cannot be recycled at the active zone and must be trafficked back and forth from the somatodendritic compartment of the cell (De Camilli et al., 2001).

Synaptic terminals often contain mitochondria; in fact, these organelles are significantly more likely to be located at synaptic sites than at any other location within the neuron (Chang et al., 2006). The proposed function of mitochondria is to provide ATP to drive the metabolic processes of the cell, and to regulate intracellular calcium. As synapses are a dynamic, high-energy environment, and subject to frequently elevated calcium, it is not surprising that mitochondria are frequently found at synaptic terminals (Shepherd and Harris, 1998),

1.2.3 Postsynaptic region

In addition to the presence of the synaptic cluster and the vesicles docked at the active zone, one of the easiest ways to identify a synapse is through the presence of a postsynaptic density (PSD). These electron-dense structures form a scaffolding which stabilises receptor proteins (Kim and Serpe, 2013) and various other major proteins, which control the cell's response to neurotransmitter (De Camilli et al., 2001).

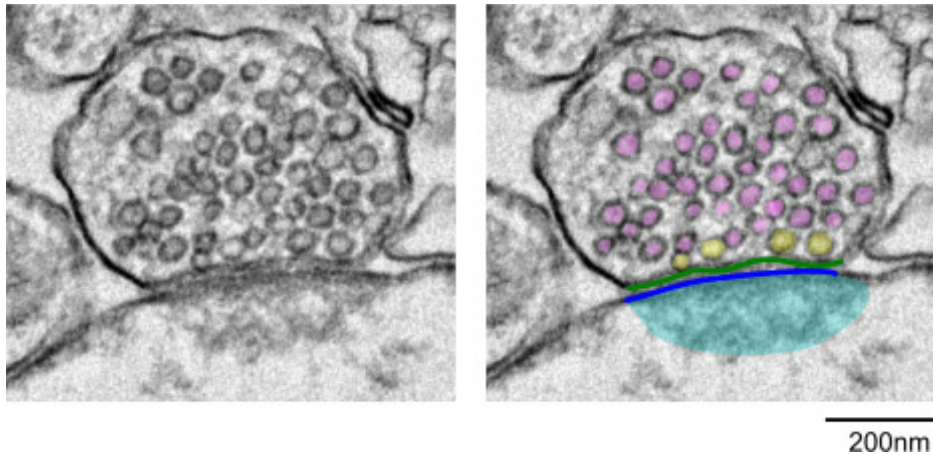


Figure 1.1 An example electron micrograph of a synapse

Sample synapse, shown unaltered (left) and with key features labelled (right): the postsynaptic density (cyan); the postsynaptic membrane (blue); the active zone (green); synaptic vesicles (pink); and docked synaptic vesicles (yellow).

1.3 Synaptic vesicle recycling

For neurotransmitter release in response to physiological stimulation to be sustained, it would require more vesicles than are present within the terminals. To create wholly new vesicles would require unsustainably large amounts of membrane to be created (Bittner and Kennedy, 1970). This suggested that there must be a mechanism for release which involved the conservation of membrane.

Heuser and Reese (1973) looked at this question using horseradish peroxidase (HRP). HRP placed into the extracellular environment, and as such encapsulated within any membrane endocytosed, was used to catalyse the oxidation of diaminobenzidine (DAB), leading to the presence of a dark, electron-dense product. Frog neuromuscular junction (NMJ) preparations were stimulated in the presence of HRP, fixed, stained with DAB, and then prepared for electron microscopy. Initially, HRP appeared within cisternae which, over time, were broken down into synaptic vesicles. If stimulated again prior to fixation, HRP was eliminated from many of the vesicles. This was clear evidence of a one-way recycling system for synaptic vesicles.

This system features two key steps, the connection of the vesicle to the external environment and the reclamation of membrane to form a new vesicle (Fig.1.2).

That this process occurs can be verified electrophysiologically, using a method first established by Neher et al. (1978) known as the 'patch clamp'. In this method, a recording electrode forms a tight seal, preferably with a very high resistance, such as a giga-ohm seal (Sigworth and Neher, 1980), against the cell membrane. There are a number of variations in how this clamp can then be used: either recording from this patch of membrane whilst it is attached to the cell (whole cell recording); or by removing it from the cell (inside-out or outside-out). Alternatively, the seal may be continuous with the cell membrane of the cell, and a recording made from the interior of the cell (whole cell attached patch clamp). (Cahalan and Neher, 1992)

Patch clamping allows for very high resolution recordings, able to record the properties of single ion channels. This method can be used to study the properties of individual synapses, albeit primarily larger ones such as ribbon synapses in retinal cells. It does this by taking time-resolved capacitance measurements of the cell. When a vesicle undergoes fusion, the cell membrane is extended, increasing its capacitance. When the vesicle is no longer continuous with the membrane, the capacitance decreases again (von Gersdorff and Matthews, 1999). Using this method, Stevens and Tsujimoto (1995) were able to gain information about the vesicle release kinetics at hippocampal synapses.

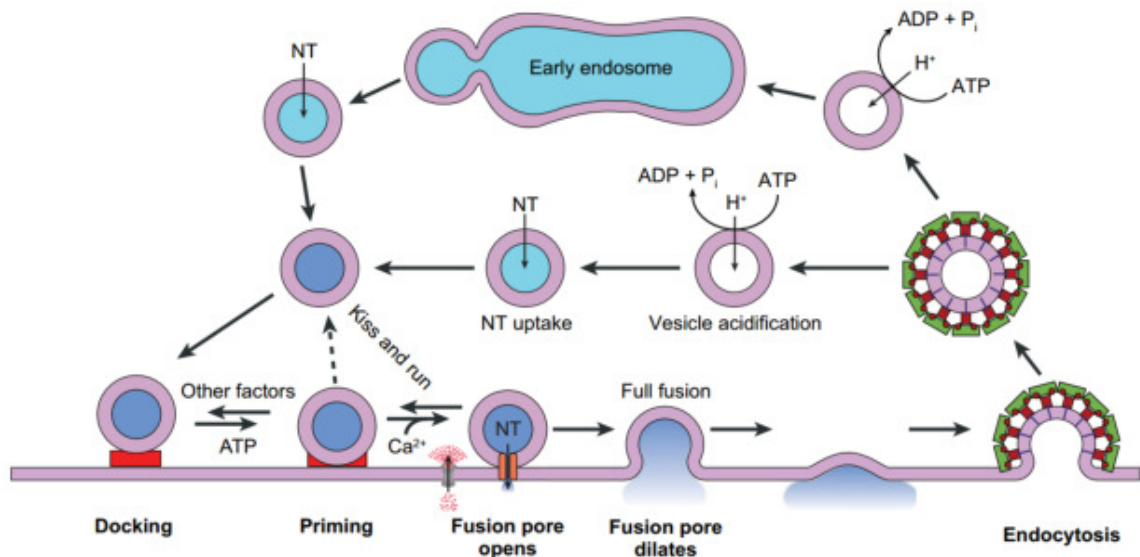


Figure 1.2 Summary of exocytosis and endocytosis in synapses

Synaptic vesicles are trafficked to docking sites, where they first dock, undergo a priming reaction, and then finally the fusion pore opens. The fusion vesicle then fully collapses into the external membrane, and is reclaimed at another location and trafficked back into the cell. This is the full collapse model of vesicle recycling. In 'kiss-and-run' recycling, the fusion pore closes again and the vesicle remains fully formed within the cell.

Figure taken from Chapman (2008).

1.3.1 Exocytosis

In order for the neurotransmitter to leave its packaging within a vesicle and make its way to receptors on the postsynaptic membrane, it must be released into the synaptic cleft. Synaptic vesicle exocytosis is a multi-step process, the key three steps being docking, priming, and fusion (Chapman, 2008, Sudhof and Scheller, 2001b) (Fig.1.2).

Bassoon and piccolo are large, fibrous proteins that guide vesicles down to the docking sites at the active zone. Bassoon in particular is critical for this purpose: without it, neurotransmission is fatally impaired (Sudhof, 2012).

The central component in exocytosis is the SNARE complex. This is formed of a vesicular membrane protein (synaptobrevin, or VAMP) and target membrane proteins (SNAP-25 and syntaxin 1). The SNARE complex provides specificity for docking, and acts as a scaffold for proteins involved in the subsequent exocytosis steps (Sollner et al., 1993). These three proteins are sometimes referred to as the 'core complex' (Sudhof and Scheller, 2001b).

The presence of a priming step was deduced by the presence of a rate-limiting step between docking and fusion. In this step, Rab3 indicates to RIM that there is a vesicle present, and then Munc13 is recruited to effect structural changes to prepare the vesicle release (Koushika et al., 2001). At this point, complexin can interact with the structure, rendering it ready for fusion to occur (Sudhof, 2013). Until the SNARE complex is formed, Munc18 prevents premature SNARE formation; but after the SNARE complex is formed and primed, Munc18 acts to promote fusion further (Chapman, 2008).

Fusion is triggered by the influx of calcium, through channels physically proximal to docking sites. The vesicular protein synaptotagmin has two calcium-sensing domains, which are responsible for triggering the final stage of exocytosis, wherein a fusion pore is opened and neurotransmitter released into the synaptic cleft (Chapman, 2008) (see Fig.1.3).

Following fusion, NSF (N-ethylmaleimide sensitive fusion protein) and α -SNAP (soluble NSF-attachment proteins) work together to disassociate the SNARE complex to prepare for further fusion events (Sudhof and Scheller, 2001b).

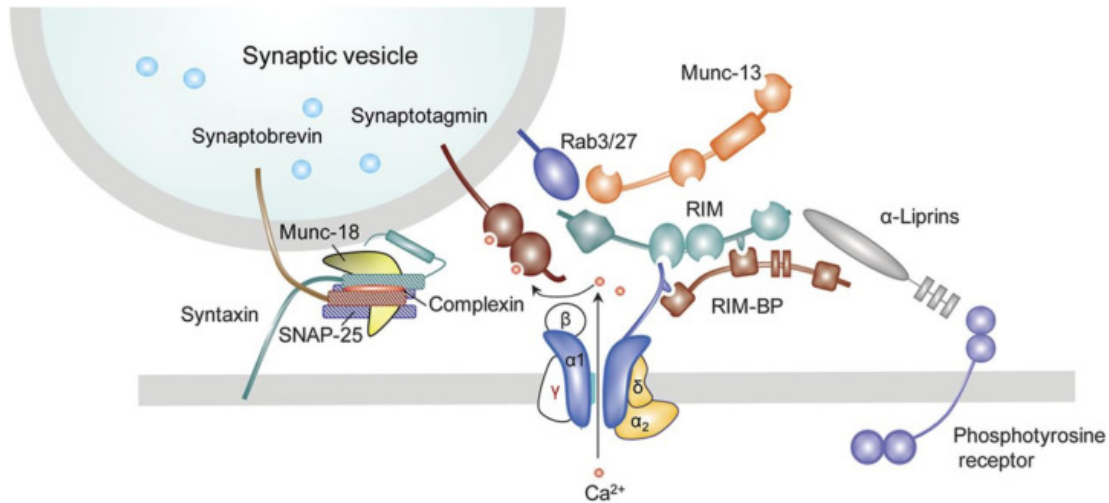


Figure 1.3 Proteins associated with synaptic vesicle exocytosis

The core SNARE complex of synaptobrevin, SNAP-25, and syntaxin has roles in docking the vesicle at the active zone. RIM and Munc13 prime the vesicle and render the vesicle ready for fusion. Complexin has a role in producing a ‘super primed’ state for vesicles. Synaptotagmin triggers fusion of the vesicle in response to calcium influx into the cell. Munc18 also facilitates fusion.

Figure adapted from Benarroch (2013)

1.3.2 Endocytosis

Depending on the type of stimulus being applied, there are several pathways taken by synaptic vesicles as they are reclaimed from the membrane (Cousin, 2014). One mechanism is termed ‘kiss-and-run’ recycling, in which synaptic vesicles do not collapse fully into the membrane upon fusion: the fusion pore instead closes and the vesicle returns to the cluster as it is. This allows for much more rapid turnover of vesicles at the active zone, taking ~1.4 s to complete (Aravanis et al., 2003). However, it remains controversial whether this mode of recycling takes place at hippocampal terminals, and if so, what role it plays in maintaining vesicle turnover. Kiss-and-run, unlike other forms of fusion, is not clathrin mediated (He and Wu, 2007).

Other forms of endocytosis occur at a much slower rate, and feature vesicles being reclaimed from the plasma membrane (Smith et al., 2008). This can occur in one of two ways, either through bulk endocytosis or through single vesicle endocytosis. In the former, this involves a large amount of membrane being taken up as an endosome, and

then vesicle budding occurs on reuptake (Clayton et al., 2008) (See Fig.1.2). This pathway for endocytosis is largely activated during the application of strong stimulation and is considered a slower route for vesicles to take (Evans and Cousin, 2007). By contrast, single vesicle endocytosis has a time scale of ~20-30 s (Saheki and De Camilli, 2012) and occurs at lower levels of stimulation. In hippocampal nerve terminals, unlike NMJ terminals, vesicles are not thought to traffic through endosomal intermediates, but instead are returned directly to the pool to allow for reuse (Murthy and Stevens, 1998).

This process is mediated by clathrin, a protein with a distinctive triskelion structure, which forms a cage around a portion of the membrane which is being internalised. This coat is visible under a TEM (see Fig.1.4) and is a distinctive sign that a vesicle has just undergone endocytosis, as the clathrin cage is dismantled by a protein known as Hsc70 (ATP-ase heat shock protein) (Popova et al., 2013).

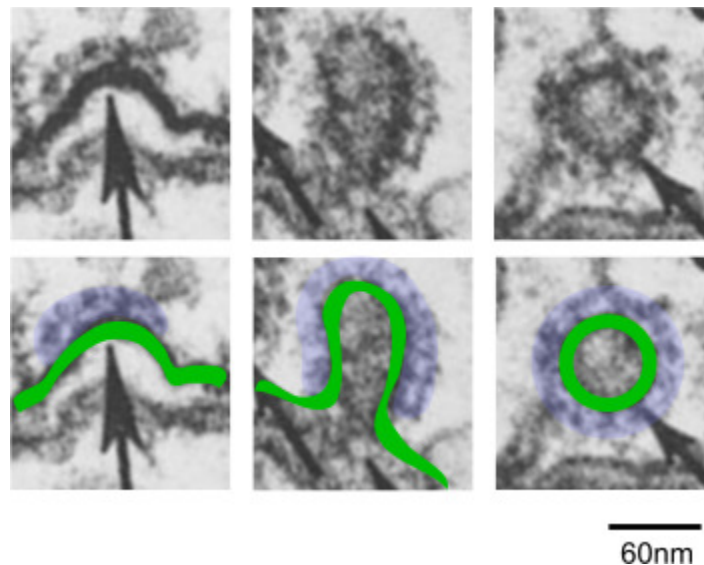


Figure 1.4 Clathrin-mediated endocytosis

This shows a clathrin-coated pit forming an invagination, before being internalised and detached from the plasma membrane. The plasma/vesicle membrane is indicated in green. The clathrin coat is highlighted in lilac.

Figure adapted from Heuser and Reese (1973).

The clathrin coat consists of an external layer formed by the clathrin triskelions, and an internal layer formed by adaptor proteins, chiefly AP-2 (Popova et al., 2013). The adaptor proteins are responsible for internalising the plasma membrane, and clathrin provides a stable cytoskeleton from which they can do this. The curve of the vesicle is provided by F-BAR, which provides a rounded shape within the vesicle as it is drawn into the cell (Suetsugu et al., 2010). Finally, when the membrane has been pulled into vesicle formation within the clathrin coat, the whole complex is cleaved from the plasma membrane by dynamin (Saheki and De Camilli, 2012) (Fig.1.5).

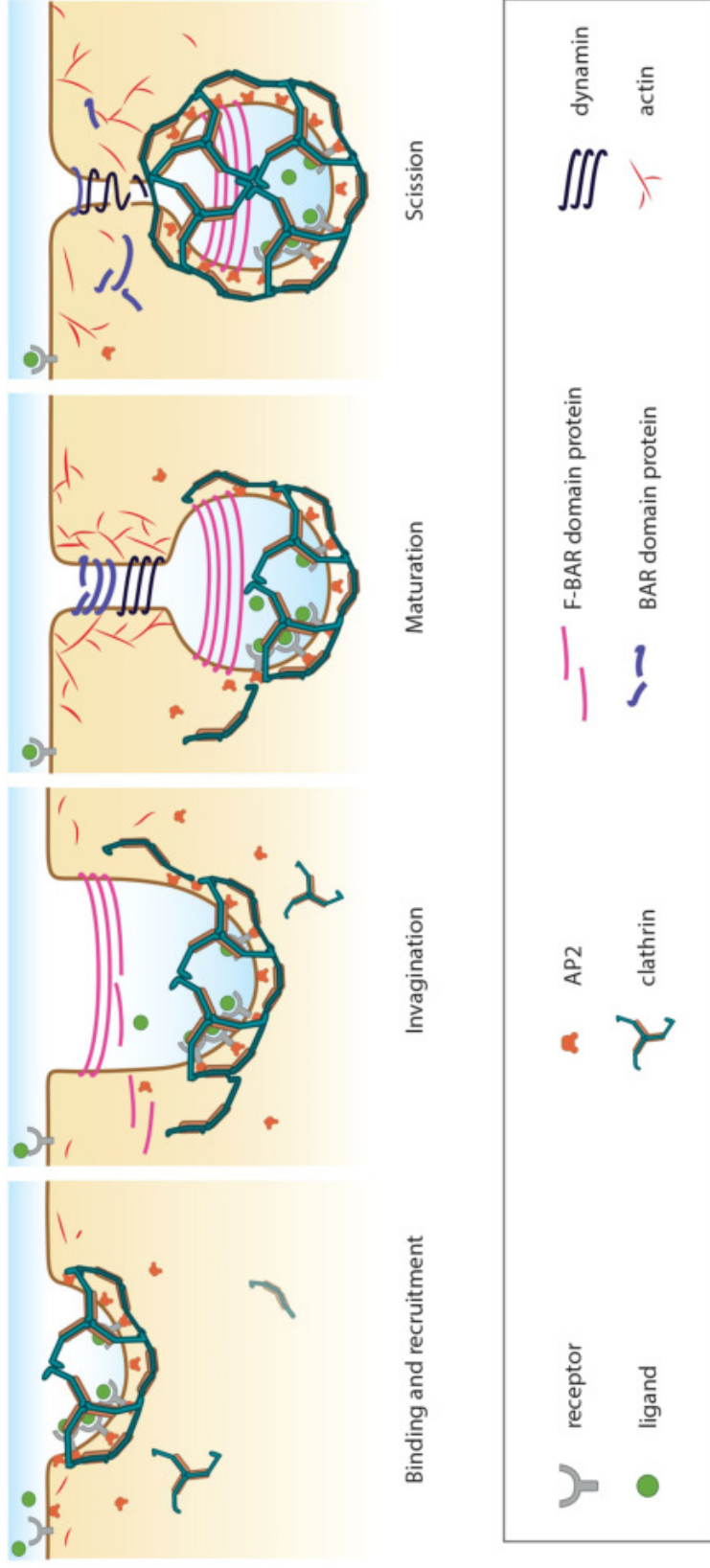


Figure 1.5 Proteins associated with endocytosis in synaptic terminals

A clathrin coat forms around the membrane to be internalised. AP2, an adaptor protein, attaches to the clathrin cage. AP2 is responsible for internalising the membrane. The curve of the vesicle is maintained by F-BAR proteins. When the vesicle is largely internalised, dynamin separates the vesicle from the membrane and it is fully internalised.

Figure adapted from MBInfo contributors, (2013).

The interior of the synaptic vesicle is more alkaline than the extracellular environment, at ~pH 5.5. Following fusion, this pH is raised following contact with the synaptic cleft, which has a pH of ~7.5. The pH is lowered again, as a V-type H⁺-ATP-ase produces an electron gradient as it fills the vesicle with neurotransmitter (Atluri and Ryan, 2006).

A recently discovered form of endocytosis, which occurs within 50 ms of the start of stimulation, and occurs over a period of ~300 ms, is known as 'ultrafast endocytosis'. It involves full collapse of vesicles, and uptake of large amounts of membrane from regions next to the active zone; this is therefore not a form of kiss-and-run, and does not appear to be clathrin-mediated (Watanabe et al., 2013).

A key question that remains unclear in synaptic neuroscience is the locations at which these modes of endocytosis occur. Kiss-and-run recycling must, by its nature, occur at the active zone, but there is some question as to whether clathrin-mediated endocytosis occurs at or near to the active zone, or at other locations within the cell. Certainly within the frog NMJ it has been shown that this occurs at sites away from the active zone, towards the side of the terminals (Betz and Bewick, 1992). There is some indication that recycling might also occur at or near the active zone (Ceccarelli et al., 1973).

Endocytosis and exocytosis are linked. This prevents the synaptic membrane from growing too large as membrane is added and not cleared. This phenomenon is thought to be linked to the elevated calcium levels in the terminal during the stimulation which causes exocytosis. Endocytosis is also a calcium-mediated process (Gundelfinger et al., 2003).

1.3.3 Calcium in synaptic vesicle recycling

Calcium has pivotal roles in both endocytosis and exocytosis within synaptic terminals. Voltage-gated calcium channels are responsible for transducing the changes in membrane potential which accompany the action potential into an influx of calcium ions into synaptic terminals (Meriney et al., 2014). These channels are located 30-300 nm away from vesicle docking sites. This variation in distance can have effects on the release probabilities of individual vesicles (Meinrenken et al., 2002). Voltage-gated calcium channels are kept in close proximity to synaptic vesicle docking sites by the transmembrane protein synaptotagmin (McNeil and Wu, 2009).

Structural analysis of the synaptotagmin revealed it to contain two copies of a domain homologous to those known to be responsible for calcium binding to membranes in

other proteins, such as protein kinase C and phospholipase A. These are known as the C2 domains, and they were shown to bind to calcium in the presence of phospholipids (Brose et al., 1992). C2A and C2B, with the former being more proximal to the vesicle, are essential for synchronous release of neurotransmitter. They each have a negatively charged pocket, which is neutralised by the presence of Ca^{2+} ions, and consequently allows synaptotagmin to interact with the negatively charged phospholipids in the plasma membrane and the proteins in the SNARE complex (Striegel et al., 2012).

Calcium also plays a vital role in endocytosis. This was first demonstrated by Ceccarelli and Hurlbut (1980) by using latrotoxin to deplete synaptic vesicles in a calcium-independent manner, in a calcium-free extracellular solution. This led to a depletion of synaptic vesicles and an accumulation of membrane, which was not seen when this protocol was carried out in solutions containing calcium. Calcium is required for the formation of the clathrin-coated pits which are essential for single-vesicle endocytosis after full fusion collapse (Gad et al., 1998), but it is also required for activity-dependent bulk endocytosis (Cheung and Cousin, 2013).

Calcium's involvement in endocytosis is through reaction with the Ca^{2+} /Calmodulin dependent phosphatase, Calcineurin. Calcineurin phosphorylates a group of proteins which are essential for endocytosis to occur (Cousin and Robinson, 2001), called the desophorins. One such protein is dynamin1, a protein which has a role in synaptic vesicle fission in endocytosis. The reaction of calcineurin-dynamin1 complex is thought to act as a calcium sensor for many of the other reactions which occur during endocytosis (Lai et al., 1999).

1.4 Synaptic vesicle pools in hippocampal terminals

Synaptic vesicles are divided into subgroups known as 'pools'. These pools are functionally defined, and as such represent important concepts in how synaptic vesicles behave, and also have important functional implications. There are many pools, including the recycling pool, the spontaneous pool, the resting pool, the reserve pool, the superpool, and the readily releasable pool (Denker and Rizzoli, 2010) (Fig.1.6).

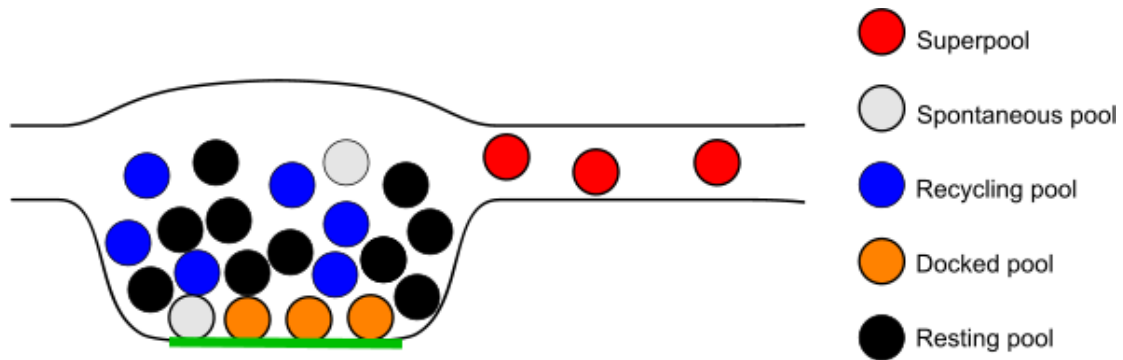


Figure 1.6 Synaptic vesicle pools in hippocampal neurons

The active zone is indicated in green, as a site where the docked pool (orange) is situated, ready to be primed and accessed as the readily releasable pool (RRP), and where spontaneous transmission also occurs (grey). Within the terminals, there are a subset of vesicles which are able to undergo recycling, and those which cannot be recruited; these are the recycling pool (blue) and the resting pool (black) respectively. There also exists a population of synaptic vesicles at extrasynaptic locations; these are the superpool (red).

1.4.1 The spontaneous pool

The spontaneous release can be seen in evidence in the to the miniature endplate potentials seen by Fatt and Katz (1952). It is thought to have a role in synaptic plasticity, and in regulating postsynaptic protein synthesis (Autry et al., 2011). There is some evidence that the spontaneous pool might be drawn from the resting pool (Fredj and Burrone, 2009, Hua et al., 2010, Sara et al., 2005), but this claim remains controversial (Hua et al., 2010).

1.4.2 The recycling pool and resting pool

The total pool consists of all vesicles within a synapse. The total recycling pool (TRP) comprises all vesicles that can be stimulated to undergo recycling. The resting pool comprises those vesicles which cannot be stimulated to undergo recycling. Estimates of the TRP vary widely depending on the protocol used, from as high as 100% (Rose et al., 2013, Ikeda and Bekkers, 2009), to ~50% (Fernandez-Alfonso and Ryan, 2008, Fredj and Burrone, 2009, Kim and Ryan, 2010, Darcy et al., 2006a) or 15-20% (Harata et al., 2001, Marra et al., 2012), with the remaining fraction presumed to be the resting pool. In all these measurements there is a huge degree of heterogeneity, providing

clear evidence that the recycling fraction is highly variable between synapses, even within a neuron.

Though the exact reasons for the presence of non-recycling vesicles, and what causes a vesicle to be consigned to this pool, are unclear, there is ample evidence that vesicles can be moved between pools. The inhibition of cyclin-dependent kinase 5 (CDK5), an important molecule in neuronal development, can increase the recycling pool fraction (Kim and Ryan, 2010, Marra et al., 2012). Altering the release properties of a terminal through a plasticity protocol to induce potentiation has also been shown to increase the recycling pool fraction (Ratnayaka et al., 2011). α -Synuclein inhibits the size of the recycling pool; there have been some suggestions that its tendency to reduce the levels of other proteins present within the cell may be the cause of this (Scott and Roy, 2012). Changes in temperature also have an effect on the size of this pool (Micheva and Smith, 2005). The adjustable nature of the recycling fraction of the total pool of vesicles points to its being a potential mechanism for regulating synaptic output (Branco et al., 2010).

The recycling pool is composed of the readily releasable vesicles, which are the first to undergo fusion on stimulation, and the reserve pool, the vesicles that begin to undergo recycling when the readily releasable pool has been exhausted (Denker and Rizzoli, 2010).

1.4.3 The readily releasable pool

A subset of the recycling vesicles are able to respond to stimulus within 0.1 ms (Sabatini and Regehr, 1999) and are released at a higher rate than subsequent vesicles. These were first identified via paired pulse experiments, in which small stimuli were applied to a cell and the response from the terminals recorded. It was found that there was a depression in the size of the response for up to 10 s following the stimulation (Stevens and Tsujimoto, 1995). This demonstrated that there was a pool of vesicles which is able to undergo release rapidly and, when this pool is exhausted, the terminal has an impaired ability to generate a response. It is therefore unsurprising that this pool, known as the readily releasable pool (RRP), is strongly correlated with the release probability of the terminals (Murthy et al., 2001, Murthy et al., 1997, Dobrunz, 2002).

The RRP can be released either by electric stimulation, or through the use of hyperosmotic sucrose (Rosenmund and Stevens, 1996). Hyperosmotic sucrose releases a higher number of vesicles than electrical stimulation, suggesting both that these vesicles are released by a non-physiological route in the presence of hyperosmotic sucrose, and that this may be caused by their proximity to the plasma membrane (Moulder and Mennerick, 2006).

There is further evidence to suggest that RRP vesicles may have preferential positioning around the active zone, and are primed and ready for release. The RRP consists of 10-12 recycling vesicles. This figure is remarkably similar to estimates of the docked pool (Schikorski and Stevens, 2001). Taken in combination, it seems likely that RRP vesicles are primed for release, but that not all vesicles at the active zone are RRP vesicles.

1.4.4 The superpool

Synapses are not isolated units: they are an outpost of transmission machinery, connected to the rest of the cell through axonal or dendritic processes. As mentioned previously, large dense core vesicles must be trafficked to release sites through the axon (De Camilli et al., 2001), as must presynaptic transport vesicles, containing membrane proteins such as bassoon and piccolo, syntaxin, and SNAP-25 (Shapira et al., 2003). Small electron lucent vesicles have also been found in these processes. Synaptic vesicles move between synapses and form a 'superpool' (Staras et al., 2010).

FM dye-labelled vesicles (see section 1.6.2.2) can be observed moving between terminals in cultured neurons, meaning that recycling vesicles leave the terminal after reuptake and travel through the processes (Krueger et al., 2003). By illuminating single terminals with a confocal microscope, the FM dye fluorescence can be eliminated through photobleaching. Over the course of ~20 min, FM dye-labelled vesicles move from neighbouring terminals and appear at the site of the terminal which has just had its fluorescence removed. This process, called 'fluorescence recovery after photobleaching' (FRAP), demonstrates that recycling vesicles move between terminals, and join the cluster within those terminals. When stimulated, the fluorescence which was recovered in the photobleached terminal is eliminated, showing that mobile vesicles are still capable of undergoing recycling, and that they join the recycling pool in their 'new' host terminal (Darcy et al., 2006a).

Around 4% of the total pool of each synapse can leave the terminal and move into the processes (Staras et al., 2010). This pool is newer than the others described, so less is known about the factors affecting this pool; however, in synapsin triple knock-out mice, there were increased numbers of vesicles in the synaptic processes. Inhibition of Cdk5 with roscovitine also increased the mobility of synaptic vesicles and the rate of FRAP (Orenbuch et al., 2012). Brain-derived neurotrophic factor (BDNF) has also been shown to reduce synaptic vesicle clustering and to lead to an increase in the number of vesicles leaving terminals (Staras and Branco, 2010). Intriguingly, α -Synuclein has an inhibitory effect on the transport of synaptic vesicles between terminals, implicating its possible modulation as a mechanism underlying disease states (Scott and Roy, 2012). Important recent work has demonstrated that the superpool is also a feature of axonal processes *in vivo* (Herzog et al., 2011).

1.5 Long-term plasticity in the hippocampus

The central principle of plasticity within the brain is that connections are created, strengthened, weakened, or eliminated in a functionally-dependent manner. The ability of neurons to do this was speculated from as early as the 1870s (Cooper, 2005). Even as the early neuroscientists attempted to determine whether nerve cells were discrete entities or continuous with one another, they also turned themselves to the question of how vital behavioural processes, such as learning and memory, can be produced by alterations in the properties of these cells.

In 1890, William James coined the term 'plasticity' to describe the ability of the brain to respond to activity within itself to "deepen old paths and create new ones" (James, 1890). Sherrington, though coining the term and concepts of the synapse, compared neuronal plasticity to the pliability of animals which had their synapses removed, and did not associate this with synaptic changes. At this point, the generally accepted theory was that neuronal resistance controlled the 'flow' of neuronal impulses, with activity decreasing resistance (Cooper, 2005). The first scientist to postulate that plasticity was regulated at a synaptic level was Eugenio Taniz, who suggested that repeated use of a pathway would decrease the distance which signal had to cross at the synaptic cleft (Berlucchi and Buchtel, 2009).

In 1949, Hebb published 'The Organisation of Behaviour'. Before the identification of the ionic activity which occurs within axons during action potential, conclusive proof that

neurons were not continuous with one another (De Robertis and Bennett, 1954, De Robertis and Bennett, 1955, Palay and Palade, 1955), and the first clues as to how neurotransmitter might be released from synapses (Fatt and Katz, 1952), this book provided ideas which were to revolutionise the way in which neuroscience approached the connections between neurons.

One of the key ideas in Hebb's work was that synchronous firing of neurons would lead to a strengthening of specific neurons. According to Hebb, "when an axon of cell A is near enough to excite a cell B and repeatedly or persistently takes part in firing it, some growth process or metabolic change takes place in one or both cells such that A's efficiency as one of the cells firing B, is increased" (Hebb, 1949). This is commonly referred to as Hebb's postulate and summarised as 'cells which fire together, wire together'.

The idea of activity-dependent alterations of synaptic strength is a key one in our ideas of learning and memory. Long-term potentiation and depression are thought to be models of learning and memory precisely because they fit the criteria predicted by Hebb, of a method of strengthening neuronal connections. Experiments in *Aplysia* were the first to demonstrate that this theory is the case, showing that synaptic changes lasting for days, and mirroring the time course of the memory process, occurred accompanying various training protocols (Kandel, 1976).

1.5.1 Long-term potentiation in hippocampal synapses

Long-term potentiation (LTP) is an enhancement of synaptic strength that follows the application of a brief tetanic stimulus and lasts several hours (as long as 48 h has been recorded). Discovered by Bliss and Lomo in 1973 (Bliss and Lomo, 1973), this phenomenon produces synapse-specific changes to the response to stimuli (Bliss and Collingridge, 1993, Malenka and Siegelbaum, 2001). This makes it a particularly interesting field for study, as the way in which synapses alter themselves to provide these changes in function has huge relevance for brain function, organism behaviour, and disease.

A major discussion point in studies on LTP is the extent to which presynaptic and postsynaptic changes are responsible for LTP expression. There is evidence for the involvement of a variety of factors at both loci.

1.5.1.1 Postsynaptic factors in LTP

Induction of LTP is generally accepted to have a postsynaptic mechanism. A transient calcium influx through calcium-permeable NMDA receptors leads to a calmodulin-dependent protein kinase II (CaMKII) activation, which in turn phosphorylates AMPA receptors containing GluR1 subunits in order to increase their permeability and produce potentiation (Lisman et al., 2012). There is also evidence that new AMPA receptors are inserted into the postsynaptic membrane following LTP induction. These can lead to synapses which were previously silent becoming active, as these new AMPA receptors can respond to glutamate release (MacDougall and Fine, 2014).

1.5.1.2 Presynaptic factors in LTP

Though these aspects alone could be a sufficient mechanism for the induction of LTP, there is significant evidence of a presynaptic involvement. It has been shown that new active zone proteins are trafficked in following LTD, and that the active zone is expanded (Bell et al., 2014). LTP induction also promotes synaptogenesis and increases the total number of vesicles present at synapses (Bourne et al., 2013). A form of potentiation in cultured neurons has been demonstrated specifically to increase the recycling fraction within terminals (Ratnayaka et al., 2012). It has been hypothesised that one possible function of the superpool (see section 1.4.4) might be to act as a substrate for the activity-driven recruitment of new vesicles to synaptic terminals to support forms of plasticity (Staras, 2007).

These changes in vesicle arrangement and properties also have implications for the function of presynaptic terminals. Inducing LTP causes an increase in release probability, showing increased reliability of response to stimulation (Lisman et al., 2012), commensurate with an increase in the number of vesicles docked at active zones (Bourne et al., 2013). In addition to this, LTP synapses have faster FM dye release properties (Zakharenko et al., 2003), thought to be due to the fusion of many vesicles simultaneously.

1.5.2 Long-term depression in hippocampal synapses

Long-term depression (LTD), the functional opposite of LTP, is a decrease in synaptic strength following sustained low-level stimulation (Dudek and Bear, 1992). It can be induced in synapses which have already undergone LTP, and in naïve synapses (Bear and Linden, 2001). Though LTD is an important concept in neuroscience, providing the

bidirectionality required for Hebbian learning, it is less well understood than its counterpart (Bear and Linden, 2001).

It has been claimed that LTD may act as a mechanism for forgetting (Bear and Linden, 2001), but this appears to be a rather large oversimplification as behavioural studies have shown that several forms of learning rely on LTD alone. In *in vivo* studies of cerebellar LTD, the abilities of mice to learn a motor control task was inhibited in mGluR1/5 knock-out mice (Aiba et al., 1994, Kashiwabuchi et al., 1995). Induction of hippocampal LTD in freely-behaving rats demonstrated that LTD has roles in object recognition and learning subtle spatial clues, such as the location of an object in a room (Goh and Manahan-Vaughan, 2013b, Goh and Manahan-Vaughan, 2013a). LTD is therefore clearly important in learning in its own right.

Like LTP, LTD has both presynaptic and postsynaptic components, but the relative roles of each of these is still being established (Malenka and Bear, 2004). Among the many possible substrates, recycling properties of vesicles represent likely targets and evidence hints at their possible involvement in LTD-related modulation of synaptic strength (Stanton et al., 2003, Zakharenko et al., 2001).

1.5.2.1 Postsynaptic factors in LTD

Because LTD induction requires lower frequency stimulation than that needed to induce LTP, many of the changes in synaptic weight are thought to be related to the intracellular calcium level. In Schaffer collateral CA1 synapses, calcium enters the cell either through Group 1 metabotropic G protein coupled receptors (mGluRs) or NMDA receptors (Upreti et al., 2013, Mulkey and Malenka, 1992). NMDA receptors require both the presence of glutamate and the activation of voltage dependent Mg^{+} channels to allow calcium influx into the cell, which makes them a particularly valuable tool for study, as they therefore act as detectors of synchronicity in presynaptic transmitter release and postsynaptic activation (Poschel and Stanton, 2007). Group 1 metabotropic glutamate receptors (mGluR1 and mGluR5) exist primarily at the edges of the postsynaptic density (De Blasi et al., 2001). In response to glutamate release, these receptors work through secondary messengers to trigger calcium release from the intracellular calcium stores (Bolshakov and Siegelbaum, 1994) (see section 1.5.4). The activation of mGluR1 receptors is particularly crucial for LTD induction (Neyman and Manahan-Vaughan, 2008, Zakharenko et al., 2002).

CaMKII activation is higher in LTP synapses (Pettit et al., 1994), and CaMKII inhibition can cause LTD in synapses (Lisman et al., 2012). At lower calcium levels, CaMKII is dephosphorylated, and consequently deactivated, instead (Lisman, 1989, Michalski, 2013). PP1 and PP2A are protein phosphatases which are very sensitive to calcium and are consequently activated at low concentrations of calcium (Mulkey et al., 1993).

Inhibition of these phosphatases has been shown to block LTD induction in the hippocampus (Mulkey et al., 1993, Mulkey et al., 1994), confirming that they are targets for LTD. An important inhibitor for PP1 and PP2A, Inhibitor-1, is also calcium dependent, being activated by Ca^{2+} and deactivated by cAMP (Ingebritsen and Cohen, 1983). The regulation by cAMP of this inhibitor adds another layer of calcium dependency, as adenylate cyclase synthesis of cAMP is calcium dependent, but is also inhibited at high calcium levels (Lisman, 1989, Standaert and Dretchen, 1979).

A key feature in the expression of LTD is the internalisation of AMPA receptors. This process is also highly dependent on calcium influx into the cell. This process is triggered by calcium influx through NMDA receptors (Beattie et al., 2000), which in turn, activates calcineurin (a calcium/calmodulin dependent protein). Calcineurin then deactivates PP1 inhibitors (Mulkey et al., 1994), allowing PP1 to phosphorylate AMPA receptors, causing a reduction in function (Lee et al., 1998), and eventually triggering AMPA receptor internalisation (Mulkey et al., 1994, Ehlers, 2000).

Mulkey and Malenka (1992) found that LTD may be dependent on calcium influx through postsynaptic NMDA receptors. This calcium influx is detected by Calcium/Calmodulin dependent protein kinase II (CaMKII), which is thought to begin the biochemical cascade which can potentiate synapses through a variety of mechanisms. CaMKII inhibition can cause LTD in synapses (Lisman et al., 2012). LTD induction is also thought to depend on both internal calcium release and activation of metabolic glutamate receptors (mGluRs) (Bolshakov and Siegelbaum, 1994), further indicated by studies showing that the inhibition of mGluR receptors can inhibit LTD (Zakharenko et al., 2001).

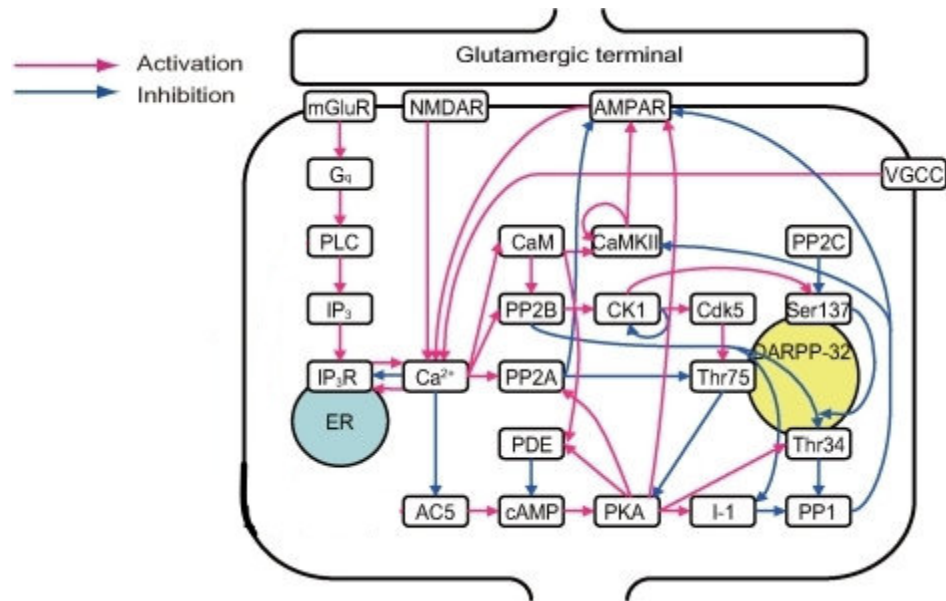


Figure 1.7 Postsynaptic pathways in LTD induction

Intracellular calcium levels are raised through calcium influx through NMDA receptors, VGCCs and G-protein-mediated release from internal calcium stores. Consequently protein phosphatases are upregulated (PP2A/B) or uninhibited (PP1), which inhibit the actions of CaMKII and trigger AMPA receptor internalisation.

Figure adapted from Nakano et al. (2010).

1.5.2.2 Presynaptic factors in LTD

Very little work has been done on presynaptic factors of long-term depression, but there are a few indications that, whereas induction may be chiefly presynaptic, expression of LTD does have a postsynaptic component (mechanisms summarised in Fig.1.8).

Two studies (Stanton et al., 2003, Zakharenko et al., 2001) which focused on FM dye labelling of hippocampal terminals in hippocampal slices showed that LTD causes a decrease in the number of labelled terminals. The decrease in the fluorescence levels of terminals labelled in slices suggests that there are fewer vesicles being labelled, and that LTD causes a decrease in the rate of FM dye release from terminals on stimulation.

These changes in FM dye release properties point to there being an effect on vesicle release to alter presynaptic transmitter release properties. Metabotropic glutamate receptors are thought to play a role here too. Group 2 mGluRs (mGluR2/3) are found presynaptically, and their activation is critically important for LTD induction (Mukherjee and Manahan-Vaughan, 2013). The two G-protein secondary messengers $G_{i/o}$ and $G_{\beta\gamma}$

both affect the properties within the terminal. $G_{i/o}$ inhibits the synthesis of cAMP and $G_{\beta\gamma}$ inhibits the activation of VDCCs, K^+ channels, and also inhibits cAMP levels (Atwood et al., 2014).

Aside from the effects on the influx of calcium as a means of controlling neurotransmitter release, mGluR2/3 activation also works on synaptic vesicle machinery to disrupt transmission (Upreti et al., 2013). $G_{\beta\gamma}$ competes with synaptotagmin1 at the C-terminus binding site of SNARE protein, SNAP25. This acts directly to inhibit vesicle release.

An additional mechanism of action is that the rise in intracellular calcium levels leads to higher levels of calcineurin. Calcineurin dephosphorylates Synapsin1, locking vesicles tight to the cytoarchitecture and preventing them from moving towards the active zone to refill the RRP (Bykhouvskaia, 2011, Hilfiker et al., 1999).

Interestingly, Stanton et al. (2003) found that this decrease in rate only affected RRP vesicles, with the rate of release of reserve pool vesicles being unaffected, suggesting that the effects on release and the active zone are much greater than the effects on the dynamics of the rest of the synaptic vesicle pools.

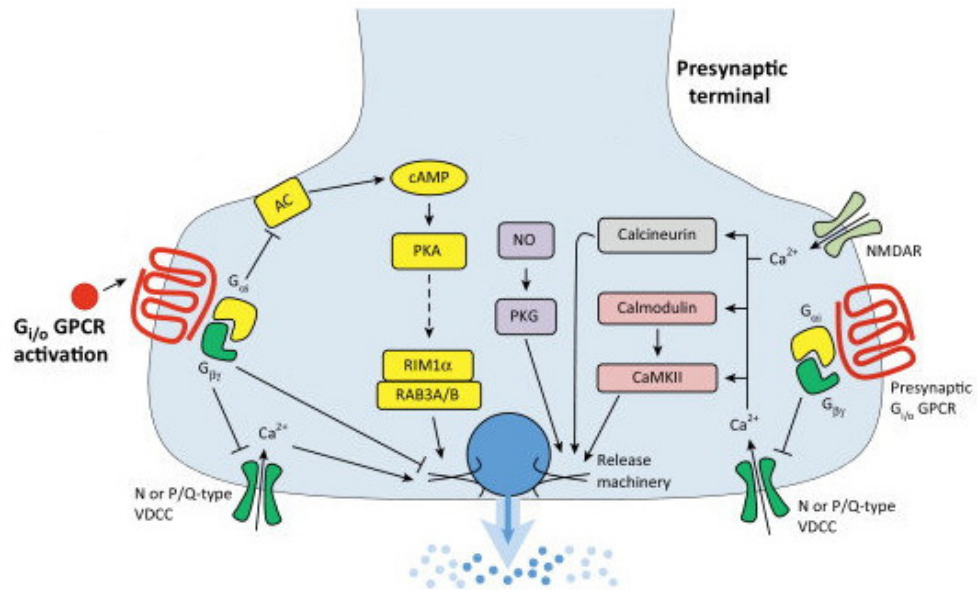


Figure 1.8 Summary of factors affecting presynaptic expression of LTD

Rises in presynaptic calcium levels, either through GPCR activation (mGluR2/3) or through activation of VDCCs and NMDA receptors, leads to deactivation of calcium receptors and phosphorylation of the vesicle release.

Figure adapted from Atwood et al. (2014).

1.5.3 Linking pre- and postsynaptic plasticity

Both the pre- and postsynaptic terminals show altered properties following exposure to plasticity protocols. In many cases, this is due to postsynaptic induction of LTP or LTD (Misner and Sullivan, 1999) leading to presynaptic expression through the medium of some chemical messenger (Bolshakov and Siegelbaum, 1994, Bliss and Collingridge, 1993). The most likely candidates for these retrograde messengers are nitrogen oxide (NO), brain derived neurotrophic factor (BDNF), and arachidonic acid, which has been shown to act on presynaptic receptors (Suvarna et al., 2015).

Arachidonic acid is a fatty acid found in high levels in the brain, which has been shown to facilitate LTD induction; blocking it prevents LTD induction (Bolshakov and Siegelbaum, 1995). It is used in the synthesis of anandamide, which activates cannabinoid type 1 receptors to induce LTD (Khlaifia et al., 2013) and impair LTP by inhibiting the amount of neurotransmitter released (Misner and Sullivan, 1999).

BDNF is a growth factor found in the brain. BDNF secretion can occur as a response to intracellular calcium levels being raised (Lanore et al., 2009), particularly to high levels like those seen in response to high frequency stimulation (Kohara et al., 2001, Kojima et al., 2001, Gartner and Staiger, 2002). High frequency stimulation has also been shown to trigger BDNF release (Hartmann et al., 2001). Postsynaptic BDNF release can cause presynaptic potentiation in a calcium dependent manner (Magby et al., 2006). Presynaptic terminals show rapid changes in function, with a time course of several minutes (Lessmann, 1998, Lu and Gottschalk, 2000).

Nitric oxide is a small molecule which can be released postsynaptically in response to changes in calcium levels (Poschel and Stanton, 2007). The receptor for NO, soluble guanylyl cyclase (GC) has been found to exist primarily in presynaptic locations (Garthwaite, 2010), and the molecule itself has been found to act on synaptic vesicle machinery targets such as the t-SNARE proteins, Munc-13 and SNAP25. NO appears to have a facilitatory effect on vesicle release, and has certainly been implicated in LTP (Hardingham et al., 2013) and LTD induction (Tamagnini et al., 2013).

1.5.4 Calcium stores and long-term plasticity

The induction of LTP is thought to require a large increase in postsynaptic calcium levels. The influx of Ca^{2+} into the cell through the NMDA receptors starts a cascade of pathways which cause potentiation of the synaptic response (Linden, 1994). Clearly, postsynaptic calcium plays a role in LTD induction, but a mechanism is required to transform transient calcium currents into long-term changes in cellular behaviour.

Intracellular calcium levels are 3-4 orders lower than those in the extracellular environment, but there are organelles within the terminals which have calcium levels similar to the extracellular environment (Korkotian and Segal, 1996); these are known as calcium stores. Mitochondria act as calcium stores, supporting metabolism and cell survival (Rizzuto et al., 2012), and the calcium stores within the spine apparatus, an extension of the endoplasmic reticulum (Spacek and Harris, 1997), support changes in calcium level during activity (Fifkova et al., 1983). Intracellular calcium stores can regulate synaptic plasticity and are involved in memory formation. Calcium can be released from these calcium stores by activation of IP3R1 and ryanodine receptors (Fujino et al., 1995). Ryanodine receptors promote long-term memory foundation and consolidation and IP3R activation is required for long-term memory (Baker et al., 2013).

IP3 and Ryanodine receptors have been implicated in the mediation of short-term plasticity (Silveira et al., 2015). Another player in the induction of short-term plasticity is protein kinase C which acts as a calcium sensor, phosphorylating downstream targets to produce post-tetanic potentiation, a form of short-term plasticity (Fioravante et al., 2014).

The postsynaptic requirement for calcium within the synapse is better understood than the involvement of presynaptic calcium in long-term plasticity. Mossy-fibre LTD certainly requires increases of presynaptic extracellular calcium to trigger downstream events which will lead to long-term plasticity (Castillo et al., 1994), mediated by protein kinases A and C (Kobayashi et al., 1999).

1.6 Methods of studying synaptic terminals

1.6.1 Electrophysiological measurement of synaptic properties

Electrophysiological recordings were central to the formation of the vesicle hypothesis. However, the results that made this discovery possible relied on recording the postsynaptic response rather than any direct properties of the presynaptic neuron, let alone the presynaptic terminal (Fatt and Katz, 1952). Today, this continues to be a limitation of electrophysiological studies of synapses: it is far easier to record the postsynaptic response to neurotransmitter release than to measure any of the presynaptic factors of it.

However, presynaptic recordings are possible. Capacitance recordings give valuable information on vesicle fusion and endocytosis, as the amount of external membrane rises and falls with exo- and endocytosis. However, these recordings are primarily done as whole cell recordings (Matthews, 1996). Individual terminals can be measured, but this is difficult and as such is not widely done, and relies heavily on a preparation which allows access to terminals, such as the NMJ or calyx of Held, which many do not (Lim et al., 1990).

1.6.2 Imaging synapses

Though electrophysiology can provide information about release and reuptake properties, it offers nothing about the spatial properties in nanoscale. For this, electron microscopy must be used.

The small size of synaptic vesicles means that, even when correctly stained, they are not visible using conventional light microscopy; however, under electron microscopy, they are easily distinguishable. Early studies involved simply imaging samples of fixed tissue to identify organelles and structures within the synapse (Palay and Palade, 1955, De Robertis and Bennett, 1955) (these findings are discussed in section 1.2.2). Later, HRP labelling of vesicles and oxidation of DAB provided a way of identifying vesicles via a functional property, namely recycling. Reese and Heuser demonstrated that vesicles were formed from the external synaptic membrane, and that the fraction of recycling vesicles is dependent on the strength of the loading stimulus. They also showed that recycled vesicles were not segregated from the rest of the vesicle population (Heuser and Reese, 1973).

1.6.2.1 Fluorescent probes for studying synaptic function

Though conventional light microscopy does not have the spatial resolution to identify individual vesicles, the properties of recycling pools can be studied using fluorescent probes.

Many of these probes must be genetically encoded, either through the development of mutant mice or through transfection into tissue cultures or organotypic cultures. A key category of genetically-encoded functional probes is the synaptopHluorins. These are pH-sensitive probes which fluoresce brightly at ~pH 7.5, but show reduced fluorescence at more alkaline pHs, e.g. ~pH 5.5 (Miesenbock et al., 1998). This is particularly important for synaptic research, for when these are tagged on to luminal synaptic proteins, the gradual decay of fluorescence as vesicles undergo reacidification gives important information on the timescales of endocytosis and reintegration into the vesicle pool (Granseth and Lagnado, 2008).

Other genetically-encoded optical probes are emerging, to give readouts of the temporal aspects of various other processes within the cell, such as glutamate release (e.g. GluSnFR, Hires et al. (2008)), or calcium influx (e.g. syGCaMP5, Akerboom et al. (2012)). Genetically encoded probes have advantages, in that they are likely to occur consistently throughout labelled neurons, but they also have disadvantages, such as long preparation times. In addition, there is not yet any certainty as to the effects of changing the genetic properties of the neuron.

1.6.2.2 FM 1-43 and the FM dyes

FM dyes, named after their creator Fei Mao, are adapted styryl dyes (Betz and Bewick, 1992). Their properties make them uniquely suited for studying synaptic vesicle recycling. FM dyes are amphiphilic, with a lipophilic tail that controls the extent to which the FM dye sticks to the membrane (e.g. this tail is shorter in FM 2-10, which has a lower affinity for plasma membranes, compared to FM 1-43), and a positively charged 'head' group, which prevents FM dyes from passing through the membrane. These are joined by a double bond bridge, which controls the fluorescence properties of the dye (Brumback et al., 2004) (Fig.1.6.A).

Because of their lipophilic properties, FM dyes bind to the presynaptic plasma membrane. When embedded in membrane, the fluorescence of FM dyes increase ~14-fold. When the synapse undergoes endocytosis, the FM dye remains embedded in the membrane, and so is trapped in the lumen of the synaptic vesicle. The external FM dye can be removed through washing, leaving behind only that fluorescent dye that is trapped inside the vesicles. A vesicle containing FM dye must have undergone recycling whilst the FM dye was present. If these vesicles undergo fusion again, the dye undergoes lateral diffusion and efficiently departs from the membrane, leading to fluorescence loss (Betz et al., 1992b) (Fig.1.6.B).

FM 1-43 has an insertion kinetic of 18 ± 5 nM/s, and dissociates with a tau of 8.0 ± 0.6 ms (Wu et al., 2009). Experimentally, Ryan et al. (1993) showed a τ_{off} of ~10 s, but this value was reached by recording the rate of surface dye elimination from neuronal cultures using a chamber perfusion system. The refill rate of the imaging chamber (~2 s in this case) likely contributed to this slow unbinding value. In full collapse fusion, the vesicle remains continuous with the plasma membrane for ~60 s (Klingauf et al., 1998), which should be sufficient to allow FM 1-43 to depart from the membrane. All FM dye destain experiments were recorded with sustained activity for 120 s, which should have allowed all recycling vesicles to be able to release any FM dye contained within them.

In addition to providing assays of function, fixable analogues of FM dyes can also be used to label recycling vesicles at an ultrastructural level (Betz and Bewick, 1992, Harata et al., 2001). DAB is typically oxidised in a reaction catalysed by horseradish peroxidase; however, this reaction can also be mediated by the photons given off when a fluorescent probe is stimulated, and FM dye is a suitable probe for this (Sandell and

Masland, 1988). Though in many ways similar to the labelling with HRP demonstrated in Heuser and Reese (1973), the fact that FM dyes are smaller and more diffusible with a high affinity for the plasma membrane means that they are more efficiently taken up into recycling vesicles, and thus more likely to provide an accurate readout of the vesicles involved with recycling.

FM dyes have many advantages compared to genetic probes, chief of which is that they do not require any alteration of the properties of the synapse being examined. FM dyes can be applied topically to recycling neurons, and work instantly. This means they can be used in many systems, including those which do not lend themselves to culturing.

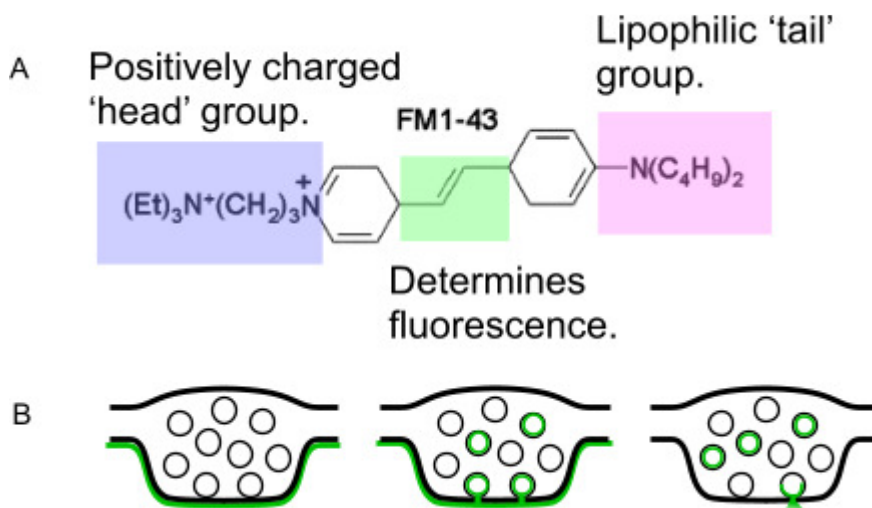


Figure 1.9 FM dye structure and mechanism of action

A) FM dyes feature a lipophilic tail group, which inserts into membranes, a bridge section which determines the fluorescent properties of the dye, and a positively charged head group. *Figure adapted from Brumback et al. (2004).*

B) FM dye embeds into the external membrane, and thus remains on the interior lumen of vesicles. When the external FM dye is washed away, that which remains is inside synaptic vesicles. When these vesicles are exposed to the external environment following exocytosis, this dye too is washed away.

1.7 Emerging techniques

1.7.1 Qdots as biomarkers

Quantum dots, or Qdots, are small spherical crystals, 2-10 nm in diameter, which have an incredibly bright and photostable fluorescence. Because of their small size and photostability, when Qdots are tagged on to a molecule, the movement of these molecules through cells can be traced accurately to within 20-30 nm (Chang et al., 2008).

This technique has been used to impressive effect with synaptic vesicles, allowing a nanoscale readout of the locations of vesicles that have undergone reuptake. For the first time ever, the fate of a newly-recycled vesicle could be observed. They appeared to re-enter at the active zone and at widely-distributed sites within the terminal, and then move to sites further or closer to the active zone, depending on the type of stimulus to which it had been exposed or the type of fusion it had undergone (Park et al., 2012).

Qdots are a valuable tool which will no doubt be exploited in future, as they bridge the gap between optical tools such as FM dyes and studies using electron microscopy. However, this technique has some limitations. One is the uptake of Qdots into synaptic vesicles: typically only one vesicle per terminal is labelled, which does not provide any population data (Park et al., 2012). Additionally there are some emerging concerns over the neurotoxicity of Qdots (Cupaioli et al., 2014).

1.7.2 Super-resolution microscopy

Super-resolution microscopy approaches are new developments in the optical imaging field, and overcome some of the diffraction limits imposed on conventional light microscopy.

One such approach has shown particular promise: stimulated emission depletion (STED) microscopy, which is now commercially available and has wide implications for the study of synaptic vesicles. STED microscopes are laser powered with a resolution approaching 35 nm (Hell and Wichmann, 1994), achieved by providing a beam of lower wavelength in a doughnut configuration which ensures the controlled decay of fluorescence around the point being imaged, and therefore permits a smaller focal spot (Requejo-Isidro, 2013).

STED microscopy has been used to image conventional fluorescent probes in organotypic cultures (Tonnesen et al., 2011) and has been shown to provide excellent images of dendritic spines (Nagerl and Bonhoeffer, 2010). However, synaptic vesicles remain at the very edge of this microscope's resolving power. In addition, the stimulated emission causes photobleaching of samples, limiting the length of time for which a probe can be imaged.

Other methods of super-resolution microscopy centre around the sequential activation of specially designed dyes to give off a specific form of fluorescence. The dyes are applied as in conventional immunofluorescence histological protocols. When activated in small numbers, the central points of these fluorophores can be pinpointed and numerous images can be combined to provide a high resolution picture. In the case of photoactivated localisation microscopy (PALM) this is done by activating small numbers of proteins of interest, locating them and imaging them until complete photobleaching occurred. When this was repeated over an area until all molecules of the dye are activated, the central locations of all the resulting fluorescent punctae are collated into a high resolution image. Using PALM it is possible to achieve a resolution of 25 nm, which is sufficient to identify the position of synaptic vesicles (Betzig et al., 2006). PALM has been turned towards the study of postsynaptic density protein distributions (MacGillavry et al., 2013) and the mobility of CaMKII in dendritic spines (Lu et al., 2014).

Using a similar principle, stochastic optical reconstruction microscopy (STORM) uses the capability of Cy5 to change between a fluorescent and a 'dark' state, in response to different wavelengths of light (Dempsey et al., 2009). Under red fluorescence, these fluorophores are in the 'off' state, but in the presence of green light, Cy5 emits fluorescence (Rust et al., 2006). In STORM, a small fraction of these photoswitchable fluorophores are activated, imaged, and centres of the resulting punctae located. Multiple images are then used to create an image with a 25 nm resolution (Bates et al., 2005).

These techniques both have the advantage of being able to be effected on live tissue, and used to look at the distribution of proteins within structures as small as a synapse. Unfortunately, the high sensitivities for light require that background fluorescence be low, limiting its use in slice-based systems. Another issue with these systems is the length of time required to image the probes. In order to collect images to provide a

resolution that would allow individual synaptic vesicles to be identified, images could be taken at no less than 33 s intervals, placing limits on the capabilities of time lapse studies (Kamiyama and Huang, 2012).

A more general challenge with such fluorescence approaches is that, whilst they provide valuable specific information on the target in question, they offer very little in the way of ultrastructural context; this limits their usefulness for many applications where vesicle organisation needs to be considered in relation to its local synaptic environment.

1.7.3 FIBSEM

Though the two methods described above are both excellent tools for providing a dynamic view of the properties of synaptic vesicles following endocytosis, they both retain the significant flaw of being able to provide information only about the vesicles which have been labelled, and thus are missing valuable context. 3D reconstructions of neurons imaged under a transmission electron microscope, containing DAB labelled functional vesicles, provide both the context required to see how recycling vesicles are organised within the terminal with respect to the non-recycling pool and also information about other structures within the terminal. However, doing this requires acquiring serial sections of samples, identifying regions, imaging them and then aligning these images manually. This is very time-consuming and relies on all serial sections remaining intact. As such, it can prove somewhat impractical for large regions of samples.

An answer to this comes with the emergence of automated electron microscopy approaches, where block sectioning is achieved under vacuum, in conjunction with imaging. In particular, focused ion beam milling scanning electron microscopy (FIBSEM) uses an ion beam to erode the surface of the sample, and a conventional electron beam to form an image of the block face from the electrons backscattered from the surface. This is repeated many times, automatically producing a stack of perfectly aligned images of regions with a volume in the region of $\sim 20 \mu\text{m}^3$ in a matter of hours (Knott et al., 2008).

Volume electron microscopy opens up new avenues for research, allowing 3D reconstructions of huge numbers of synapses in an automated way. Currently, the resolution is too poor to allow reliable differentiation of each non-recycling vesicle, but these properties are improving and a better resolution for optical study is likely to emerge in time.

1.8 Conclusions and aims

It is clear that elucidating the fundamental mechanisms of synaptic operation is of fundamental importance in neuroscience, relevant to our understanding of basic brain function, plasticity, and disease. There have been major advances in our knowledge-base, particularly in the last five or six decades, helped by ever-improving technological advances. Nonetheless, key questions remain unanswered. In the context of the current work, we consider a number of core questions in synaptic vesicle regulation which are largely unresolved. One such issue relates to vesicle fate – specifically, the location release properties and ultrastructural location of a vesicle after it has undergone recycling.

The site of reuptake is the beginning of this fate: with ultrafast endocytosis in hippocampal terminals during stimulation having been shown occurring at the sites to the edge of the active zone (Watanabe et al., 2013), clathrin-based endocytosis in the frog NMJ having vesicles re-entering the pool at the sides of the terminal (Betz and Bewick, 1992), and re-entry via kiss-and-run mechanisms defined by its mechanism (He and Wu, 2007), we have some idea as to where vesicles return to the synapse, but we have little idea what happens to their identity from this point and how their ultrastructural arrangement reflects this. Using spatial information about vesicles following reuptake, we hope to address the question whether the identity of a vesicle informs what pool it is in, or whether the pool to which it belongs is simply defined by its function.

1) To address this issue, I shall first look at the RRP. This pool of vesicles is characterised by its fast response to a stimulus and high release probability. Following an RRP-depleting stimulus, the synapse's response to a stimulus is reduced, and it takes ~10 s for the release properties to return to the prestimulus level. This is thought to be due to the time taken to replenish the RRP (Rosenmund and Stevens, 1996). A key issue addressed in this thesis is what forms this replenished RRP: whether membership of the RRP is an intrinsic property and the previous RRP vesicles are returned there, or whether the RRP is refilled with whichever vesicles are spatially convenient. A study in the frog NMJ by Rizzoli and Betz (2004) found that RRP vesicles re-entered the terminals at non-active zone membrane sites, and a fraction of these (~30%) were transferred to the resting pool. In cultured neurons, Schikorski and

Stevens (2001) found that recycling vesicles were closer to active zone than might be expected through random reintegration into the pool.

To answer questions of fate of RRP vesicles upon re-entry into the terminal, I shall outline the validation of a new method for labelling recycling vesicles with fluorescent probes, including FM dye, in the hippocampal slice system, and photoconverting these to allow identification of recycling vesicles at an ultrastructural level. This will provide a read-out of the properties of recycling synaptic vesicles in a physiologically relevant system.

2) Another advantage of conducting this research in the hippocampal slice system is that it is an established model for long-term plasticity. In this thesis, I use our novel method for labelling recycling vesicles in the hippocampal slice system to study the effects of LTD induction on the properties of the total recycling pool and the docked pool in CA1 terminals. I look at how changes in functionality are reflected in the membership of these pools, pointing to a possible mechanism for plasticity.

3) Finally, I provide the first examination of the properties of extrasynaptic recycling vesicles in the hippocampal slice system at an ultrastructural level. Using conventional 3D EM techniques, I look at the organisation of recycling vesicles outside terminals and try to draw conclusions as to what causes a vesicle to move from the recycling pool to the superpool. This question is further examined using a newly-available EM approach, which allows for volume imaging of large regions of the brain and reconstruction of large lengths of processes, allowing further insight into this question.

Taken together, these findings offer major new understanding of core processes in synaptic function and provide further insight into the concept of vesicle pools and of the identity of the vesicles that make up these pools.

Chapter 2: Materials and methods

The experiments presented in this thesis revolve around three major techniques: the use of hippocampal neuronal cultures to study functional vesicle dynamics; the use of hippocampal slice preparations to examine dynamic properties of functional vesicles; and the use of photoconversion of FM dye and electron microscopy to look at the ultrastructural properties of functional synaptic vesicles in hippocampal slices.

2.1 Animal handling

All experiments were carried out in accordance with the Animals (Scientific Procedures) Act 1986. Sprague Dawley rat pups were delivered at p 0-1 by Harlan Scientific or littered onsite.

2.2 FM dye loading in hippocampal neuronal cultures

2.2.1 Chemicals / reagents / products for culturing

Table 2.1

| Product | Product Code | Company |
|--|--------------|---------------------------|
| Basal Medium Eagle (BME) | 41010-026 | Gibco (Life Technologies) |
| Foetal Bovine Serum | 10500-056 | Gibco (Life Technologies) |
| 100 mM Sodium Pyruvate | 11360-070 | Gibco (Life Technologies) |
| Glutamax Supplement | 35050-038 | Gibco (Life Technologies) |
| B27 Supplement-Serum Free | 17504-044 | Gibco (Life Technologies) |
| HEPES | H-4034 | Sigma-Aldrich |
| Hanks Balanced Salt Solution (HBSS) x10 | 14065-056 | Gibco (Life Technologies) |
| 0.05% Trypsin EDTA | 25300-54 | Gibco (Life Technologies) |
| Poly-D-Lysine | P-1024 | Sigma-Aldrich |
| Trypan Blue Solution 0.4% | T-8154 | Sigma-Aldrich |
| Penicillin-Streptomycin | P-4333 | Sigma-Aldrich |

2.2.2 Solutions and buffers

Table 2.2

| Solution | Composition | Storage | Usage Temp |
|---|--|------------------------|------------------|
| Astrocyte Growth Media | Eagle's Basal Media (BME) with 20 mM glucose, 10 mM HEPES buffer, 1 mM sodium pyruvate, Glutamax, 10% foetal calf serum (FCS), B27 Supplement, 50 units/mL penicillin-streptomycin solution. | 4°C | 37°C |
| Neuronal Growth Media | BME with 20 mM glucose, 10 mM HEPES buffer, 1 mM sodium pyruvate, Glutamax | 4°C | 37°C |
| Dissection Solution | Hanks Balanced Salt Solution (HBSS), 10 mM HEPES | 4°C | 'Ice cold' |
| Poly-D-Lysine (PDL) | 60 µg/ml in H ₂ O | -20°C as 4 mg/ml stock | Room temperature |
| Cytosine β-D-arabinofuranoside (ara-C) | 0.6 µM in Neuronal Growth Media | -20°C as 5 mM stock | 37°C |

2.2.3 Dissection

Sprague Dawley rat pups of either sex were selected at p 0-1 and sacrificed by cervical dislocation. The head was then removed using dissection scissors, and the skin was opened using a No#22 scalpel blade. The skull was opened using curved spring scissors, cutting as shown (Fig.2.1.A). The brain was then removed and placed into an ice cold HBSS and HEPES solution. The olfactory bulb and cerebellum were removed, and the brain was hemisected down the central sulcis using a No#22 scalpel blade (Fig.2.1.B). Fine forceps and fine spring scissors were used to remove the midbrain and turn out the cortex to reveal the hippocampus. The hippocampus was dissected away from the cortex, and the meninges were removed.

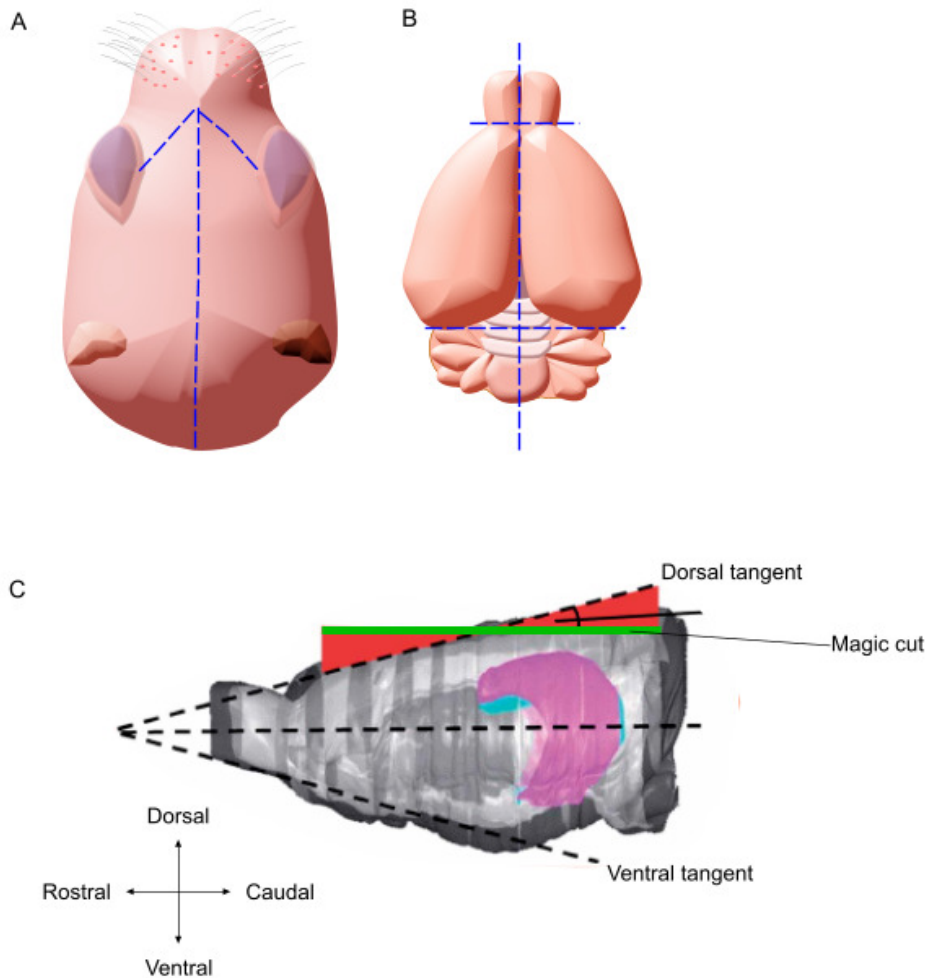


Figure 2.1 Dissection and preparation of rat brain for slicing

A) Cartoon of rat pup head, with blue lines showing cuts to make in skull and skin in order to extract the brain. B) Cartoon of rat brain with blue lines showing cuts to prepare the brain for dissection of hippocampus or for slicing. C) Rat brain with hippocampus shown in pink and turquoise. The green line indicates the ‘magic cut’, with the red section showing the extent to which the blade should be offset from the dorsal tangent.

Figure adapted from Bischofberger et al. (2006).

2.2.4 Astrocytic feeder layer

Following dissection, the removed hippocampus was washed three times in neuronal media (see Table 2.2) and homogenised in 1 ml of astro-glia media using a sterile

Pasteur pipette. The total volume was then increased to 3 ml. 200 μ L of this cell mixture was added to a 125 cm² tissue culture flask with 5 ml astro-glia media. Cells were allowed to proliferate freely in this flask until full confluency was achieved.

12 mm diameter circular coverslips were cleaned using absolute ethanol and placed into the central wells of 24 well plates, with the peripheral wells filled with distilled water to help prevent the culture wells from drying out, and to guard against changes in temperature. The coverslips were then placed in a 60 μ g/ml solution of Poly-D-Lysine and left at 37°C for a minimum of 4 h. The coverslips were then rinsed three times in distilled water and twice with PBS. Into each well was placed 2 ml of astro-glia media (see Table 2.2) heated to 37°C.

Astro-glia media contains a high (10%) level of foetal calf serum (FCS), required to promote astrocyte growth. The addition of 10% FCS renders the media toxic to neurons, and thus provides an environment for selective growth of only astro-glia cells (Ye and Sontheimer, 1998).

To dissociate the cells and apply them to the cover slips, 1 mL of 0.05% Trypsin EDTA was applied to the astrocyte culture for 10 min at 37°C. It was then removed, and the culture was gently rinsed with PBS and 3 ml of astro-glia media was added. The flask was agitated until all cells were dissociated.

The concentration of the dissociated cell solution was calculated using a haemocytometer and 0.04% trypan blue solution. ~ 10 000 cells were added to each well and allowed to settle and grow for 24 h at 37°C with 5% CO₂.

When cells reached 80-90% confluency, ara-C was added to each well to give an in-well concentration of 0.6 μ M concentration. ara-C is a mitotic inhibitor which prevents astrocyte proliferation.

2.2.5 Hippocampal neuronal culture

The method for producing these cultures was a variant of the method described by Banker and Cowan (1977).

Following dissection, the removed hippocampus was washed three times in neuronal media (see Table 2.2) and homogenised in 1 ml of astro-glia media using a sterile Pasteur pipette. The total volume was then increased to 3 ml.

The astro-glia media was replaced with neuronal media containing ara-C, which had a lower FBS content (2% vs 10%) which inhibits astrocyte proliferation and provides an environment much more suited to neuronal growth. In addition to preventing astrocyte proliferation, ara-C also promotes neurite outgrowth (Oorschot and Jones, 1986).

The concentration of the dissociated cell solution was calculated using a haemocytometer and 0.04% trypan blue solution. 20 000-35 000 neurons were added to each well of neuronal media and placed at 37°C with 5% CO₂. These cells grow into neuronal networks which are mature and ready to use at 14 DIV (Fig.2.2).

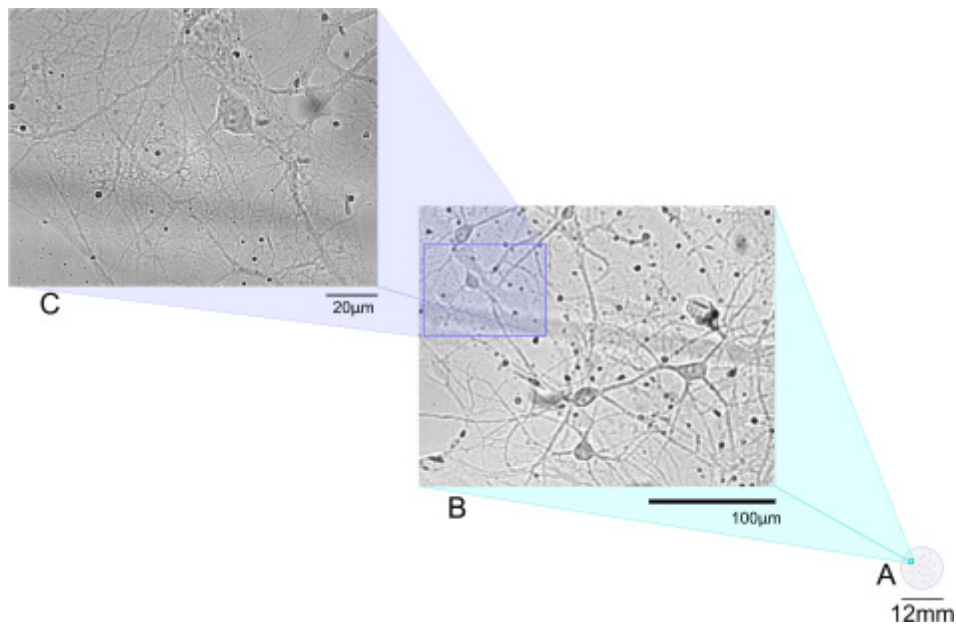


Figure 2.2 Brightfield images of hippocampal neuronal cultures

Hippocampal neurons are isolated by selective growth media and grown onto glass coverslips where they form networks. A) Cartoon of cover slip. B) Hippocampal neurons with a 10x objective. Scale bar represents 100 μm. C) Hippocampal neurons imaged using 60x objective. Scale bar represents 20 μm.

2.3 Optical probe labelling of hippocampal cultures

Table 2.3

| Product | Product Code | Company |
|--------------------|--------------|-------------------|
| CNQX disodium salt | 1045 | Tocris Bioscience |
| D-AP5 | 0106 | Tocris Bioscience |
| FM 1-43 | T-35356 | Life Technologies |
| Oregon Green 488 | O-6807 | Life technologies |
| BAPTA-1 | | |
| syOyster550 | 105 311C3 | SYSY |

Table 2.4

| Solution | Composition | Storage | Usage Temp |
|------------------------|--|---------|------------|
| External Bath Solution | 137 mM NaCl, 5 mM KCl, 2.5 mM CaCl ₂ , 1 mM MgCl ₂ , 10 mM D-Glucose, 5 mM HEPES | 4°C | 37°C |

2.3.1 Electrical stimulation of hippocampal neuronal cultures

This method was derived from several previously featured, primarily based on that described by Ryan and Smith (1995), using electrical stimulation to load cultured neurons.

In order to induce activity simultaneously in all neurons in the culture, we created a custom field stimulation chamber. This consisted of a plastic chamber with a capacity of 0.7 ml, with a glass coverslip base. Attached to the centre of this, approximately 1 cm apart, were two parallel platinum wire electrodes, 0.5 mm in diameter (Fig.2.3.B). These were attached to a Grass stimulator (Astro-Med Inc, USA), which was used to deliver electrical pulses of 0.2 ms duration of voltages between 5 and 20 V at rates of 10-20 Hz.



Figure 2.3 Method for labelling neuronal cultures with FM dye

A) Protocol for labelling cultured synapses with FM dye, stimulating and imaging its release. B) Schematic of stimulation chamber showing parallel platinum wires and wires leading to Grass stimulator.

Coverslips containing hippocampal neuronal cultures were loaded into the stimulation chamber below the platinum electrodes, and covered with 0.5 ml of external bath solution (EBS) containing 10 μM FM 1-43 dye. The stimulation protocol was applied to the neurons from the Grass stimulator to force them to undergo recycling. This was typically 1200 AP at 10 Hz or 40 AP at 20 Hz.

Following the application of the stimulus protocol, the slice was left in the presence of the dye for a further 60 s to allow recycling to complete. The FM dye solution was then replaced three times with 0.7 ml of EBS with 20 μM CNQX and 50 μM AP5 added to prevent recurrent activity and spontaneously generated signals from propagation. At this point, recycling vesicles have been labelled with FM dye (summarised in Fig.2.3.A).

2.3.2 Imaging functional properties of cultured synapses

Experiments were carried out using an Olympus BX61 microscope with an XM10 camera, controlled by an MT10 imaging system. Loaded cultures were viewed using excitation and emission filter sets 470/22, 520/35. A region of interest was identified using a 10x 0.3 NA objective and then located under a 60x 1.0 NA dipping objective. Images were obtained with 1x1 binning with an exposure time of 100 ms. Images were taken every 2 s for each experiment unless otherwise stated.

2.3.3 Calibration of stimulation chamber for hippocampal neuronal cultures

In order to verify that the chamber was successfully and reliably delivering a stimulus to the neurons in the culture, and to attempt to minimise the voltage levels of the stimulus to a submaximal level, we used a combination of two optical probes: Oregon Green 488

BAPTA-1 (OGB), a calcium ionophore which fluoresces green; and syOyster550, a red fluorescent probe attached to an anti-synaptotagmin1 antibody, which binds to the internal lumen of recycling vesicles (Kavalali and Jorgensen, 2014). This allowed us to measure the activity of a neuron in response to a stimulus, and to identify synaptic regions along the process.

Cultures were placed in wells containing neuronal media, ara-C, and 12 μ M OGB. These were then incubated for 2 h at 37°C in 5% CO₂, before being rinsed in EBS and loaded into the imaging chamber. Cultures were then placed in a 1:100 solution of syOyster550 in EBS and exposed to a 1200 AP/10 Hz stimulation protocol. Following this, synapses were allowed to recover for 60 s (Ryan et al., 1996) in order to allow recycling to complete. The culture was then washed in EBS containing 20 μ M CNQX and 50 μ M AP-5.

Regions containing punctate syOyster550 labelling along processes were imaged using an Olympus Cell M imaging system and emission filter sets 470/22, 520/35 for OGB, and 556/20, 609/54 emission sets for syOyster550. Single DIC images, and fluorescence imaging with syOyster550 were taken. Time lapse images of the OGB labelled process were taken with a frame rate of 1 frame per ~80 ms for 4.8 s. During this timeframe, the region was exposed to a 9 AP/10 Hz stimulus. This was done multiple times for each of 0 V, 5 V, 10 V, 15 V, 20 V, 25 V, and 30 V.

Using ImageJ software (NIH, US), the regions demonstrating punctate staining of syOyster550 were selected as regions of interest of uniform size. The locations of these regions of interest were then transposed into the OGB image stacks showing the time lapse of the application of calibration stimuli. Using ImageJ, the average fluorescence of each of these regions was extracted for each time point in the image stack, normalised, and plotted into a graph. This allowed us to identify a voltage which elicited a submaximal response from the tissue. We selected this voltage, 20 V, for use in all future culture experiments.

2.4 Labelling functional synapses in hippocampal slices

The methods described in this section are summarised in Marra et al. (2014).

Table 2.5

| Product | Product Code | Company |
|---------------------------|--------------|-------------------|
| CNQX disodium salt | 1045 | Tocris Bioscience |
| D-AP5 | 0106 | Tocris Bioscience |
| FM 1-43FX | F-35355 | Life Technologies |
| Bromophenol Blue | 10040040 | Fisher Scientific |
| syOyster | 105 311C3 | SySy |
| syCypHer5 | 105 311CpH | SySy |

Table 2.6

| Solution | Composition | Storage | Usage Temp |
|---|---|--|--|
| Artificial cerebro-spinal fluid (ACSF) | 125 mM NaCl, 2.5 mM KCl, 2 mM CaCl ₂ , 1 mM MgCl ₂ , 25 mM D-Glucose, 1.25 mM NaH ₂ PO ₄ , 26 mM NaHCO ₃ , saturated with gaseous mix of 95% O ₂ / 5% CO ₂ | N/A | 'Ice cold', room temperature and 37°C as described |
| Calcium-Free ACSF | 125 mM NaCl, 2.5 mM KCl, 2 mM MgCl ₂ , 25 mM D-Glucose, 1.25 mM NaH ₂ PO ₄ , 26 mM NaHCO ₃ , saturated with gaseous mix of 95% O ₂ / 5% CO ₂ | N/A | Room temperature |
| Bromophenol Blue | 2 µM in ACSF | Room temperature as 20 µM bromophenol blue in 1.25 M NaCl, 25 mM KCl, 12.5 mM NaH ₂ PO ₄ , 0.26 M NaHCO ₃ , saturated with gaseous mix of 95% O ₂ / 5% CO ₂ | Room temperature |

2.4.1 Preparing hippocampal slices

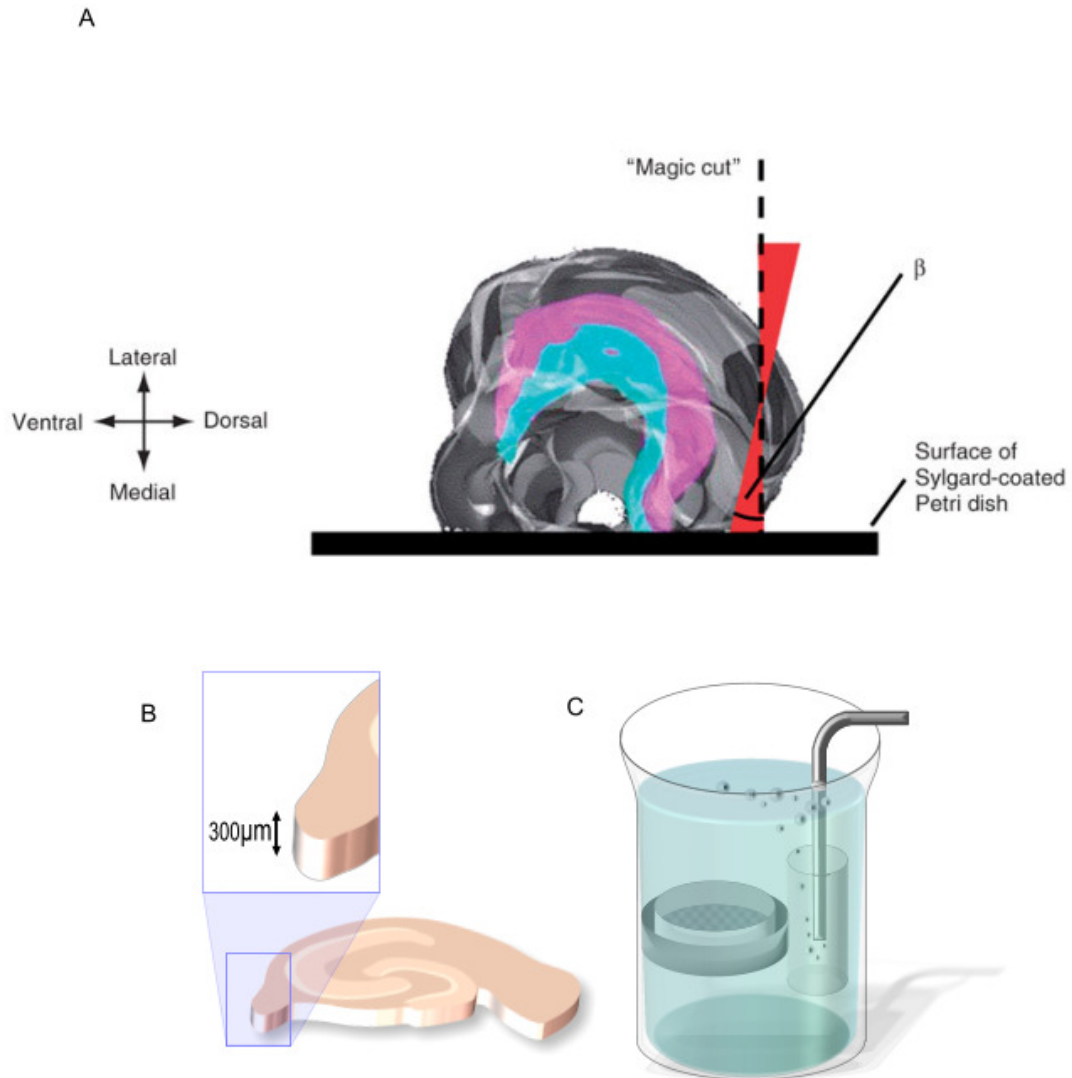


Figure 2.4 Preparing hippocampal slices for FM dye loading

A) An illustration to demonstrate how to prepare the brain for sectioning following hemi-section using the “magic cut” (from Bischofberger et al. (2006)). B) Cartoon of slices of hippocampus prepared with 300 μm thickness. C) Diagram of holding chamber showing Petri dish with nylon mesh stretched across the bottom, held in place by a tube which contains a scintillator to deliver bubbles of 95% O_2 / 5% CO_2 (as described in Gibb and Edwards (1994)).

Rats aged 21-28 d of either sex were sacrificed using cervical dislocation. The head was then removed with scissors and placed into ice cold ACSF where it was kept fully submerged for 1 min. The skin and skull were then cut in a similar manner to that described in Fig2.1.A and B, using dissecting scissors, and the brain was removed using a spatula.

The brain was then placed into a dish of Sylgard containing ice cold ACSF, and the olfactory bulb and cerebellum were removed. Using a single-edged razor blade, the brain was hemisected. The brain was levelled off along the dorsal surface (see Fig.2.4.A, adapted from Bischofberger et al. (2006)) using the 'magic cut' to ensure that the Schaffer collaterals are running parallel to the direction of cutting. The slice was then attached to the magnetic stage using superglue and loaded into a Leica VT 1200S cutting system and covered with ice cold ACSF. A cutting speed of 0.05 mm/s with a horizontal deflection of 0.1 mm was used to produce slices of 300 μm thickness (Fig.2.4.B). The slices were removed from the cutting bath and placed in a Sylgard dish where the hippocampus was cut out. Each slice was then transferred to a holding chamber containing 37°C ACSF using a wide mouthed pipette. The holding chamber was constructed as described by Edwards & Konnerth (1992): specifically, nylon mesh was stretched tightly over a hoop formed by removing the base from a 35 mm Petri dish, and fixed halfway up a 150 ml beaker, using a plastic tube into which a glass scintillator was placed. The rising air bubbles caused solution to move upwards, creating a downward current which passed over the slices (Gibb and Edwards, 1994).

The slices were then allowed to settle at 37°C for a minimum of 30 min before the holding chamber was allowed to return to room temperature.

2.4.2 Experimental set-up

2.4.2.1 Imaging system

Experiments were carried out in an imaging chamber with a glass coverslip base mounted on a BX51WI upright microscope attached to an anti-vibration table. The microscope was attached to an Olympus Fluoview FV300 imaging system, with HeNe and multi-argon lasers.

2.4.2.2 Electrophysiology rig

Axon CV-7B headstages were mounted onto Scientifica Starlab manipulators and fed into an Axon Multiclamp 700A amplifier, and then to an Axon digidata (1322A). Stimulation was carried out using a Grass SD 9 stimulator.

2.4.3 Stimulating Schaffer collaterals in hippocampal slices

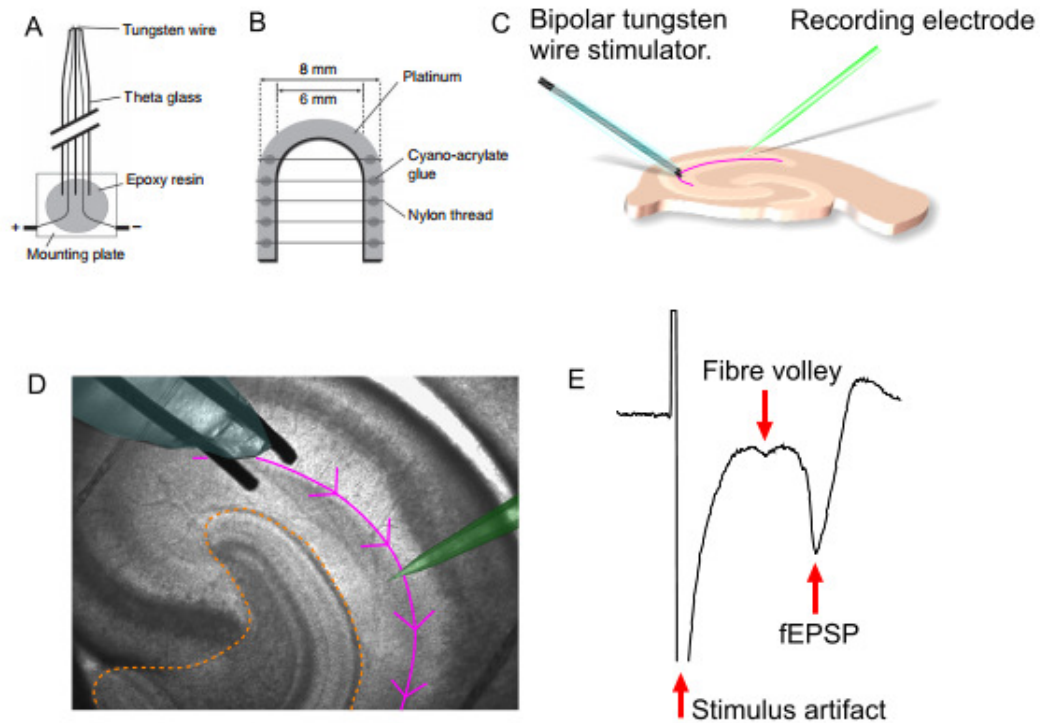


Figure 2.5 Producing a field excitatory postsynaptic potential in CA1 of a hippocampal slice

A) Schematic of bipolar tungsten stimulating electrode. B) Diagram of platinum harp used to hold hippocampal slice in place for experiments. C) Cartoon showing placement of stimulating and recording electrodes in hippocampal slice. D) Example brightfield image of slice with stimulating electrode (left – blue) and recording electrode (right – green) in place. E) Representative fEPSP response with characteristic features labelled.

Images A & B from Marra et al. (2014).

Hippocampal slices were placed in the experimental chamber and held in place with a platinum harp with nylon strings attached with superglue (Fig.2.5.B) and allowed to acclimatise for 15 min. The system was perfused with ACSF at a rate of 3 ml/min. All experiments were carried out at room temperature unless otherwise stated. We found that conducting experiments at 35°C reduced the lifespan of the slice and caused unacceptable drifts in the plane of focus.

A bipolar stimulating electrode was constructed by placing two tungsten wires of 0.075 mm thickness in each compartment of a theta glass capillary, then elongating the tip in a Bunsen burner until the wires were ~0.2 mm apart and sealed within the capillary. The platinum wires were then attached to a Grass stimulator using suitable wires (Fig.2.5.A).

The tip of the stimulating electrode was then placed across the stratum radiatum at the CA2/CA3 boundary. A glass electrode (Harvard apparatus, GF150F-10) was pulled on a Narishige PC-10 vertical electrode puller to give a resistance of 3-5 M Ω , measured in the Axon Multiclamp software. The electrode was then filled with ACSF. The tip of the recording electrode was placed ~50 μ m below the surface of the stratum radiatum of CA1. A series of pulses of 5-10 V, 2 ms duration at 0.03 Hz were delivered to test whether successful activation of Schaffer collateral synapses was achieved (Fig.2.5.C, D). When a trace was obtained that showed a field excitatory postsynaptic potential (fEPSP), it was concluded that a successful stimulation of synapses had been achieved (Bortolotto et al., 2001). Good response traces were characterised by a stimulus artefact, a fibre volley and a large deflection in voltage which corresponds to a compound response from all synapses activated by the pulse. This was typically between 0.5-2 mV (Fig.2.5.E).

To calibrate the stimulation, increasing voltage steps were applied to the slice, and the amplitude and slope of the fEPSP were measured using Clampfit Software (Axon Instruments). A stimulus voltage was selected which elicited a response from the tissue which was slightly submaximal. This was used for experiments conducted on this slice.

2.4.3.1 Electrophysiology trace analysis

Compound synaptic responses were recorded using Clampex 10.3 and analysed in Clampfit 10.3 (Axon Instruments). Values for the maximum amplitude of the fEPSP response and the time to the peak of the response were obtained using the software's

'statistics' function. These were used to calculate the slope of the response. Figures depicting electrophysiology results were high pass filtered with a Gaussian filter at 1000 Hz.

2.4.4 FM dye labelling in hippocampal slices

To prevent propagation of signal and spontaneous signal generation in the slice, 50 μ M CNQX and 20 μ M AP-5 were added to the ACSF perfusion system running at 3 ml/min. The size of the fEPSP was checked at regular intervals until it was no longer visible. At this point the blockers were considered to have taken effect and experiments commenced.

In order to carry out fluorescence labelling of the healthiest parts of the slice, it was necessary to use a pressure injection system (Picospritzer, Parker) to apply the dye locally. In experiments where loading with FM dye was to occur, the solution of the recording electrode contained 20 μ M FM-1-43FX (or 1:100 antibody concentration, as appropriate) in ACSF. Using a 60x 1.0NA dipping objective, we located the tip of the recording electrode and observed it under polarised light through an infrared filter. Observation was continued for a few seconds following the activation of the Picospritzer until the stream of dye could be seen being applied to the tissue. This is in order to verify that the pipette is not blocked and there has been no mechanical failure in applying the dye.

We used the Picospritzer at a pressure of 1.5 psi to eject the dye from the pipette into the slice. In each case, this was done for 3 min prior to stimulation to induce recycling to ensure that the area was saturated with the probe. After this application, a loading protocol of either 1200 AP/10 Hz or 40 AP/20 Hz was applied at the voltage determined by testing in the previous step. During this time the dye was continuously ejected into the tissue. Following the completion of the stimulation protocol, the application of dye into the tissue continued for 2 min to ensure that all recycling was completed.

2.4.5 Measuring fluorescence levels of native terminals

Imaging of fluorescent probes in labelled presynaptic terminals was performed using an Olympus BX51WI microscope and a FV-300 confocal system (Olympus, UK). FM 1-43FX was imaged using a 488 nm Argon laser and a 520/10 emission. Oyster and CypHer antibodies were imaged using a He/Ne laser with 609/54 and 692/40 emission filter sets respectively.

The microscope was focused on the tip of the electrode and the plane of focus was raised towards the top of the slice until the surface was identified. The surface of the slice typically exhibited large numbers of unstained cell bodies with high levels of background fluorescence. Regions 10-20 μm below the surface with numerous bright punctae – presumed to represent functional synapses – were then selected for imaging.

Using an appropriate look-up table, the level of the PMT and laser power were adjusted so the punctae visible in the region selected for imaging did not reach the maximum level of intensity saturation. The region of interest was clipped to a region that could be imaged in <2 s at 1028x1028 resolution. Time lapse images were taken of each sample at a rate of 1 Hz.

2.4.5.1 Determining calcium dependence of experiments

Experiments using calcium free ACSF were carried out to verify that this response was due to calcium-dependent neurotransmitter release, and also to verify that the loading described above was calcium dependent. In this step, following the verification of a response, calcium-free ACSF was applied via the perfusion system at 3 ml/min. The response was tested until no response from the tissue was visible. The experiment was conducted as described above using calcium-free ASCF in place of normal ACSF. Following the conclusion of the experiment, the perfusion was switched for one of normal ACSF and left until the response returned.

2.4.6 Analysing fluorescence data

ImageJ software was used to analyse the data collected from fluorescence experiments. Image stacks were opened in ImageJ and regions of interest of uniform size were selected according to desired criteria (e.g. responsive punctae representing synapses), and the mean grey values for these regions in each image in the stack was extracted. Areas containing little to no fluorescence were used as backgrounds for comparison.

2.5 Ultrastructural studies of recycling vesicles

Table 2.7

| Product | Product Code | Company |
|-------------------------------|---------------------|-----------------|
| 25% Glutaraldehyde | AGR1312 | Agar Scientific |
| 16% Formaldehyde | AGR1026 | Agar Scientific |
| Diaminobenzidine (DAB) | 4170 | Kem-En-Tec |

| | | |
|--|----------|-----------------------------|
| Sodium Cacodylate | AGR1104 | Agar Scientific |
| Oxoid Phosphate Buffered Saline (PBS) Tablets | BR0014 | Thermo Scientific |
| Osmium Tetroxide | O012 | TAAB Laboratories Equipment |
| Potassium Ferrocyanide | 455989 | Sigma-Aldrich |
| Uranyl Acetate | AGR1260A | Agar Scientific |
| TAAB 812 | TO23 | TAAB Laboratories Equipment |
| DDSA | DO27 | TAAB Laboratories Equipment |
| DMP-30 | DO32 | TAAB Laboratories Equipment |
| NBA | MO11 | TAAB Laboratories Equipment |
| Propylene Oxide | AGR1080 | Agar Scientific |

Table 2.8

| Solution | Composition | Storage | Usage Temp |
|--|---|--------------------|-------------------|
| Ammonium Chloride | 100 mM ammonium chloride in PBS | 4°C | Room temperature |
| Phosphate Buffered Saline (PBS) | 160 mM NaCl, 3 mM KCl, 8 mM NaH ₂ PO ₄ , 1 mM KH ₂ PO ₄ (tablets made up as directed) | Room temperature | Room temperature |
| Glycine | 100 mM glycine in PBS | 4°C | Room temperature |
| DAB | 1 mg/ml in PBS. Keep away from light, sonicate for 30 min, and filter before use. | N/A | Room temperature |
| Fixative | 6% glutaraldehyde, 2% formaldehyde in PBS | Room temperature | Room temperature |
| Cacodylate Buffer | 0.1 M sodium cacodylate, pH 7.4 with HCl | 4°C | Room temperature |
| Uranyl Acetate | 4% uranyl acetate in 70% ethanol. Vortex for 5 min and filter before use. | N/A | Room temperature |
| EPON Resin | TAAB 812, MNA, DDSA and DMP-30 in a 24:16.5:9.5:1 ratio respectively | 4°C (for 48 h max) | Room temperature |

2.5.1 Calibrating microwave for rapid fixation

For rapid fixation it is essential that the temperature of the sample is raised to 50-55°C (Login et al., 1998). In order to absorb reflective radiation and provide uniform fixation of the sample, a 200 ml beaker filled with room temperature water was placed in the corner of a conventional microwave oven and the microwave was run with the power at 700W until the temperature of the beaker reached 40-45°C. In our system, this process took 30 s. The time taken to raise 4 ml of fixative to 50-55°C when placed in the centre of the microwave was then determined using an electronic temperature probe. In our system this was 12 s. This was then used for all fixation experiments.

2.5.2 Microwave enhanced fixation

Because of the requirement of preserving the fluorescent signal of FM dye and the structural arrangement of the vesicles, a rapid method of fixation was required. Samples were transferred in ACSF and CNQX+ AP5 to a 35 mm Petri dish with a plastic ring in the centre and held in place with a glass harp and placed in 4 ml of 37°C fixative solution. A 200 ml water load was then heated for 30 s. The central island of the microwave was covered with an upturned Petri dish. The fixative solution was then replaced with a fresh 4 ml of 37°C fixative solution and the Petri dish was placed on the central island and the sample was irradiated for 12 s. The fixative solution was disposed of appropriately and the sample was rinsed three times in PBS.

2.5.3 Photoconversion of DAB

Fluorescent dyes can be used to catalyse the photoconversion of DAB to an electron-dense product (Sandell and Masland, 1988). Fixed samples were then placed into a 100 mM solution of glycine in PBS in order to quench the free aldehyde groups, washed three times in PBS, and then placed into an 100 mM ammonium chloride solution also to bind and block aldehyde groups, and then washed five times in PBS, leaving 10 min between washes.

The samples were then put into a 1 mg/ml solution of DAB in PBS, which was then bubbled with 95% O₂ / 5% CO₂ for 10 min. The DAB was then refreshed, the bubbling continued, and the region in which the FM dye was injected was identified under the microscope using a dedicated x50 NA 0.8 water immersion objective, with objective power density of ~1500 mW/cm². After focusing the objective on the top of the slice at this region, the sample was illuminated at <500 nm from a 100 W Mercury lamp.

When the photoconversion process was complete, a dark black spot was visible in the region which was exposed to the fluorescent light. The sample was checked every 5 min from the start of photoconversion until the point that this state was reached.

Following photoconversion the slice was washed in PBS and marked so that the photoconverted region could be identified later.

2.5.4 Preparation for conventional electron microscopy

Slices were placed in cacodylate buffer. Samples were placed in 1.5% potassium ferrocyanide, 1% osmium tetroxide and 0.1 M cacodylate buffer for 1 h. The sample was then washed five times in cacodylate buffer, with 10 min intervals between washes. The sample was then placed in to 1% osmium tetroxide in 0.1 M cacodylate buffer for a further hour. The sample was again put through a series of 5 x 10 min washes in cacodylate buffer, and one in 50% ethanol. Samples underwent en-bloc staining with 4% uranyl acetate in 70% ethanol for 1 h.

To prepare the sample for embedding, the hippocampal section was then moved through the following series of alcohols, spending 20 min in each, with the solution refreshed after 10 min: 75% ethanol, 90% ethanol, 95% ethanol, 100% ethanol.

Using blunt forceps and a scalpel blade, the sample was then transferred into a foil dish containing a 1:1 mix of EPON resin and propylene oxide. Using the blunt forceps, the sample was gently held at the bottom of the dish until penetration of the tissue was sufficient to prevent it from immediately floating to the top. Samples remained in this solution overnight.

Samples were then placed into EPON resin for 24 h, with the resin being refreshed twice in this time. Following complete impregnation with EPON resin, the sample was placed in to the lid of a BEEM capsule, and pressed flat. At this point, it was ensured that the photoconverted region was 'face down' into the lid of the capsule. The capsule was then filled with EPON resin and left to harden for 48 h at 60°C.

When the resin had polymerised, the photoconverted region of interest was identified both visually and using the photos taken at the time of photoconversion. This region was then marked with a scalpel so it could be located for sectioning.

2.5.5 Ultrathin serial sections

The EPON capsule containing the sample was mounted onto a Leica Ultracut ultramicrotome. A single-edged razor blade was used to trim excess resin from around the scored region containing the photoconverted area of the slice. The sample was aligned to the blade of a diamond knife, and 70 nm sections were produced. These were collected in the waterboat attached to the knife, and placed onto 300 mesh thin bar nickel grids (Agar Scientific, AGG2740N).

2.5.6 Image acquisition

Images were obtained using a Gatan Ultrascan 1000CCD camera, mounted axially on the TEM. Images were obtained at 8000-12000x magnification, depending on their intended use.

2.5.7 Analysis

The images obtained from the electron microscope were annotated and prepared for analysis using Xara Designer Pro (Xara Ltd, UK).

Spatial data was extracted from EM images using Reconstruct software (Fiala, 2005). This allowed us to obtain calibrated absolute distances between features inside synaptic terminals. It can also provide coordinates of the centres of features to allow information about the arrangement of these vesicles to be extracted. Reconstruct software was also used to create 3D reconstructions of serial sections.

2.5.7.1 Density maps in MATLAB

In order to provide an alternative visual representation of the distribution of synaptic vesicles within the terminals, density plots of vesicle locations were produced. To do this, a custom-written script for MATLAB was used (supplied by Prof K Staras).

This involved extracting coordinate data of the centre of vesicles and the centre of active zones from ImageJ software, and using it to generate a plot of the location of vesicles. This plot was then normalised with respect to the furthest vesicle in lateral and dorsal directions to produce a rectangular profile for each cluster. This was done in order to allow synapses of different sizes to be compared. This normalised plot was then reflected bilaterally in order to remove any influence of x axis distribution, which is entirely an artefact of imaging.

Individual plots from every synapse used were then collated to form a single plot, which was used to generate a density map. This was then smoothed using ImageJ, and a look-up table was applied (summarised in Fig.2.6).

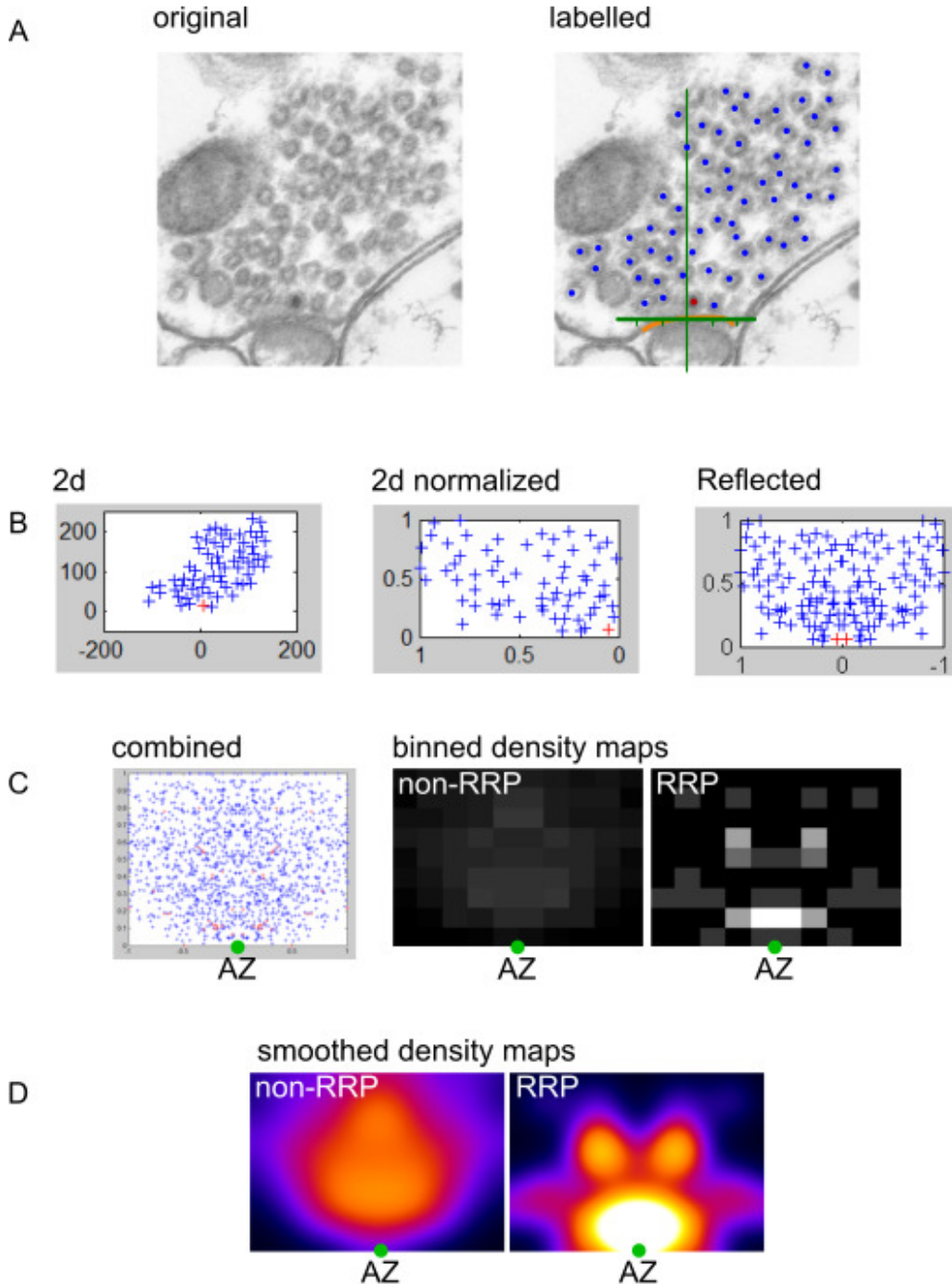


Figure 2.6 Producing density plots using MATLAB

A) In 2D images of synapses, the centre of the active zone was marked, and all vesicles were marked as either recycling or non-recycling. These key features were

then marked in Reconstruct and coordinates of the positions of these features were generated. B) These were generated as plots in MATLAB. They were then normalised to the furthest point from the active zone, and the information regarding which side of the active zone the vesicle occurred on was removed. This was then reflected, to provide a normalised plot of the location of recycling vesicles in a bilateral fashion. C) This was carried out for all vesicles in a group and then combined into a single plot. A density map of this plot was then generated using MATLAB. D) Smoothed density maps were then produced using ImageJ and coloured look-up tables were applied.

Figure generated with assistance from Prof K Staras.

2.6 Preparation of samples for FIBSEM electron microscopy

Table 2.9

| Product | Product Code | Company |
|--------------------------------|---------------------|--------------------------------|
| Osmium Tetroxide | O012 | TAAB Laboratories Equipment |
| Potassium Ferrocyanide | 455989 | Sigma-Aldrich |
| Uranyl Acetate | AGR1260A | Agar Scientific |
| Thiocarbohydrazide(TCH) | 88535 | Sigma-Aldrich |
| Acetone | 10314930 | Fisher Scientific |
| Durcupan component A | 44611 | Sigma-Aldrich |
| Durcupan component B | 44612 | Sigma-Aldrich |
| Durcupan component C | 44613 | Sigma-Aldrich |
| Durcupan component D | 44614 | Sigma-Aldrich |

Table 2.10

| Solution | Composition | Storage | Usage Temp |
|--------------------------|--|----------------|-------------------|
| Cacodylate Buffer | 0.15 M sodium cacodylate, pH 7.4 with HCl, with 2 mM CaCl ₂ . | 4°C | 'Ice cold' |
| Uranyl Acetate | 1% uranyl acetate in ddH ₂ O. Vortex for 5 min and filter before use. | N/A | 4°C |
| TCH | 1% TCH in ddH ₂ O, filtered with 0.22 µm Millipore filter before use. | N/A | Room temperature |
| Aspartic Acid | 0.03 M | 4°C | 60°C |

| | | | |
|---------------------------|--|-----|------------------|
| Lead Aspartate | 20 mM lead nitrate in 0.03 M aspartic acid. | N/A | 60°C |
| Durcupan AMC Resin | 11.4 g Part A, 10 g Part B, 0.3 g Part C, 0.05-0.1 g Part D. | NA | Room temperature |

This protocol was taken directly from Deerinck et al. (2010), picking up at the steps following the fixation of the tissue. Hippocampal slices were loaded, fixed and photoconverted as described above. Following completion of the photoconversion steps, the slices were placed directly into ice cold 0.15 M cacodylate buffer containing 2 mM CaCl₂, which was refreshed three times over 15 min. Slices were then placed into ice cold 1.5% potassium ferrocyanide / 2% osmium tetroxide solution in 0.15 M cacodylate buffer containing 2 mM CaCl₂ for 1 h.

The samples were then washed three times in ddH₂O over the course of 15 min. The sample was then placed into a 1% TCH solution for 20 min. The washing step was then repeated. The sample was placed in 2% osmium tetroxide for 30 min before once again being washed three times with ddH₂O within 15 min. The sample was then refrigerated in 1% uranyl acetate solution overnight.

The sample was once again washed three times over the course of 15 min with H₂O. It was then incubated at 60°C in lead aspartate for 30 min; after this, the washing step was repeated.

The hippocampal section was then dehydrated using the following series of ice-cold ethanol solutions, spending 5 min in each solution before being moved to the next concentration: 20%, 50%, 70%, 90%, 100%. The sample was then transferred to ice-cold 100% anhydrous ethanol which was then allowed to warm to room temperature for 10 min before being refreshed with room temperature anhydrous ethanol.

The hippocampal section was then transferred to 25%, 50% and 75% durcupan / acetone solutions, spending 2 h in each. The sample was then placed in 100% durcupan resin and left overnight. The following day, the durcupan was refreshed 2 h prior to the sample being mounted in a BEEM capsule as described above.

The region of interest was identified on the sample and scored using a scalpel blade.

2.6.1 Analysis

The resulting stack of images was analysed by identifying recycling vesicles and mapping their positions and the positions of the active zones using Trak2EM for FIJI, a modified version of ImageJ. Coordinates for the positions of vesicles relative to the centre of the active zone were extracted from Trak2EM.

Using a variant of Pythagoras' theorem adapted for three dimensions $d = \sqrt{(x1 - x2)^2 + (y1 - y2)^2 + (z1 - z2)^2}$, we calculated the distance between each vesicle and all other vesicles of its classification, and the distance between each vesicle and its nearest active zone.

2.7 Statistics

Typically, values shown are the mean value of a group, \pm standard error of the mean.

When comparing two groups, a two-tailed unpaired Student's *t*-test for unequal variance is performed unless stated otherwise.

For more than two groups, typically a one-way ordinary ANOVA was carried out to determine whether there was a significant difference between groups. If significant differences existed, groups were compared using Student's *t*-test.

2.8 Collaborators

Non-serial sections were produced by Dr JR Thorpe. Serial sections were produced by Dr JJ Burden.

Although I prepared FIBSEM samples according to the protocol outlined, the sample used for analysis was produced by Dr V Marra. Prof M Hausser and colleagues ran the FIBSEM dataset collection.

Chapter 3: Fundamental properties of presynaptic terminals in culture and acute slice

3.1 Introduction

Chemical synapses are the key sites for information transmission in the central nervous system. Each synapse is comprised of two principal components, a presynaptic and a postsynaptic terminal. Presynaptic terminals can primarily be characterised by the presence of a large cluster of synaptic vesicles, each containing neurotransmitter, organised close to a release site on the membrane (Palay, 1956). The postsynaptic region contains the receptors and machinery necessary for signal propagation, and can be identified chiefly by its position, closely apposed to the active zone, and by the presence of a postsynaptic density, an array of proteins associated with the receptors (Ziff, 1997). A key feature of synapses is that the strength of signalling is both variable and adjustable in response to changing functional requirements; this operational flexibility provides the nervous system with powerful information-processing capacity. Factors that contribute to basal synaptic strength, and the substrates that support changes in operation, are of key interest in contemporary neuroscience, but still remain poorly defined.

Studies on the ability of the postsynaptic terminal modulated synaptic response have a much longer history than studies in of presynaptic terminals. In addition to electron microscopy and other image-based methods of determining the properties of the postsynaptic terminals, the susceptibility of the postsynaptic neuron to electrophysiological study provided scientists with a method of obtaining a detailed, real-time readout of the activity of a synapse; through pharmacological agents, a great deal of information about the causes and effects of neuronal activation could be determined. This was more difficult in presynaptic terminals. For example, capacitance readings can be used to measure the exocytosis through vesicle fusion in uniquely large synapses, such as the calyx of Held (Leao and von Gersdorff, 2009); however

central terminals are typically <500 nm in size, making this approach impractical. Using a method known as 'continuous amperometry', the release of neurotransmitter can be measured directly using a carbon fibre electrode; however, this must be calibrated to the specific neurotransmitter, making it impractical for more generalised studies of synaptic vesicles (Gonon et al., 1993).

In the last two decades it has become much easier to study presynaptic terminals, thanks to the development of an array of different sensitive imaging systems and synaptic reporters. Genetically engineered presynaptic probes, fluorescent stains, and nano-engineered reporters now offer direct readouts of presynaptic events, leading to a growing fundamental understanding of basal presynaptic operation, regulation, plasticity, and disease-related dysfunction.

One key determinant of transmission strength, and therefore a significant target for study, is the synaptic vesicles themselves. Although vesicles appear anatomically similar (Alabi and Tsien, 2012), they are known to be divided into functionally distinct sub-populations, or 'pools', which are differentially recruited by specific patterns of synaptic activation. These pools are important concepts in understanding the properties of synaptic transmission and have been the focus of much study in recent years. Functionally defined pools that have been defined and characterised include a recycling pool, responsible for the majority of the terminal's activity (Schikorski and Stevens, 1997, Harris and Sultan, 1995), a readily releasable pool which corresponds to the vesicles that first respond to activity (Rosenmund and Stevens, 1996, Schikorski and Stevens, 2001), and a synapse spanning superpool (Darcy et al., 2006a, Staras et al., 2010). This work has also included efforts to characterise features of vesicle recycling and fusion (Ariel and Ryan, 2010, Granseth and Lagnado, 2008, Ryan et al., 1996), and the mechanisms that underlie these properties.

In spite of this significant progress in understanding the characteristics of vesicle pools, most studies are based on primary cultured neurons. These preparations have been harnessed because they offer distinct advantages for such research. For example, they are more-or-less two-dimensional and so offer significant benefits for imaging work. Moreover, they can be easily accessed for the introduction of fluorescence markers and pharmacological agents and for electrophysiological manipulation (e.g. field stimulation). In addition, introduction of genetically-encoded cDNA reporters, using transfection or viral constructs, is straightforward and conveniently allows expression of

the protein of interest within the development period of the culture. However, inevitably, the conclusions drawn from these studies must be treated with caution, since they likely include artefacts related to the reconstituted circuits from which they are derived. As such, the relevance of these findings for circuits in intact nervous system remains unclear. Without doubt, similar information from acutely-derived brain tissue, where neurons remained connected in native networks, and with locally-relevant cytoarchitecture, would offer significant new insights for understanding fundamental synaptic operation. However, to date, with very few exceptions, there is little available information regarding synaptic function in native preparations. The objective of this chapter is to develop a methodology that addresses this knowledge shortfall by providing the means to label selectively functional vesicle pools in acute hippocampal tissue slices. The longer-term aim is to use this method in conjunction with ultrastructural approaches to provide information about how functional pools are structurally organised, and the relevance of these properties as potential substrates for supporting flexible synaptic operation.

This chapter is organised as follows. The initial section establishes conventional approaches based on optical imaging probes in cultured neurons, in particular using the styryl dye FM1-43 and antibody-based probes such as SytI-Oyster. These experiments provide an important baseline in dissociated neurons for the use of similar approaches in native brain tissue. Subsequently, the chapter outlines the development of an acute brain slice preparation whereby functional labelling of synaptic terminals can be readily achieved, characterises the key properties of these terminals, and includes a comparative study of these findings and the culture work. The wider objective of the development of this approach is to harness the same functional readout ultrastructurally in subsequent chapters.

3.2 Fluorescence readout of recycling vesicle properties in cultured hippocampal neurons

3.2.1 Establishing dissociated hippocampal cultures

As outlined above, a key first step was to establish optical readouts of synaptic function in culture as the basis for development of the use of similar approaches in hippocampal slice preparations. We prepared hippocampal neurons derived from p0 rat pups, using a variant of the established method first described by Banker and colleagues (Banker

and Cowan, 1977). This was a two-step culturing protocol, whereby astrocytes were first plated onto poly-d-lysine coated coverslips to form a feeder layer, and then neurons were plated onto the astrocytes to provide the best conditions to support robust development. This two-step plating approach allowed for much more robust and healthy neurons than co-plating of neurons and glia (unpublished pilot experiments in the lab) (Fig.3.1.A). To promote strong astrocyte growth in the initial, astrocyte-only phase, we used culture media which included 10% FBS (Ye and Sontheimer, 1998). After 5 d, when neurons were plated onto this astrocyte feeder later, we reduced the FBS concentration to 2% to encourage neuronal growth and to limit further astrocyte proliferation. Additionally, we used 0.6 μM cytosine arabinoside (ara-C), a DNA synthesis inhibitor, to restrict further astrocyte development. Throughout the culturing period, neurons were kept in an incubator at 37°C in 5% CO₂. Cultures were typically maintained for ~14 d, to allow the growth of mature networks and synaptic connections (Grabrucker et al., 2009). After this point, it was possible to see defined networks of inter-connected neurons (Fig.3.1.B).

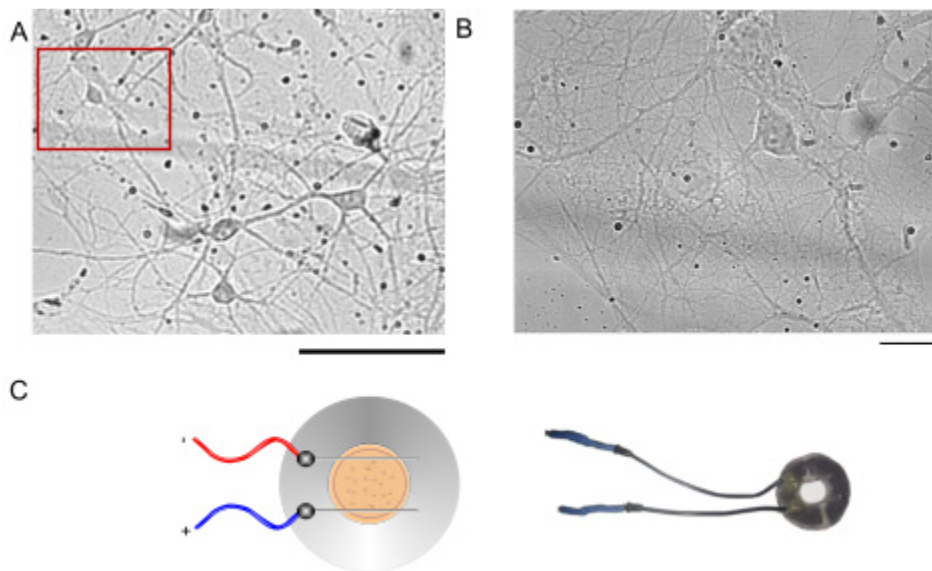


Figure 3.1 Culture and stimulation of hippocampal neurons

A) Cultured hippocampal neurons, DIC imaged using the 10x objective. Scale bar indicates 100 μm . B) Region indicated by the red square in A) was imaged using the 60x objective. Scale bar represents 20 μm . C) A cartoon and photograph of the custom-built stimulation chamber. A coverslip is placed between two parallel platinum electrodes, placed ~10 mm apart, and the wires are attached to a Grass stimulator.

3.2.2 Establishing conditions for effective synaptic activation

An experiment involved the transfer of a coverslip from the incubator to a custom designed imaging chamber (shown in Fig.3.1.C) with parallel platinum electrodes for field stimulation. This chamber was placed on an upright microscope setup, with a dipping objective designed for simultaneous time lapse imaging and electrical stimulation. Recent advances in imaging probes offer a variety of possible reporters which are highly suitable for this calibration experiment. One such example is Oregon Green™ 488 BAPTA (OGB), a membrane-permeable probe which displays a 14-fold increase in fluorescence upon binding with calcium (Paredes et al., 2008). This makes it an accurate probe to measure Ca^{2+} increases, which can be used to confirm that a synaptic response is being generated by the stimulus delivered to the tissue.

Coverslips grown with neuronal cultures were placed in conditioned neuronal media (see Table 2.2) containing 12 μM of OGB and incubated for 2 h at 37°C in 5% CO_2 . Following this, coverslips were placed into the holding chamber described above, and washed with 37°C EBS, and placed into EBS. A region containing visibly labelled processes was selected (Fig.3.2.A).

In order to identify synaptic regions successfully, we had to use an additional probe. sytIOyster550 is a red fluorescent marker attached to an antibody raised against the luminal domain of the synaptic vesicle protein, synaptotagmin. Synaptotagmin is a transmembrane calcium binding protein that plays a key role in exocytosis (Sudhof and Rizo, 1996). Coverslips were placed into a 1:100 solution of sytIOyster550 in EBS, and exposed to a 1200 AP/10 Hz stimulus. The sample was allowed 60 s to complete recycling (Ryan et al., 1996), before once again being washed in EBS and finally placed into EBS containing 20 μM of the AMPAR blocker CNQX, and 50 μM of the NMDAR blocker AP-5. These blockers were used to prevent recurrent firing of neurons, and to ensure that activity seen was induced by the stimulus and was primarily presynaptic.

The application of sytIOyster550 in the presence of a stimulus led to functional terminals being labelled. These appeared as discrete red fluorescent punctae along processes, representing synapses. These were used to select regions of interest in which we could measure the levels of OGB fluorescence.

A 9 AP/10 Hz stimulus was applied with each of the following voltages: 0 V, 5 V, 10 V, 15 V, 20 V, 25 V, 30 V. As the dye was not eliminated from the process, multiple regions from the same coverslip could be used. During the application of the stimulus, the region was imaged at a frame rate of 1 frame per 81 ms using a cooled CCD camera, operating at -77°C . During the stimulation period, the fluorescence of the process increased, and then decreased again following the cessation of the stimulus (Fig.3.2.B). We measured the fluorescence levels of OGB over time of these regions before, during, and after the 9 AP stimulus.

There was no significant difference in fluorescence between when no stimulus was applied (0 V) and when a stimulus of 5 V ($n=468$ synapses from 4 coverslips, Student's *t*-test for unequal variance, not significant, $p=0.372$) or 10 V ($n=468$ synapses from 4 coverslips, Student's *t*-test for unequal variance, not significant, $p=0.826$) was applied. When the stimulus voltage was increased to 15 V, there was a sharp rise in fluorescence to a level significantly different from the baseline, and then a slow decrease in fluorescence ($n=494$ synapses from 4 coverslips, Student's *t*-test for unequal variance, $p<0.002$), showing this is the minimum voltage at which the chamber elicits a response which can be detected with this probe. When the stimulus voltage was increased from 15 to 20 V, there was a further significant increase in the levels of fluorescence displayed ($n=494$ synapses from 4 coverslips, Student's *t*-test for unequal variance, $p<0.002$). At this point, an increase in voltage ceased to produce a significant increase in fluorescence level. There was no significant increase in fluorescence between 20 V and 25 V ($n=494$ synapses from 4 coverslips, Student's *t*-test for unequal variance, not significant, $p=0.113$), or between 25 V and 30 V ($n=494$ synapses from 4 coverslips, Student's *t*-test for unequal variance, not significant, $p=0.253$). Because of this, 20 V was identified as a submaximal stimulus voltage and was used for all future experiments (Fig.3.2.D).

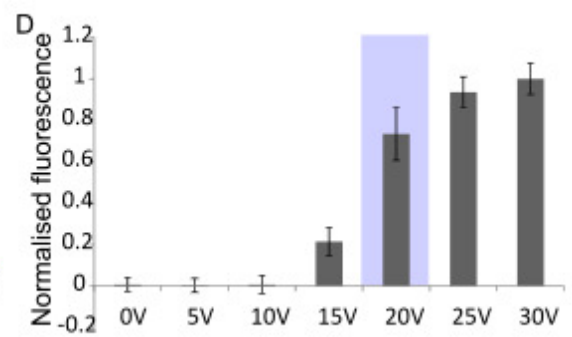
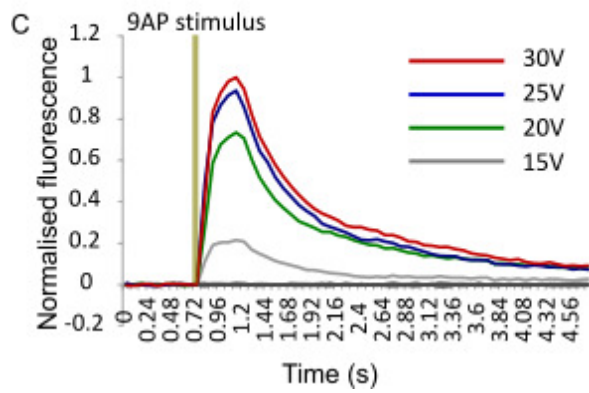
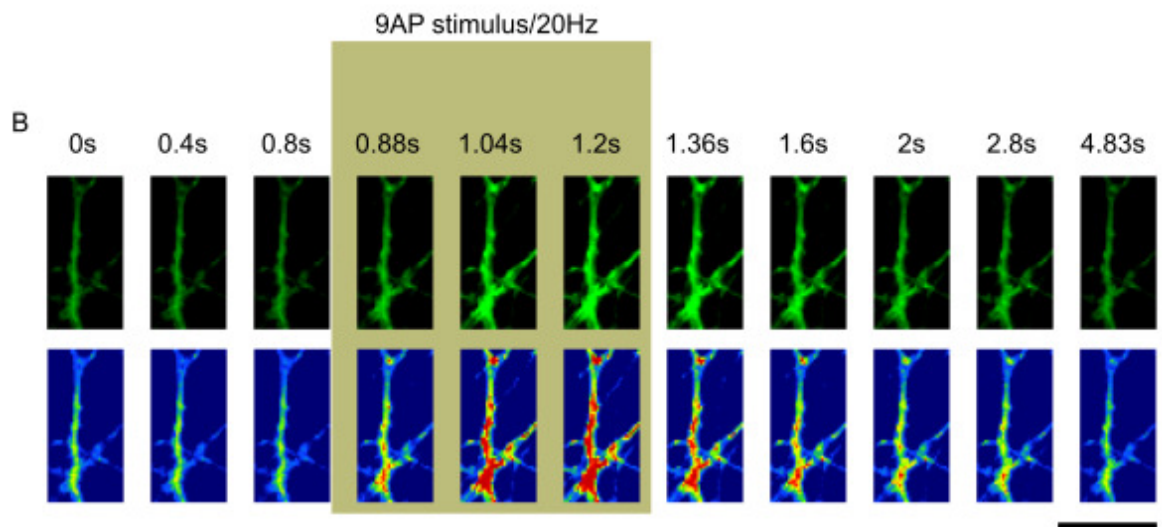
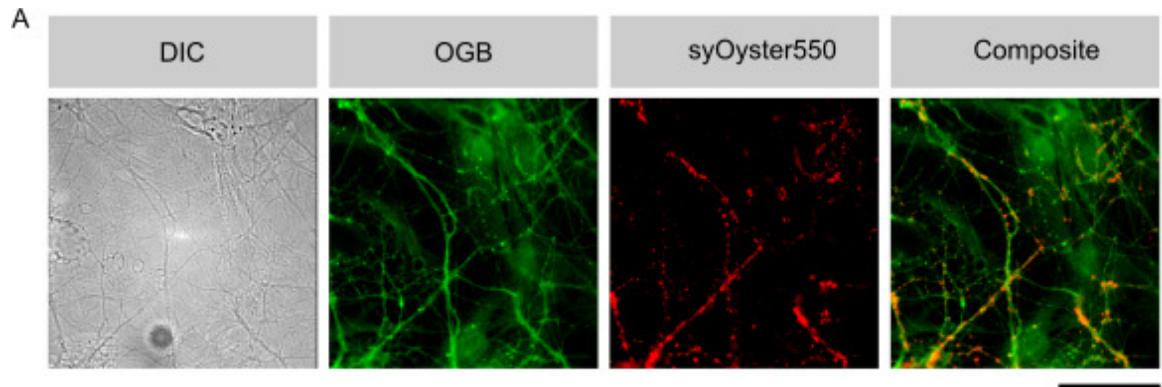


Figure 3.2 Calibrating tissue culture stimulation chamber)

A) Hippocampal neuronal cultures were incubated for 2 h in a 12 μ M solution of membrane permeable Oregon Green BAPTA, in neuronal media. The cultures were then washed in EBS and loaded with 1:100 syt1Oyster550. B) OGB displays an increase in fluorescence in response to calcium influx, caused by stimulus. C) Sample normalised fluorescence response of region to varied stimulus voltages. D) Stimuli at 0-10 V caused no significant difference in fluorescence (n=468 synapses from 4 coverslips, Student's *t*-test for unequal variance, not significant, 0 V-5 V, p=0.372, 0 V-10 V, p=0.826). However, there was a significant rise in fluorescence when a 15 V stimulus was applied (n=494 synapses from 4 coverslips, Student's *t*-test for unequal variance, p<0.002), and further when the stimulus voltage was increased from 15-20 V (n=494 synapses from 4 coverslips, Student's *t*-test for unequal variance, p<0.002). There was no significant increase between 20 V and 25 V (n=494 synapses from 4 coverslips, Student's *t*-test for unequal variance, not significant, p=0.113), or between 25 V and 30 V (n=494 synapses from 4 coverslips, Student's *t*-test for unequal variance, not significant, p=0.253). Accordingly, 20 V was selected as a stimulus voltage. Cultures provided by Ms MM Wagner, who also assisted with high frequency imaging.

3.2.3 FM dye labelling of hippocampal synapses in culture

Having established the basic conditions for neuronal activation in our cultures, we next set out to label dissociated neurons with FM 1-43, a styryl dye that has been widely used as a reporter of synaptic vesicle turnover (Ariel and Ryan, 2010, Betz and Bewick, 1992, Betz et al., 1992b, Betz et al., 1996, Darcy et al., 2006b, Moulder and Mennerick, 2005, Darcy et al., 2006a). The mechanism of action of FM dyes is outlined at length in the introduction: they work by binding to the extracellular leaflet of the presynaptic membrane and being taken up into the luminal surface of the vesicle membrane during endocytosis (see Fig.3.3.A for schematic). After extensive washing of the extracellular membrane, punctate staining corresponds to individual synapses containing recently dye-labelled vesicles (example shown in Fig.3.3.C).

We carried out FM dye labelling using 14-21 DIV cultured hippocampal neurons, prepared as described in section 3.2.1. The coverslip with cultured neurons was placed into the stimulation chamber containing extracellular bath solution (EBS) and 10 μ M FM 1-43 dye. The EBS also contained 20 μ M CNQX and 50 μ M AP-5 to prevent recurrent excitation of the network. For dye loading, the culture was field stimulated with 20 Hz, 1200 AP (60 s duration). This is an established loading stimulation protocol, widely

used for hippocampal cell culture experiments, which is employed as a saturating stimulus, and likely to recruit all functional vesicles in the synapse (Harata et al., 2001, Ryan and Smith, 1995). After a further period of 60 s to allow the completion of endocytosis, the coverslip was washed extensively for ~10 min with fresh, dye-free, EBS (protocol summarised in Fig.3.3.B). After labelling and washing, synapses were imaged on an upright microscope using an EM-CCD camera with an excitation filter 480/30, and a 530/30 emission filter. A typical example of labelling for this experiment is shown in Fig.3.3.C. In a bright field image, the soma and neuronal processes are readily observed. The image in fluorescence is characterised by the same structures, but now with clear punctate staining, approximately 500-1000 nm in diameter, presumably corresponding to the labelling of individual functional synaptic punctae.

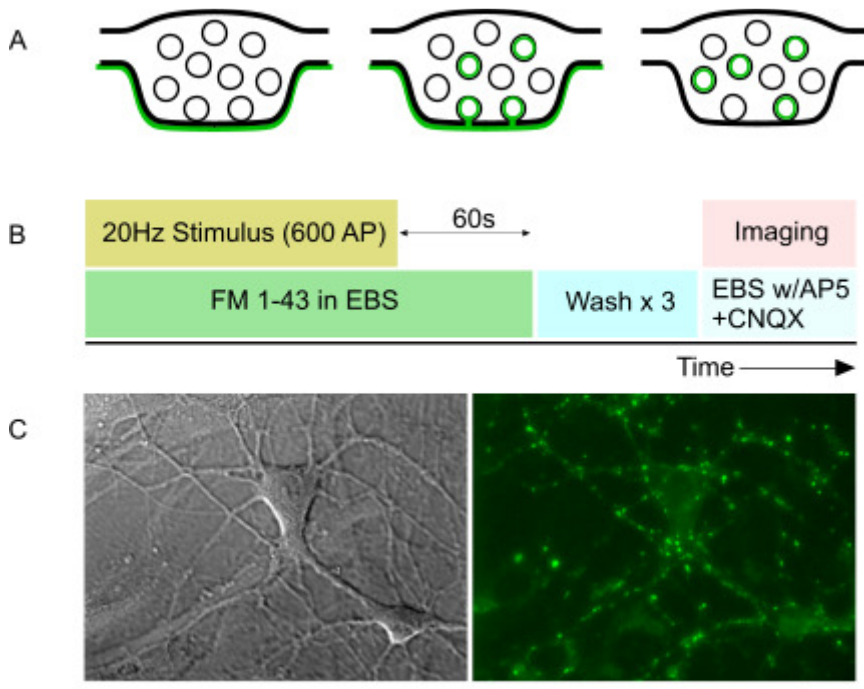


Figure 3.3 Activity dependent labelling of cultured neurons with styryl dye

A) Schematic of the mechanism for labelling of recycling vesicles using FM 1-43. FM 1-43 embeds into the exterior membrane of the synapse, and consequently is contained within the lumen of the vesicle following endocytosis. Remaining external dye can be removed by washing steps. B) Schematic of the protocol for labelling hippocampal neurons with FM 1-43. Neurons are stimulated to activity in the presence of FM 1-43, washed with EBS containing CNQX and AP-5, and then imaged.

3.2.4 Assaying ongoing synaptic function using FM 1-43 dye destaining

A key characteristic and major benefit of styryl dye labelling experiments is that, in addition to their usefulness for functional synaptic labelling, they also provide a means to assay the ongoing functionality of a terminal. The rationale for this is that a dye-labelled terminal actually comprises a population of recently recycled, dye-filled vesicles. As such, a further round of stimulation can evoke their activity-evoked fusion. Since there is now little or no dye in the extracellular solution, the internalised FM dye molecules rapidly depart from the vesicle membrane as it comes to the extracellular surface. In this way, FM dyes provide a sensitive readout of vesicle exocytosis as a function of dye loss at a labelled synapse (described as a schematic in Fig.3.4.A).

To test this functional readout directly in our cultures, synapses were FM dye labelled as above. For destaining, we set up a time lapse imaging experiment (every 2 s) and, after collecting four baseline images, we stimulated at either 10 Hz or 20 Hz whilst continuing imaging. The fluorescent punctae, described above, had stable fluorescence levels prior to the application of the synapse, at which point they underwent rapid dye loss (Fig.3.4.B). When the fluorescence levels over time in these punctae were measured using ImageJ software, they produced a profile showing a plateau followed by an exponential decay curve, the beginning of which coincided with the beginning of the stimulus (Fig.3.4.C). There was a range in the profiles of dye release within samples, demonstrating heterogeneous rates of synaptic activity within the population (Fig.3.4.D).

Further evidence that FM dye release is a good readout of synaptic function is the frequency dependence of the rate of dye loss. We compared the mean normalised dye loss curves from samples which were exposed to a 10 Hz destain stimulus to those exposed to a 20 Hz destain stimulus. The 10 Hz stimulus resulted in dye loss with a time constant (τ) value of 52.58 ± 3.6 s, and the 20 Hz stimulus caused a destain with a time constant of 35.84 ± 7.39 s. These values were significantly different, with the 20 Hz punctae showing a much steeper destain curve (10 Hz, $n=107$ synapses from 3 coverslips, 20 Hz, $n=43$ synapses from 2 coverslips, Student's t -test for unequal variance, $p < 0.05$). We then calculated the time constant tau values of the destain curves generated by fluorescence loss from punctae in each of the two groups. These values were significantly smaller, signifying a faster rate in samples destained using the

higher frequency stimulus (10 Hz, $n=107$ synapses from 3 coverslips, 20 Hz, $n=43$ synapses from 2 coverslips, Student's t -test for unequal variance, $p<0.05$).

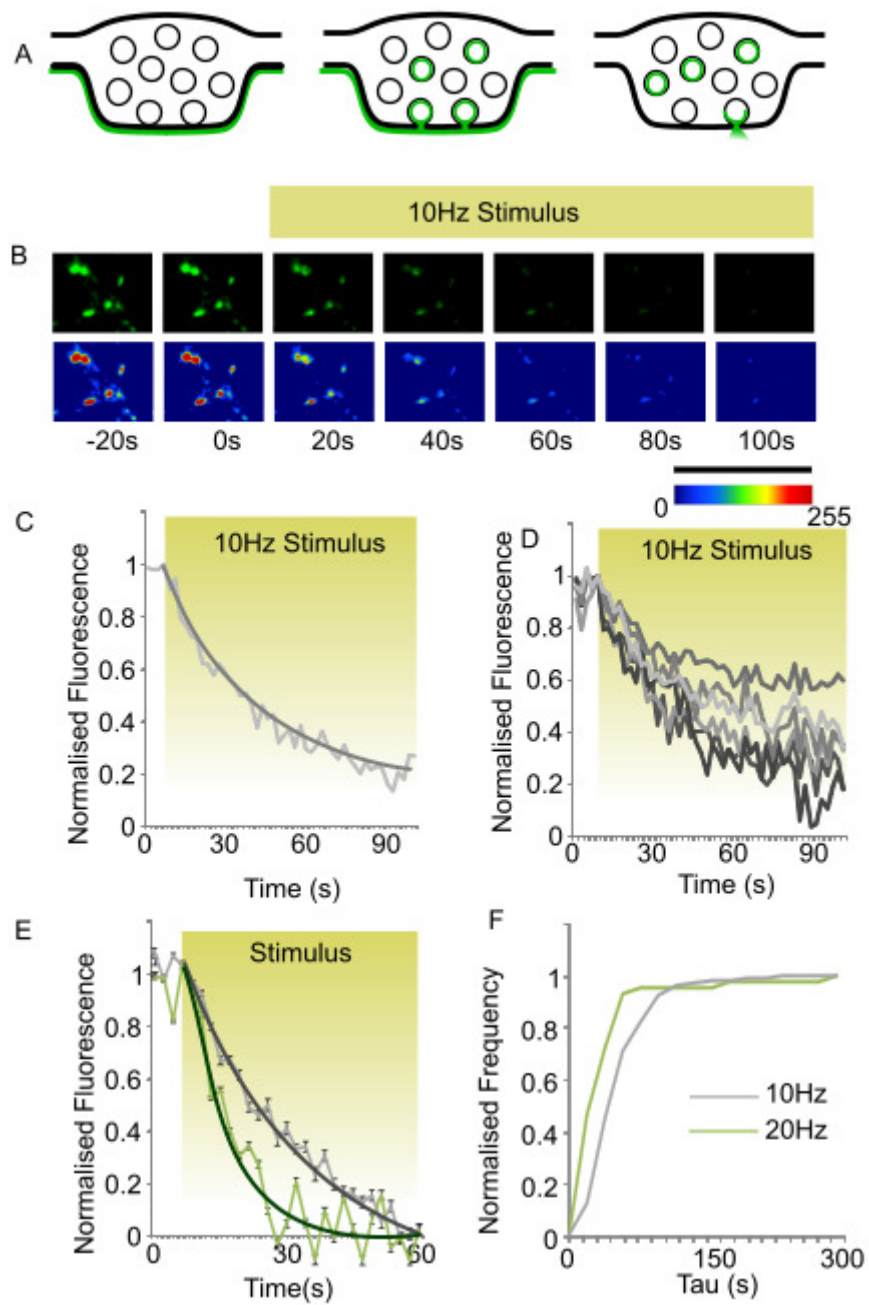


Figure 3.4 Visual assay of synaptic recycling in hippocampal cultures

A) Schematic of mechanism of FM dye release: vesicles which were labelled with FM 1-43 during the loading stimulus application release the dye into the synaptic cleft when the fusion pore opens the lumen of the vesicle to the intracellular environment upon the application of a further stimulus. B) Upon stimulation the FM dye is released by vesicles and washed out of the membranes, causing a decrease in fluorescence. C) Fluorescence levels can be measured through time lapse imaging and produce an exponential decay curve. D) The FM dye destain rates of these curves are heterogeneous within samples, displaying different rates. E) Average fluorescence loss over time curves for cultures destained using a 10 Hz ($\tau=52.58 \pm 3.6$ s), or 20 Hz stimulus ($\tau=35.84 \pm 7.39$ s). These curves were normalised against both fluorescence levels at the point of stimulation, and the levels remaining at the end of imaging. Exponential decay curves shown. These are significantly different (10 Hz, $n=107$ synapses from 3 coverslips, 20 Hz, $n=43$ synapses from 2 coverslips, Student's *t*-test for unequal variance, $p<0.05$) (green – 20 Hz, grey – 10 Hz). F) Cumulative distribution curves of time constant tau values. These values were significantly smaller, signifying a faster rate, in samples destained using the higher frequency stimulus (10 Hz, $n=107$ synapses from 3 coverslips, 20 Hz, $n=43$ synapses from 2 coverslips, Student's *t*-test for unequal variance, $p<0.05$).

3.2.5 Alternative acutely-applied reporter for monitoring vesicle recycling

The work so far has verified the usefulness of FM-dye as a reporter for the readout of functional vesicle recycling and this probe is an important possible option to trial for activity-driven labelling in acute slice (see section 3.3.7). Along the same lines, we also wanted to consider other alternative acutely-applied probes that might be relevant for synaptic labelling in culture, and that may also be applicable and perhaps beneficial in slice preparations.

It is notable that with the rise in genetically-encoded constructs – which can be specifically targeted to proteins or other structures in neurons and not contingent on preceding activity – there has been relatively little effort invested in the development of probes that can label vesicles directly in the manner of FM dye loading. As such, there are limited options to consider: for example, recently, Qdots, small (2-10 nm), intensely fluorescent crystals, which can be attached to a wide variety of proteins in an immunospecific manner, using a biotinylated-streptavidin complex (Bruchez, 2011). When attached to vesicular proteins, such as the luminal domain of the vesicle protein synaptotagmin1, these provide huge advantages over styryl dyes, in that they are very

photostable; small enough that their fluorescent signal can be tracked to provide real-time information with regards to the movement of vesicles within terminals; and exocytosis can be tracked, through the use of an extracellular fluorescence quencher, such as trypan blue (Park et al., 2012). With such benefits, it may seem a wonder that they do not seem to dominate the world of synaptic functional studies. This is in part due to the technical challenges involved with getting sufficient Qdot labelling within synapses. Park et al. (2012) were able to label only a single vesicle in each bouton from which they recorded. This magic bullet for linking ultrastructure and function can only provide us with data from one randomly-selected recycling vesicle per experiment. Sadly, no other approach yet provides the ability to track specific proteins through tissue, but the other desirable property of Qdots was more achievable. For our approach we wanted to combine the photostability of Qdots with the population-labelling capabilities of styryl dyes.

One alternative which has become available only in the last few years is the use of commercially-available probes based on fluorescent-conjugated antibody targeted to the vesicle protein synaptotagmin (discussed briefly in section 3.2.2). This becomes exposed when the protein moves onto the membrane surface. Analogous to FM dye, acute application of the tagged antibody during vesicle recycling can lead to selective labelling of functional vesicles as the probe binds to the protein and is taken up into vesicles during endocytosis. With extensive washing, residual fluorescent tag on the plasma membrane surface can be removed and the remaining signal is vesicle-specific. Sytl-Oyster features a highly photostable fluorophore, which is ideal for long-term studies (e.g. Ratnayaka et al. (2011)).

Prior to their use in the hippocampal slice system, use of this probe was trialled in cultured neurons. A coverslip was immersed in a 1:100 solution of Sytl-Oyster550 and exposed to a 600 AP/10 Hz stimulus to allow loading. The slice was then washed well with EBS containing CNQX and AP-5. The sample was then imaged at a rate of 0.5 Hz using a 556/20 emission filter set. This produced red punctate staining, similar to that seen with FM 1-43 labelling (Fig.3.5.A). When exposed to a destaining stimulus, the fluorescent punctae underwent fluorescent dye loss, similar to that seen with FM 1-43 (Fig.3.5.B). However, punctae stained with Sytl-Oyster550 retained $71.34 \pm 3.4\%$ of their fluorescence following destaining (Fig.3.5.C). This lack of fluorescence loss is because the affinity between the antibody for synaptotagmin I and its corresponding protein is

much greater than that between FM 1-43 and the membrane. Dyes attached to immunological probes would be difficult to remove from the membrane, requiring the applications of solutions at pH 2.5-3.5, which is not suitable for application to living systems (Li et al., 2007).

This demonstrated that sytIOyster550 has some ability to act as a probe for demonstrating synaptic vesicle recycling; because of its photostability, it would be a very useful tool to use for functional studies regarding vesicle mobility in the hippocampal slice system.

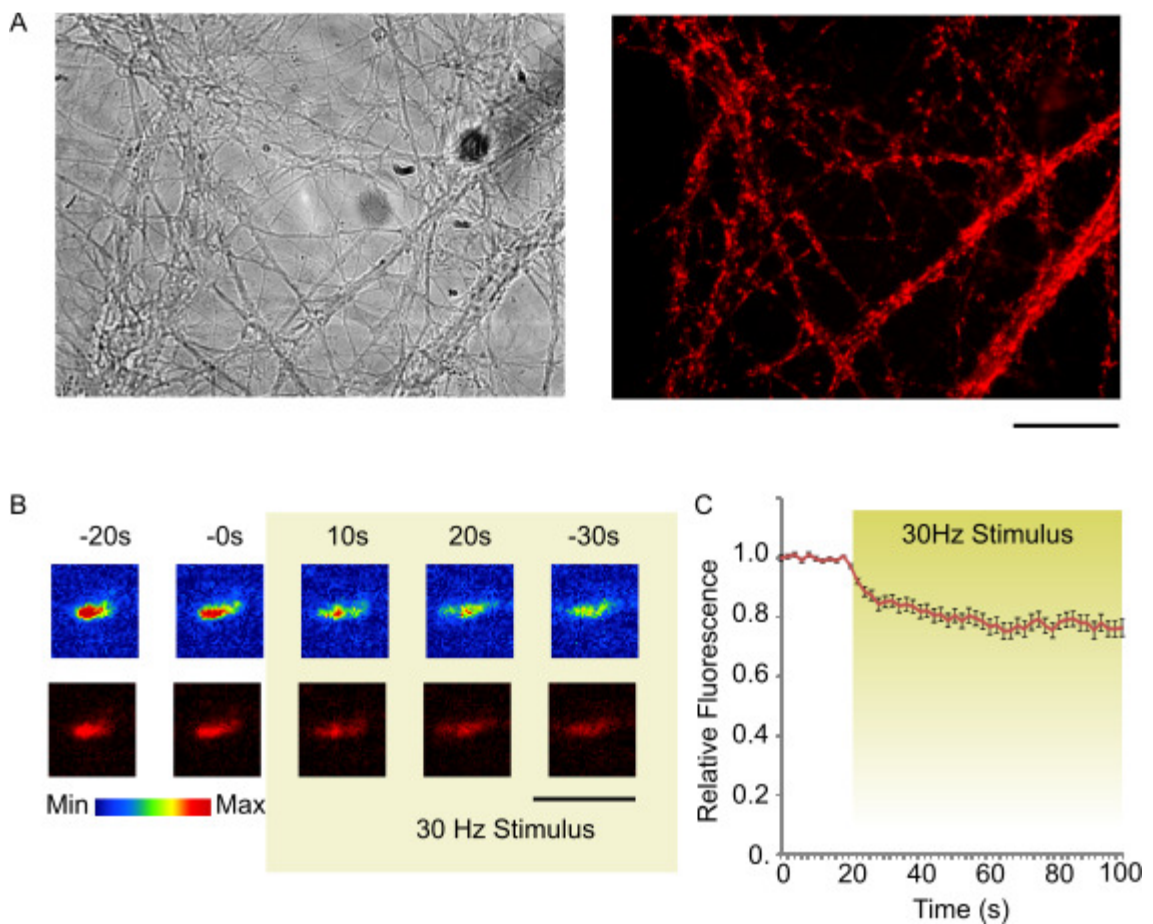


Figure 3.5 Using sytIOyster550 antibodies to provide readouts of synaptic function

A) Polarised bright field image, and image taken with emission excitations sets 556/20 of a hippocampal culture labelled with SytIOyster550. Punctate staining indicate functional synapses. Scale bar represents 30 μ m. B) A representative synapse

exhibiting stimulation dependent dye loss. C) Labelled punctae demonstrate a stable prestimulation fluorescence level, and a stimulus dependent exponential decrease in fluorescence (n=56 neurons from 1 coverslip).

Image stack provided by Dr JA Ratnayaka.

3.2.6 Acute probes for optical measurement endocytosis timings in cultured neurons

The most commonly used optical probes for endocytosis in cultured neurons are synaptopHluorins and sypHy (Granseth and Lagnado, 2008, Royle et al., 2008, Ryan et al., 1996), but these must be transfected into cell cultures and expressed before they can be used. This process has a low yield, has unknown effects on the health and function of the cell, and, crucially, prolonged periods for the proteins to be expressed.

Anti-synaptotagmin CypHer5E is a pH dependent probe attached to an antibody which binds to the luminal domain of the synaptotagmin protein. The use of this probe is important as it provides a read-out of endocytotic function in native terminals, which cannot otherwise be achieved without the use of organotypic cultures (Halff et al., 2014) or the use of a strain of genetically modified mice with a tag of synaptopHluorin on the luminal domain of vesicle associated membrane protein 2 (VAMP2) (Bozza et al., 2004, Nicholson-Tomishima and Ryan, 2004). Both of these reduce the physiological relevance of the results, involving either a prolonged period of growth following extensive traumatic damage to tissues, or another involving genetic manipulation of protein expression, which has been shown to reduce the size and dynamics of vesicle pools (Bozza et al., 2004).

As with sytlOyster550, sytlCypHer5E gains entry to the vesicle lumen when the fusion pore opens during exocytosis, and it binds to synaptotagmin I. When inside the presynaptic terminal, the interior of a synaptic vesicle is pH ~5.5, at which CypHer5E fluoresces. When the fusion pore opens and the lumen of the vesicle is in contact with the extracellular environment, the pH rises to pH 7.4, which quenches the fluorescence. When endocytosis occurs and the fusion pore closes, vesicles undergo a process of reacidification, bringing the pH back down to 5.5, which causes the CypHer5E probe to fluoresce again.

As described above, we immersed the coverslip in a solution of 1:100 syt1CypHer5E in EBS and exposed it to a 600 AP/10 Hz stimulus. When imaged at this point, bright fluorescent punctae, indicative of functional synapses, were visible (Fig.3.6.A). Due to the high level of photobleaching recorded for this probe, time lapse images were taken every 10 s. Upon application of a 100 AP/10 Hz stimulus, there was a significant decrease in the levels of fluorescence, after which the fluorescent signal gradually recovered to levels not significantly different from background levels (n=29 synapses from 1 culture, Student's *t*-test for unequal variation, $p < 0.002$).

This probe was capable of giving an optical readout of fluorescence in the culture system and thus was suitable for trial in the hippocampal slice system.

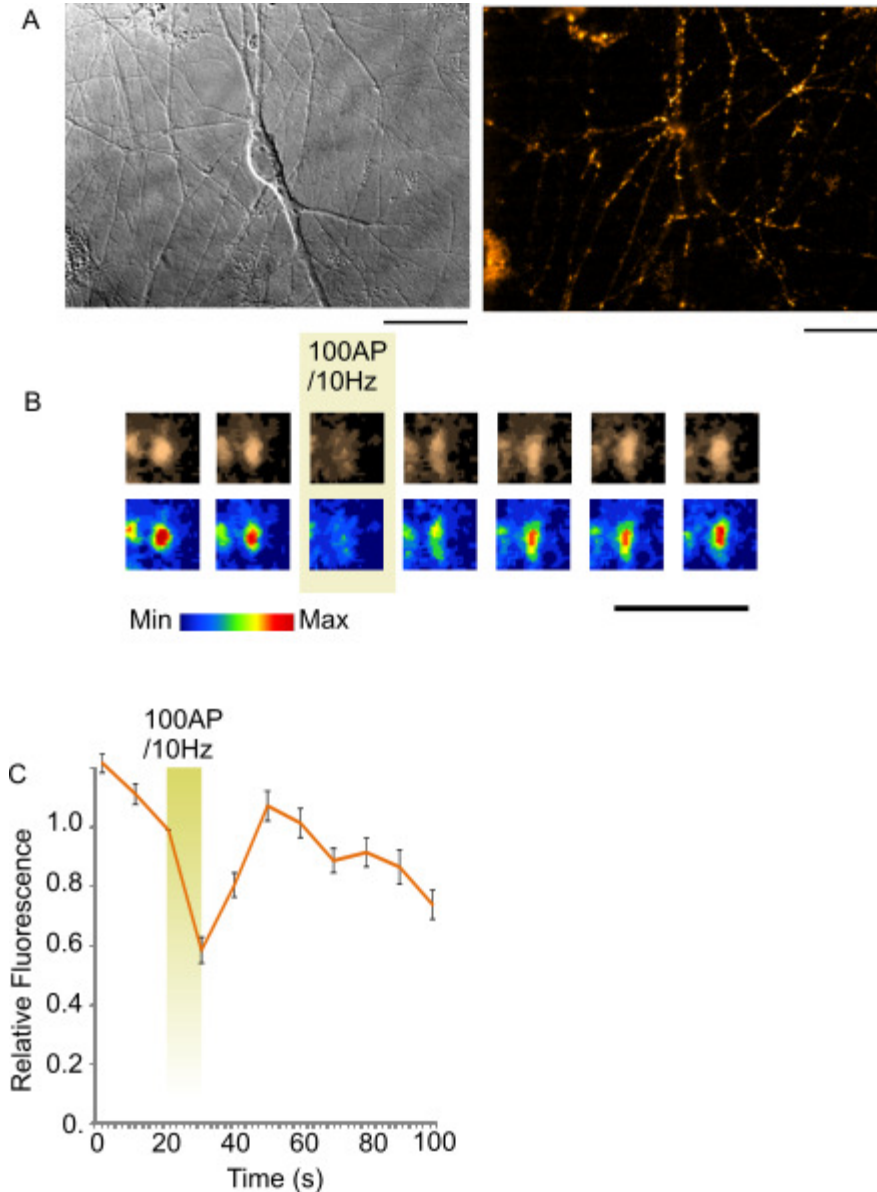


Figure 3.6 Obtaining an optical readout of endocytosis in cultured neurons using an acutely applied probe

A) DIC image and image taken using 628/40 emission-excitation filter sets, of a cultured neuron labelled with syt1CypHer5E. Scale bars represent 30 μM . B) Representative punctae showing dye loss and recovery following a brief period of stimulation. C) Normalised fluorescence levels of responsive punctae, showing dye loss and recovery following stimulation (n=29 synapses from 1 culture).

Cypher image stack provided by Dr JA Ratnayaka.

3.3 Developing FM-dye-labelling in the native slice system

The experiments outlined above established the basic paradigm for FM-dye loading in cultured neurons. The next aim was to employ the principles of this methodology to allow activity-driven synaptic labelling in acute hippocampal slices. This permits exploration of properties of synapses in native cytoarchitecture, but brings with it a number of technical challenges owing to the nature of the tissue. First, the slice is a three-dimensional structure such that ready access of FM-dye to a target region of synapses is made difficult. This is compounded by the fact that the superficial structures of the slice are a newly-cut surface, comprised of dead material and neuronal structures which are presumably structurally compromised. For this reason, readout of functional synapses requires an imaging system which can optically section through tissue.

The simplest possible approach would be to use a population-level stimulation method, combined with tissue-wide exposure to FM dye in the extracellular solution. This was the approach used by Staras et al. (2010), and was achieved by placing hippocampal slices into ACSF containing 40 mM KCl and 10 μ M FM 1-43 for a time period of 45 s and then washing with normal ACSF again. This process required a 30 min washing procedure with ACSF containing FM dye chelator Advasep-7. The resulting staining was largely superficial and required the penetrating power of a multiphoton microscope to reach the levels of optical sectioning required to produce acceptable ratios of signal to noise fluorescence levels. In this work, a multi-photon microscope was not available, but there was ready access to a confocal microscope. This made it necessary and desirable that we should develop a new method allowing for loading using a more localised and defined stimulation, which would be more analogous to the experiments described in culture, and that it should allow for FM dye to be applied below the damaged cutting surface of the slice.

The protocol for this was based on an approach first established by Zakharenko et al. (2001) and Pyle et al. (1999). The hippocampal slice system certainly provides advantages, such as physiological relevance and context, but it poses a series of technological challenges which are not present when using cultured neurons.

3.3.1 Generating synaptic activation in hippocampal slice preparations, and basic calibration

In order to load synapses with FM 1-43, it was first important to establish that we could effectively stimulate synapses in the hippocampus. An established method of stimulation and recording in the hippocampus is to stimulate the Schaffer collaterals (Bortolotto et al., 2001, Schiess et al., 2010, Stanton et al., 2003, Zakharenko et al., 2003). The Schaffer collaterals are projections from neurons in CA3, which synapse onto processes in CA1 (Szirmai et al., 2012). To activate these synapses we adapted the method described by Zakharenko et al. (2001), and produced a bipolar tungsten electrode and placed it across the stratum lucidum and stratum radiatum at the CA2/CA3 boundary, then placed a recording electrode with resistance 5-8 M Ω into the stratum radiatum in CA1 (Fig.3.7.A).

With the stimulating and recording electrodes in place, as shown in Fig.3.7.A, we delivered a 0.2 ms square wave pulse to the tissue to see if a response could be detected. If there was no response from the tissue, the recording electrode was relocated until one could be detected. Following the detection of a response, the tissue was left for 15 min, to allow the slice to 'settle' around the electrode.

A typical response from the tissue consisted of: a stimulus artefact, caused by voltage which reached the recording electrode non-axonally, i.e. it travelled across the bath solution and surface of the tissue; a fibre volley, caused by current passing in nearby axons; and finally, a field excitatory postsynaptic response (Fig.3.7.B). This is formed by all stimulated synapses proximal to the recording electrode responding simultaneously (Bortolotto et al., 2001).

The first step was to validate the stimulation used for this work, for which there are a number of key expectations which it is important to confirm. First, it should be readily possible to show that this response is voltage dependent. To do this, we applied a stimulus with a gradually increasing voltage, and recorded the response given by the tissue. Example responses from the tissue are shown in Fig.3.7.C. The amplitude and latency of the peak of the fEPSP were also calculated, and these were used to calculate the slope of the graph. We could use these measures to calibrate our stimulation. Although the positioning of the electrodes and the distance between the stimulus and recording electrodes have an effect on the size and time course of the

response, we found under our conditions that the maximum synaptic recruitment was at 7 V, with 6 V and 5 V still <90% of the maximum. As seen in Fig.3.7.D, 1 V stimulus was below the threshold required to generate a response; at 2 V, a response was not reliably generated in all samples, explaining a standard error some 30 times larger than that of other data points. We used a 5 V stimulus as it was the lowest voltage which provided a slightly submaximal response.

A second expectation is that responses should be more-or-less stably evoked over time. This is a key requirement for any experiment dependant on repetitive stimulation. To test this, we measured the responses given by tissue when we applied 22 x 2 ms pulses at the 5 V stimulus that we determined above (Fig.3.7.E). When aligned, these traces showed little variation (Fig.3.7.F), but in order to test whether this was the case or not, we once again measured the slope of the graph as described above. There was no significant difference in the variation of the responses given over multiple samples (n=5 slices, ordinary one way ANOVA, not significant, p=0.99) or between the responses (n=18 responses from 5 slices, repeated measures one way ANOVA, not significant, p=0.98). This provides strong evidence to show that our approach permits a stable response from the tissue over time.

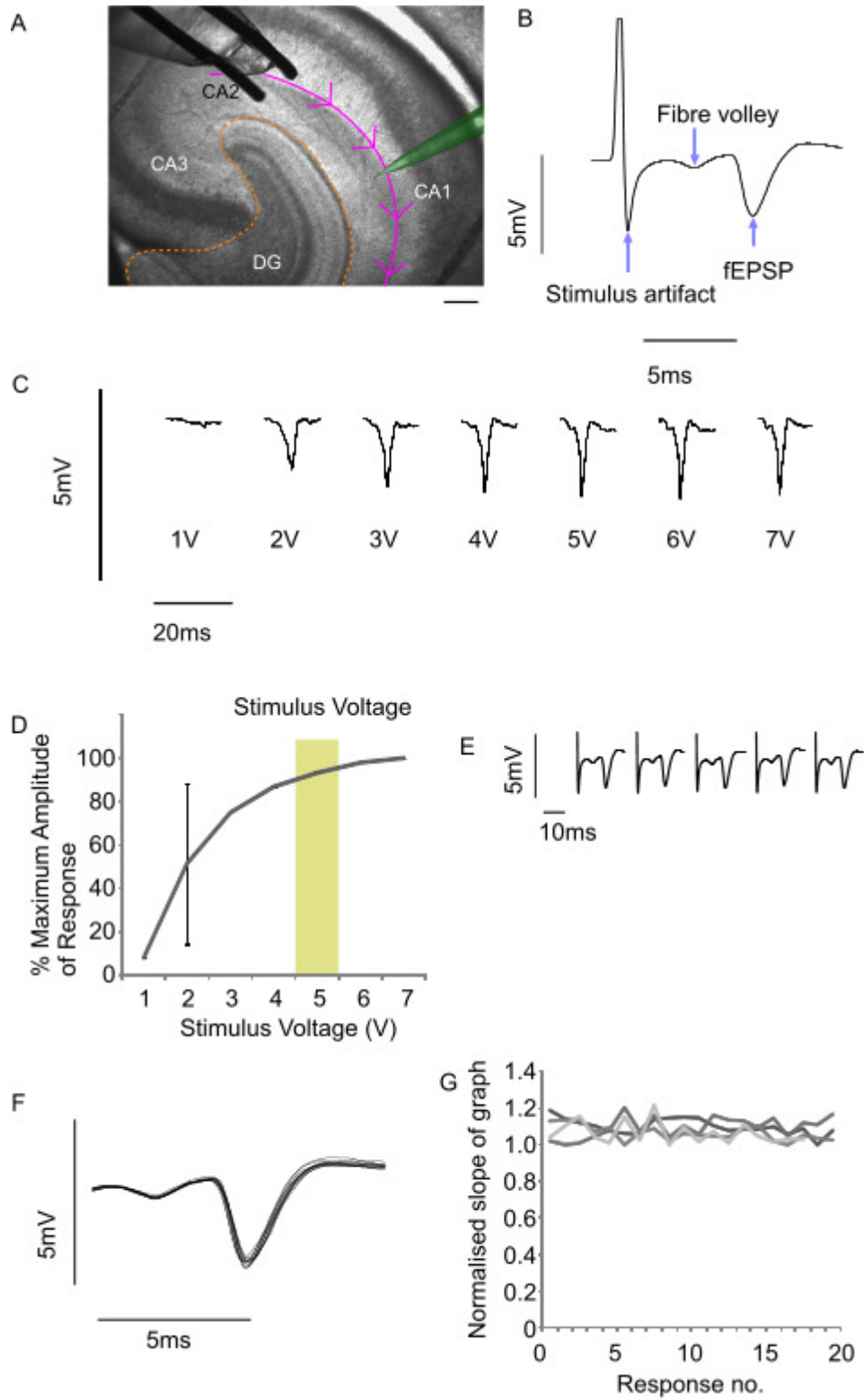


Figure 3.7 Establishing a robust synaptic response from the hippocampal slice system and basic calibration of stimulus

A) Brightfield image of hippocampal slice, with the stimulus electrode in CA2 and the recording electrode highlighted in green in CA1. The Schaffer collaterals are indicated in pink. Scale bar is 200 μm . B) A sample response from CA1 of a hippocampal slice, with key features labelled. C) The response generated by the tissue is dependent on the voltage of the stimulus. Sample responses from a slice exposed to a stimulus of increasing voltage. D) We measured the amplitude of these responses across three different slices. The percentage of the maximum amplitude of the fEPSP at each voltage is shown here. We selected 5 V (response at this voltage indicated in yellow) as a sub-maximal response, for use in all other experiments. E) Example of trace given through repetitive stimulation of the same slice. F) A typical response obtained from the tissue over the course of 20 APs, all aligned. Smoothed using a low band pass filter at 1000 Hz. G) The slope of the downward phase of the fEPSP, calculated by dividing the amplitude of the peak by the latency from the beginning of the fEPSP to its peak. The slope of the graph in responses, applied at 0.003 Hz, over a period of 10 min, and normalised to the minimum response given, is displayed from 5 slices. There is no significant difference between the variation in responses over multiple samples ($n=5$ slices, ordinary one way ANOVA, not significant, $p=0.99$) or between the responses ($n=18$ responses from 5 slices, repeated measures one way ANOVA, not significant, $p=0.98$)

3.3.2 Confirming calcium dependence of hippocampal responses

Synaptic vesicle fusion is triggered by the influx of calcium into the presynaptic terminal leading to neurotransmitter release and postsynaptic effect. As such, synaptic transmission is highly calcium dependent (Sudhof and Scheller, 2001a). It was important to verify this dependency in our system, and thus that the activity generated by the stimulating electrode was due to presynaptic neurotransmitter release.

Experiments were carried out in which a robust initial response to a 0.05 Hz protocol was obtained in 3 slices. These slices were then washed in ACSF where the calcium had been replaced with magnesium, and the protocol was repeated. Subsequently, the Ca^{2+} -free ACSF was again replaced with normal ACSF, and the stimulation protocol was repeated a further time (summarised in Fig.3.8.A).

As described in the previous section, we located a robust response when the tissue was placed in normal ACSF. When Ca^{2+} -free ACSF was added to the perfusion system and given time to access the tissue, there was a significant decrease ($n=22$ responses from 3 slices, Student's t -test for unequal variance, $p= <0.0005$) in both the slope and

the amplitude of the fEPSP. The response was effectively eliminated, with the amplitude showing no significant difference to the prestimulation baseline recordings ($n=22$ responses from 3 slices, Student's t -test for unequal variance, $p=0.225$) (Fig.3.8.B). In order to verify that this was due to the absence of calcium, rather than some toxic effect of the Ca^{2+} -free ACSF on the system, we washed the sample with normal ACSF for several minutes until the response was recovered. At this point, the response reached on average, $78.12\pm 0.6\%$ of its previous amplitude. This difference was significant to the value obtained prior to the application of Ca^{2+} -free ACSF ($n=22$ responses from 3 slices, Student's t -test for unequal variance, $p<0.0005$) (Fig.3.8.C). These findings provide further confirmation that we are recording signals dependent on a Ca^{2+} -triggered synaptic mechanism.

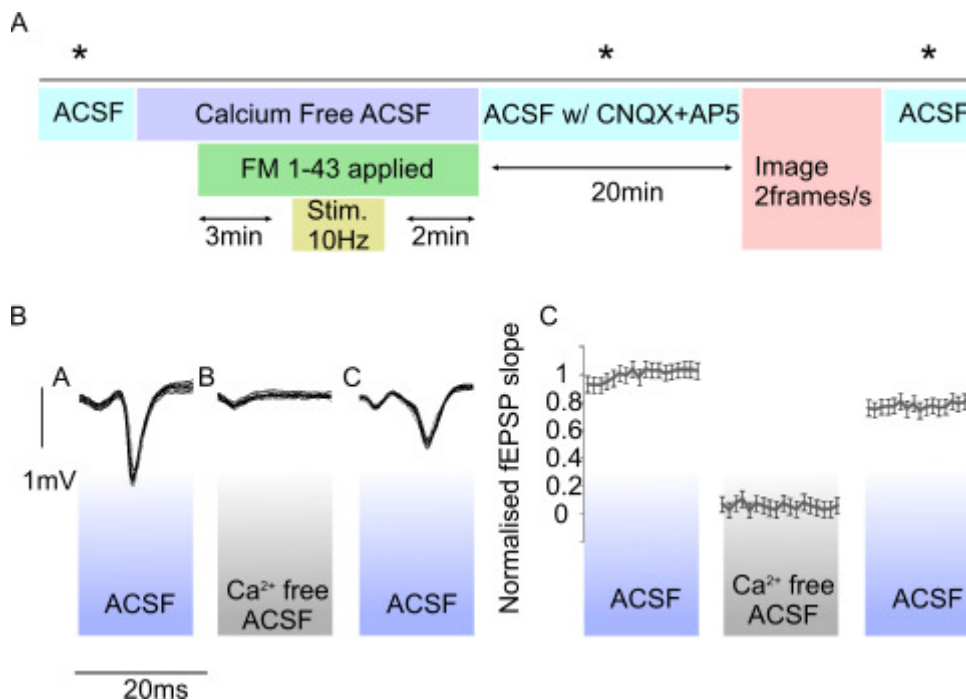


Figure 3.8 Measured fEPSP is calcium dependent

A) Stimulation protocol for determining the calcium dependence of a response. Electrophysiology recordings are taken at the points indicated by asterisks (*). B) The tissue response prior to, during, and after the application of Ca^{2+} ACSF. After the application of Ca^{2+} -free ACSF, the fibre volley remains but the response is entirely eliminated. When Ca^{2+} -free ACSF is replaced with normal ACSF, the response is recovered. C) Slope of the graph normalised against the maximum slope. Following the application of Ca^{2+} -free ACSF, there was a significant decrease in the slope of the graph ($n=22$ responses from 3 slices, Student's t -test for unequal variance, $p<0.0005$) to levels which were not significantly different from the baseline recorded prior to

application of the stimulus (n=22 responses from 3 slices, Student's *t*-test for unequal variance, not significant, $p=0.225$). Following replacement of the Ca^{2+} -free ACSF with normal ACSF, the fEPSP slope recovered to $78.12\pm 0.6\%$ of the size seen previously. This was not a significant difference compared to the responses seen prior to the application of Ca^{2+} -free ACSF (n=22 responses from 3 slices, Student's *t*-test for unequal variance, $p<0.225$).

3.3.3 Fluorescent labelling of hippocampal slices in acute slice preparation

The next objective was to adapt the stimulus protocols established above to activate synapses in order to fluorescently label them using the activity dependent dye, FM 1-43. In experiments using FM dye in culture, providing neurons with access to the dye simply required the replacement of extracellular solution with one containing a solution of FM 1-43. In slices, however, the superficial layers of the slice are the cut surface of the slice, which is likely to have several microns of dead tissue overlying healthy neurons. This presents a major technical challenge for FM dye loading studies, since FM dye is readily taken up by dead tissue membrane. In the acute slice preparation, most experimenters target cells that are at least 10 μm below the cut surface. In our system, a bath application of FM 1-43 would mean the dye either 1) can access the healthy layer but the signal is contaminated by the intense fluorescence from above it, or 2) the dye cannot penetrate into the healthy layer, in which case it will not be present to load synapses. To circumvent these issues, a method was devised which relied on the use of a Picospritzer and a large pipette (resistance 5-8 $\text{M}\Omega$) to microinject FM dye at the target region, 50 μm below the surface of the slice.

A 20 μM solution of FM 1-43 was added to the ACSF of the recording electrode. A response from the tissue was located as described in Fig.3.7, with the tip of the recording electrode ~ 50 μm beneath the surface of the slice (Fig.3.8.B). The dye was ejected into the tissue at a pressure of 15-20 psi for 3 min to allow the tissue to be saturated with the dye, and then a 1200 AP/10 Hz stimulation was applied to instigate vesicle recycling. This system was then washed for 20 min to allow excess dye to be removed and was then imaged using a Olympus Fluoview FV-300 confocal imaging system, with a multiline Argon laser at 488 nm excitation and BP556/20 emission filters (summarised in Fig.3.9.A).

When imaged, this protocol resulted in the region near to the recording pipette being characterised by bright, discrete punctae, approximately 0.5-1 μm in diameter (Fig.3.9.C). The appearance of these fluorescent signals in CA1 is consistent with labelled presynaptic terminals being similar to the size reported for small hippocampal synapses in previous studies (Harris and Sultan, 1995).

Further to the results shown in section 3.3.2, we carried out the above protocol in the absence of calcium in order to determine whether this labelling profile was calcium-dependent, providing further verification that what we were seeing is function of vesicle recycling. When FM dye was applied and a stimulus delivered in the absence of calcium, there was no punctate labelling visible: further evidence that FM 1-43 is labelling functional synapses (Fig.3.9.D).

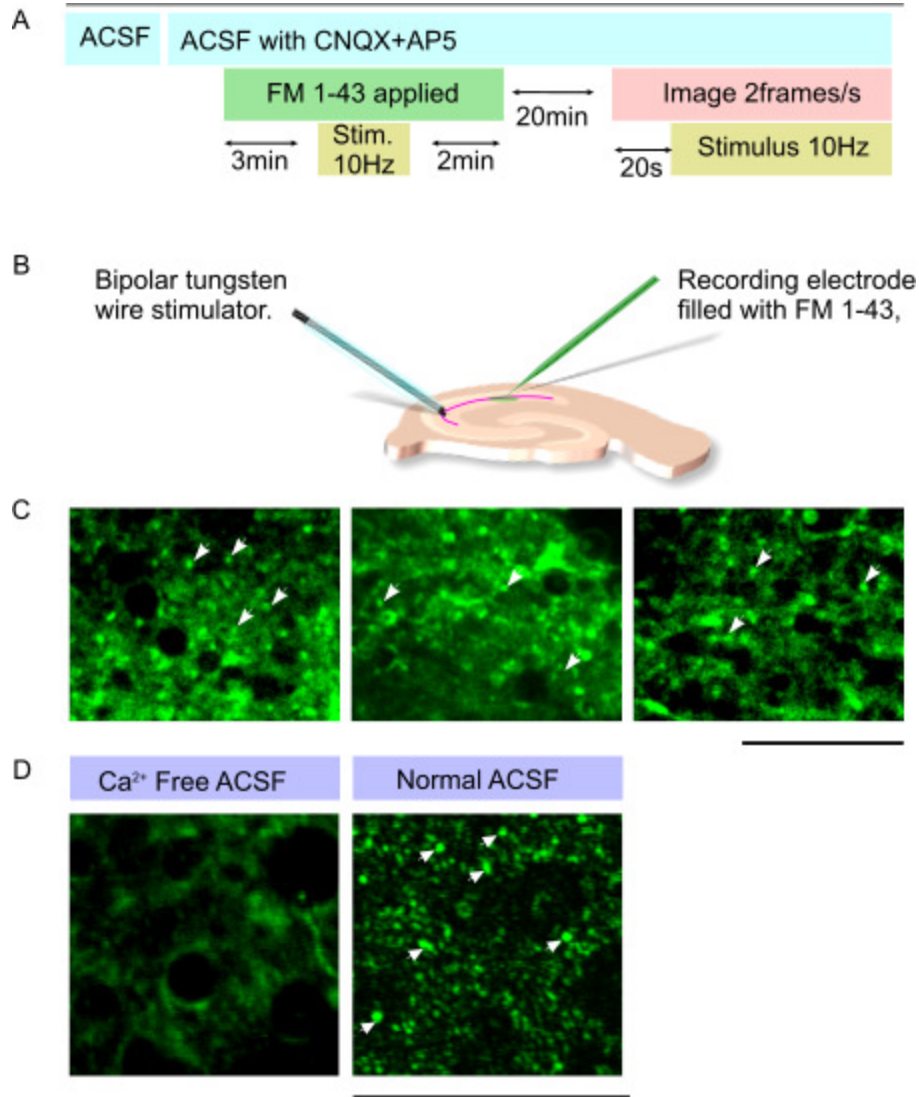


Figure 3.9 FM dye labelling of functional synapses in hippocampal slices

A) Protocol for labelling recycling vesicles with FM 1-43 and obtaining a functional readout. B) Cartoon of the mechanism of FM dye delivery into the slice. FM dye is pressure injected into the slice, and a stimulus is applied along the Schaffer collaterals. C) Example slices featuring FM dye loading of functional synapses. These synapses appear as small, discrete fluorescent punctae. D) This labelling is calcium dependent. When FM dye is injected into tissue without the presence of calcium, these fluorescent punctae do not appear.

3.3.4 Challenges of background dye elimination

One of the clear challenges with this approach is to achieve the best signal to noise ratio possible; that is, discrete fluorescent signal corresponding to synaptic punctae, set against a low-fluorescence background. A likely source of background signal is residual dye on external membranes that has not been effectively removed.

Previous groups addressing this problem, such as Pyle et al. (1999) and Zakharenko et al. (2001), found an effective solution in the use of FM-dye chelator, Advasep-7. Advasep-7, developed by Kay et al. (1999), is readily soluble in water, and binds to FM dye with a greater affinity than the plasma membrane. This leads to a greater degree of FM dye wash out. However, Advasep-7 itself is intensely fluorescent and sticks readily to glassware, plasticware, and objective lenses. These issues meant that it was desirable to avoid its use if possible.

The studies mentioned previously have advocated a 15-20 min washing period in order for Advasep-7 to have a full effect (Kay et al., 1999, Zakharenko et al., 2001). Hippocampal slices loaded with 1200 AP/10 Hz with FM 1-43 were washed for 20 min with either 0.2 mM Advasep-7 ACSF or normal ACSF (control). These were then imaged using confocal microscopy.

Both in the Advasep-7 samples and the control samples, bright fluorescent punctae were clearly identifiable against the background levels of fluorescence (Fig.3.10.A). In the collected images of FM 1-43 labelled synapses, using a uniform sized region of interest, 50 samples were collected of areas which contained these bright punctae, and 50 samples of areas which contained no fluorescent bodies.

There was a little overlap in the levels of fluorescence of punctuate regions versus background ones in the control samples (Fig.3.10.B), and none in those of the Advasep-7 group (Fig.3.10.C). The ratio of fluorescence in punctae to background fluorescence was significantly higher in Advasep-7 compared to control samples (3.76 ± 0.1 Advasep-7; 2.8 ± 0.1 controls, background regions $n=50$, fluorescent punctae, $n=50$, Student's *t*-test for unequal variance, $p < 0.02$). However, in both Advasep7 and control slices, the fluorescent punctae showed significantly higher levels of fluorescence compared to the background, meaning that the two categories could be clearly distinguished (two-tailed Student's *t*-test, $p < 0.00002$ in both cases).

Though the addition of Advasep-7 made several improvements in reducing background levels of FM 1-43, they were not material differences. Labelled punctae could be easily differentiated from background levels using a 20 min wash with normal ACSF. Because of the technical difficulties raised by the adhesive and fluorescent properties of Advasep-7, it was decided that the advantages were not great enough to warrant its use.

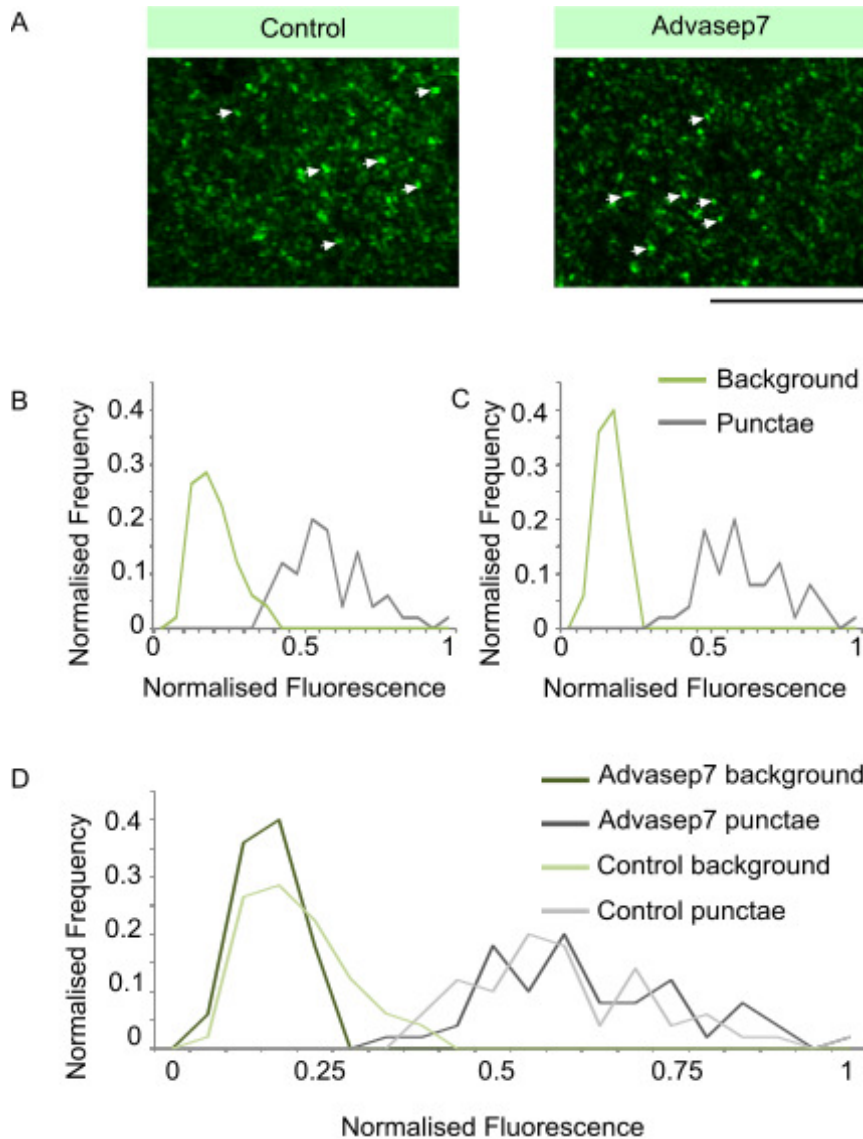


Figure 3.10 Using an FM-dye chelator to improve signal to noise ratio

A) Images of FM 1-43 labelled slices washed with either ACSF or 0.2 mM Advasep-7 ACSF for 20 min. B) In control samples there is a significant difference between the fluorescence levels in background regions compared to those in fluorescent punctae (background regions $n=50$, fluorescent punctae $n=50$, Student's t -test for unequal variance, $p < 0.0002$). C) In samples washed with Advasep-7 ACSF, the fluorescence levels were also significantly different in punctate and background regions (background regions $n=50$, fluorescent punctae, $n=50$, Student's t -test for unequal variance, $p < 0.0002$). D) The ratio between the background and punctate region fluorescence levels was significantly greater in Advasep-7 samples compared to controls (background regions $n=50$, fluorescent punctae, $n=50$, Student's t -test for unequal variance, $p < 0.02$).

3.3.5 Assay of function in native hippocampal terminals

The next important step was to determine the functionality of the fluorescent punctae that were observed. Assuming that the fluorescent signals correspond to healthy synaptic terminals, an expectation is that stimulation should evoke activity-dependent dye loss caused by exocytosis and subsequent dye departitioning. Similar to the method used in culture, we also used electrical stimulation to evoke dye destaining. After the wash out period, we located an area with numerous discrete punctae and low background fluorescence, and took a series of time lapse images of the region, with one image every 2 s. After ten slices had been collected to establish a baseline, a 10 Hz stimulus was applied for 90 s. Responsive punctae were then selected as regions of interest in ImageJ software, and the background levels of fluorescence were subtracted. Fluorescence levels were then normalised against the baseline levels (summarised in Fig.3.11.A).

The fluorescence level in the punctae was reduced dramatically following the start of the stimulus (examples shown in Fig.3.11.B.). When the fluorescence levels from ImageJ were plotted against time, they showed a profile demonstrating a maintained or slightly decreasing fluorescence level prior to the start of the stimulus, followed by an exponential decrease at the point at which the stimulus begins. The curves were significantly different from those seen in cultured neurons (Fig.3.11.C).

The exponential decay curves of the fluorescent signal in hippocampal slices showed an average time constant (τ) of 73.88 ± 4.0 s. Although not an order of magnitude different, this value was significantly slower than the rate obtained in cultured neurons using the same stimulation protocol (10 Hz destain in culture, $\tau=52.58 \pm 3.5$ s, two tailed Student's *t*-test, $p < 0.0005$). A longer time course of destaining in the slice system was consistent with the findings of (Pyle et al., 1999) who found a $\tau_{1/2}$ value of ~ 200 s compared to typical findings of a $\tau_{1/2}$ of ~ 30 s in cultured neurons (Ryan and Smith, 1995). One possible explanation for the discrepancy in rate between culture and native tissue is that in the confined and dense tissue of acute slice, dye released onto the membrane presumably does not diffuse and departition as efficiently, and perhaps even some undergoes reuptake into recycling vesicles (Fig.3.11.D) (culture, $n=107$ synapses from 3 coverslips, hippocampal slice, $n=112$ synapses from 6 slices, Student's *t*-test for unequal variance, $p < 0.02$).

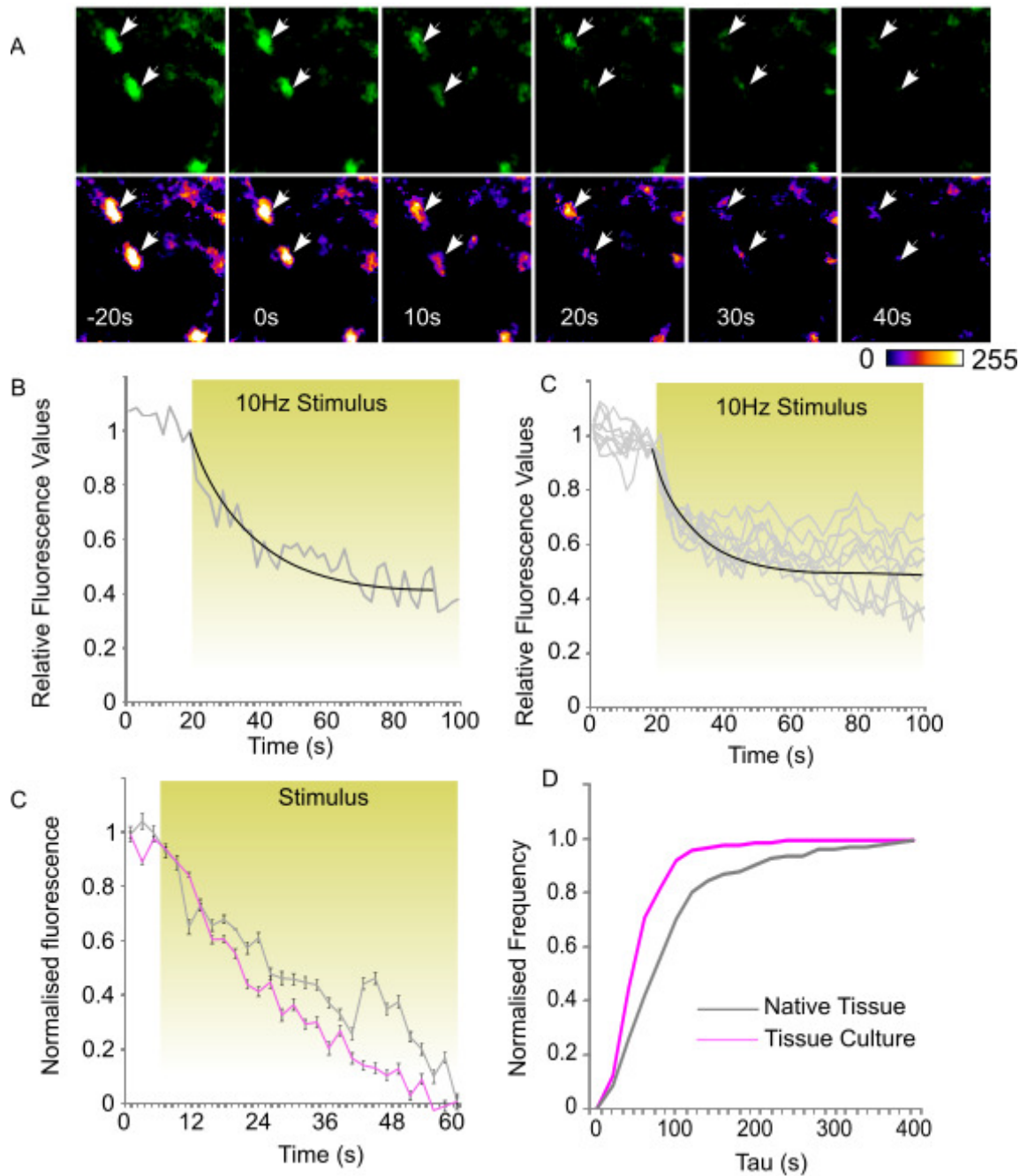


Figure 3.11 Visual assay of synaptic function in hippocampal slices using FM 1-43

A) Example puncta, labelled with FM 1-43. Upon stimulation, the puncta releases FM dye, leading to a loss of fluorescence. B) FM 1-43 destain curve from a single puncta within a slice. It demonstrates an exponential dye loss. C) Dye loss curves from 10 different puncta from one hippocampal slice. They demonstrate a wide variety of dye

loss rates, indicative of functional heterogeneity. C) Mean destain curve for synapses in cultured neurons (pink) and in hippocampal slices (grey). Both are normalised against the level of fluorescence immediately before fluorescence begins, and the fluorescence level once dye loss is complete. In tissue culture the curve is significantly steeper than that in culture (culture, $n=107$ synapses from 3 coverslips, hippocampal slice, $n=112$ synapses from 6 slices, Student's t -test for unequal variance, $p<0.02$). D) We calculated the time constant tau values for each exponential decay curve and produced a cumulative frequency plot. The time constants in tissue culture were significantly higher in native tissue than they were in cultured neurons, indicating that the rate of dye release was significantly slower (tissue culture, $n=107$ synapses from 3 coverslips, hippocampal slice, $n=112$ synapses from 6 slices, Student's t -test for unequal variance, $p<0.0002$).

3.3.6 Frequency dependent recycling in native terminals

In section 3.2.4 it was demonstrated that the dye release rate from cultured hippocampal terminals was frequency-dependent. Determining the dye loss described above to be frequency dependent is an important factor in verifying that we are exploiting the same exocytosis mechanisms seen in cultured neurons. In order to examine this important parameter in native tissue, we used trains of 10 Hz or 20 Hz action potentials to stimulate exocytosis within the terminals labelled with FM 1-43 in the presence of a 1200 AP/10 Hz stimulus, and recorded the resulting dye loss.

As previously shown in culture, faster destain profiles were demonstrated when a higher frequency stimulus was applied (e.g. Fig.3.12.A). Time constant tau values were significantly smaller at 20 Hz, $48.00 \text{ s} \pm 13.6 \text{ s}$, compared to $73.88 \text{ s} \pm 4.0 \text{ s}$ at 10 Hz (20 Hz, $n=43$ synapses in one slice, 10 Hz, $n=112$ synapses in 6 slices, Student's t -test for unequal variance, $p<0.002$), demonstrating that destain rates were quicker overall (Fig.3.12.A). There was also an increase in the standard deviation of the tau values, with those for synapses destained with a 10 Hz stimulus having a standard deviation of 50.65 s, whereas those for samples which were destained with 20 Hz were 86.95 s. This showed an increase in heterogeneity of the sample. This could be due to a higher frequency leading to activation of more synapses: those only activated at higher frequencies might have different destaining properties from those only activated at lower frequencies.

Interestingly, there was no significant difference in the tau values between 20 Hz destain slices in culture and in the hippocampal slice system. This points to 20 Hz frequencies reaching some sort of functional limit in how fast FM dye can be eliminated in synapses (20 Hz in slice, n=43 synapses in one slice, 20 Hz in cultured neurons, n=43 synapses in 2 coverslips, Student's *t*-test for unequal variance, not significant, $p=0.434$). The standard deviation of the tau values calculated for 20 Hz samples in culture was 48.48 s, compared to 86.98 s in slice, showing a widely increased heterogeneity.

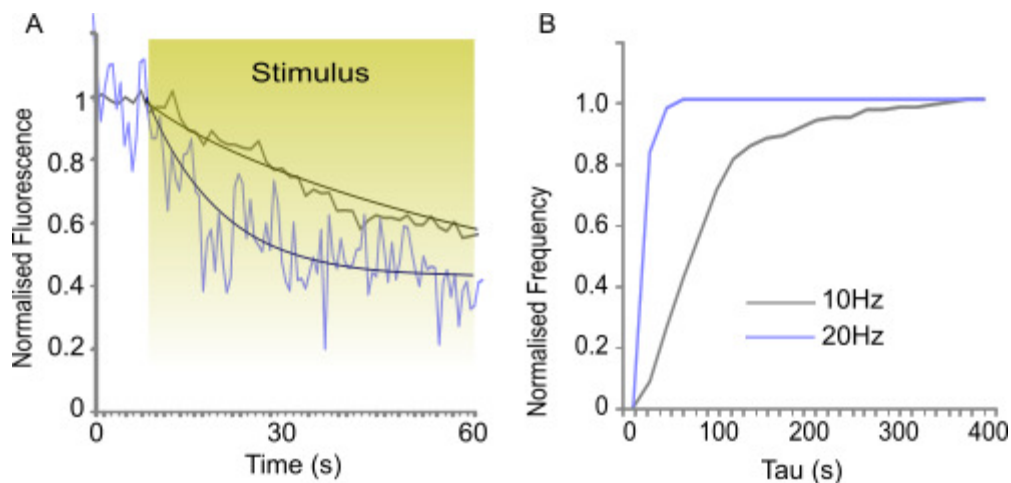


Figure 3.12 Release of FM 1-43 in native hippocampal terminals is frequency dependent

A) Representative fluorescence loss from a single puncta in a slice loaded with FM dye and exposed to a 20 Hz destaining stimulus (purple) or a 10 Hz destaining stimulus (grey). B) The time constant tau of the exponential decay curves of the fluorescence in labelled punctae in slices destained at 20 Hz vs 10 Hz were significantly higher (20 Hz, n=43 synapses in one slice, 10 Hz, n=112 synapses in 6 slices, Student's *t*-test for unequal variance, $p=<0.002$).

20 Hz destain image stack provided by Dr V Marra.

3.3.7 Alternative methods of viewing synaptic function in hippocampal slice

The approach demonstrated in this chapter provides a robust method of recording functional properties of live synapses in the slice system. In addition to the use of FM dye, we wanted to establish whether this method was suitable for use with other optical

probes of synaptic proteins and function. There are two main reasons for this. First, success with another probe would provide us with an independent validation of the punctate labelling we observe with FM dye. Second, there may be additional benefits of other synaptic reporters for readout of vesicle recycling properties.

Due to its photostability and specificity, we used the Synaptotagmin 1 Oyster550 antibody described in sections 3.2.2 and 3.2.5. As with FM dye, we applied the antibody by placing a 1:100 dilution of 1 mg/ml stock (working solution: 10 μ g/ml) in ACSF into the pipette and using a Picospritzer to pressure inject the dye into the tissue at 50 μ m below the surface of the slice. We then applied a 1200 AP/10 Hz stimulus to allow the antibody access to the interior of the vesicles. Following this, the slice was perfused with ACSF with AP-5 and CNQX for 20 min, to ensure that all unbound antibody was removed, and the slice was imaged using confocal microscopy (Fig.3.13.A).

On imaging hippocampal slices exposed to Sytl-Oyster550 and stimulated to induce uptake, small punctate regions were visible within the slice, as shown in Fig.3.13.B. The presence of high levels of fluorescence in punctae, like those seen in FM dye loaded samples indicates that the anti-synaptotagmin Oyster antibody has successfully labelled synapses in hippocampal slices.

These punctae can undergo a form of fluorescence loss on further stimulation, in a manner reminiscent of FM-dye (an example is shown in Fig.3.13.A). We speculated that this might be due to unbound antibody remaining within the vesicles, which is washed away causing a small drop in fluorescence. These had a mean time constant tau value of 63.61 ± 6.81 s (calculated from 44 synapses, from four slices from three animals) compared to the mean tau of 73.88 ± 4.02 s decay time constant of fluorescence loss seen when FM dye 1-43 is stimulated (calculated from 112 synapses, from 6 slices, from 6 animals). These values showed no significant difference ($p=0.951$, unpaired Student's *t*-test), indicating that these punctae do represent functional synapses and the mechanism of dye release is similar to that of FM dye. This dye could offer significant benefits for long-term imaging studies. This will be returned to in chapter 6.

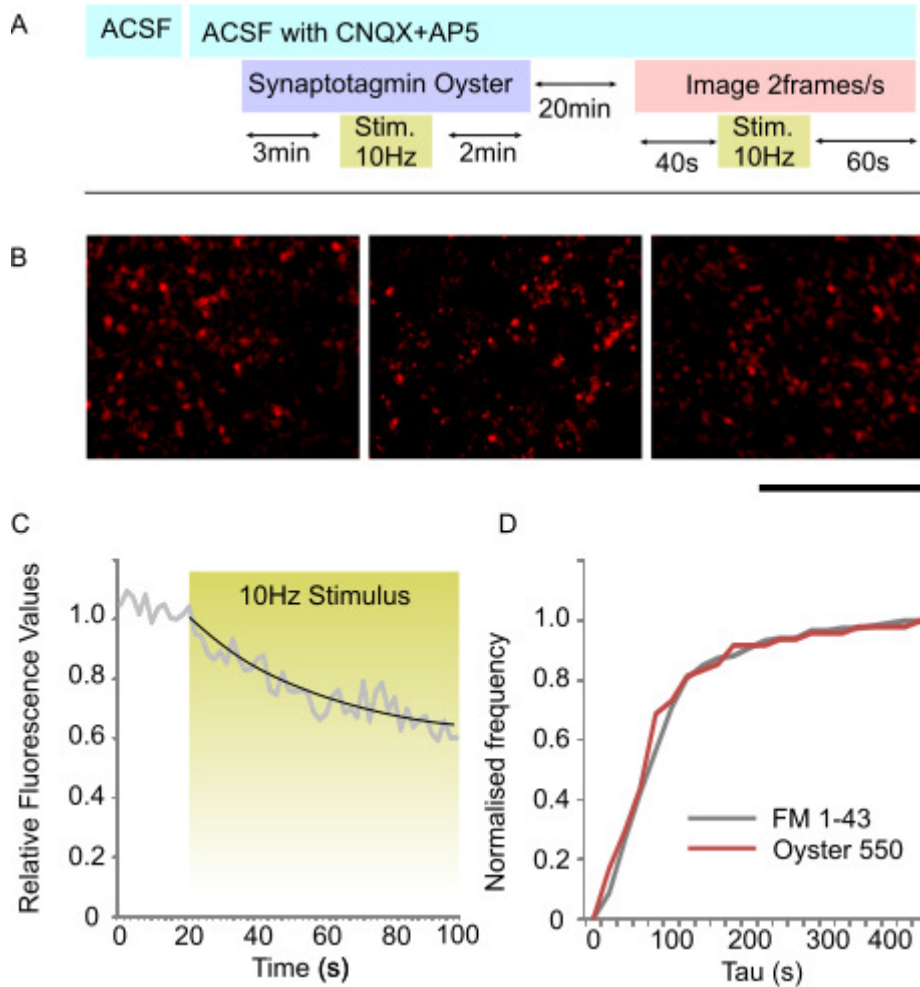


Figure 3.13 An alternate method of viewing functional synapses in the hippocampal slice system

A) Summary of the protocol for labelling hippocampal synapses with a 1:100 solution of syt/Oyster550 antibody, and obtaining readings relating to vesicle turnover. B) Examples of hippocampal slices labelled with syt/Oyster 550. The red punctae are indicative of functional synapses. Scale bar represents 20 μm . C) Example response from a single puncta, demonstrating exponential loss of fluorescent signal in response to stimulation. D) We calculated time constant tau values for the exponential dye loss curves of responsive punctae and compared them to those seen in FM 1-43 labelled synapses. There was no significant difference in the rates observed with these two probes (syt/Oyster550, n=44 synapses from 4 slices, FM 1-43, n=112 synapses from 6 slices, Student's *t*-test for unequal variance, not significant, $p=0.951$).

A second type of antibody-based probe, CypHer, offers the possibility for readout of endocytosis. We successfully trialled this probe in culture (section 3.2.5). Having established that we can adapt this protocol to label synapses with immunological probes, the next question was whether we could use a recently developed probe to look at another property of synaptic vesicle turnover, endocytosis.

Using a protocol as described above, we placed a 1:100 (10 $\mu\text{g/ml}$) solution of Sytl-CypHer5E in ACSF into the recording electrode, located a response from the tissue, and used a Picospritzer to apply the antibody to the tissue. We then exposed the tissue to a 1200 AP stimulus to allow the antibody access to the interior of synaptic vesicles. Following this, we imaged the tissue using confocal microscopy (Fig.3.14.A).

As with FM dye and anti-synaptotagmin Oyster, bright punctae were visible (Fig.3.14.B), indicating that we had successfully labelled native hippocampal synapses with the anti-synaptotagmin probe. We next had to ascertain whether we could use the pH dependent fluorescence of the probe to look at another functional property of the synapses. After imaging for 30 s to establish a baseline of fluorescence, we then applied a 300 AP/10 Hz stimulus to drive activity dependent vesicle recycling. We continued to image the sample for a further 90 s following the end of the stimulus.

Prior to the start of the 300 AP stimulus, there was no significant change in the levels of fluorescence detected (paired two-tailed Student's *t*-test $p=0.84$). At the end of the period of stimulation there was a significant decrease in the levels of fluorescence (paired Student's *t*-test $p=<0.0002$). This fluorescence loss happened with a mean time constant of 20.56 ± 5.12 s. In the time period following the completion of the stimulus the fluorescence returned to levels which were not significantly different from those recorded prior to stimulation (paired Student's *t*-test $p=0.07$), but they did show some fluorescence loss due to photobleaching (Fig.3.14.C, D). Fluorescence recovery occurred with a mean tau value of 29.35 ± 6.12 . This was very similar to that found in culture (31.61 ± 14.7 s, two-tailed Student's *t*-test, $p=0.887$) and was similar to values which might be expected from the literature.

This method is a potentially useful tool which allows a functional read-out of the dynamics of endocytosis in slice, without altering the genetic makeup of the animal, with

untold effects on functionality. However this method is not without its challenges. These results were taken from 11 punctae, from three slices from two animals. Though large numbers of punctae were visible, very few experienced fluorescence loss or recovery, many fewer than we typically observed in FM dye release experiments, or those using the sytI-Oyster550 antibody previously described. The CypHer5E ester has a molecular weight of 848, which is larger than the molecular weight of Oyster550 of approximately 720 (GE-Healthcare, 2006, Luminartis, 2011). This difference in the size of the molecules may have an effect on their ability to access the luminal domain of the synaptic vesicle. These values are both larger than the molecular weight of FM 1-43, even without the antibody attached. This may account for decreased levels of labelling observed. This suggests that the antibody may have trouble reaching its targets, or that non-specific labelling is occurring. Work needs to be done to optimise this method but it does allow successful imaging of endocytosis in native hippocampal terminals.

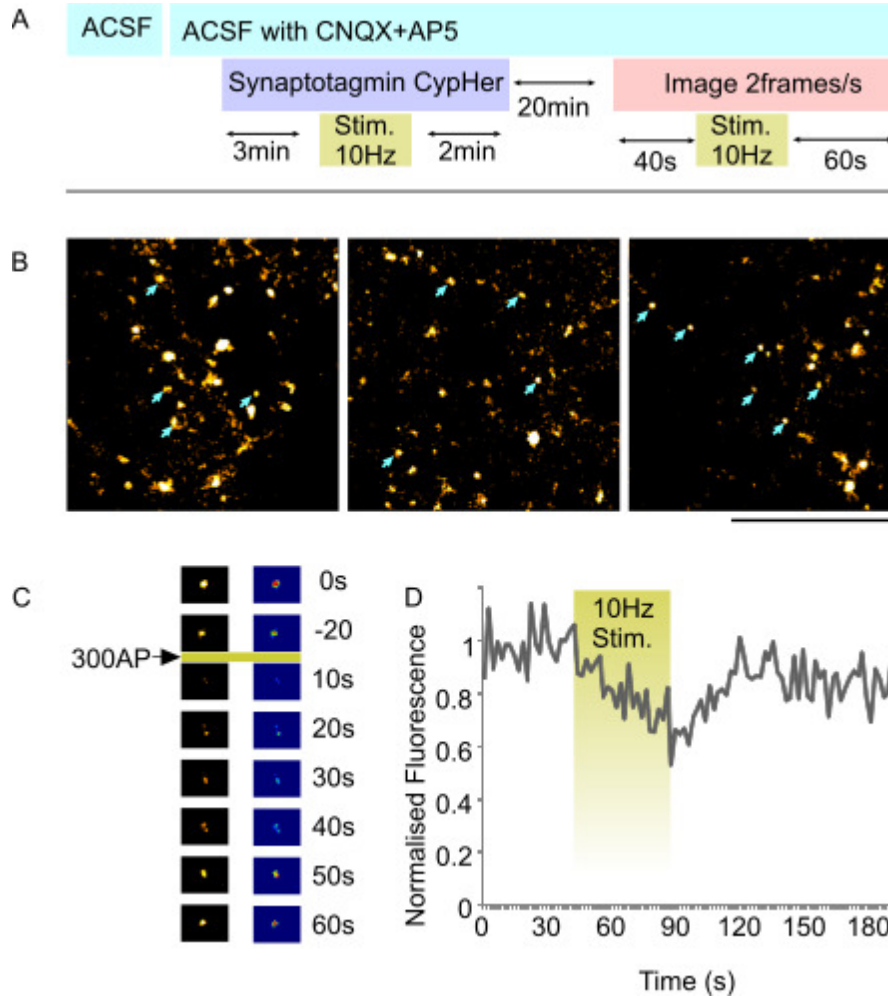


Figure 3.14 Observing endocytosis in the hippocampal slice system

A) Cartoon of protocol used to label hippocampal slices with 1:100 CypHer antibody and provide readout of endocytosis. B) Examples of slices labelled with CypHer, with functional synapses appearing as fluorescent punctae. Blue arrows indicate example functional synapses. Scale bar represents 20 μm . C) Example of a synapse undergoing fluorescence loss, indicating exocytosis and fluorescence recovery, a measure of endocytosis (shown in two different look-up tables). D) The curve of CypHer fluorescence profile in response to a stimulation protocol designed to allow observance of both endo and exocytosis.

3.4 Discussion

3.4.1 FM dye labelling and release from hippocampal neurons

Studies of function in hippocampal synapses are hugely important in providing information on the way that neurotransmission is supported, and provide an understanding of the fundamental processes which are altered in disease, plasticity, learning, and memory. Using activity-dependent optical probes has provided immense insight into the functional properties of synapses, and about the organisation and mechanisms of synaptic vesicles in cultured neurons. It was highly desirable to produce a reliable, robust method of labelling functional synapses using styryl dyes in a much more physiologically relevant system.

One of the major advantages of this dye is that labelling works effectively with its acute application to a neuronal preparation (within the extracellular solution) before activity-driven endocytosis. In this way, it offers excellent potential for use in native preparations where genetically-encoded constructs are not readily available. Here, the demonstration of successful dye-labelling experiments in cultured neurons is intended as an important experimental prerequisite for trialling the use of the same dye label in native tissue in the second half of the chapter, where the two labelled preparations, side by side, provide important information for a comparative study. Several studies had made steps towards being able to demonstrate FM dye labelling in the acute slice preparation, loading synapses through immersion of the slice in solutions of FM 1-43 and applying high potassium ACSF to generate activity to load the slice (Staras et al., 2010, Pyle et al., 1999). In Pyle et al. (1999), slices were imaged using confocal microscopy, producing poor results, with high levels of background staining.

Staras et al. (2010) obtained better results by imaging using a two-photon microscope. However, this provided a stimulus that was hard to control, and a two-photon microscope was not available for this work. A way to ensure clearer labelling using a confocal microscope was to pressure inject FM dye into the tissue, avoiding excess dye congregation in the dead tissue on the cut surface; this was drawn from Zakharenko et al. (2001). FM 1-43 was ejected into the slice using a patching pipette into the tissue, and uptake was stimulated using a bipolar tungsten pipette, providing a method of controlling activity absent in previous experiments. As demonstrated above, and in work done concurrently in the lab presented in Marra et al. (2012), this produced easily identifiable fluorescent punctae representing functional synapses.

We found that the rate of dye loss from vesicles in the total recycling pool had a time constant τ of 48 ± 14 s at 20 Hz and 74 ± 4 s at 10 Hz. These values were larger than those we observed in cultured neurons. Values for comparison in the literature are surprisingly hard to come by. In the paper by Marra et al. (2012), the work which uses the most similar method to the one stated here, despite comparing the tau values at different frequencies, they do not provide them. This is a common pattern with work on synaptic vesicle exocytosis. Similar techniques used by papers by Zakharenko et al. (2001) also do not state rate values, and use τ_{50} rather than τ to express their time constant information meaning that values are not comparable. From their graph, it appears that at 10 Hz, their values are approximately 20-25 s. Pyle et al. (1999) found their samples to have a half time constant of ~ 200 s at 10 Hz. From these values, we can see that comparing the tau values of FM dye destaining in slice between different systems can provide wildly different answers, and can gain some idea why studies only compare the rates within similar systems.

There is a greater degree of agreement in cultured neurons on the half time constants of FM dye release following 10 Hz stimulus. Values of 20-30 s for FM 1-43 dye loss were found in studies by Ryan and Smith (1995) and Klingauf et al. (1998), and this value was confirmed in studies using FM 4-64 (Welzel et al., 2011), which has similar partitioning properties (Wu et al., 2009). These values give approximately a similar tau value to the ones seen in our experiments.

Despite the difficulty in obtaining conclusive measures of the kinetics of dye release from the literature, the dye elimination was significantly slower and the standard deviation was higher. This is an excellent indicator as to why a more physiologically relevant model is needed for study: the significantly lower rates could be caused by normal physiological activity shaping synaptic function (Moulder et al., 2006).

3.4.2 Immunological methods for studying functional properties in hippocampal slice

We also demonstrate that this method has use in the application of other probes, such as those with an immunological tag. The luminal domain of synaptotagmin is a target used by both probes described in this chapter. Access to the lumen only occurs when the fusion pore is open, meaning that these too provide a measure of labelling functional vesicles. Though syt1Oyster provides a read out of activity-dependent dye loss, its higher affinity for the epitope of synaptotagmin I means that it is much more

difficult to remove from the vesicle, making it good for longer term experiments, but worse for studying vesicle turnover. Styl-CypHer5E is a pH-dependent probe, giving off fluorescence at 663 nm when protonated, and becoming quenched at neutral pHs (Briggs et al., 2000). Its mechanism of providing endocytosis information is similar to that of synaptophluorin and sypHy, both of which exploit pH dependent probes and the difference in pH between the acidic environment of the interior of the vesicle and the more neutral pH of the synaptic cleft (Granseth and Lagnado, 2008, Royle et al., 2008). An advantage over other methods of measuring endocytosis is that this one can be used via acute application rather than via transfection into cultured neurons.

The main use for CypHer so far has been to track GPCRs as they are internalised in response to agonist stimulation and moved to endosomes for recycling, producing a desensitisation effect (Adie et al., 2002, Perez-Aso et al., 2013). It has also been used to gain information about the structural arrangement of vesicular transporter proteins by tagging against short chains of VGAT proteins to determine whether these fragments were located within the vesicle or not (Martens et al., 2008).

Raised against synaptotagmin1, CypHer5E has been previously used only to confirm that other functional probes are accurately labelling functional synapses (Welzel et al., 2011). This chapter demonstrates the first use of CypHer to measure properties of synaptic vesicle recycling. In our hands, we found that CypHer can provide a suitable method for measuring endocytosis, but very few synapses in each labelled preparation displayed the desired dye-loss-and-recovery profile, meaning that large numbers of recordings would have to be taken. In cultured neurons, this would prove difficult, as CypHer is incredibly prone to photobleaching and the fluorescent light illuminates the entire sample during imaging. In hippocampal slices, we found that there was less noticeable photobleaching, so regions could be imaged more freely. Confocal imaging illuminates only a small, specific region of the slice, which combined with the antibody labelling leading to very little dissociation of the probe from vesicle lumens, means that the slice may undergo many rounds of stimulation, and multiple regions can be imaged from each slice. An advantage to CypHer5E should be that it can be used for co-localisation studies with other probes. However FM dyes, which are major functional probes in synaptic function studies, quench the fluorescence of CypHer5E (Welzel et al., 2013). This reduces the dual fluorescence studies which can be run in this model, limiting future use.

Unfortunately, tagging a protein does not allow for tracking of individual vesicles through multiple rounds of stimulation, only the tracking of a protein. Kononenko et al. (2013) found that vesicle identities are not conserved on recycling, but instead form a pool on the membrane and are sorted to ensure that the newly formed vesicles contain the correct proportions of vesicles. This is not an issue on the first round of stimulation, but means this tool is not suitable for tracking vesicle identity over multiple rounds.

3.4.3 Future development for methods of studying vesicle properties in slice

A major way that the physiological relevance of this technique may be increased is by conducting these experiments at physiological temperature. Previous work has found that the rate of endocytosis is highly temperature dependent (Renden and von Gersdorff, 2007, Fernandez-Alfonso and Ryan, 2004). Electron microscopy studies of synapses loaded with HRP at physiological temperatures show an increased number of large endocytic structures (Micheva and Smith, 2005), indicating that fast endocytosis plays a higher role in synaptic vesicle recycling than studies at room temperature would indicate. Further evidence towards this being the case is that the rate of 'slow' endocytosis in experiments at physiological temperature is similar to the rate of endocytosis at room temperature (Renden and von Gersdorff, 2007). This confirms the findings of Watanabe et al. (2014), which suggest that there is an ultrafast mode of endocytosis, which involves the recruitment of large vesicles, which then join into endosomes

The rate of exocytosis at physiological temperature is not so conclusive a story. Some studies have found the rate of exocytosis to be unchanged by an increase in temperature (Fernandez-Alfonso and Ryan, 2004), whereas others have shown there to be an increase (Micheva and Smith, 2005). Decreases in release probability and increases in refilling have been shown (Pyott and Rosenmund, 2002). A key finding of research into the temperature dependence of synaptic vesicle recycling is that the size of the recycling pool has been shown to double at physiological temperature (Renden and von Gersdorff, 2007), similar to the results we saw on conducting similar experiments. This brings results closer to those seen by Rose et al. (2013), suggesting that the striking difference between their calculations of the size of the recycling pool and those commonly seen in FM dye based experiments was not due to a flaw in the labelling mechanism of FM dye, but due to their experiments being conducted at

physiological temperatures. Future work improving the stability of these experiments at higher temperatures would improve their physiological relevance and provide key new insight on the behaviour of vesicles *in vivo*. The method outlined in this chapter is highly suitable for further study and presents an important step forward in terms of the physiological relevance of hippocampal study.

3.5 Acknowledgements

Additional cultures were supplied by Ms MM Wagner (Fig.3.2), who also provided assistance for high frame rate imaging. Dr JA Ratnayaka assisted in providing image series of syt1Oyster550 (Fig.3.5) and syt1CypHer5E labelling and responses in cultured neurons (Fig.3.6). 20 Hz destain in tissue provided by Dr V Marra (Fig.3.12).

Chapter 4: Characterising release ready vesicles in acute slice preparation

4.1 Introduction

The previous chapter outlined an approach for using fluorescent probes to study functional properties of synapses in the hippocampal slice system. This approach offers important information about the activity of functional vesicles and the efficiency of neurotransmission in native synapses; however, it gives little insight into the size of recycling fractions, the arrangement of recycling and non-recycling vesicles within the terminal, and the relationship between vesicles and their ultrastructural context. Though newly developed methods, such as Qdots (Park et al., 2012), allow a real-time readout of data with nanoscale resolution, these have their own problems, such as concerns about probe access and technical challenges in providing a readout of the entire pool. They also do not provide any information about unlabelled vesicles or the detailed arrangement of functional vesicles in relation to other structures (e.g. active zones) or organelles (e.g. mitochondria). To investigate these properties, it was desirable to develop an ultrastructural approach. A major advantage of FM dyes is that they can be used to photoconvert DAB into an electron-dense product, allowing labelled vesicles to be specifically identified in EM (Henkel et al., 1996).

This reaction has previously been used to allow a nanoscale examination of recycling vesicles in large peripheral terminals such as neuromuscular junctions (Denker et al., 2011, Denker et al., 2009, Henkel et al., 1996, Richards et al., 2000, Richards et al., 2003, Rizzoli and Betz, 2004), large central terminals such as the calyx of Held (de Lange et al., 2003), and cultured hippocampal neurons (Branco et al., 2010, Darcy et al., 2006, Harata et al., 2001, Ratnayaka et al., 2011, Ratnayaka et al., 2012, Schikorski and Stevens, 2001, Staras et al., 2010). Studies of ultrastructure of recycling vesicles have been made in the calyx of Held in slice, using FM dye injected *in vivo* (Denker et al., 2011). However, small, central terminals in native tissue remain largely unexplored,

with only Marra et al. (2012) examining the recycling vesicles in the hippocampal slice system – a study conducted in parallel with this work. Whereas Marra et al. focused on the characteristics of the total recycling pool, this chapter aims to use the same approach to characterise the properties of the readily releasable pool (RRP).

The RRP comprises the vesicle population at synaptic terminals that is the first to be released when exposed to a minimal stimulus (Rosenmund and Stevens, 1996). The RRP was initially defined by whole-cell current clamp recordings of mEPSPs of cells exposed to a hyperosmotic sucrose solution to stimulate exocytosis. The recorded rate of exocytosis was initially rapid, before dropping exponentially (Stevens and Tsujimoto, 1995). It was hypothesised that this result was due to the initial peak being caused by the release of vesicles from docking sites, and the time taken for new vesicles to be moved into position. It was found that a train of 10 AP at 20 Hz would have a similar effect (Rosenmund and Stevens, 1996). The response to a hyperosmotic challenge is also an indicator that these vesicles correspond with vesicles docked at the active zone. A previous study of functional RRP vesicles at an ultrastructural level found that the recycling fraction and the docked pool size were equivalent (Schikorski and Stevens, 2001).

Characterisation of the RRP is an interesting focus of study, not only because the low stimulus levels required to label it are well within the physiological range (Mizuseki and Buzsaki, 2013, Csicsvari et al., 1999), but also because the vesicles have a very specific functional definition and their positions prior to labelling with FM dye can be presumed. Previous studies have claimed that RRP vesicles are preferentially reused for further activity (Pyle et al., 2000, Rizzoli and Betz, 2004) and retain a specific identity; however, there is also evidence that membership of the recycling pool is transient and that, following reuptake, a new population is recruited to the recycling pool (Atluri and Ryan, 2006, Li et al., 2005). When studying FM dye labelled vesicles, the pool under observation comprises vesicles that were previously at docking sites and were amongst the first vesicles released; this makes it an excellent tool for studying the fate of these vesicles, to attempt to resolve these results.

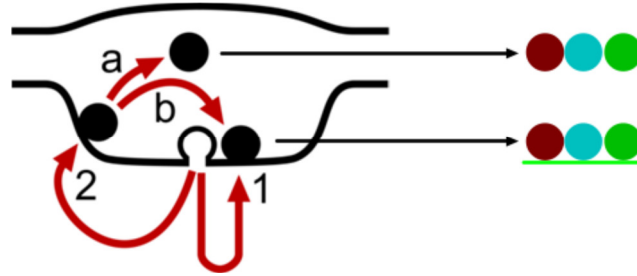


Figure 4.1 Possible routes of vesicle re-entry and reuse

Schematic describing possible routes of vesicle re-entry and reuse. Vesicles may be retrieved either at the active zone (1) or at sites away from the active zone (2). On re-entry, vesicles might be returned to the cluster with no preferential positioning (a) or returned to positions near the active zone (b). At this point (a) or (b), they might either be preferentially handled for reuse, recycled in line with the rest of the pool, or moved into the resting pool (indicated by the brown, blue, and green balls).

This chapter aims to use the method described in the previous chapter to obtain a functional readout of the RRP in the hippocampal slice system, and then to develop a method to label RRP vesicles for nanoscale analysis under an electron microscope. This approach is then used to establish whether this RRP vesicle reuse is reflected in the arrangement of recycling vesicles within the terminal. To determine this, a key element is to look at the fate of RRP vesicles following recycling. Following fusion, there are several possible routes for a recycling vesicle (summarised in Fig.4.1). The vesicle must first re-enter the synapse. This might occur at the active zone, either via a rapid, possibly kiss-and-run style, event, or via slower clathrin-based endocytosis, or reuptake may occur at sites away from the active zone. Upon reuptake, the next question is how these vesicles become repositioned in the terminal with time: do they take up a segregated place near the active zone, or do they become randomly distributed in the vesicle pool as a whole? Understanding the regulation and timing of vesicle fate offers key insights about whether the RRP represents a unique sub-population of vesicles, one that is selectively labelled and preferentially handled to support ongoing transmission. The experiments in this chapter aim to address these questions.

4.2 Ultrastructural properties of RRP vesicles in the hippocampal slice system

4.2.1 Establishing a robust method of labelling the RRP in native tissue

In the previous chapter, I outlined the method for labelling synaptic vesicles in the acute hippocampal slice preparation with FM dye in order to provide functional readouts of vesicle labelling and recycling. This approach makes use of a saturating stimulus to label the total recycling pool; in other words, accessing all the recycling vesicles. This is a convenient pool for study because it has a large signal in fluorescence; however, its physiological value is less clear, given that it requires a stimulation loading protocol that far exceeds the physiological firing patterns of these hippocampal neurons (Mizuseki and Buzsaki, 2013, Csicsvari et al., 1999). Here, the aim was to characterise a pool with substantially more relevance to the operational performance of the terminal, the RRP. We elected to use a protocol consisting of 40 AP at 20 Hz. This stimulus duration is shorter than the time period for the RRP to replenish and has been used previously to label the RRP (Burrone et al., 2006, Li et al., 2005, Murthy et al., 1997, Murthy and Stevens, 1999, Schikorski and Stevens, 2001) (for protocol, see Fig.4.2.A).

Labelling and imaging procedures were broadly similar to those described in the previous chapter. Briefly, after locating an fEPSP response to a stimulus to the Schaffer collaterals, we applied FM 1-43FX, a fixable analogue of FM dye, for 3 min to allow saturation of the tissue with FM dye, and then delivered a 40 AP/20 Hz stimulus. FM application was allowed to continue for 2 min to allow recycling to complete. Samples were then allowed to wash for 20 min to remove excess FM dye. Subsequently, samples were imaged using confocal microscopy. Similar to labelling of the TRP described in the previous chapter, discrete bright punctae were visible, offering us the first view of the RRP in native hippocampal synapses. As might be expected, the fluorescence levels of the punctae representing RRP terminals were strikingly lower than those found in TRP-labelled synapses (see Fig.4.2.B). When samples with the TRP labelled and samples with the RRP labelled were imaged with identical settings and compared, the fluorescence levels in the RRP punctae corresponded to $13 \pm 5.6\%$ of that of the total recycling pool. This was a significant difference in fluorescence (Student's *t*-test, unequal variance, $n=60$ synapses from 3 slices, $p < 0.005$).

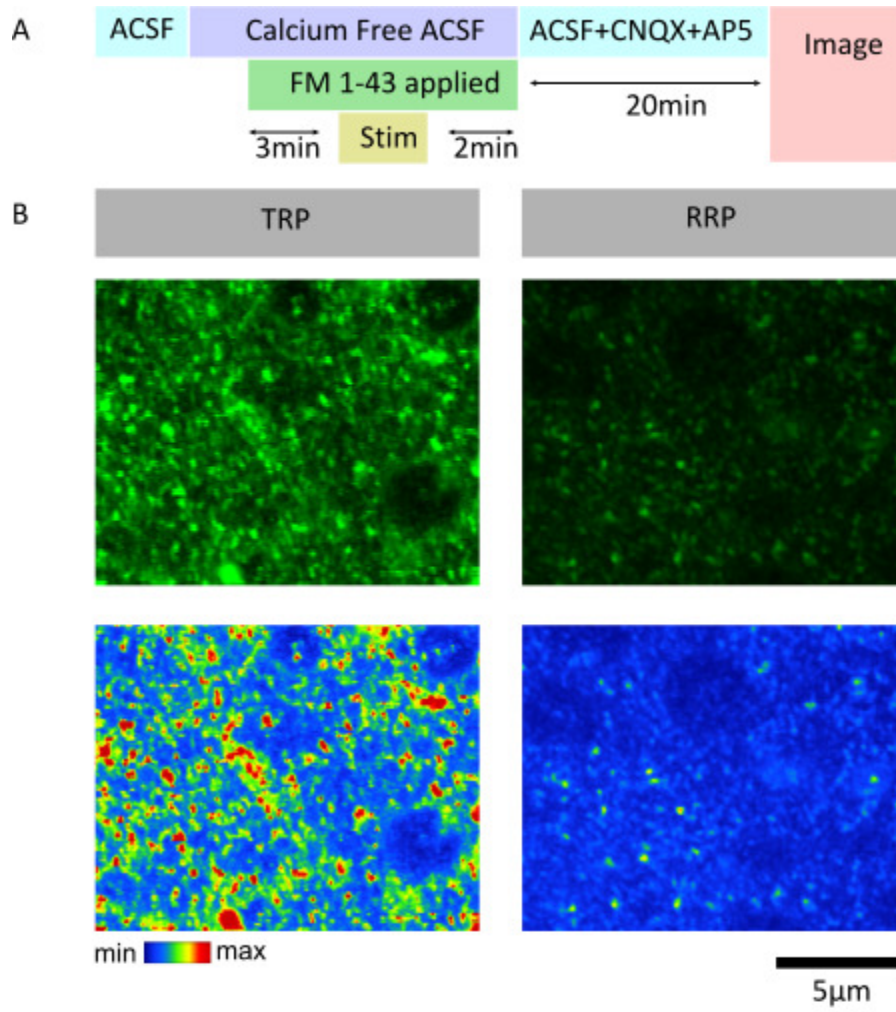


Figure 4.2 Lower levels of fluorescence labelling of RRP compared to TRP

A) Synapses in hippocampal slices were exposed to FM dye and then a stimulation of 1200 AP at 10 Hz (TRP) or 40 AP at 20 Hz (RRP) was applied to the tissue. B) TRP labelled synapses exhibited a much higher level of labelling compared to RRP synapses, when imaged using identical microscope settings. C) This corresponded to $13 \pm 5.6\%$ of the fluorescence values of the TRP (Student's *t*-test, unequal variance, $n=60$ synapses from 3 slices, $p < 0.005$)

4.2.2 Development of a procedure for photoconversion of the RRP

Having successfully established robust labelling of RRP vesicles, the next objective was to adapt a method previously established in cultured neurons and other systems for use with hippocampal slices. The method outlined in this section is described in detail in both the Methods chapter (section 2.5) and in Marra, Burden, Crawford and Staras (2014).

After the slice had been labelled as described in section 4.2.1, the next step was to halt vesicle activity. Because of the mobile nature of vesicles and the relative fragility of a fluorescent probe, it was not possible to allow several hours for fixation through immersion in fixative alone to take place. Instead, we used rapid microwave fixation with 6% glutaraldehyde and 2% paraformaldehyde to allow complete fixation of the slice in under a minute (Jensen and Harris, 1989). The slice was then placed into a 1 mg/ml DAB solution bubbled with 95% O₂ / 5% CO₂ and incubated for 10 min. The solution was then refreshed and the sample illuminated with 480 nm light with a mercury lamp until a black photoconverted spot formed on the surface of the slice. The slice was imaged to allow later relocation of this area, as this spot indicates the region of interest. The sample was then processed for electron microscopy, including fixation with osmium tetroxide and potassium ferrocyanide, heavy metal staining with uranyl acetate and dehydration, before being embedded in EPON resin and polymerised at 60°C. Sections were then produced at 70 nm thickness and placed on nickel grids and examined under a transmission electron microscope (summarised in Fig.4.3.A).

When sections from within the region of interest were examined under the electron microscope, black vesicles were visible within synapses, distinct in appearance from the other vesicles present (see Fig.4.3.B).

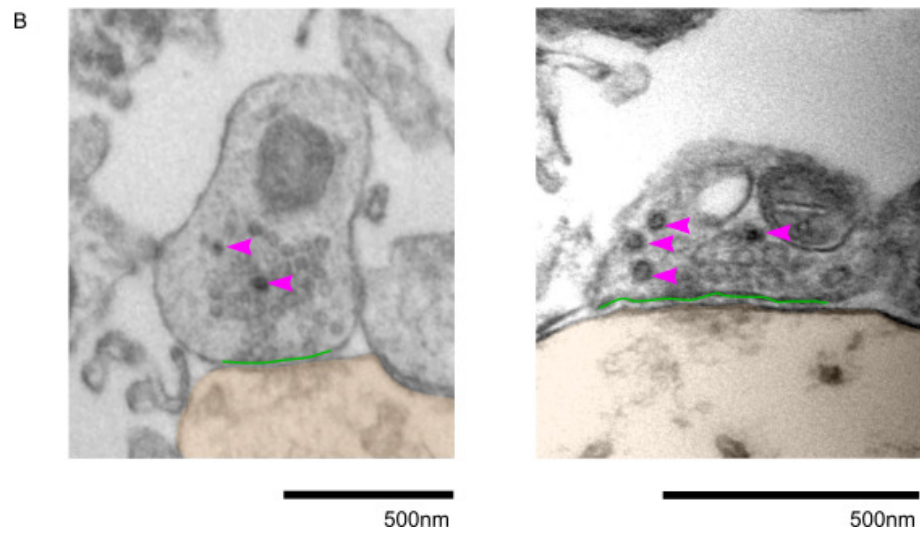
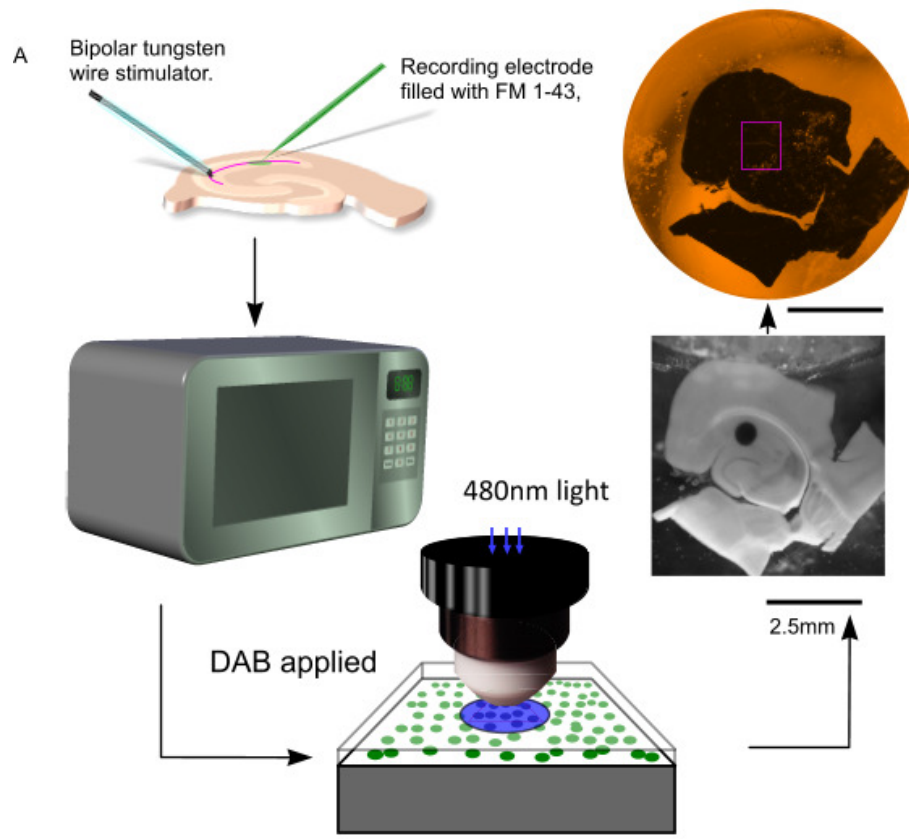


Figure 4.3 Photoconversion of DAB labelled functional vesicles at an ultrastructural level

A) Synaptic vesicles in slices were labelled with FM 1-43FX as described in the previous chapter, and were then fixed in glutaraldehyde and formaldehyde using rapid microwave fixation. Samples were then incubated in 1 mg/ml DAB solution and irradiated with light at 480 nm by a mercury lamp. This produced a black region of interest on the surface of the slice. Samples were then fixed for electron microscopy, dehydrated and embedded in EPON resin blocks. The region of interest was then located and sectioned for electron microscopy. B) At an ultrastructural level, synapses with a clear active zone and photoconverted vesicles were selected. Pink arrows indicate photoconverted vesicles, green line indicates the active zone. Postsynaptic region labelled in orange.

4.2.3 Characteristics of photoconverted vesicles

It was important to be able to identify recycling vesicles routinely and reliably within terminals in order to ensure uniform analysis across the sampled vesicle population. To do this, we had to establish a series of rules for identifying photoconverted vesicles.

Non-photoconverted vesicles have a dark membrane with the central lumen being similar in appearance to the surrounding environment in the terminal. Photoconverted vesicles have the same dark membrane, but they have an even darker lumen, filled with electron dense material where FM 1-43 was present to drive the photoconversion of DAB (Lubke, 1993) (see Fig.4.4.A). When a plot of the absorbance of these vesicles across their diameter is taken, non-photoconverted vesicles show a profile with a high absorbance in the membrane, but a lower absorbance in the lumen, similar to that outside the membrane. Photoconverted vesicles have a domed profile, with the lumen having a greater absorbance than even the membrane surrounding it (Fig.4.4.B).

In order to check whether there might be confusion between photoconverted and non-photoconverted vesicles under these criteria, the absorbance was measured from a 3 pixel diameter spot in the centre of the lumen of 50 photoconverted and 50 non-converted vesicles. Whereas the density of photoconverted vesicles varied widely, the lumen density of non-photoconverted vesicles showed less variation. The groups did not show any overlap of lumen density so this was determined to be sufficient for photoconverted vesicle identification (Fig.4.4.C).

The presence of photoconverted vesicles indicated that the synapse had been activated by the applied stimulus. As can be seen in Fig.4.5.A, synapses proximal to those

containing photoconverted vesicles do not necessarily contain photoconverted vesicles themselves, suggesting that they do not receive activation by the portion of the Schaffer collaterals that we stimulated. This was confirmed in samples that were exposed to FM dye and photoconverted, but with no stimulus applied. In this case, no photoconverted vesicles were visible in any synapses (Fig.4.5.B).

The black vesicles were a result of photoconversion, as sections taken from outside the photoconverted region (indicated by the black spot – see Fig.4.2.A) contained no photoconverted vesicles (e.g. Fig.4.5.C).

Another possible problem with regards to misidentifying photoconverted vesicles are artefacts and other structures which also appear electron dense under the microscope. Synaptic vesicles typically have a distinctive round shape and a diameter of 40-60 nm (De Robertis, 1965). Artefacts smaller than this, or of a different shape were eliminated on this basis (Fig.4.5.D). Large dense core vesicles, which are involved in neuropeptide transmission, also appear in synaptic terminals, and naturally have a black lumen without photoconversion. These vesicles are unlikely to be confused with small synaptic vesicles, owing to their large size (100-300 nm) (Torrealba and Carrasco, 2004) (see Fig.4.5.E).

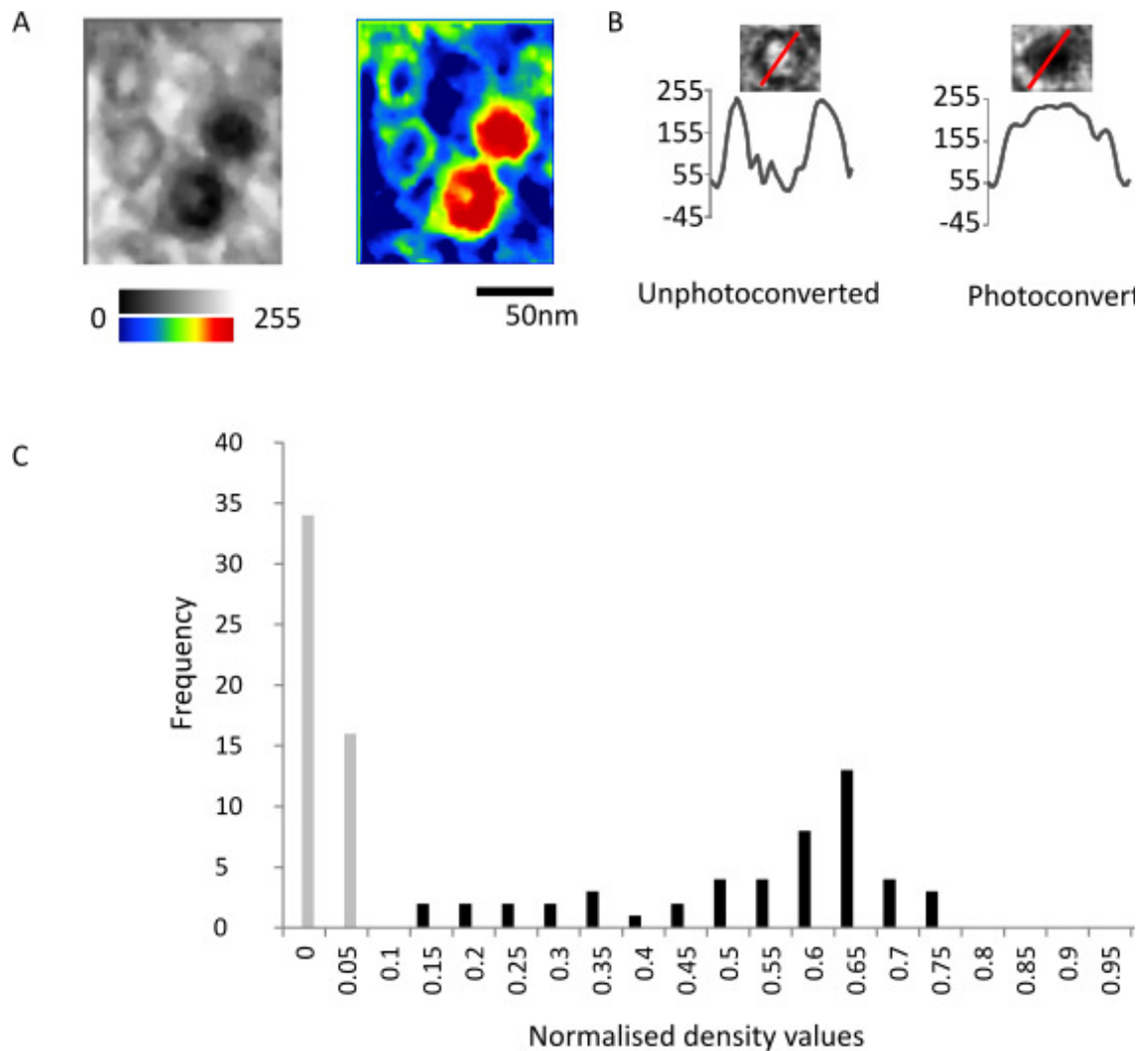


Figure 4.4 Photoconverted vesicles are readily identifiable under the electron microscope.

A) Photoconverted vesicles have a dark lumen, compared to non-photoconverted vesicles which have a paler lumen. B) Photoconverted vesicles give a density profile with the highest density in the lumen, at least as dense or denser than the surrounding membrane; in non-photoconverted vesicles, the membrane is the most electron-dense part, with the lumen being closer in electron density to the space around the vesicles. C) The electron density of the lumen of non-photoconverted vesicles had a smaller range and was much lower, compared to photoconverted vesicles, which had a larger range across the higher electron densities (n=50 photoconverted and n=50 non-photoconverted vesicles). Black bars represent the electron density of the central lumen of the photoconverted vesicles, and grey bars represent the central lumen of non-photoconverted vesicles.

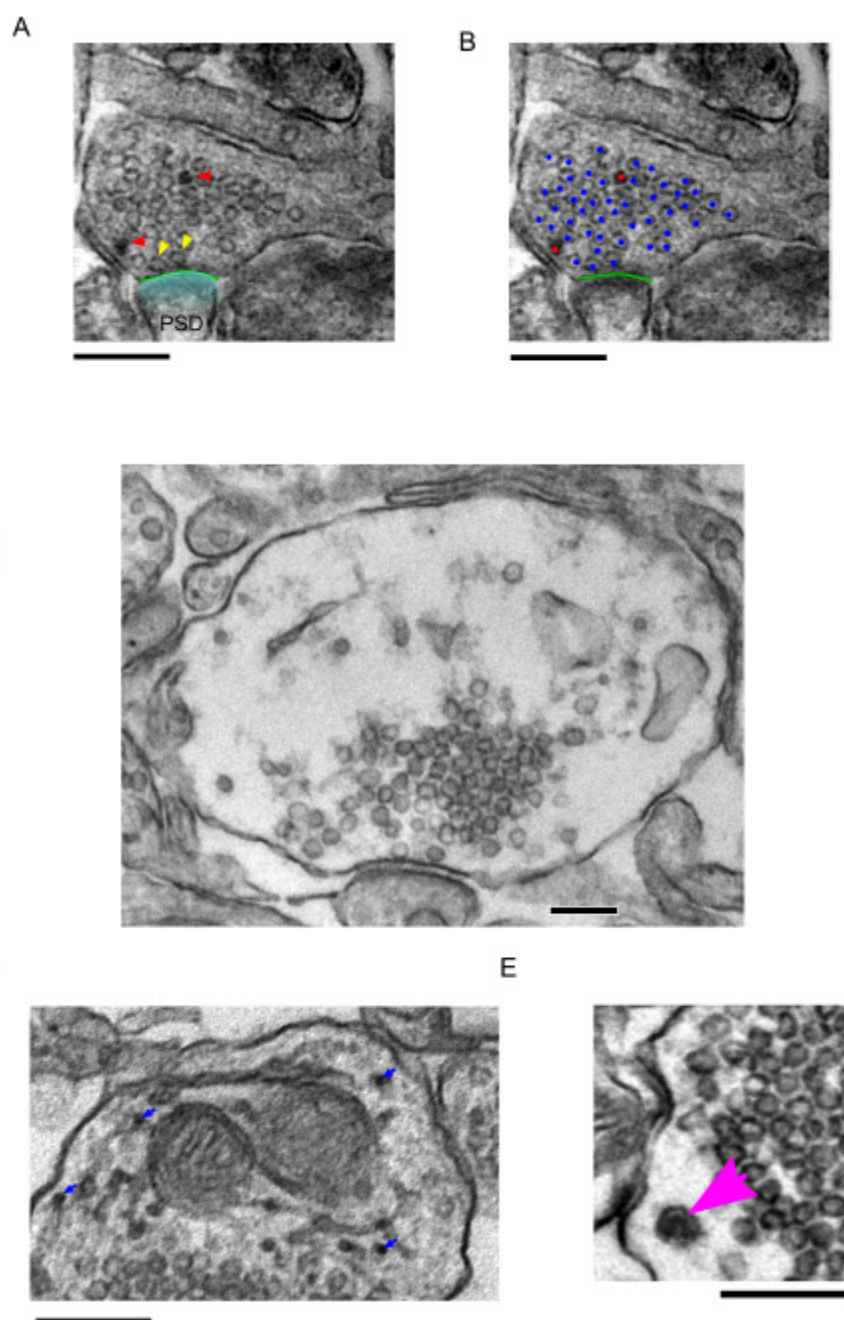


Figure 4.5 Black vesicles are specific to FM dye loading and photoconversion

A) Sections containing a complete cross-section of a synapse, an active zone and photoconverted vesicles were selected for analysis. PSD - postsynaptic density (shaded blue), green line indicates active zone, yellow arrows indicate docked vesicles, red arrows indicate photoconverted vesicles. C) For analysis, vesicles were classified as either photoconverted or non-photoconverted, and the active zone was defined. Blue indicates non-recycling vesicles, red indicates recycling vesicles. Green indicates the active zone. C) Outside of the photoconverted region, no photoconverted vesicles are present. Not all synapses within photoconverted region contain photoconverted vesicles. D) Electron-dense artefacts may be present, but these can be distinguished from photoconverted vesicles by their size and shape. E) Large dense core vesicles also have a black appearance, but they have a typical diameter of 80-120 nm and can therefore easily be distinguished from photoconverted vesicles. All scale bars indicate 200 nm.

4.2.4 RRP vesicles as a fraction of the total pool

The first question was to establish the size of the RRP in native terminals. In order to do this, synapses were labelled with FM 1-43FX and photoconverted using the method described above. Sections from these samples were observed under the electron microscope. Synapses containing photoconverted vesicles were selected for analysis on the basis of having a complete membrane around the synaptic vesicle cluster, a visible active zone, identified by the presence of a postsynaptic density, and docked vesicles (e.g. Fig.4.5.A). Vesicles were classified as photoconverted or non-photoconverted and the active zone was labelled. These features could then be used for analysis.

Recycling vesicles corresponding to the RRP make up $5.518 \pm 2.81\%$ of the total pool (Fig.4.5.B), a value highly consistent with that reported for RRP size in a previous study using cultured neurons (5.4% in Schikorski and Stevens, 2001) (n=56 synapses from 4 animals). It is noteworthy that this value appears to be a little higher than that indicated by our fluorescence data (Fig.4.2 and section 4.2.1), but the estimates based on the latter approach were made using a two-step process where errors in estimation are likely to be compounded: first, it involved estimating the fraction of the TRP represented by the RRP, and second, by estimating the fraction of the total pool represented by the TRP, a value which is known to have high heterogeneity between samples and is typically between 20 and 40% (Darcy et al., 2006, Denker et al., 2011, Harata et al., 2001, Marra et al., 2014). Given the errors in fluorescence-based measurements in

acute tissue slices, these values seem to be in reasonable agreement with those from the ultrastructure-based analysis.

The results outlined so far provide a promising initial characterisation of the pool. Next, to look at the fate of recycling RRP vesicles, we designed a protocol that would capture the positional organisation of vesicles at three time points post stimulus. The time points selected were 1 min after fixation, 5 min after fixation, and 20 min after fixation. The minimum time period allowed by this particular method was 1 min, which incorporated 45 s to allow recycling to complete. These will be referred to as the RRP 1 min, RRP 5 min, and RRP 20 min respectively throughout the rest of this chapter.

We first established the RRP fractional size at these three time points. Notably we found that the percentage of RRP vesicles was extremely stable across these time points, showing 5.7 ± 0.42 , at 1 min ($n=11$ synapses), $5.8 \pm 0.52\%$ at 5 min ($n=15$ synapses), and $5.02 \pm 0.47\%$ at 20 min ($n=25$ synapses) (Fig.4.6.A). A one-way ANOVA revealed no significant difference ($p=0.50$) (Fig.4.6.A). The distribution of RRP fractions within the sampled synapses was also similar at all time points, and showed no significant differences over time (Fig.4.6.B). This finding is important, indicating that time after stimulation does not result in vesicle loss due to release, giving us further confidence in the value of this approach for readout of vesicle fate over time.

We also examined the relationship between RRP size and total pool size. We found that the number of vesicles in the RRP was correlated with the size of the total number of vesicles in each section, with the number of recycling vesicles increasing with total pool size (Fig.4.6.C). Nonetheless, the recycling fraction was not correlated with total pool size; in other words, with larger synapses did not have a larger proportion of RRP vesicles (Fig.4.6.D).

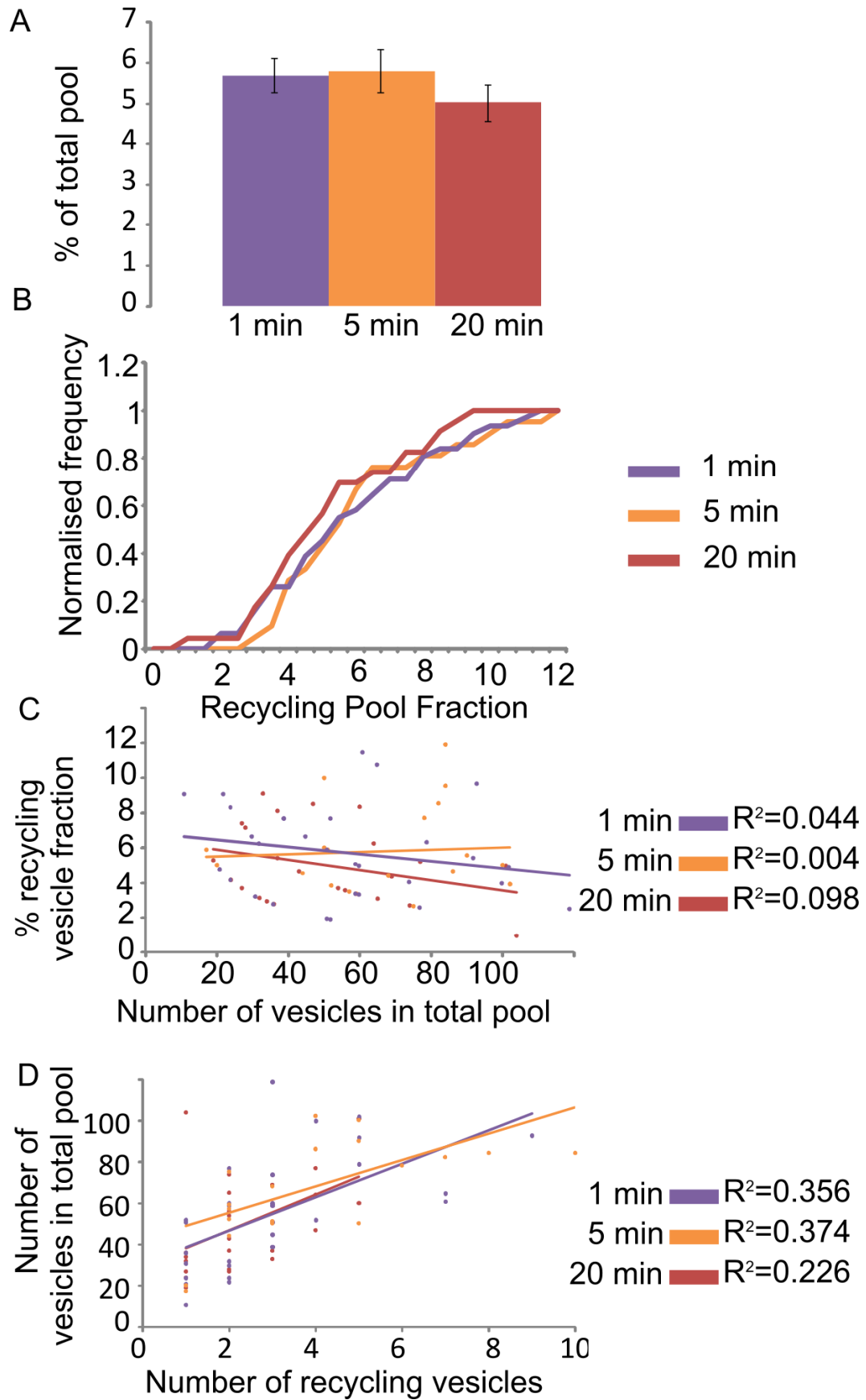


Figure 4.6 Recycling pool fraction is stable over time and is not related to synapse size

A) In slices fixed 20 min, 5 min, or 1 min following stimulation, the recycling fraction was $5.017 \pm 0.469\%$, $5.805 \pm 0.522\%$, and $5.695 \pm 0.422\%$, respectively. There was no significant difference between recycling fractions at any of the time points. B) Nor was there any significant difference in the distribution of the fractions within any of the populations. C) Number of vesicles in the recycling pool is linked to the size of the total pool. D) However, recycling pool fraction is not linked to the size of the synapse. Red – RRP 20 min, orange – RRP 5 min, purple – RRP 1 min.

4.2.5 Arrangement of readily releasable vesicles following reuptake

Next we exploited the information obtained from the three different fixation time points (outlined above) to follow the fate of recycling RRP vesicles. Key questions to address include whether RRP vesicles re-enter the synapse at points close to the active zone, or at points further away from the active zone; and whether they subsequently segregate within the total terminal space (e.g. front, back, or cluster edge), or insert randomly.

In order to gain insight into these questions, we took synapses from each time point and measured the distance from the active zone of all vesicles within the terminal and compared the distribution of distances for recycling vesicles and non-recycling vesicles. (see Fig.4.7). These were normalised to the size of the synapse, so that all synapses could be compared. The synapse size was determined by the furthest vesicle from the active zone. To represent the organisation of the RRP within the terminal in a visual form, we also generated density maps of vesicle positions using a custom-written MATLAB script (supplied by Prof K Staras). The plots show normalised 2D coordinates of each vesicle with respect to the active zone and the vesicle cluster boundaries with vesicle densities represented by a colour look-up table (see section 2.5.7.1).

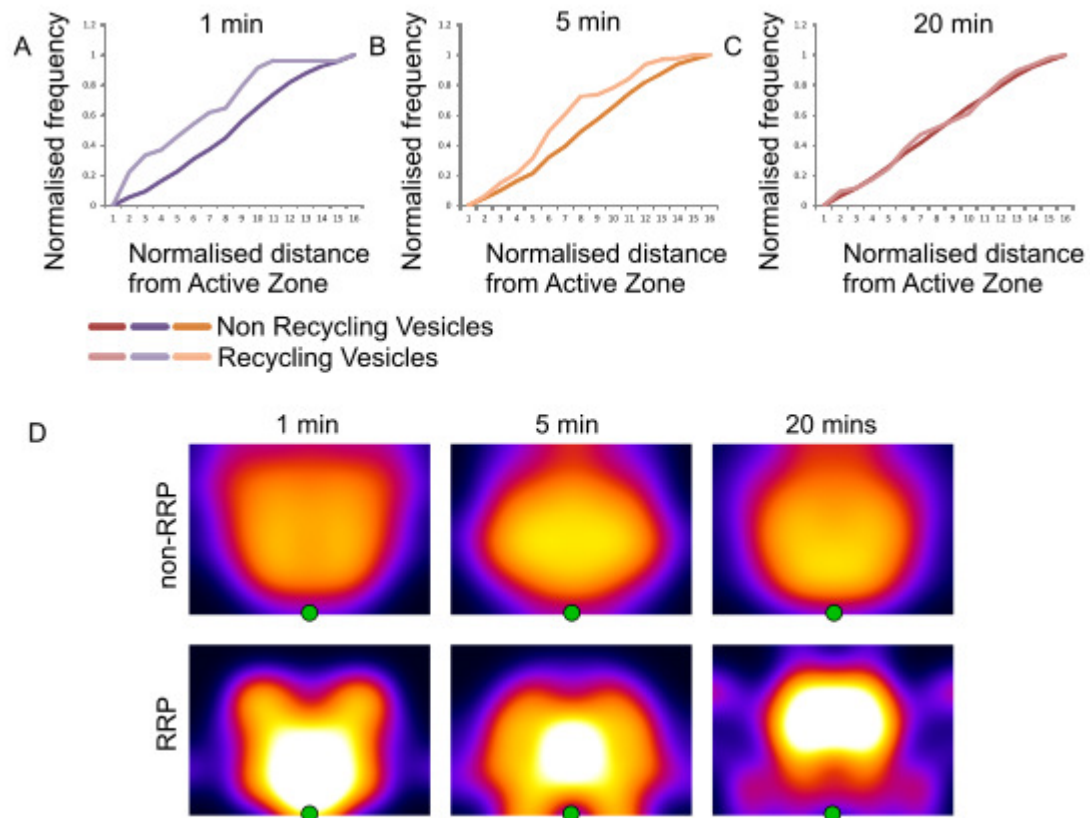


Figure 4.7 Recycling vesicles are positioned towards the back of the cluster over time

A) In samples fixed 1 min after FM dye loading, recycling vesicles are significantly shorter distances from the active zone compared to the rest of the cluster ($n=11$ synapses, unpaired Student's t -test for unequal variance, $p<0.002$). B) In samples fixed at 5 min after FM dye loading, the positioning of RRP vesicles within the cluster was still significantly closer to the active zone than non-recycling vesicles, but the preferential positioning was reduced ($n=15$ synapses, unpaired Student's t -test for unequal variance, $p<0.05$). C) 20 min after loading, recycling vesicles showed no significant difference in their distribution compared to non-recycling vesicles ($n=25$ synapses, unpaired Student's t -test for unequal variance, not significant, $p=0.706$) D) Density maps of vesicle distribution at 1, 5 and 20 min time points. At later time points, the distribution of RRP vesicles is less towards the active zone, and more similar to that of the non-recycling vesicles. Green spots indicate centre of active zone.

In all cases, the distribution of non-recycling vesicles was very similar. The cumulative frequency curves closely matched each other, and showed no significant differences to each other (one-way ordinary ANOVA, $p=0.859$). The heat maps reveal that the cluster of non-recycling vesicles form an approximately circular distribution in each case.

These findings strongly support that the integrity of the cluster as a whole is not influenced by the stimulation protocol, and that objective comparisons of RRP vesicle distributions at different time points are justified.

The organisation of RRP vesicles was strikingly different. At 1 min, vesicles adopt positions close to the active zone, seen in both the leftward shift of the cumulative frequency plot (Fig.4.7.A.) and the high density vesicle representation at sites directly behind the active zone and at the lateral margins in the heat plot (Fig.4.7.D). At 5 min, this distribution bias is substantially less clear, with vesicles adopting positions nearer the centre of the cluster volume; this is revealed both by the rightward shift of the RRP curve in the cumulative frequency plot and the movement in vesicle density in the heat plot towards the cluster volume centre (Fig.4.7.B, D). This pattern is emphasised further for the 20 min time point. Now the cumulative frequency plots for RRP and non-RRP vesicles are virtually indistinguishable and the heat plot likewise shows that the RRP recycling vesicles have a similar distribution to the non-recycling vesicles.

How are these RRP vesicles arranged with respect to each other? They could be arranged in small clusters, or mixed fully with the rest of the vesicle cluster. Close positioning over time might indicate that there is a specific site to which these vesicles are returned in the cluster, rather than reintegrating at random. To address this question, we carried out a simple cluster analysis, based on the use of a grid of six concentric circles, each one vesicle width apart. The central circle was placed over a recycling vesicle, and the fraction of recycling vesicles in each of the subsequent circles was calculated (Fig.4.8.A). Plots of average fractions from all vesicles for each time point against increasing distance from the vesicle target are shown in Fig.4.8.B. This analysis shows that recycling vesicles tended to cluster together at 1 min (high fractional values at short distances, falling away at longer distances), hinting at a specific location for vesicle reuptake. When taken in concert with the previous data, this suggests that the site for vesicle re-entry is at or close to the active zone. Interestingly, there is also clear clustering at 20 min after stimulation, consistent with the reaccumulation of vesicles at a specific area within the synapse. The data from the previous analysis suggests that this site is further back in the synapse, away from the active zone. Meanwhile, at the 5 min time point, there is no clear clustering of vesicles, and photoconverted vesicles appear to be spread further apart, possibly consistent with

a period during which they are transiting between endocytic sites and final reintegration sites (Fig.4.8.B).

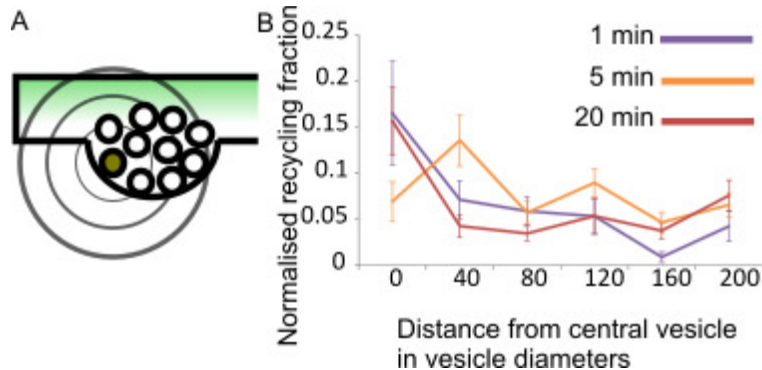


Figure 4.8 Clustering of recycling vesicles at multiple time points

A) Schematic of measuring system. Using a circular grid of six concentric circles, each one vesicle width apart, the number of recycling vesicles in each circle was expressed as a fraction of the overall number of vesicle in that circle. B) Mean fraction of recycling vesicles within 1-6 vesicle widths of each recycling vesicle. Red – RRP 20 min, orange – RRP 5 min, purple – RRP 1 min. Recycling vesicles cluster together at 1 min and 20 min following stimulation, but display less clustering at 5 min following stimulation. An ordinary one-way ANOVA was performed, and there was no significant difference between the distributions at these time points ($p=0.89$).

4.2.6 RRP vesicles and the docked pool

Vesicles in the readily releasable pool are defined by their preferential release characteristics (Rosenmund and Stevens, 1996), and there is some evidence that vesicles which were previously labelled as part of the RRP are preferentially reused (Pyle et al., 2000, Rizzoli and Betz, 2004). For vesicle release to occur, these vesicles must have access to docking sites. As such, looking at the representation of photoconverted recycling vesicles in the docked pool is an important next step in discovering whether RRP vesicles retain their identity following reuptake.

To address these ideas, we first looked at the overall representation of the RRP pool in the docked pool, determining how many previously RRP vesicles were at docking sites. At 1 min after stimulation, $19.52 \pm 5.8\%$ of the labelled RRP is at positions at the active zone. By 5 min, this value drops significantly (Student's *t*-test for unequal variance, $p < 0.05$) to $5.967 \pm 2.898\%$ of the RRP vesicles at docking sites. There was no

significant decrease between 5 min and 20 min when $4.751 \pm 2.714\%$ was contained at the docked pool (Fig.4.9.A).

We next looked at the fraction of docking sites filled with recycling vesicles. This showed a similar decrease over time. At 1 min following stimulation, $12.95 \pm 4.2\%$ of the docked pool was taken up by what had previously been RRP vesicles. By 5 min, the fraction of the RRP vesicles in the docked pool had dropped to $5.97 \pm 2.5\%$, dropping further to $3.04 \pm 1.7\%$. There is a significant difference between the fraction of RRP vesicles at the docked pool between 1 min and 20 min (Student's *t*-test, unequal variance, $p < 0.05$), but there is no significant difference between either point and the 5 min time point (Fig.4.9.B).

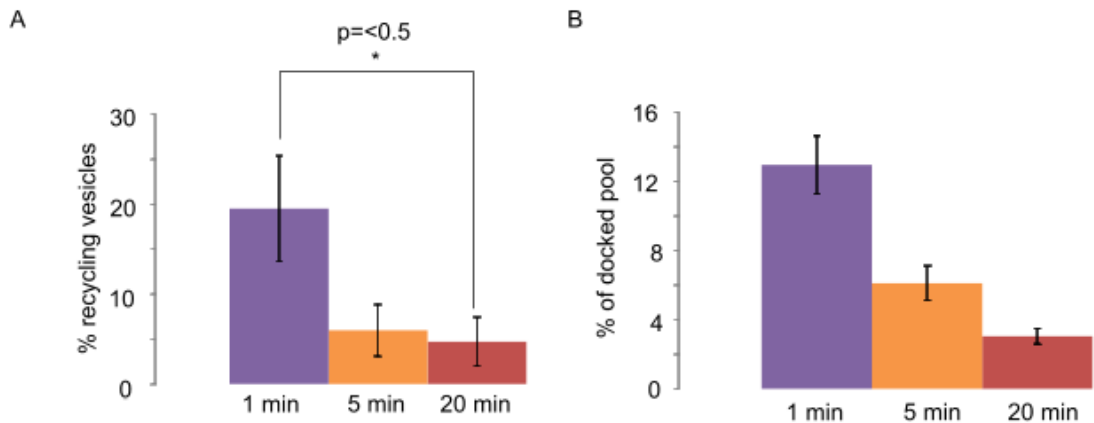


Figure 4.9 Recycling vesicles are more common at docking sites at shorter times following stimulation

A) At 20 min, the docked pool contains $4.8 \pm 2.7\%$ of the RRP. At 5 min, $6.0 \pm 2.9\%$ of the RRP is at docking sites, and at 1 min, the $19.2 \pm 5.9\%$ of the RRP is at docking sites. These figures show a significant difference between the time points (ordinary one way ANOVA, $p < 0.05$), with a significant difference between 1 min and 20 min time points (1 min $n=11$, 20 min $n=25$, unpaired Student's *t*-test for unequal variance, $p < 0.05$), and the 5 min and 20 min time points (5 min $n=15$, 20 min $n=24$, unpaired Student's *t*-test for unequal variance, $p < 0.05$); however there was no significant difference between the 1 and 5 min time points (1 min $n=1$, 5 min $n=15$, Student's *t*-test for unequal variance, $p=0.314$). B) At 20 min after loading, the docked pool consists of $3.0 \pm 1.685\%$ recycling vesicles, at 5 min $6.0 \pm 2.5\%$ recycling vesicles, and with only 1 min between loading and fixation, recycling vesicles comprise $13.0 \pm 4.2\%$ of the docked pool. These differences were not significant (one-way ordinary ANOVA, $p=0.09$), but do represent a clear trend in the number of recycling vesicles at docked sites.

These results show a decrease in the number of the previous RRP at the active zone over time. The most obvious interpretation of this is that endocytosis occurs at or near the active zone and then RRP vesicles are inserted randomly into the synaptic vesicle cluster. In order to determine at which part of the active zone this endocytosis occurs, we divided positions at the docked pool into central or peripheral (Fig.4.10.A), and calculated the fraction of recycling vesicles at either of these positions. The active zones used can be seen described in Fig.4.10.B. All docking pools of a single vesicle were eliminated as this indicated that a non-representative cross-section of the active zone was obtained in that section. The mean value for each category is listed in Fig.4.10.E.

At 1 min ($n=11$, unpaired Student's t -test for unequal variance, $p=0.35$) and 5 min ($n=11$, unpaired Student's t -test for unequal variance, $p=0.73$), there was no significant difference in fraction of peripheral and the fraction of central docking sites occupied by recycling vesicles; however, 20 min following labelling, there were significantly higher numbers of vesicles at peripheral sites compared to those at central sites at the active zone ($n=23$, unpaired Student's t -test for unequal variance, $p<0.05$). There was no significant difference in the fraction of recycling vesicles at peripheral sites across the time points measured (ordinary one-way ANOVA, not significant, $p=0.45$), but there was a noticeably higher fraction of recycling vesicles at peripheral sites at the 1 min time point. In central vesicles, there was a significant difference between the time points (ordinary one-way ANOVA, $p<0.002$): specifically, there were significantly higher numbers of recycling vesicles at central docking sites at 5 min (unpaired Student's t -test for unequal variance, $p<0.05$) and 1 min (unpaired Student's t -test for unequal variance, $p<0.05$) compared to 20 min, when all recycling central vesicles had been eliminated. There was a marked but not significant increase in the number of recycling ventral vesicles between 1 min and 5 min after stimulation (unpaired Student's t -test for unequal variance, not significant, $p=0.165$). (Fig.4.10C) The ratio of recycling vesicles between peripheral and central vesicles drops over time, as the central docking sites are no longer occupied by recycling vesicles. (Fig.4.10)

This suggests that there is greater vesicle mobility at centrally located docking sites on the active zone, and that if reuptake occurs around that region, then the vesicles are more likely to be reintegrated into the pool.

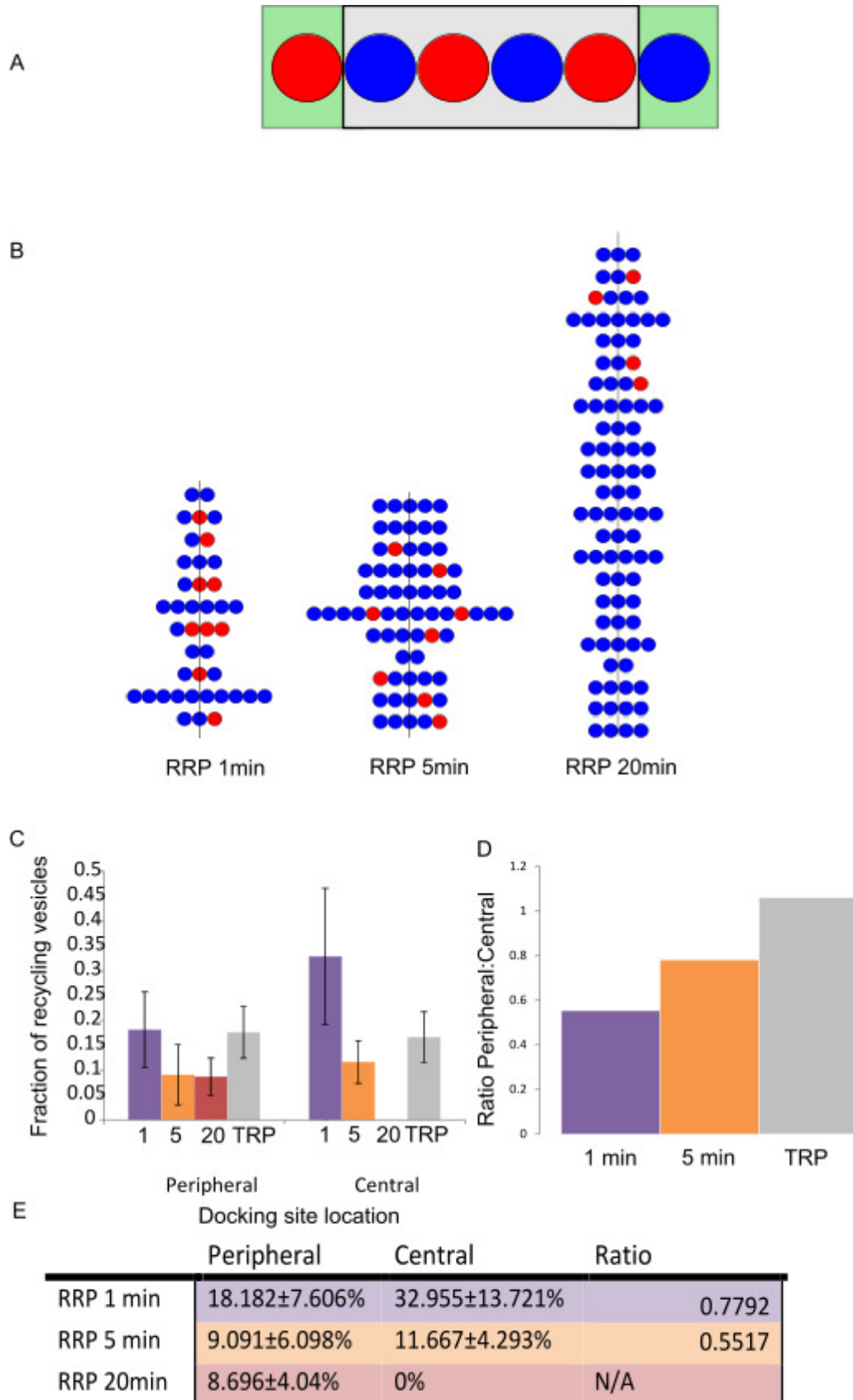


Figure 4.10 Recycling vesicle positioning at docking sites at three different time points

A) Vesicles at the active zone were defined as either peripheral (indicated in green) or central (indicated in grey), and as photoconverted or non-photoconverted. Red – photoconverted, blue – non-photoconverted. B) Cartoon of all active zones used. C) The fraction of recycling vesicles at the active zone in peripheral and central locations. There are no recycling vesicles in central docking sites at 20 min. D) Ratio of peripheral to central vesicles. Red – RRP 20 min, orange – RRP 5 min, purple – RRP 1 min, grey – TRP 20 min. E) Mean fractions \pm standard error of the mean of each position at each time point, with ratio of RRP vesicles at peripheral / central sites.

4.3 Functional properties of RRP vesicles in the acute hippocampal slice preparation

The ultrastructural information gathered in section 4.2 provides valuable insight into the arrangement of vesicles on reuptake. The hypothesis that is most consistent with the data is that RRP vesicles undergo endocytosis and are subsequently reclaimed at sites at or adjacent to the active zone. However, at later time points, they are reintegrated into the vesicle cluster, adopting a random spatial distribution. Such a finding has parallels with the work by Rizzoli and Betz (2004) in the frog neuromuscular junction, showing that RRP vesicles are not preferentially segregated after recycling. In this previous study, they also demonstrated that those vesicles are still reused preferentially, indicating that position may not be a key factor for privileged release. Next we looked at the same issue in small central terminals using a fluorescence-based approach.

4.3.1 Rate of fluorescence depletion in RRP labelled synapses

Having used the method described in section 4.2.1 to label RRP vesicles, the next step was to establish whether they retained their functionality, or whether RRP vesicles moved out of the recycling pool entirely. RRP vesicles in the presence of FM dye were exposed to a stimulation protocol of 40 AP/20 Hz, and CNQX and AP5 were applied to prevent signal propagation causing fluorescence loss, and the slice was allowed to wash for 20 min prior to imaging. The slice was then imaged using time lapse confocal microscopy, at a frame rate of 0.5 fps. Following 20 s of imaging, a 10 Hz destaining stimulus was applied.

A selection of the fluorescent punctae experienced stimulus dependent fluorescence loss as the FM dye was released when the labelled vesicles underwent recycling

(Fig.4.11.A). The profiles generated by this fluorescence loss over time demonstrated a heterogeneous rate of dye loss, but a stable period, followed by a period of exponential dye loss which coincided with the start of the 10 Hz stimulus was exhibited in all cases (Fig.4.11.B).

The mean of all curves fitting this profile for RRP labelled synapses was compared to a similar curve generated by TRP labelled synapses, both with their minimum fluorescence normalised to zero, and normalised against the fluorescence at the point that the stimulus started (Fig.4.11.C). The destain profile of the RRP synapses shows a steeper exponential decay than that of the TRP synapses indicating a faster rate of dye loss.

This was confirmed by collecting the time constant tau values for the generated destain curves for RRP vesicles and comparing them to those for TRP destain curves. The mean time constant tau of destain rates in TRP synapses was 94.24 ± 8.1 s, which was nearly twice that which we found in RRP synapses 43.27 ± 6.3 s. This is a significant difference (Student's *t*-test for unequal variance, $p < 0.002$) (Fig.4.11.D). When we compared the frequency distributions of the tau values, there was a definite skew of RRP values towards the shorter time constants, confirming that the rate of destain is faster in RRP synapses compared to those labelled with a TRP labelling stimulus (Fig.4.11.E).

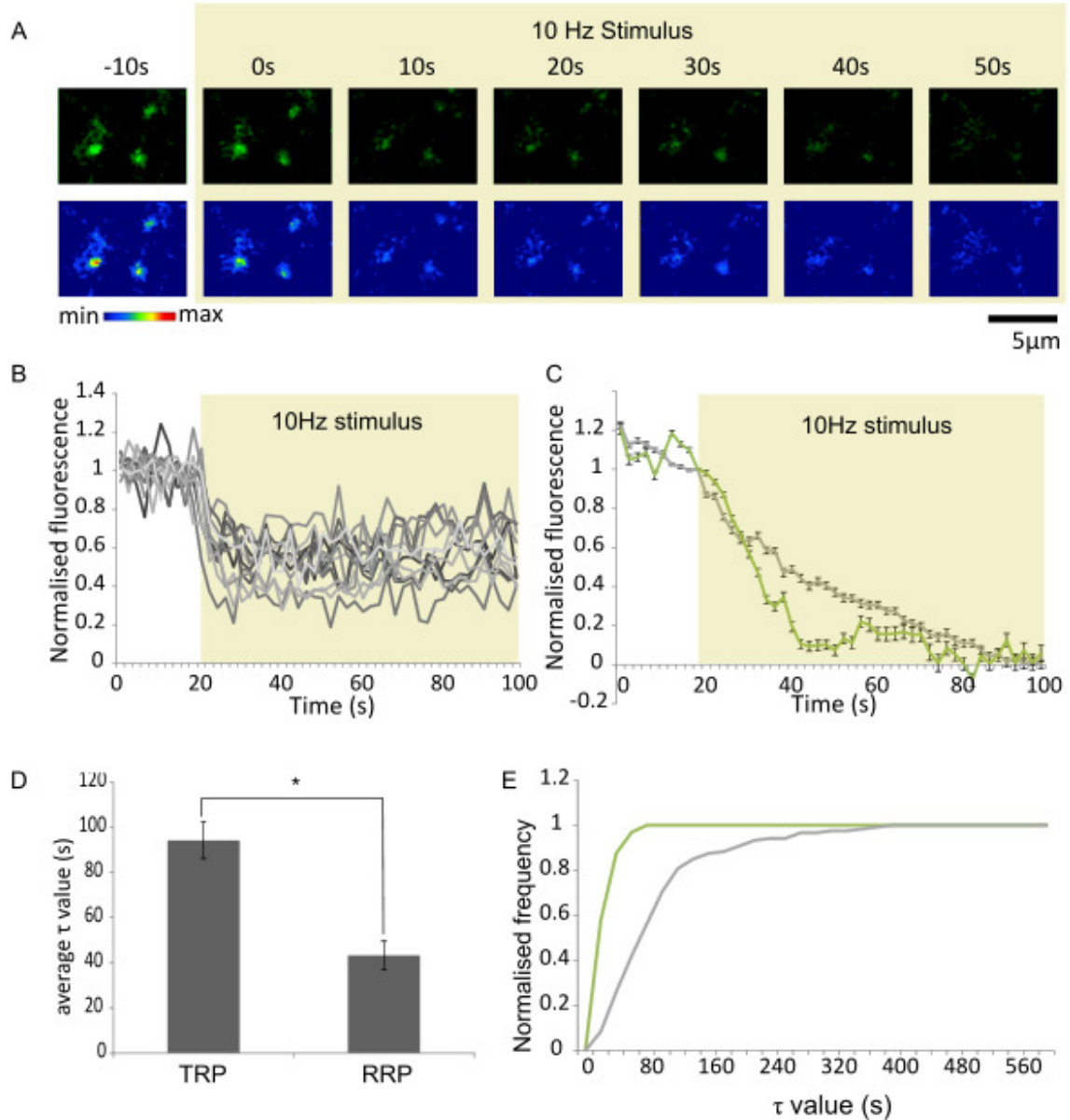


Figure 4.11 Functional activity of RRP vesicles in native tissue

A) Vesicles in synapses labelled with an AP stimulus in the presence of FM dye retained their functionality and exhibited dye release when exposed to a 10 Hz destaining stimulus. B) Functional punctae typically show a profile of a roughly maintained fluorescence level prior to the start of the stimulus, followed by a stimulus-driven fluorescence loss. The rate of this fluorescence loss is heterogeneous between synapses. C) The average profile of RRP synapses ($n=89$ from 4 animals) shows more rapidly completed dye release than in TRP labelled synapses ($n=107$ from 5 animals). Green – RRP synapses, grey – TRP synapses. D) The mean time constant τ of destain rates in TRP synapses is 94.242 ± 8.145 s, compared to 43.270 ± 6.345 s in RRP synapses. This is a significant difference (Student's t -test for unequal variance, $p < 0.002$) E) Though both TRP and RRP synapse populations have a level of

heterogeneity, the range of tau values in RRP synapses is skewed towards smaller values than those of TRP synapses. Green – RRP synapses, grey – TRP synapses.

4.3.2 Using fluorescence based assays of function for short time scales

In section 4.2.6, we establish that 1 min after stimulation, there are large numbers of FM-labelled RRP vesicles at the active zone. What remains unclear is whether these vesicles are release competent at this time point, or whether they need to cycle through the pool to participate in further release events. To examine this idea, we aimed to compare the destain rate of FM dye labelled synapses at 1 min versus 20 min after loading.

This posed a technical challenge. The 20 min washout period, which lowered the background fluorescence to suitable levels for responsive punctae to be identified, could not be used under these conditions. Use of an FM dye collating agent, such as Advasep, requires several minutes of application in order to have an effect (Kay et al., 1999). A rapid method of removing background fluorescence was required in order to visualise labelled RRP synapses only 1 min after stimulation. In a previous study, Harata et al. (2001) used BPB as an approach to quench external fluorescence to study fast fusion events, such as kiss-and-run recycling. BPB rapidly quenches the fluorescence of FM dye, and as such makes it ideal for our purposes.

As in previous experiments, FM dye was puffed into the slice for 3 min, and then the loading stimulus applied. At this point, the surface of the tissue was located under the electron microscope, and a point 10-25 microns below it was selected for imaging. The application of FM dye was terminated 45 s after the stimulus concluded, the perfusion system was stopped, and the ACSF in the imaging chamber was gently replaced with ACSF containing 50 μ M CNQX, 20 μ M AP5 and 2 mM BPB; the slice was then imaged. The application of BPB caused an instant drop in fluorescence (see Fig.4.12.A). Small fluorescent punctae were clearly visible.

We measured the fluorescence level of 50 punctae and 50 background regions of the same size in a BPB-labelled slice, compared to a slice which experienced a 20 min wash with normal ACSF as a control. We found that the fluorescence levels throughout the samples were reduced in the presence of BPB, with decreased background

fluorescence and the levels of fluorescence in visible punctae also lowered (Fig.4.12.B). When comparing the frequency distributions of the punctae and background fluorescence of the BPB -reated slice and the control slice, normalised against the maximum fluorescence level of the punctae in each category, we found that there was no change in contrast between the punctae and brightness levels, but the distribution of the values are smaller (Fig.4.12.C).

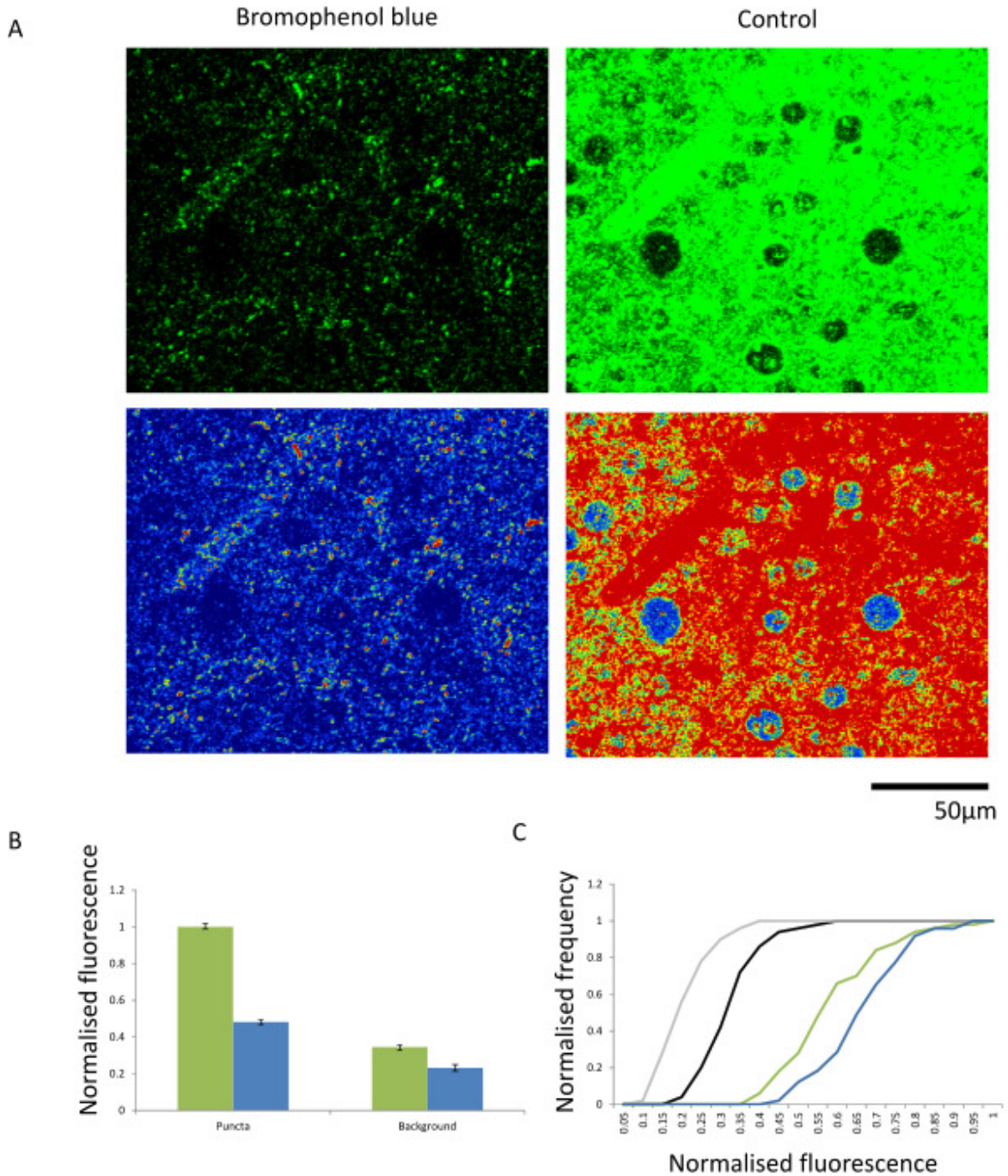


Figure 4.12 BPB quenches FM 1-43 fluorescence

A) Same slice imaged with the same settings both before and after the application of 0.2 mM BPB solution. B) Levels of fluorescence in punctae was reduced, as was the fluorescence in the background. C) BPB causes overall decrease of fluorescence levels. However, the difference between background and responsive punctae levels was significant (Student's *t*-test, $p < 0.002$) in both control and BPB samples. Green – control punctae, blue – BPB punctae, grey – control background, black – BPB background.

Having established that BPB is a suitable tool to allow the study of fluorescence loss in RRP vesicles immediately following loading, we compared the rate of fluorescence loss in a slice which was allowed to incubate for 20 min following FM dye loading to one which was only allowed 45 s to recover. In each case, a region of interest was selected, the perfusion system was stopped and the ACSF in the imaging chamber replaced with BPB ACSF containing CNQX and AP5, and the region of interest was imaged at a rate of 0.5 fps, with a destaining 10 Hz stimulus applied after 10 frames.

An unforeseen technical difficulty posed by this method is that the perfusion system provides a current over the surface of the slice which contributes towards holding the slice flat in the chamber, preventing the slice from drifting in the z-plane when imaged. The absence of the perfusion system meant that obtaining these readings without z-drift was difficult. As such, replicates were limited: for BPB RRP 20 min $n=16$ synapses from 2 animals; and for BPB RRP 1 min $n=11$ synapses from 1 animal.

There was no clear difference between the average destain curves of these synapses (Fig.4.13.A). When comparing the distribution of the time-constant tau values for these two time points, it also showed no significant difference (20 min $n=16$ synapses from 2 animals, 1 min $n=11$ synapses from 1 animal, unpaired Student's *t*-test for unequal variance, not significant, $p=0.475$), but may potentially point to a slight decrease in rate between the BPB RRP 1 min destain punctae and the BPB RRP 20 min punctae (Fig.4.13.B).

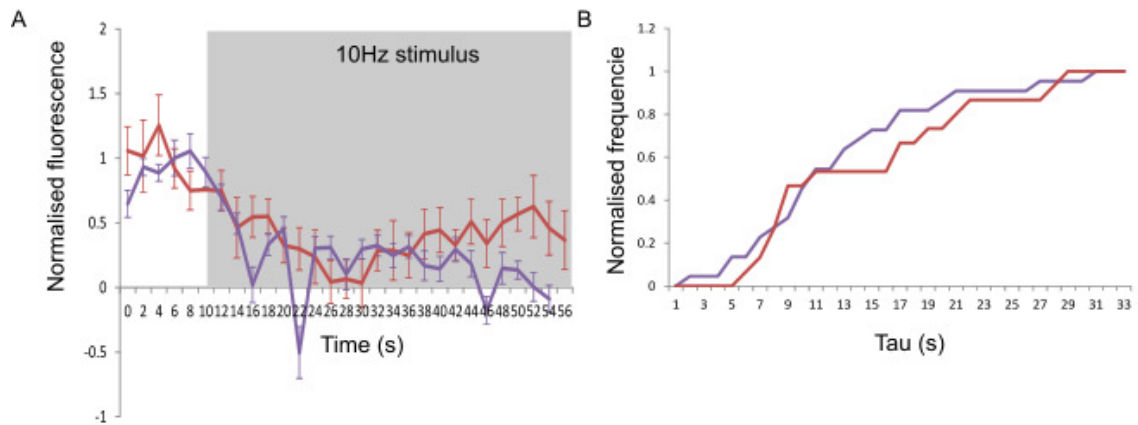


Figure 4.13 Rate of fluorescence loss at 1 min vs 20 min after stimulation

A) Average fluorescence loss over time of BPB treated synapses, 1 min (purple) or 20 min (red) after fluorescence loading. B) Frequency distribution of tau values for BPB RRP 20 min (red) and BPB RRP 1 min (purple) punctae destain curves (20 min $n=16$ synapses from 2 animals, 1 min $n=11$ synapses from 1 animal, unpaired Student's t -test for unequal variance, not significant, $p=0.475$).

4.4 Discussion

In this chapter the primary aim was to exploit an ultrastructural readout of functional vesicles to establish the fate of the readily releasable pool following endocytosis at native central synapses. By quantifying the location of these vesicles at various time points after loading, the overall temporal dynamics of this pool could be characterised. This is a particularly interesting question with regards to RRP vesicles since it has previously been suggested that these vesicles are preferentially reused to maintain vesicle recycling (Denker et al., 2011, Pyle et al., 2000).

4.4.1 Labelling the RRP in the hippocampal acute slice preparation

With the aim of labelling and then characterising the properties of this pool, an initial consideration was to choose the best paradigm for labelling. Many researchers have used hyperosmotic sucrose as an approach to access this pool (Rosenmund and Stevens, 1996, Moulder and Mennerick, 2005) Although this has been highly informative, the mechanism by which it brings about the release of the RRP is not clearly understood. It is known to be calcium independent, suggesting that it does not rely on the normal release mechanism. Indeed, Moulder and Mennerick (2006) suggest that hypertonic release of vesicles based on sucrose application shows higher numbers of released quanta than an exhausting stimulus train, indicating that it may be releasing

additional 'reluctant' vesicles with unclear physiological meaning. Moreover, the fact that sucrose-induced release appears to be resistant to drugs altering release probability indicates that an entirely different mechanism of action is at work (Rosenmund and Stevens, 1996).

From a technical and experimental point of view, there are also potential problems with the precise and discrete application of sucrose. In addition, we anticipated problems with eliminating the hypertonic sucrose following injection into the tissue at the site of FM dye uptake, as we would not be able to control the duration of the hypertonic solution. As such, sucrose-induced release offered few clear advantages for this work

We were able to label the readily releasable pool for quantification at an ultrastructural level using FM dye photoconversion. Our finding of an RRP recycling fraction of $5.5 \pm 2.8\%$ of the total pool is within the range previously described in the literature, (Sudhof, 2000, Rizzoli and Betz, 2005, Schikorski and Stevens, 1997b, Murthy et al., 1997) and is broadly consistent with our fluorescence findings (see section 4.2). As previously stated, it is possible that one might confuse large dense core vesicles with recycling vesicles, or even endosomes which will later be parcelled off into recycling vesicles. The low occurrence rate of these large dense core vesicles also means that, were they somehow to be confused with normal recycling vesicles, this would be unlikely to have a significant bearing on the results. The low incidence of large dense core vesicles in samples and the absence of photoconverted vesicles in the control samples provide support for this.

The consistency of the recycling fraction over the course of multiple time periods is good evidence that this pool is not being lost, either through spontaneous fusion or through transfer to the superpool (Staras et al., 2010) (see sections 1.3.4). This suggests that RRP recycling vesicles are largely maintained within terminals. An interesting future experiment would be to see to what extent RRP vesicles do leave terminals and appear at extrasynaptic locations. This would help clarify whether recycling vesicles in this pool behave differently to recycling vesicles in the total pool (Darcy et al., 2006).

4.4.2 Distribution of RRP vesicles following recycling

After undergoing recycling, RRP vesicles were reintroduced into the vesicle pool. At 1 min following reuptake recycling vesicles appeared to show a preferential distribution

towards the active zone. Over the course of 20 min, recycling vesicles were intermingled with non-recycling vesicles, showing no preferential distribution.

Our initial finding of a trend of recycling vesicles towards the front matches the findings of Park et al. (2012), who also found that recycling vesicles to be positioned close to the active zone after recycling. However, the method used by Park et al. differed in that they used a 10 AP stimulus to label RRP vesicles, leading to a subset of the RRP being labelled. It is possible that the RRP defined by Rosenmund and Stevens (1996) is actually made up of a small group of vesicles with a specific, preferentially releasable identity, like that suggested by Denker et al. (2011), Pyle et al. (2000), and Rizzoli and Betz (2004), and recycling vesicles from the TRP which just happened to be in the right place at the right time. Looking at the positioning of a pool labelled using this 10 AP stimulus would be an interesting experiment to explore this idea further.

These results also complement previous findings in the frog neuromuscular junction which found that RRP vesicles clustered together upon re-entry into the cluster and did not mix with the rest of the recycling pool (Richards et al., 2000). In a later paper in the same system, comparing the position of RRP vesicles when fixed immediately after stimulation and when fixed 10 min later, they also found vesicles clustered at the membrane in vesicles fixed immediately, and that over the course of 8-10 min, recycling vesicles were delivered into clustered where they slowly mixed with the other vesicles in the terminal (Richards et al., 2003).

In synapses fixed 20 min after a loading stimulus, we found that RRP vesicles did not show any preferential distribution towards the active zone, and were, if anything, distributed towards the back of the cluster. This was in direct contrast to the findings of Marra et al. (2012) when investigating the total recycling pool in the same system. They found that in TRP labelled synapses, after 20 min, recycling vesicles showed preferential positioning around the active zone. One possible explanation for this is that following re-entry, vesicles are returned to the back of the cluster, and are moved to positions near the front in an activity-dependent manner, as those vesicles in front of them are released and then endocytosed and returned to the back of the cluster. The duration of the TRP loading stimulus would allow those vesicles which were loaded at the start of the stimulus to be returned to the front, as all the other vesicles in front of them in the queue are cleared. In order to test this in future experiments, perhaps by labelling the RRP with a non-releasable activity dependent probe such as syOyster (see

sections 3.2.4 and 3.3.7) and applying a further stimulus after allowing vesicles to re-enter the pool, we could see whether the previous RRP vesicles move towards the front. Subsequent studies in the lab, based on this idea, have confirmed this finding (Dr S Rey, personal communications).

4.4.3 RRP vesicle re-entry around the active zone

An important finding in this chapter is the indication that vesicle re-entry occurs around the active zone and at the lateral edges of the vesicle cluster. This is in broad agreement with the classical models of endocytosis. The high numbers of recycling vesicles present at the docking sites, and at positions around the active zone at earlier time points, and moving away from with time, indicate that this is a major site for vesicle turnover.

Previous work has indicated that a rapid form of endocytosis is predominantly used when recycling RRP vesicles, and that this is an important mechanism in maintaining presynaptic function, suggesting full collapse fusion is not something which could sustain transmission alone (Pyle et al., 2000). This result backs up a suggestion made by Alabi and Tsien (2012) that the depression seen when synapses are repeatedly exposed to an RRP-depleting stimulus (von Gersdorff and Matthews, 1997, Abbott and Regehr, 2004) is caused by an accumulation of former RRP vesicles around the active zone, which cannot be cleared in time to allow efficient refilling of the pool.

A recent paper by Watanabe et al. (2014) found that an ultrafast mode of recycling occurred over the course of 5-6 s after the end of short bursts of stimulation. This involves large clathrin independent vesicles being taken up from the synaptic membrane, fusing to form endosomes, and then being apportioned off via a clathrin-based method. This method could potentially play a part in the recycling of RRP vesicle, but bulk endocytosis vesicle reclamation methods are more likely to replenish the reserve pool (Cousin, 2014), so the vesicles which are returned to the RRP are more likely to be recycled by an alternative method.

In order to identify the role that ultrafast endocytosis plays in recycling RRP vesicles, future experiments could include exploiting the clathrin dependence of full fusion

endocytosis, and the clathrin independence but actin dependence of ultrafast vesicle recycling Watanabe et al. (2013). By applying an actin polymerisation inhibitor, such as Cytochalasin B, and checking the extent of recycling vesicle labelling and comparing it to the labelling following exposure to a clathrin inhibitor, such as Pitstop, this may help determine which modes of endocytosis are involved in vesicle reuptake following short bursts of activity.

4.4.4 Functional properties of RRP vesicles on reuse

When performing fluorescence loss experiments of FM 1-43 labelled RRP vesicles, we found that the fluorescence in the synapses was lost at faster rates than that in FM 1-43 labelled TRP synapses. Though TRP synapses have a larger number of labelled vesicles, if all vesicles are used without preference then we should have seen an equal time course with lower fluorescence levels. This results points to a greater degree of reuse of RRP vesicles in future recycling events. TRP destaining also includes a population of RRP vesicles, so slower time course of release may be due to a slow rerecruitment of non-RRP vesicles. This is further evidence toward the suggestion above that a subset of RRP vesicles is preferentially reused. The notion of heterogeneity within pools has been suggested recently by Alabi and Tsien (2012), linking studies which have shown a subset of RRP vesicles which are pre-primed and released within much smaller timescales than the rest of the RRP (Hanse and Gustafsson, 2001, Wu and Borst, 1999, Moulder and Mennerick, 2005).

At 1 min following labelling, RRP vesicles are at locations close to the active zone, but at 20 min following labelling, RRP vesicles display no preferential positioning relative to the other vesicles within the terminal. This did not translate into a change in synaptic vesicle function. One possible reason for this, suggested by Rizzoli and Betz (2005), is that resting pool vesicles are 'glued' together, making it difficult for them to break away to undergo recycling.

In the synapsin knock-out mouse model, the clustering of synaptic vesicles is compromised, and larger numbers of vesicles are present outside the cluster (Orenbuch et al., 2012). Performing similar experiments on these mice would determine whether the rigidity of the cluster is what provides RRP vesicles with their increased mobility. If this is the mechanism behind preferential reuse, it points to a specific identity of the recycling pool vesicles from which the RRP are preferentially drawn.

Alternatively, the even distribution through the terminal which is displayed after 20 min actually has some recycling vesicles near the front of the terminal. It is possible that these specific vesicles are at these locations closer to the active zone owing to properties which allow them to be preferentially reused for recycling. Experiments looking at the locations of the remaining pool, when the vesicles which can be released with 10 AP have been destined, would give an interesting insight into whether this is actually the case. This idea would to some degree match the findings of Neves and Lagnado (1999) in their experiments on bipolar cells in goldfish retina. Using capacitance measuring, they found three tiers of rates of recycling, fastest in the first 10 ms, gradually decreasing over the next second, and then maintaining a slower steady rate subsequently. The terminals in goldfish bipolar cells are far larger, containing thousands of vesicles, but this three-tier rate system may be in evidence in hippocampal terminals.

This chapter demonstrated that the ultrastructural arrangement of recycling vesicles has implications for the function of the synapse. In the next chapter, we examine how altering synaptic function has an effect on the ultrastructural arrangement of recycling vesicles.

Chapter 5: The effect of long-term plasticity on ultrastructure and function of recycling vesicle pools

5.1 Introduction

In the previous chapter, we looked at the implications of the ultrastructural arrangement of recycling vesicles in presynaptic terminals for the functionality of those synapses. In this chapter, the overarching objective is to take this investigation of the link between function and ultrastructure to the obvious next step, by using a well-established method to modulate synaptic strength, followed by the use of the approaches detailed in the previous chapter to examine how this modulation acts on organisational properties of recycling vesicles. Specifically, we aim to induce a form of long-term depression in CA3-CA1 connections in acute hippocampal slices and employ FM dye labelling, fluorescence imaging, photoconversion, and electron microscopy to assay properties of functional pools.

Long-term depression (LTD) is an excellent candidate for further study: it is a topic of considerable interest, but little is known about the cellular and molecular mechanisms underlying it. LTP, first discovered in 1973 (Bliss and Lomo, 1973), has been the subject of extensive study since then, and is a valuable model for learning and memory. LTP was intended as a future direction for this work and would certainly support any conclusions drawn, but LTD was chosen due to its having been the subject of less study since its rather more recent discovery (Dudek and Bear, 1992). This allowed more scope for original investigation into the presynaptic properties of this form of long-term plasticity, and increased the impact of this work.

LTD is a reduction in synaptic strength, lasting hours or days, caused by the brief application of a low frequency stimulus (Dudek and Bear, 1992). This effect is reversible and, after having been induced, the response from the tissue can be elevated to, and indeed beyond, its previous levels through application of a protocol for inducing long-

term potentiation (LTP) (Mulkey and Malenka, 1992). LTD is also more reliably induced than LTP, making it more convenient for inclusion as part of a complex protocol where ultrastructural information is also obtained (Bear and Linden, 2001).

The investigations into the postsynaptic mechanisms of LTD have shown there to be two major forms of LTD, one requiring the activation of NMDA receptors, a rise in postsynaptic calcium level, and an activation of protein phosphatase cascades (Mulkey et al., 1994, Malenka and Bear, 2004). The other key form of LTD, and the one addressed by Zakharenko et al. (2002), is caused by internal calcium release following activation of metabotropic glutamate receptors (mGluR) (Bolshakov and Siegelbaum, 1994). This form is particularly prevalent in CA1 LTD. Antagonists against mGluR1s can inhibit LTD successfully in this model (Zakharenko et al., 2002). The activation of mGluR2s, which are typically found presynaptically, have been shown to be critical for persistent induction of LTD (Mukherjee and Manahan-Vaughan, 2013). AMPA receptor internalisation also plays a role in the reduction in the size of the postsynaptic response in LTD synapses (Hanley and Henley, 2005) (full summary in chapter 1.5.2). However, less is understood about the role played by presynaptic factors in LTD.

In their tour-de-force study, Zakharenko et al. (2002) demonstrate that synapses in hippocampal slices loaded by incubation in FM dye and imaged with a two-photon microscope demonstrate a reduced rate of dye release after induction of a form of LTD. They demonstrated the opposite effect, an increase in dye release rate following LTP in a subsequent series of experiments (Zakharenko et al., 2003). In cultured neurons, Ratnayaka et al. (2012) demonstrated that induction of LTP leads to recruitment of vesicles from the resting pool to increase the recycling pool fraction. Clearly then, synaptic vesicle pools are affected by long-term plasticity protocols, but the precise nature of their involvement is not yet known.

A key hypothesis we shall test is that LTD arises in part from a reduction in the absolute or fractional number of functional vesicles at the terminal. The mechanistic basis for this hypothesis is already established in the literature. It has previously been reported that release probability, one of the fundamental parameters defining synaptic strength, is positively correlated to the size of the recycling pool (Murthy et al., 1997). Homeostatic plasticity paradigms, such as long-term silencing of neuronal activity by TTX, produce results consistent with this theory, showing a rescaling of the functional pool (Murthy et al., 2001, Thiagarajan et al., 2005).

A second possible vesicle pool parameter that could undergo changes associated with synaptic plasticity is the physical organisation of vesicles in the terminal. The rationale for this is the recent observation that the absolute position of functional vesicles in the terminal is a determinant of its release characteristics (Marra et al., 2012). We shall test the hypothesis that the induction of long-term depression acts on the structural organisation of the recycling pool, such that the physical arrangement of the recycling vesicles with respect to the release sites is less advantageous for efficient release.

The docked pool is a site of particular interest in this case. The size of this population has been shown to be affected by long-term plasticity protocols (Murthy et al., 1997). The size of the recycling fraction of the docked pool released with hypertonic sucrose in LTD (Stanton et al., 2003) and LTP (Stanton et al., 2005) synapses have been shown to be lowered and raised respectively. These fluorescent studies provide a tantalising glimpse as to the role that the docking sites play in long term plasticity.

The aim of this chapter is to investigate the effect of using LTD to alter synaptic function on the properties of synaptic vesicles in the presynaptic terminal on FM dye release as an assay of recycling. More importantly, we aim to provide the first look at the ultrastructural arrangement of functional vesicles in functionally altered terminals. We shall use this information to determine the organisation of these vesicles with respect to each other and the active zone, and how the induction of LTD affects the composition of the vesicle pools at the active zone.

5.2 Functional labelling of recycling vesicles in hippocampal slices with LTD induced

5.2.1 Protocol of LTD in Schaffer collateral synapses

The initial objective was to establish a robust paradigm for LTD. LTD induction protocols have been widely outlined in the literature and several different mechanisms have been described. For these experiments, we adapted a protocol for a conventional form of hippocampal LTD used by Zakharenko et al. (2002). A basic outline of the procedure was as follows. Slices were prepared as described in previous chapters, using rats aged 21-28 d. This upper limit on age is important, as previous studies suggest that animals exceeding 35 d are much more unreliable for LTD induction (Bear and Linden, 2001). As described in previous chapters, following sectioning and a period

bubbling in 95% O₂ / 5% CO₂, a slice was placed into the recording chamber and then left for a further 15 min to acclimatise, as suggested by Edwards and Konnerth (1992). Next, a baseline was established. Specifically, a response was elicited by stimulating the Schaffer collaterals in CA3 and recording the evoked activity in CA1 (Fig.5.1.A). As outlined previously, this response typically had three distinct components: a stimulus artefact, the fibre volley, a small signal which is the electrode detecting the axonal transport of the stimulus, and an fEPSP which is a compound response of all synaptic activity in the area surrounding the recording electrode tip (Bortolotto et al., 2001) (Fig.5.1.B). As described in chapter 3, a sub maximal voltage was selected and used for these experiments.

LTD is induced by using sustained activity which is of insufficient frequency to induce LTP (Cummings et al., 1996, Dudek and Bear, 1992), and as such there are a wide variety of induction protocols, based on sustained stimulation at <10 Hz, which can be used to bring about LTD (Bear and Linden, 2001, Dudek and Bear, 1992). We chose to use 3 Hz for 900 AP (5 min), the protocol used previously by Zakharenko et al. (2002) to examine presynaptic components of LTD, as well as in numerous other studies (Hrabetova and Sacktor, 1996, Hrabetova et al., 2000, Xu et al., 2010).

Prior to the application of the LTD induction protocol, we collected synaptic responses at 0.033 Hz for 10 min. The low frequency stimulus was used to prevent the induction of metaplasticity (Zorumski and Izumi, 2012), which can affect the development of long-term plasticity changes. This was important for use as a basis of comparison for all subsequent responses. Following the LTD protocol of 3 Hz stimulus for 5 min, we sampled the response at 0.033 Hz for 25 min to ensure that the changes in response were sustained. The same protocol was carried out in control experiments and time matched, except here the LTD induction step was not included (outlined in Fig.5.1.C).

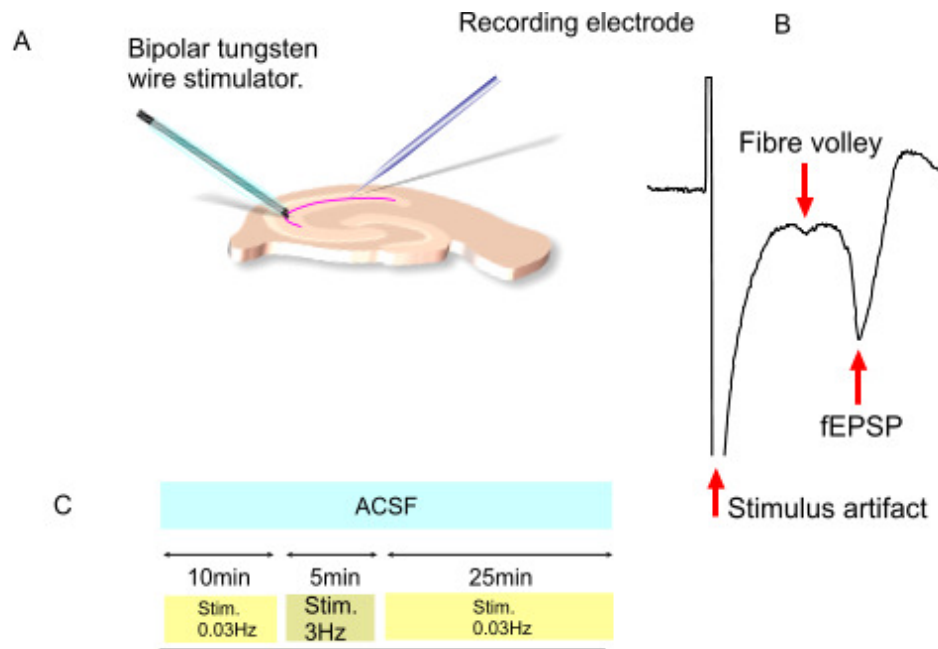


Figure 5.1 Location of a tissue response for plasticity induction

A) The tissue was stimulated along the Schaffer collaterals by a bipolar tungsten electrode placed along the CA2/CA3 boundary. A recording electrode measuring activity in the stratum radiatum of CA1 (for more details on set-up, see section 2.4.3). B) A typical response showed an artefact from the stimulus, a fibre volley, caused by axonal transmission, and a field excitatory postsynaptic potential (fEPSP). C) After using very low frequency (0.033 Hz) stimulation to measure the postsynaptic response for 10 min, a 3 Hz / 5 min plasticity protocol was applied. The postsynaptic response was monitored for 25 min, using a 0.033 Hz stimulus.

5.2.2 Electrophysiological evidence for LTD induction

In order to test for the successful induction of LTD and quantify its extent, we compared the amplitude and slope of the components of the fEPSP in pre- and post-LTD conditions. These changes reflect changes in the response amplitudes of the individual synapses and the number of synapses activated, and are standard parameters that are known to undergo modulation during LTD. The latency is the time from the start of the descending phase of the fEPSP to the end of the rising phase. The amplitude is the deflection from the baseline to the peak of the fEPSP. The slope is calculated by dividing the amplitude by the 'time to peak', which is measured from the start of the descending phase of the LTD (Fig.5.2.B).

An example comparison of the responses from one experiment is shown in Fig.5.2.A. The baseline responses typically showed little variation prior to LTD induction. Following the induction of LTD there was a striking increase in the response latency, taking several milliseconds longer to return to baseline levels. We compared the latency and size of the fibre volley in pre- and post-LTD responses from the tissue. There was consistently no significant difference in the timing of the fibre volley of the pre- and post-LTD response (control latency 54.1 ± 0.16 ms, LTD latency 54.3 ± 0.11 ms, Student's *t*-test, unequal variance, $p=0.167$). However the amplitude of the fibre volley in the pre- and post-LTD responses was significantly decreased (Student's *t*-test, unequal variance, $p < 0.02$). This indicates that transduction of the response through the axon is not inhibited, but there is a factor upstream of the synapse which affects the generation of the response.

The amplitude, time to peak, and consequently slope of the fEPSP were all consistently significantly lower in post- vs pre-LTD tissue responses (Student's *t*-test, unequal variance, $p < 0.002$ in all cases) (Fig.5.2.C and 5.2.D).

We deemed a successful LTD induction to have occurred if the slope of the fEPSP was still significantly lower than the baseline recordings at 25 min following the 3 Hz / 5 min stimulation. This is a relatively short time period after induction: many studies rely on a test of LTD at ~50 min, but it was important in this case to use a shorter sampling time point so that the additional aspects of the protocol related to fluorescence imaging could be included. To be assured that the plasticity induction we achieved was consistent with a long-term form of synaptic depression, we also ran experiments for periods up to 50 min, and demonstrated that LTD expression was sustained.

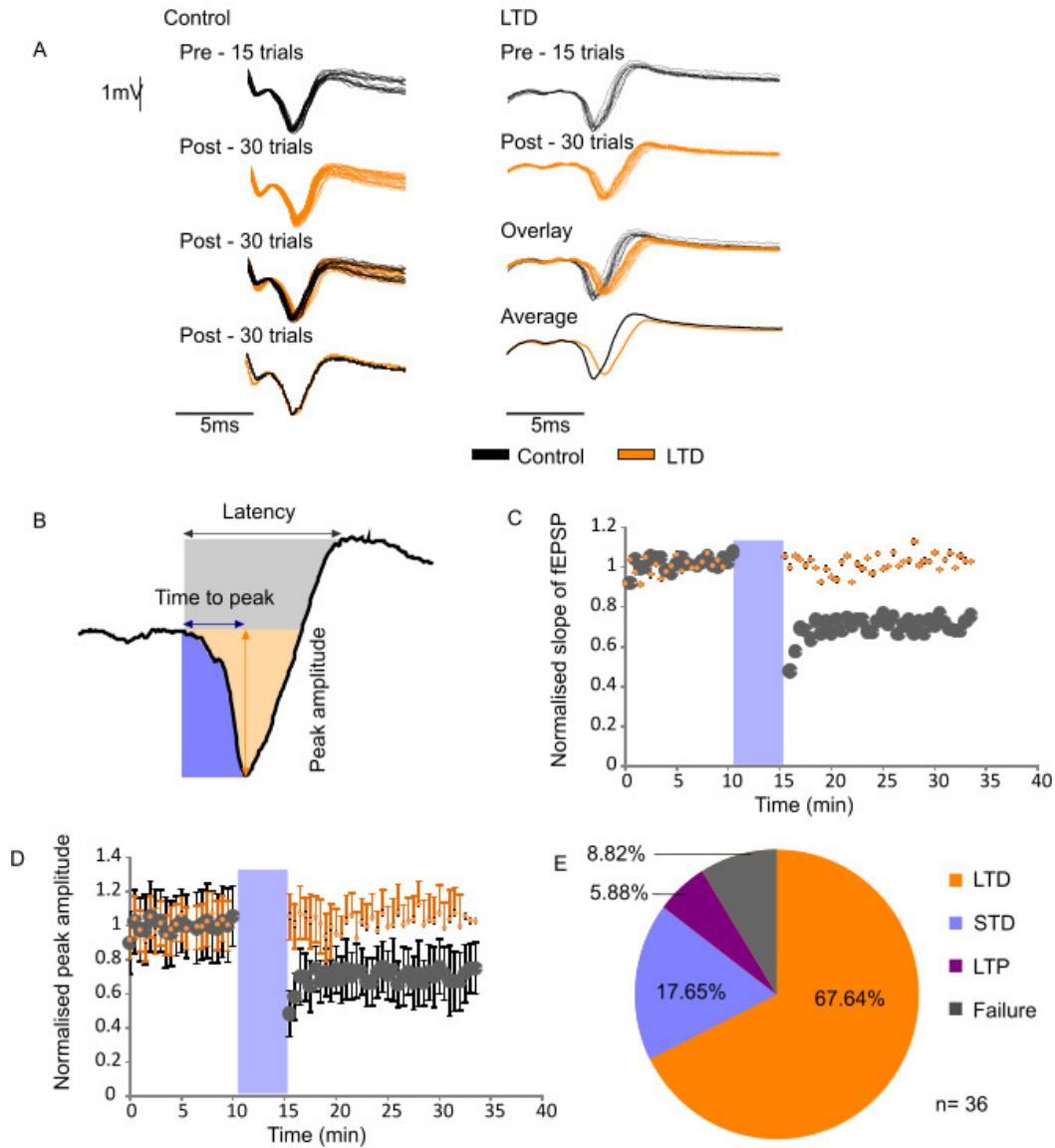


Figure 5.2 Low frequency stimulation alters parameters of the tissue response.

A) Trace responses from tissue showing the fibre volley and fEPSP, comparing those taken prior to exposure to a plasticity-generating stimulus, demonstrating the effect that a decreased amplitude and increased latency has on the trace generated. B) Diagram illustrating the different measurements taken from the trace. Latency is the time between the start of the descending phase of the fEPSP and the end of the ascending phase, peak amplitude is the maximum deflection reached by the trace from baseline levels, and the time to peak is the time from when the descending phase of the fEPSP begins and the peak amplitude being reached. C) The slope of the fEPSP was calculated by dividing the peak amplitude by the time to peak. This indicates the properties which were measured to obtain these values. This was calculated,

normalised against the mean level in the pre-LTD protocol readings, and plotted over time. D) The peak amplitude of the response generated, normalised against the mean peak amplitude in the pre-LTD readings. In C and D: orange – control, grey – LTD. In the 5 min period indicated by the purple bar, in LTD readings, a 3 Hz stimulus was applied, or in the control readings, no stimulus was applied. n=4, error bars show standard error of the mean E) Chart showing the frequency of LTD induction compared to other outcomes. From a total n of 36 experiments, a 3 Hz/5 min protocol resulted in the induction of LTD in 23 cases, short term depression (STD) in 6 cases, LTP in 2 cases, and in 3 cases, there was no change from baseline readings 1 min following the stimulus protocol, classified here as failure.

5.2.3 Anomalies of LTD induction

While robust LTD was the common outcome, there were instances in which the stimulation protocol produced a different response (Fig.5.2.E). On six occasions we observed a clear depression which was not sustained. In these cases a marked decrease in the size of the trace was clearly visible immediately following the application of the 3 Hz / 5 min stimulus, but the signal had returned to normal within 15 min (Fig.5.3.A). Both the latency and the amplitude show signs of having recovered (Fig.5.3.B). The fEPSP response slope (Fig.5.3.C) and amplitude (Fig.5.3.D), whilst showing clear and immediate evidence for LTD, gradually returned to baseline levels (or even above) over approximately 20 min. Why this occurs was not clear. One potential reason is that the stimulus is around the threshold level for the induction of LTP, and it is causing a balance of potentiation and depression. The precise placing of the electrodes may be what determines the overall outcome seen in the fEPSP. These multiple potential outcomes underline the sometimes tentative nature of plasticity induction and maintenance.

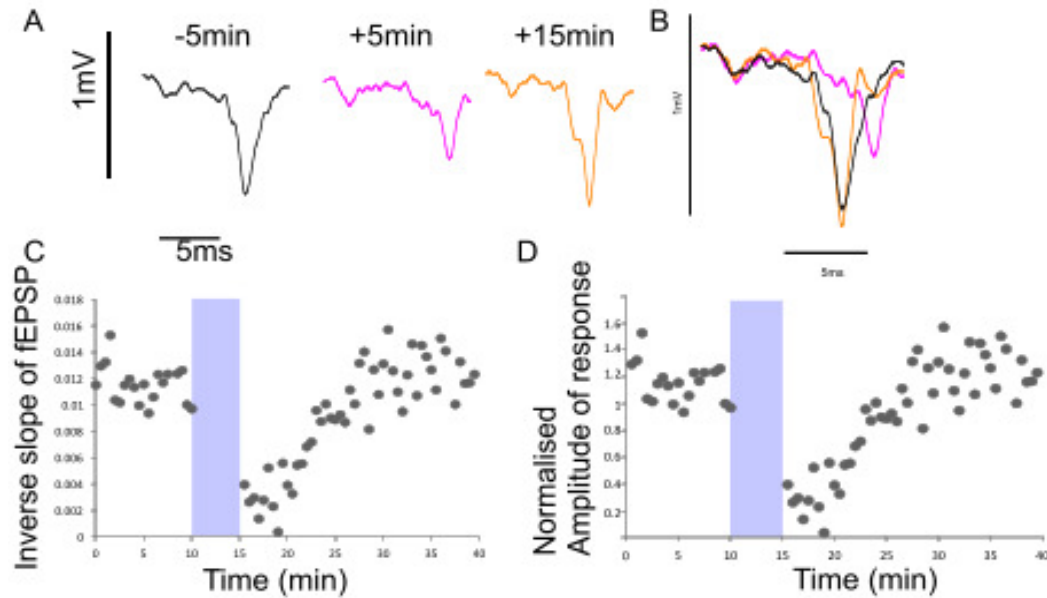


Figure 5.3 Short-term plasticity induction in Schaffer collateral synapses

A) An example trace of a system which underwent short-term LTD, showing an initial decrease in amplitude and then gradually returning to a higher amplitude over the course of 15 min. B) An overlay of the three traces: black – 5 min pre-stimulus, pink – 5 min post-stimulus, orange – 15 min post-stimulus. C) The slope of the graph showed a large decrease in size before returning to levels higher than the baseline. D) The amplitude of the fEPSP exhibited a sharp drop before returning to levels higher than baseline. In all cases the purple bar represents the application of a 3 Hz / 5 min stimulus.

Much less common but also worthy of mention was the finding that the LTD induction protocol would occasionally cause a potentiation of the synaptic response. An example of this is shown in Fig.5.4, where the various response characteristics outlined above all indicated an increase in the strength of the synaptic response: a significant decrease (Student's *t*-test, unequal variance, $p < 0.002$) in the time to peak of the fEPSP (Fig.5.4.B), a significant increase in the amplitude (Student's *t*-test, unequal variance, $p < 0.002$) (Fig.5.4.D), leading to a significant increase in the slope of the fEPSP (Student's *t*-test, unequal variance, $p < 0.002$) (Fig.5.3.E).

Once again, the explanation for these anomalous findings is unclear, but indicate that protocols for inducing a particular form of plasticity are not guaranteed and presumably relate to a complex range of variables such as the activity history of the synapse, which it may not be possible to fully control. The induction of LTD is caused when elevated

calcium does not reach a threshold level for the induction of LTP (Dudek and Bear, 1992). It could be that the particular positioning of electrodes in these slices and the sensitivity of these synapses to stimulation meant that the stimulation caused the internal calcium levels to rise above the threshold level for LTP induction.

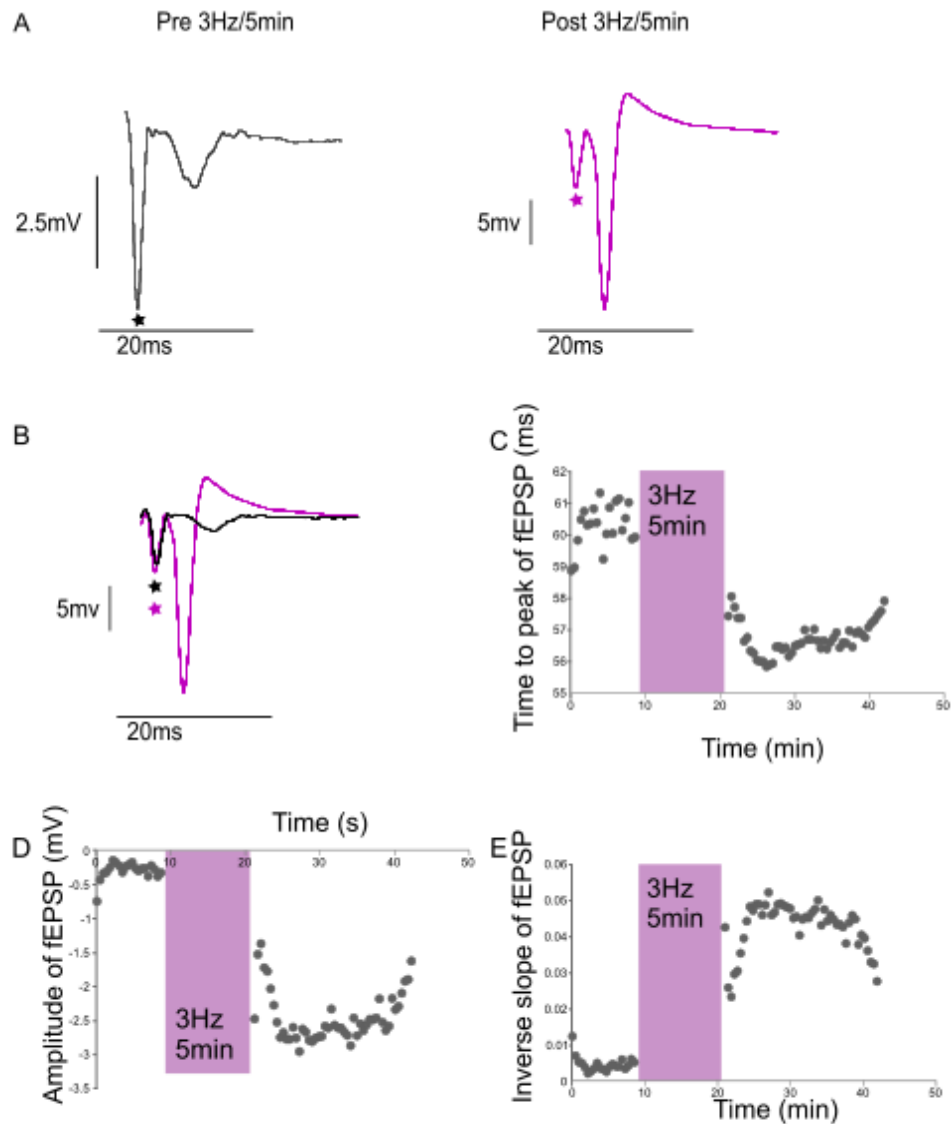


Figure 5.4 Induction of LTP using 3 Hz / 5 min protocol

A) In some cases the use of a 3 Hz / 5 min protocol induced a robust increase in the size of the postsynaptic signal. The average traces for an slice in which a 3 Hz / 5 min protocol resulted in potentiation is presented here, on different scales to demonstrate

best the different components. The fibre volley and fEPSP are shown, the fibre volley indicated by a star. B) Overlay of the pre-3 Hz / 5 min stimulus and post-3 Hz / 5 min stimulus trace on the same scale (fibre volleys indicated by a star). C) The time to peak of the fEPSP showed a significant decrease following the stimulus application (Student's *t*-test, unequal variance, $p < 0.002$). D) The amplitude of the fEPSP was greatly increased, reaching significantly more negative values after the stimulus was applied (Student's *t*-test, unequal variance, $p < 0.002$). D) When the slope of the graph was calculated, the changes to amplitude and time to peak lead to a significant increase in the slope of the fEPSP (Student's *t*-test, unequal variance, $p < 0.002$).

5.2.4 Labelling synapses with FM 1-43 for fluorescence imaging

Work by Zakharenko et al. (2002) found that mGluR1-dependent LTD had an effect on the rate of exocytosis at hippocampal synapses, thus linking the observed decrease in electrical transmission to changes in synaptic vesicle recycling and suggesting that this process has a presynaptic component. As a step towards the overall objective of this chapter, aimed at characterising the ultrastructural properties of presynaptic terminals that have undergone LTD, it was important next to establish the functional presynaptic consequences of LTD in our experiments. To do this, we again took advantage of the activity dependent styryl dye, FM 1-43, to label functional synapses and to look at properties of recycling vesicle pools in networks influenced by recent LTD induction.

NMDA and AMPA receptors are known to play critical roles in the strengthening and weakening of synaptic signals in LTD and LTP (Dudek and Bear, 1992, Mulkey and Malenka, 1992). Addition of the NMDA receptor blocker AP5 during the application of the LTD stimulus alone can increase the depression of the fEPSP in response to the LTD induction protocol (Cummings et al., 1996). As such, the induction step of the protocol needs to be carried out in the absence of postsynaptic receptor blockers. However, for the subsequent readout of vesicle pools, it is important that we are only labelling functional vesicles based on presynaptic activity and not driven in part by any recurrent activation of the network, leading to pre- and post-stimulus transmission and complex consequences for interpretation.

In order to avoid this recurrent activity, we therefore needed to silence the postsynaptic response after LTD induction, but before the dye labelling step of this experiment. We chose a 25 min period after induction, to allow time to confirm a robust LTD induction before proceeding with the imaging steps.

The effectiveness of blockers is very evident in experiments. Following the application of 50 μM CNQX and 20 μM AP-5, there is no significant difference in the slope or timing of the fibre volley after the application of CNQX and AP5 ($n=3$, Student's t -test, unequal variance, $p=0.2904$ and $p=0.572$), demonstrating that axonal transmission is not affected. There is a significant decrease in the slope and amplitude of the fEPSP following the application of the blockers (Student's t -test, unequal variance, $p<0.05$ and $p<0.002$). After the application of CNQX and AP5, there is no significant difference between the amplitude of the response and the baseline prior to the stimulus (Student's t -test, unequal variance, $p=0.589$). Thus, the postsynaptic response is entirely eliminated by these blockers, and all labelling is from activity generated by the stimulating electrode.

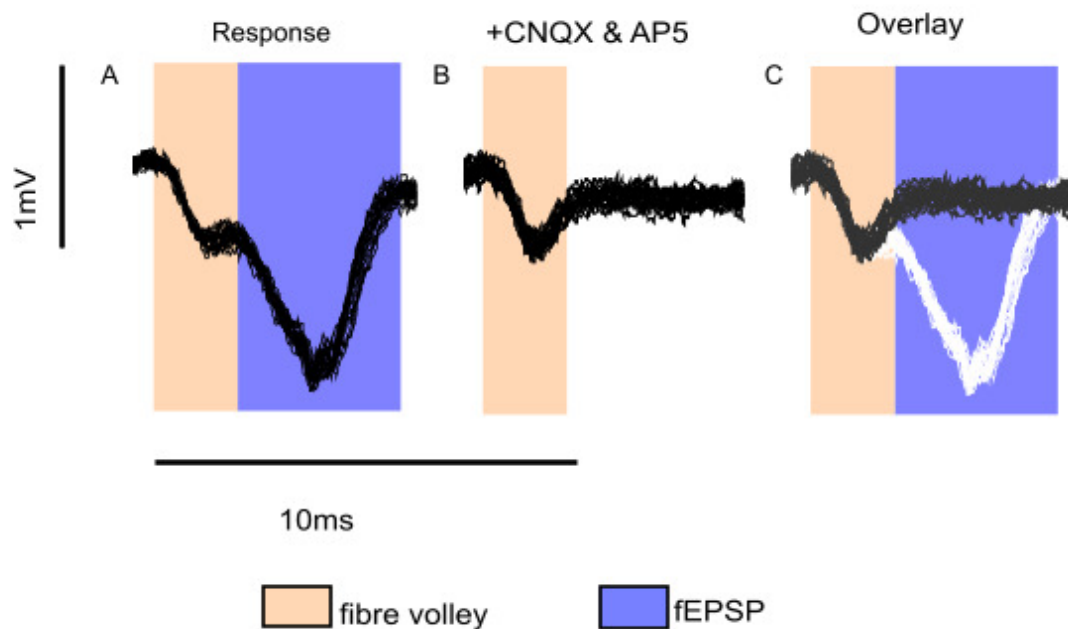


Figure 5.5 CNQX and AP5 effectively eliminate the post synaptic response

A) In ACSF without blockers, a response from the tissue consists of a fibre volley, caused by axonal transmission, and a fEPSP. B) When CNQX and AP5 are applied to the tissue, the fibre volley is still in evidence, but the field excitatory postsynaptic signal is effectively eliminated. C) The traces overlaid.

Synapses in both LTD and control samples were labelled as in previous chapters. Briefly, the recording electrode filled with 20 μM FM 1-43 was placed around 50-100 μm

below the surface of the hippocampal slice, and the FM dye was pressure injected into the tissue using a Picospritzer for 7 min. Following 3 min of dye application, a 1200 AP/10 Hz stimulus was applied to the tissue using the stimulating electrode. FM dye was applied for a further 2 min to ensure that, for vesicles undergoing recycling in that time, dye availability was not a limiting factor. Slices were then left in a 3 ml/min perfusion of ACSF with 50 μ M CNQX and 20 μ M AP5 for 20 min, a process which removed excess dye. The slices were imaged by confocal microscopy at a rate of 0.5 fps. Areas demonstrating discrete punctate staining at depths of between 10-20 μ M into the tissue were selected for imaging.

5.2.5 Functional properties of synaptic vesicle pools in LTD synapses

As discussed in previous chapters, FM dyes provide an excellent tool for looking at functional properties of synapses, particularly with regards to recycling. As such, if there is a presynaptic component to the functional changes in LTD synapses, there should be evidence of this in the dynamics of stimulus-dependent dye loss of FM dye. As such, we applied a further stimulus to the FM loaded synapses and imaged at a rate of 0.5 fps using confocal microscopy, and measured the fluorescence level of the punctae using ImageJ. Following the acquisition of 10 frames to establish a baseline of fluorescence, a 10 Hz stimulus was applied for 90 s.

Punctae were identified as functional synapses if they exhibited a fluorescence decay upon application of the 10 Hz stimulus (Fig.5.6.A). When the fluorescence levels of these punctae were measured over time, they gave an exponential decay curve, which related to the rate of exocytosis. These curves were highly heterogeneous and corresponded to highly heterogeneous rates of decay (Fig.5.6.B, D).

The mean curve of FM dye release was shallower compared to controls, indicating a slower rate of dye release. When time constant tau values were collected, they too showed a large range of values, demonstrating release rate heterogeneity within LTD synapses (Fig.5.6.D). The distribution of tau values trends towards higher values (and thus slower release rates) in LTD synapses. There is a significant difference (Student's *t*-test, unequal variance, $p < 0.05$) between the tau values for LTD synapses versus controls.

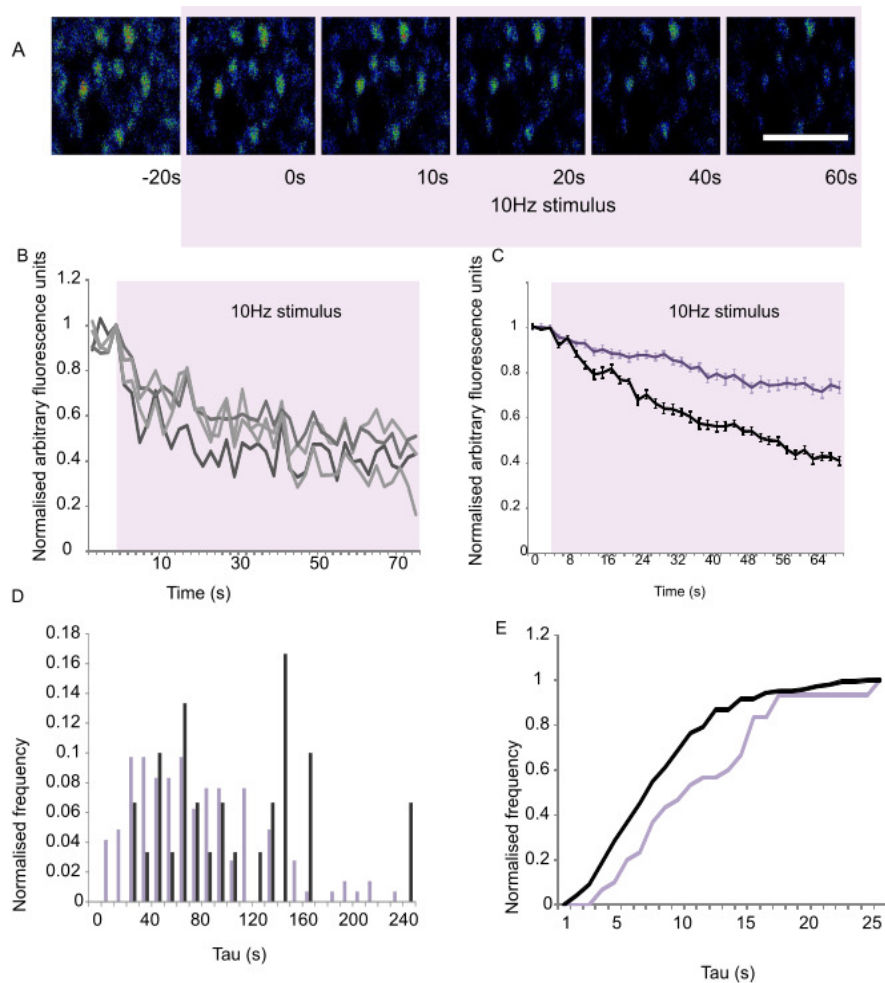


Figure 5.6 Activity dependent fluorescence loss in LTD synapses

A) Labeled synapses lose fluorescence in a stimulus-dependent manner. Scale bar is 2 μm . B) Fluorescence levels are stable prior to the application of a stimulus, upon which they experience exponential dye loss. Synapses release dye at many different rates. C) Average dye loss curves from LTD and control samples (Black – control, $n=130$ synapses from 5 slices, purple – LTD, $n=32$ synapses from 3 slices). D) Cumulative frequency of time constant τ values. The τ time constants of the dye-release curves are significantly higher in LTD synapses (Student's t -test, unequal variance, $p < 0.05$).

5.2.6 Ultrastructural properties of the total recycling pool in LTD synapses

Consistent with the previous work by Zakharenko et al. (2002), we find that altering synaptic function through LTD does involve a presynaptic element, namely a change in the rate of FM dye release in synapses. The work in the previous chapter indicated that there is a link between the function of the synapse and the arrangement of synaptic

vesicles. To investigate the link between LTD-modulated synaptic function and ultrastructure, we exploited the approach outlined previously to enable detailed ultrastructural characterisation, using the ability of FM dye-labelled vesicles to be photoconverted to an electron-dense product. As before, following loading with the fixable analogue of FM 1-43, the labelled slices were fixed with rapid microwave fixation, incubated in DAB, and illuminated with blue fluorescent light in order to catalyse the oxidation of DAB. The hippocampal slice was then prepared for electron microscopy as previously described (Fig.5.7.A), and either sectioned to produce single sections for analysis or a section series which could be used to produce 3D reconstructions of synapses (Fig.5.7.D).

We were successfully able to identify photoconverted vesicles in LTD synapses, and were able to create two reconstructions which provide more detailed information of the arrangement of recycling vesicles within a synapse. (Fig.5.7.B, C, D)

To demonstrate the changes in recycling vesicle properties caused by the induction of LTD, it was necessary to select an appropriate control. In these experiments it was slices which, instead of experiencing a 10 min 0.033 Hz sampling period followed by a 5 min application of a 3 Hz stimulus, they experienced the same sampling period followed by 5 min without stimulation. These controls were also exposed to a 1200 AP/10 Hz stimulus in the presence of FM dye, and this labelled the total recycling pool. These synapse provided a baseline level for comparison of the properties of LTD synapses.

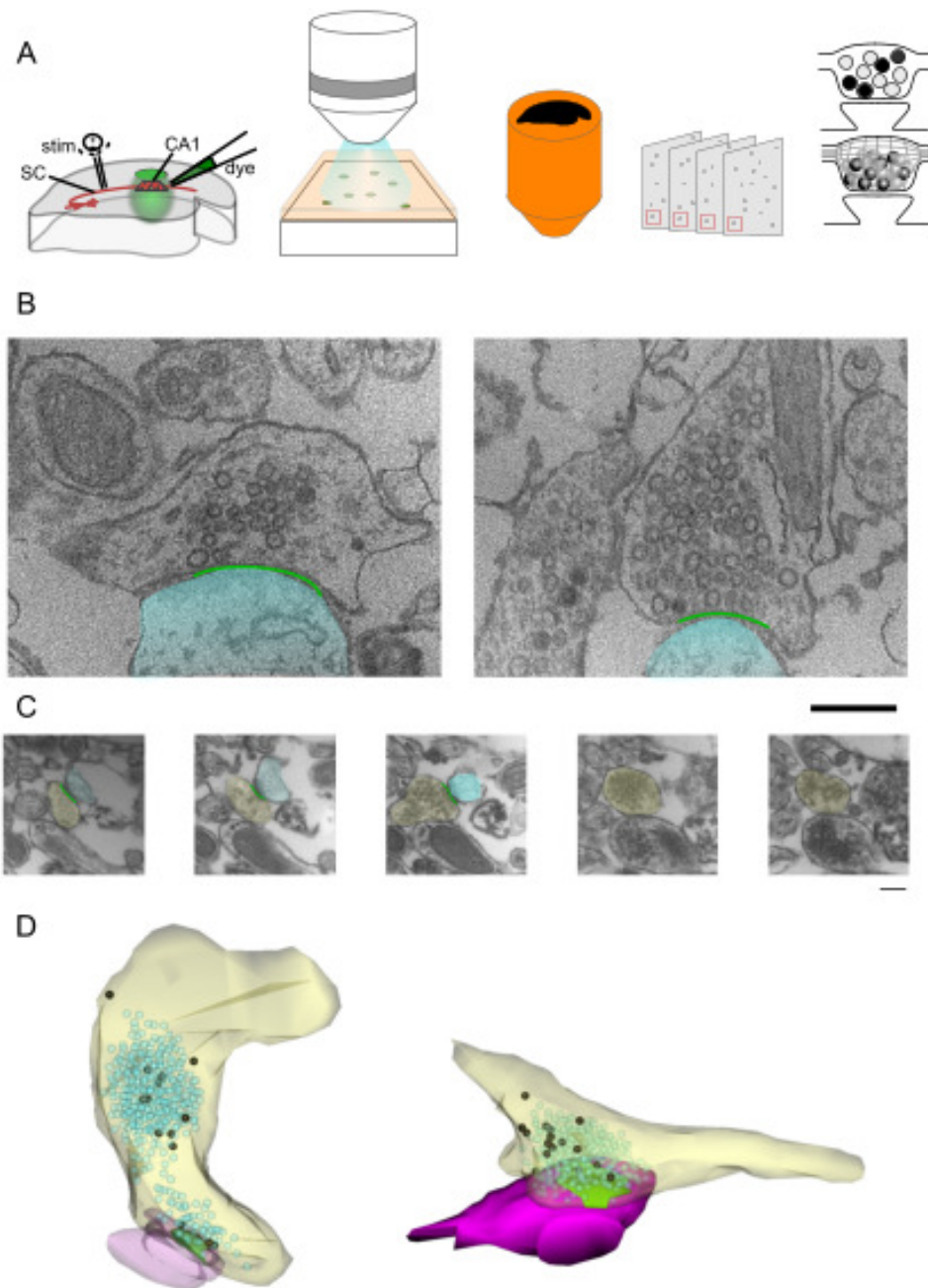


Figure 5.7 Visualising the total recycling pool in LTD synapses

A) A cartoon summarising the process for ultrastructural labelling of synaptic vesicles. The dye is loaded in the slice using a Picospritzer and bipolar tungsten electrode. The slice is then fixed, placed in DAB and exposed to a blue light ($<500\text{ nm}$) to catalyse the DAB oxidation reaction, then the sample is prepared for electron microscopy with several fixation, heavy metal staining and dehydration steps, before it is embedded in a block of EPON resin. The photoconverted region is then sectioned and imaged. B) Examples of photoconverted LTD vesicles. Blue indicates postsynaptic region, the

green line indicates the active zone of the synapse. C) Serial sections were produced by Dr JJ Burden, allowing regions to be tracked across multiple sections to produce a 3D image of the synapse. D) Example reconstructed synapses, produced using Reconstruct software. Scale bars are 200 nm.

The first parameter to explore is the effect of LTD on the recycling fraction. The loading stimulus we used was a saturating stimulus which should label the entirety of the recycling pool in control synapses. We counted the total number of vesicles in the terminals, and the number of recycling vesicles and calculated the recycling fraction. There were larger numbers of recycling vesicles present in the control samples (Fig.5.8.A) compared to the LTD samples (Fig.5.8.B). Specifically, recycling vesicles made up $23.4\pm 4.3\%$ ($n=19$ synapses from 2 samples) of the total pool in control synapses, whereas the recycling fraction was significantly lower at $12.2\pm 1.2\%$ in LTD synapses ($n=29$ synapses from 2 samples) (Student's *t*-test, unequal variance, $p<0.02$) (Fig.5.8.C).

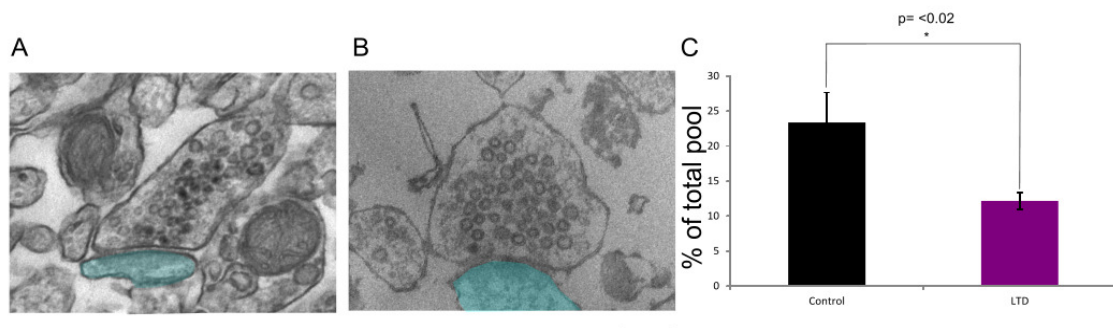


Figure 5.8 Recycling fraction of LTD versus control synapses

A) A control synapse containing photoconverted vesicles. B) An LTD synapse containing photoconverted vesicles. In A and B, the blue shaded area is the postsynaptic zone. C) The recycling fraction in control synapses is $23.4\pm 4\%$ of the total vesicle pool, but in LTD synapses, the recycling fraction is significantly lower at $12.2\pm 1\%$ of the total pool (Student's *t*-test, unequal variance, $p<0.02$).

This reduction in the size of the recycling vesicle fraction provides strong evidence that vesicle pools are modulated as part of the mechanism of adjusting synaptic strength. This poses the question: are vesicles positioned differently within LTD synapses in such a way as to reduce synaptic efficiency and strength, or is positioning not altered? Under basal conditions, previous work from the lab has demonstrated that functional vesicles

belonging to the total recycling pool are preferentially positioned towards the active zone at a time point 20 min after loading (Marra et al., 2012). An interesting question was to establish if this was disrupted in LTD synapses. To determine this, we categorised vesicles within our sample synapses (control, n=19 from 2 samples; LTD, n=28 from 2 samples) as either recycling or non-recycling, and then defined the active zone of the synapse. Active zones were identified by the presence of a postsynaptic density and by the presence of a docked pool of vesicles, aligned in contact with the synaptic membrane.

Using Reconstruct software (Fiala, 2005), the distance between the centre of each vesicle and the nearest point on the active zone was calculated. This data was normalised against the largest linear distance in each synapse, allowing the normalised cumulative frequencies to be compared to look at the relative distribution of recycling vesicles across the two conditions.

In order to get a better idea of the distribution of these vesicles within the terminal we generated density maps of vesicle position using a MATLAB script (supplied by Prof K Staras). As described in section 4.2.5 and 2.5.7.1, this involved plotting the normalised 2D coordinates of the distance between each vesicle and the active zone, normalising these plots for lateral direction, and then plotting vesicle density against a look-up table.

The distribution of the non-recycling vesicles is similar, giving a rounded cluster with the highest distribution in the centre and the density steadily decreasing away from this point. The recycling vesicles do however show specific clustering locations. In control synapses, this clustering is towards the active zone. In LTD synapses, we also see a high density of recycling vesicles immediately at the active zone. This is presumably the representation of the 'bump' seen on the cumulative frequency curve, representing a high number of recycling vesicles in positions immediately around the active zone. The rest of the recycling vesicle pool in the LTD synapses appears to be around the edges of the cluster, towards the middle of the synapse (Fig.5.9).

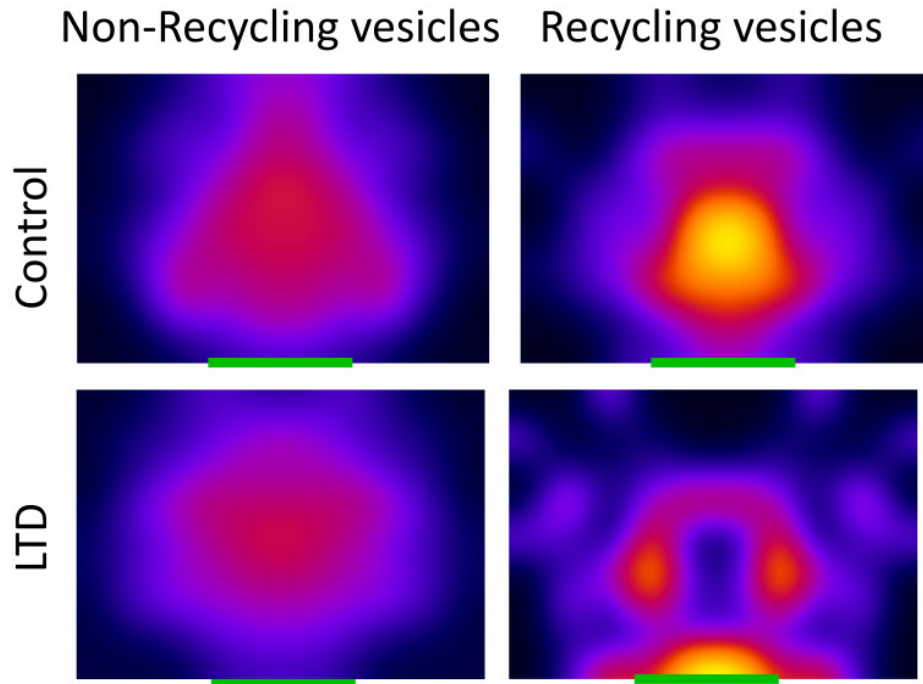


Figure 5.9 Density maps of synaptic vesicles within LTD and control terminals

Heat density plots of vesicle distribution within terminals for non-recycling vesicles and recycling vesicles within control and LTD terminals (control synapses $n=16$, LTD synapses $n=18$).

The non-recycling vesicles in both groups displayed similar distributions, although they appear to be more compressed towards the active zone in control synapses. This is to be expected as these vesicles are not involved in recycling, and so should only form the shape of the cluster within the synapse. In both the control and the LTD synapses, there was a preferential arrangement of vesicles towards the active zone. When the distances of recycling vesicles from the active zone in these synapses were compared, this trend was not shown to be significant in either case (Student's t -test for unequal variance, LTD recycling vs non recycling, $p=0.473$, control recycling vs non recycling, $p=0.439$), but was noticeable (Fig.5.10).

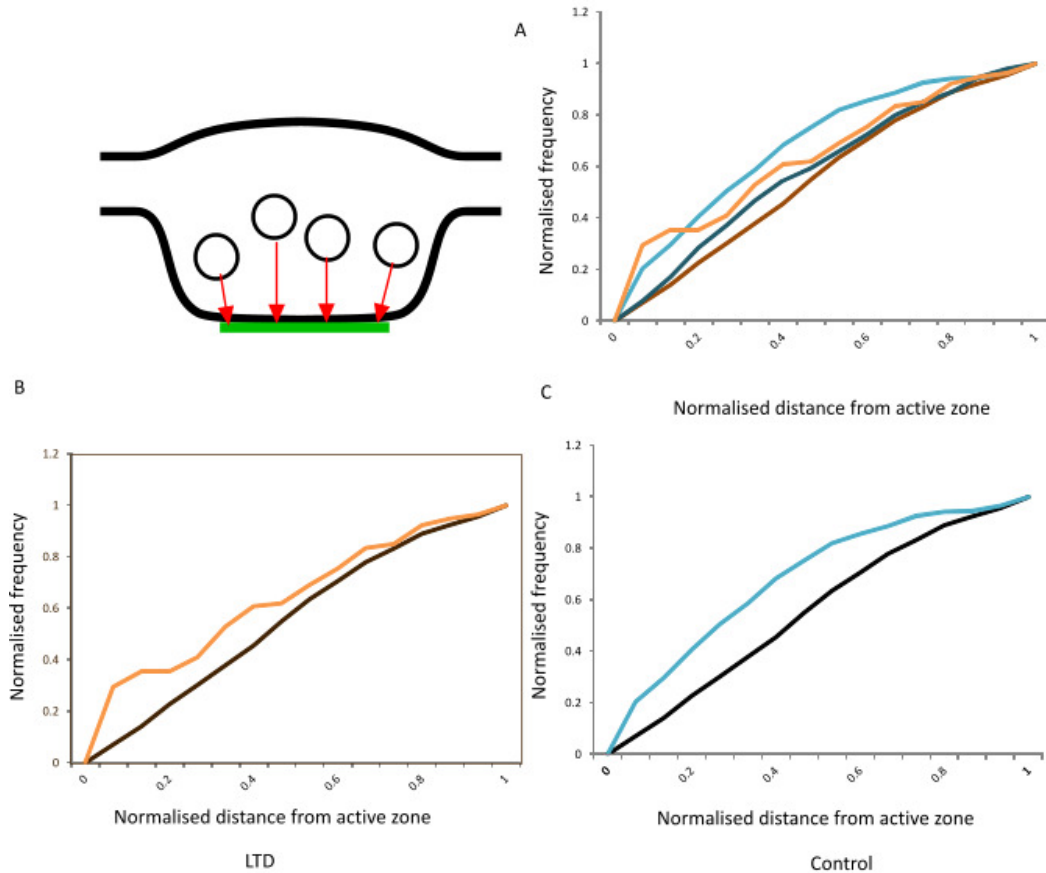


Figure 5.10 Distance from active zone of vesicles in control and LTD synapses

A) There is no significant difference between the distribution of non-recycling vesicles in LTD and control synapses (control $n=18$, LTD $n=23$, Student's t -test for unequal variance, $p=0.784$), and there is no significant difference between the distribution of the recycling pool vesicles between control and LTD synapses (Student's t -test for unequal variance, $p=0.706$). B) Recycling vesicles in LTD synapses tend to be closer to the active zone of the synapse, but they do not have a significantly different distribution compared to the non-recycling vesicles (Student's t -test for unequal variance, $p=0.473$). C) Vesicles in control synapses also cluster towards the active zone, but do not have a significantly different distribution than non-recycling vesicles (Student's t -test for unequal variance, $p=0.439$).

Dark brown – LTD non-recycling vesicles, orange – LTD recycling vesicles, dark blue – control non-recycling vesicles, light blue – control recycling vesicles.

5.2.7 Properties of the docked pool in LTD synapses

One of the most striking findings from the analysis of recycling vesicle pool positions in LTD synapses is the presence of a cluster of vesicles close to the active zone. This provides compelling evidence suggesting that the composition of the docked pool in particular is affected by LTD. As such, we wanted to consider this finding in more detail to understand how this sub-pool of vesicles might have implications for function. We considered that one hypothesis was that the number of active docking slots (i.e. those containing functional vesicles) in the active zone could be a key substrate for setting presynaptic efficacy. As such, deactivation of docking sites would serve to limit the number of easily released vesicles, and thus reduce the rate at which vesicles can release their contents into the synaptic cleft.

To examine this hypothesis, we first looked at the number of docked vesicles (disregarding their photoconversion status) present in LTD synapses compared to control synapses to test whether total docked vesicles counts were influenced by LTD; for example, consistent with dismantling of docking site apparatus, we should expect to see fewer docked vesicles at the active zone. As can be seen in Fig.5.11.A, we actually saw a slight increase in the percentage of vesicles present at docking sites: LTD synapses had $9.6 \pm 3\%$ of the total pool at docking sites, compared to $7.8 \pm 1\%$ at control synapses. This was not a significant difference in the size of the active zone (control $n=18$, LTD $n=23$ Student's *t*-test, for unequal variance, $p=0.50$) Without the ability to look at large populations of synapses, a real estimate of changes in docked pool size cannot be made.

Next we looked at the number of recycling vesicles present at the active zone. In control synapses, recycling vesicles made up $23.37 \pm 4.2\%$ of the total pool and $24.35 \pm 6.4\%$ of the docked pool. There is no significant difference between these fractions ($n=18$, Student's *t*-test for unequal variance, $p=0.89$). In LTD synapses the total pool is made up of $12.16 \pm 1.3\%$ recycling vesicles, but the docked pool is made up of $20.91 \pm 5.9\%$ recycling vesicles. Though this is a marked difference, it is not significantly different ($n=23$, Student's *t*-test for unequal variance, $p=0.16$) (Fig.5.11.B). We next considered how this corresponded to the fraction of the recycling pool as a whole. This was even more dramatic. In control synapses, $11.13 \pm 3.7\%$ of the recycling pool vesicles are situated at the active zone. In LTD synapses, there is $35.68 \pm 10.6\%$ of the recycling pool

situated at the active zone. This is significantly higher (control $n=18$, LTD $n=23$, Student's t -test for unequal variance, $p<0.02$).

Although there is no significant difference in the composition of the docked pool, there is a significant difference in the fraction of the recycling pool that is at the active zone. This suggests that trafficking of recycling vesicles away from the active zone is reduced in LTD synapses, potentially leading to a reduction in the efficiency of release.

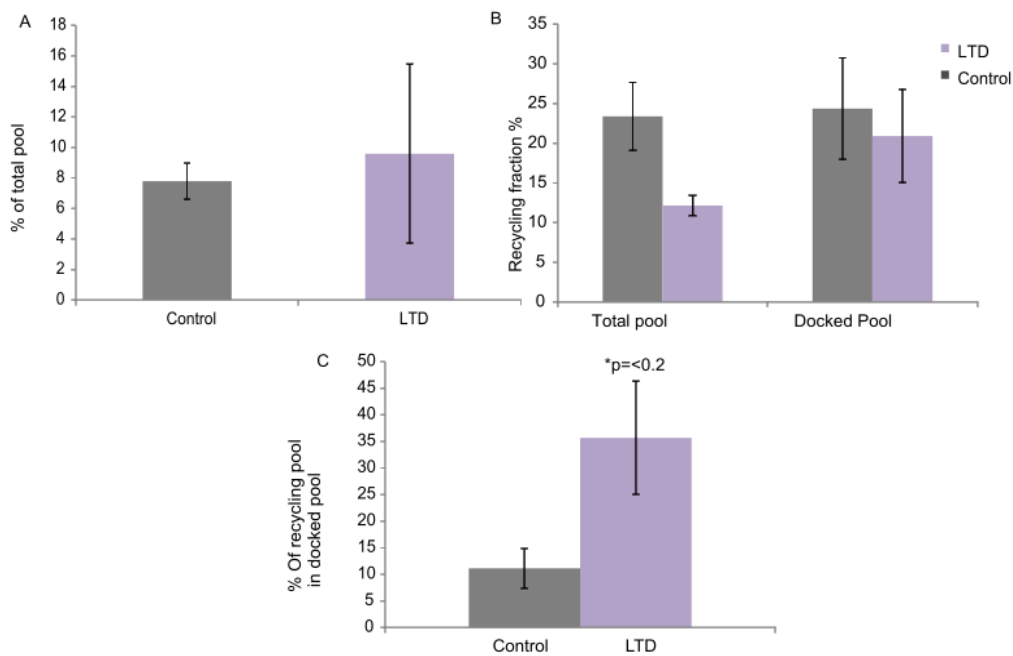


Figure 5.11 Recycling fractions in the docked pool in LTD and control synapses

A) The fraction of the total pool of vesicles which is located at docking sites in LTD ($9.6\pm3\%$) and control synapses ($7.8\pm1\%$) (control $n=18$, Student's t -test for unequal variance, $p=0.50$). B) The percentage of vesicles which are recycling vesicles within the total pool compared to the fraction of vesicles which are recycling vesicles in the docked pool. In control synapses, the recycling fraction comprises $23.4\pm4\%$ of the total vesicle pool. In LTD synapses, the recycling fraction is significantly lower at $12.2\pm1\%$ of the total pool (Student's t -test for unequal variance, $p<0.02$). In control synapses, recycling vesicles make up $24.35\pm5\%$ of the docked pool. In LTD synapses, recycling vesicles make up $20.9\pm6\%$ of the docked pool. C) The fraction of the total number recycling vesicles present in the synapse located in the docked pool in LTD synapses is significantly higher ($35.7\pm11\%$) compared to control synapses ($11.14\pm4\%$) (Student's t -test for unequal variance, $p<0.02$).

In the previous chapter (section 4.2.6), we observed that recycling vesicles were more likely to be retained at sites at the periphery of the active zone, and trafficked away from sites towards the centre of the active zone. This led us to hypothesise that vesicle recycling occurs largely at the centre of the active zone. An interesting question is whether the change in vesicle recycling, effected when LTD is induced, is reflected in the positions at which recycling vesicles occur in the active zone. In order to examine this, we next produced cartoons of the vesicles at the active zone of each synapse used (Fig.5.12.B), eliminating those with only one vesicle at the active zone, and then divided vesicles into recycling or non-recycling. The docking sites were then categorised as either peripheral or central (Fig.5.12.A). The fraction of recycling vesicles at each category of docking site was then calculated.

There is no significant difference between peripheral and central sites in active zones of LTD synapses (Student's *t*-test for unequal variance, $p=0.24$) or control synapses ($p=0.90$). There is no significant difference in the number of recycling vesicles at peripheral sites in LTD synapse active zones and those of control synapses ($p=0.81$), nor is there a significant difference between the recycling vesicle fraction at central sites ($p=0.429$) in control and LTD synapses. Though results were not sufficiently replicated to achieve statistical significance, there was marked difference in distribution of vesicles in control vs LTD synapses. In control synapses, the ratio of recycling vesicles at central vs peripheral sites was 0.944, suggesting that they occurred at roughly similar frequencies. In LTD synapses, recycling vesicles were much more common at peripheral sites, giving a ratio of 0.552, showing that vesicles are approximately twice as common at the periphery as they are in central sites.

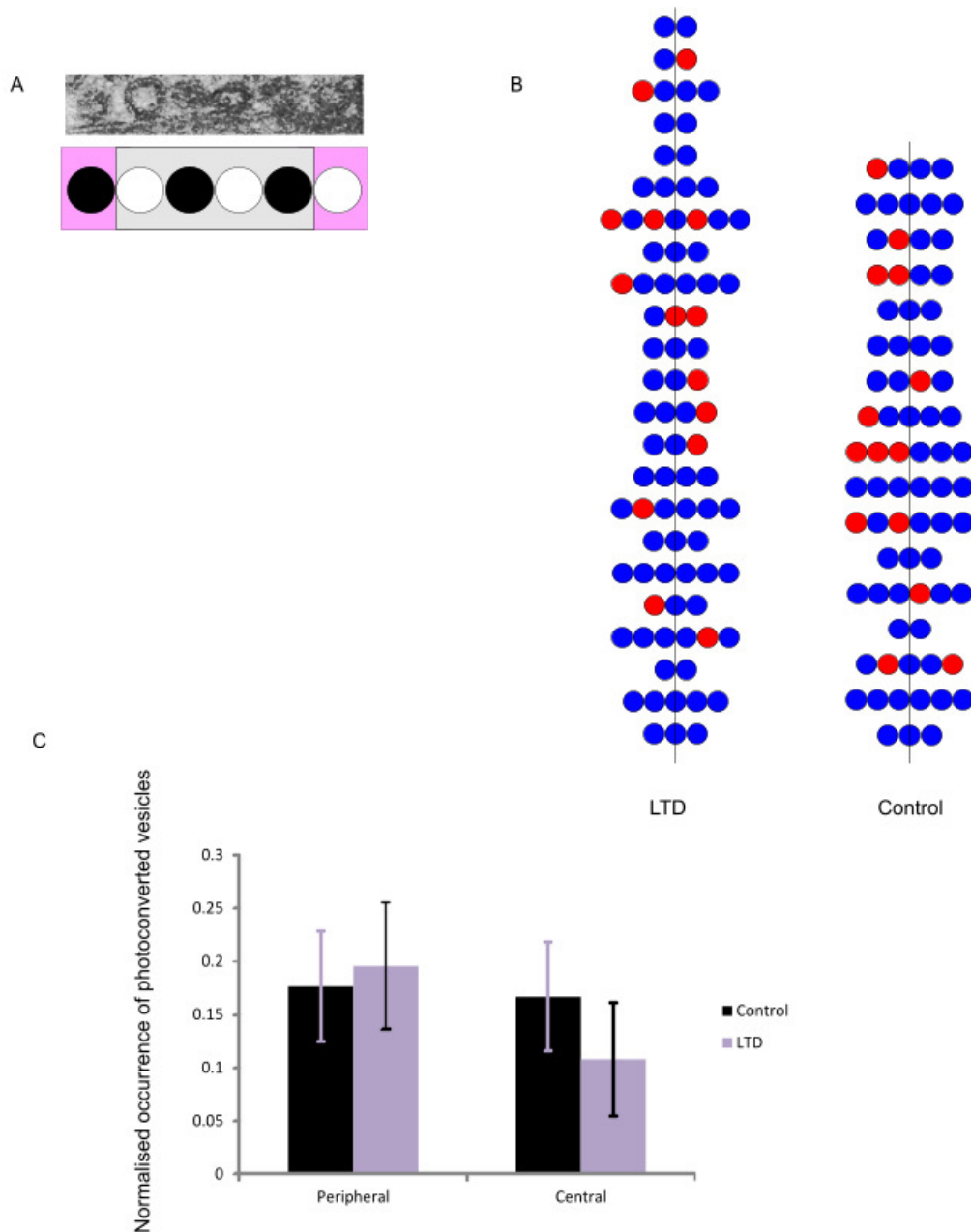


Figure 5.12 Location of recycling vesicles within the docked pool

A) Cartoons of the vesicle population at the docked pool of each synapse were created. Vesicles were termed recycling or non-recycling, and peripheral (indicated by pink boxes) or central (indicated by the grey box). B) Cartoons of all active zones used. Active zones containing only a single vesicle were eliminated. C) Fraction of recycling vesicles at peripheral vs central sites in LTD and control synapses. In control synapses, recycling vesicles are present at 17% of peripheral docking sites, and 16% of central ones. There is no significant difference between peripheral and central sites in LTD

synapses. (Student's *t*-test for unequal variance, $p=0.24$) or control synapses ($p=0.90$). There is no significant difference in the number of recycling vesicles at peripheral sites in LTD and control synapses ($p=0.81$), nor is there a significant difference between the recycling vesicle fraction at central sites ($p=0.429$).

5.3 Discussion

In this chapter we established a method for the reliable induction of LTD to examine possible relationships between this type of persistent change in synaptic strength and underlying modulation of the functional vesicle pools. We demonstrated that, after LTD, synapses show less efficient release capabilities, smaller functional pool size and specific changes in the arrangement of functional vesicles docked at the active zone.

5.3.1 Functional properties of LTD synapses

The findings from our fluorescence studies were broadly consistent with those of Zakharenko et al. (2002), the first study that showed robust vesicle recycling kinetic changes in depressed central terminals. Specifically, we observed that FM dye-labelled synapses displayed lower average levels of fluorescence and a decrease in the rate of release. This suggests a reduction in the efficiency of neurotransmitter release, as FM dye release is linked to fusion. Zakharenko et al. (2002) suggested that this may be due to a switch from full fusion exocytosis events to fusion pore events. This may be the case and further experiments, such as conducting the FM dye destain in the presence of BPB, might help determine whether the rate of dye leaving the vesicles rather than the rate of vesicle fusion is the limiting factor. As previously discussed in section 4.3.2, BPB has previously been used in experiments to determine the occurrence of kiss-and-run recycling (Harata et al., 2001). As a water soluble compound, it can access and quench FM-dye within vesicles much more quickly than the dye molecules can dissociate from the membrane. This would eliminate the possibility that in LTD the fusion pores are opening for a shorter period of time, or that there is a shift towards a different mechanism of vesicle fusion.

Our results are in direct opposition to those shown by Xu et al. (2013) in their experiments using biotinylation of vesicle transporters, showing increased neurotransmitter release that they believed to be as a homeostatic response to the internalisation of postsynaptic AMPA receptors. However, these experiments were

conducted using high K^+ extracellular solution on cultured neurons, which might recruit a different pool from that of electronic stimulation in slice.

5.3.2 Relating ultrastructure and function in LTD synapses

In our control samples, the recycling pool made up $23.4 \pm 1.2\%$ of the total pool. This is in line with the findings of Marra et al. (2012) working in the same system. The recycling fraction was significantly reduced in recycling synapses that had undergone LTD. The decrease in the number of recycling vesicles in LTD synapses compared to controls confirmed the idea of a presynaptic component to LTD. This result is complementary to previous research, suggesting that LTP produces an increase in release probability (Bekkers and Stevens, 1990) and the findings of this lab that potentiation increases the recycling pool fraction (Ratnayaka et al., 2012). This does not suggest whether this is due to a mechanism which occurs within the synapses, or perhaps whether this is further evidence of the role for retrograde messengers in long-term plasticity.

In the previous chapter we discussed the possibility of a system of vesicle recycling in which vesicles are taken in at sites proximal to the active zone and returned to the cluster, and suggested that they return to sites closer to the active zone on further activity as those vesicles which are positioned closest to the active zone undergo fusion and reuptake and are returned to the back of their cluster in turn. The results described in this chapter show further evidence for this. The revelation of a reduced rate of vesicle turnover (Fig.5.6.E) combined with the information regarding positioning of vesicles within the cluster (Fig.5.11B) gives further support for this theory. If there are lower numbers of vesicles released in a given time, fewer vesicles will be cleared from the front of the queue, and thus the vesicles will not proceed as far towards the active zone. In addition, the less frequent occurrence of recycling vesicles at the central docking sites in the active zone also suggests that previous recycling vesicles are not being put forward for further fusion events.

Bourne et al. (2013) found that the number of vesicles at docking sites in LTP showed an initial decrease, and then an increase after 2 h. In our experiments, samples were fixed nearly 1 h following the induction of LTD, and at this point we saw no reduction in the size of the active zone. There is a question as to whether we are seeing part of a two-phase change in docking vesicle arrangement, or whether we are seeing the final arrangement. There was a greater variation in the size of active zones in LTD synapses, which could be caused by active zone restructuring. Looking at later time

points in future experiments would be a useful direction of study, to see whether similar longer-term changes to those found by Bourne et al. (2013) are found in LTD synapses. The use of volume electron microscopy data would allow larger numbers of synapses to be screened, reducing selection bias, and giving a clearer picture of the stimulus-based changes in properties.

It has previously been identified that the prolonged silencing of synapses in neuronal cultures leads to a decrease in certain key synaptic proteins, specifically CAST/ELK, bassoon, piccolo, RIM1, Munc13-1, liprin-ALPHA, and synapsin. Other synaptic proteins levels remained unaffected (Lazarevic et al., 2011). CAST/ELK, two closely-related proteins which are responsible for the maintenance and stability of active zones, bind with RIM1, bassoon, piccolo, and Munc13-1 (Hida and Ohtsuka, 2010). RIM1 and Munc13-1 are key factors for synaptic vesicle priming, and the localisation of RIM1 at the active zone is CAST/ELK dependent (Betz et al., 2001).

In a recent paper, Sugie et al. (2015) identified changes in the size of the active zone in *Drosophila*. They noted this to be due to a decrease in the level of the CAST/ELK homologue BRP (Wagh et al., 2006). The decrease in BRP caused a decrease in the density of calcium channels in the active zone, an over-expression of kinesin, and the dispersal of RIM1 from the active zone to other locations in the cell. They also found that other active zone protein levels remained the same.

This provides a potential mechanism for the reduction in the number of docking sites available: the reduction in CAST/ELK may lead to the trafficking of RIM1 away from the active zone, consequently impairing vesicle priming at some sites. This leaves the docking sites otherwise assembled, meaning they can be reactivated if the activity demands of the synapse change.

A hypothesis we put forth in this chapter is that part of the mechanism for the reduction of the rate of vesicle turnover can be reduced by deactivating docking sites. Our results showed some evidence for this theory. In chapter 4, we found that recycling vesicles appeared to be cleared from the centre of the active zone over time after the cessation of stimulus. In section 5.3.2, we found that there was a decrease in the frequency of recycling vesicles at central docking sites, compared to those at peripheral sites. This hints that fewer of these docking sites may be responsible for recycling in LTD

synapses. Looking at LTD synapses at different time points would help elucidate whether this is actually a mechanism of controlling release rate.

In their paper, Zakharenko et al. (2001) discuss the possibility that LTD might cause a move away from full collapse endocytosis towards a fusion pore model. This would be one way to reconcile Xu et al. (2013) with the results described in this chapter: if a smaller pool was undergoing heavy recycling, and the majority of the total recycling pool was moved into the reserve pool after labelling. The reduction of recycling vesicles at central positions in the active zones is evidence against this theory: one would expect an increase in recycling vesicles if this were indeed the case.

This would support the results described in the previous chapter, namely a small subset of vesicles which are preferentially recycled, and a larger pool which is recycled more slowly.

5.3.3 Linking pre- and postsynaptic factors of LTD

This chapter conclusively demonstrates that there is a presynaptic component to LTD, confirming the findings of (Zakharenko et al., 2002), but the literature provides no evidence that LTD can be generated within the synapse. As LTD is induced postsynaptically, but leads to changes presynaptically, the involvement of a retrograde messenger is likely (Bolshakov and Siegelbaum, 1994). The retrograde messengers which have previously been associated with LTD are arachidonic acid and NO (Bolshakov and Siegelbaum, 1994). Arachidonic acid has been shown to be essential for the induction of certain forms of LTD and limiting neurotransmitter release, similar to that seen in our results (Misner and Sullivan, 1999). Meanwhile, NO has been shown to act on synaptic vesicle docking machinery, which would result in both a reduced recycling rate, and would potentially explain the relatively high levels of recycling vesicles at the docking sites (Hardingham et al., 2013). Comparing the effects of inhibiting the endocannabinoid receptors and the guanylyl cyclase would give clearer ideas as to the mechanisms of LTD which caused the effects seen here.

This chapter provides a clear insight into vesicle recruitment and organisation in LTD synapses, paving the way for further work into the presynaptic mechanisms of this form of plasticity. Future directions could include comparisons to vesicles in LTP synapses, and time stamp comparisons, like those in the previous chapter, to provide clues as to how vesicles are reintegrated into the cluster. There are also a number of

pharmaceutical targets which might be exploited to demonstrate their effects on vesicle pool properties, such as cdk5 and calcineurin, which have been shown to have an effect on vesicle scaling. Certainly, this demonstrates an exciting new method for linking a well-established functional model of long-term plasticity to real-time optical readouts of synaptic function, and to an ultrastructural view of vesicle recycling.

Chapter 6: Recycling vesicles at extrasynaptic locations in hippocampal slice

6.1 Introduction

The approach outlined in previous chapters for studying fundamental properties of small central nerve terminals in a physiologically relevant environment can also provide us with information regarding the vesicles within the processes that connect them. We can perform optical assays of vesicle function in native tissue, use photoconversion of DAB to identify recycling vesicles at an ultrastructural level, and use established plasticity protocols to study the presynaptic effects. The objective of this chapter is to exploit the methods established previously, as well as a new approach based on cutting edge imaging technology, to address questions about the 'superpool', a population of mobile vesicles which move between synapses and can contribute to recycling (Staras and Branco, 2010).

In previous chapters we focused on the study of vesicle pools within defined synaptic terminals: those close to an active zone and organised in tightly clustered groups. An emerging theme in the literature is a role for these extrasynaptic vesicles (Staras and Branco, 2010). To date, little is understood about the organisation of such vesicles, or their potential role in neuronal signalling.

The synaptic vesicles clustered in terminals are not discrete isolated units, but connected by short lengths of axon, typically $<3 \mu\text{m}$. This raises the possibility that vesicles, and other synaptic components, could move between synapses and join the recycling pool at different terminals along the axon. In recent years this concept of vesicle transport and sharing between boutons has been explored, and it has been shown that this is indeed the case. Molecular components such as receptor proteins, active zone proteins, and vesicle precursor proteins are trafficked within neurons (Sorra et al., 2006, Fejtova and Gundelfinger, 2006), and there is evidence that receptor and

scaffolding proteins are transported laterally between postsynaptic sites (MacGillavry et al., 2011). These processes are implicated in synaptogenesis and in responding to plasticity. More importantly, synaptic vesicles can also be laterally mobile (Chen et al., 2008, Hopf et al., 2002, Krueger et al., 2003, Ahmari et al., 2000, Staras et al., 2010, Darcy et al., 2006a).

This movement of labelled vesicles has been observed since the earliest days of experiments using the FM dyes (Betz et al., 1992a) and has been noted in several studies since. Vesicles have been shown to be able to move to neighbouring synapses, and can then be recycled at these destination synapses, showing that mobile vesicles are an important new element of synaptic function (Darcy et al., 2006a). Further studies using stimulated emission depletion microscopy (STED), which provides a high resolution to observe fluorescent labelled vesicles, showed that vesicles were consistently moving, in both retrograde and anterograde directions, between boutons (Westphal et al., 2008). Recycling vesicles were revealed to be shared amongst the vesicle clusters at neighbouring boutons, at which point they re-entered the recycling pool. This pool has been theorised to have important functions for plasticity and for maintaining vesicle turnover (Staras and Branco, 2010).

Studies of the superpool have been made in a number of systems, primarily cultured neurons (Staras et al., 2010, Darcy et al., 2006a), and recently Ratnayaka et al. (2011) have shown evidence of lateral movement of recycling vesicles in the hippocampal slice system. Recently, an important study has established this pool *in vivo* (Herzog et al., 2011). Key questions remain: how are recycling vesicles organised extrasynaptically, what are their dynamics, and to what extent do recycling vesicles occur in extrasynaptic locations?

The initial aim of this study is to gather evidence using fluorescence imaging to examine dynamics of vesicle traffic in slices, using established approaches based on FM dye, but also live antibody labelling where specific protein classes can be targeted. The second objective is to reveal vesicle pool arrangements in ultrastructure and define novel features of organisation. Finally, we shall outline experimental results based on the same principles of ultrastructural investigation, but exploiting the latest technology for automated, high throughput volume analysis of tissue samples.

6.2 Fluorescence imaging of extrasynaptic vesicles

6.2.1 FM dye imaging mobile vesicles in cultured neurons

As a starting point, we set out to confirm the phenomenon of extrasynaptic vesicle mobility in acute brain slice using fluorescence approaches. As a baseline for comparison, we first examined this process in dissociated cultured neurons, where most work to date has been carried out (Ratnayaka et al., 2011, Staras et al., 2010, Darcy et al., 2006a). Neuronal cultures were prepared as described in previous chapters: hippocampal neurons from 0 d rat pups were dissociated and plated onto astrocytic feeder layers grown onto glass coverslips. These neurons were then used at 14-21 DIV. These cultures were placed into a custom-built imaging chamber with parallel platinum electrodes which could be used to stimulate neurons. In the presence of 10 μM FM 1-43 in EBS, these cells were stimulated with 1200 AP/20 Hz and washed thoroughly in ACSF containing 20 μM AP5 and 50 μM CNQX. These cells were then imaged at a rate of 0.2 fps, with a 20 Hz stimulus applied after 20 s, in order to establish that labelled recycling vesicles were still release competent.

When these time lapse images were analysed, small packets of fluorescence were visible moving along processes (Fig.6.1.A). We made a number of quantitative measurements to characterise this process. First, we established the approximate size of mobile packets relative to the synapses represented by fluorescent punctae. In order to do this, from each culture we sampled the average intensity of the FM dye fluorescent signal in 15 laterally moving packets (extrasynaptic vesicles) and 15 stationary punctae (intrasynaptic vesicles) which responded to a destaining stimulus. When the background fluorescence levels were subtracted, and these values were normalised to the maximum fluorescence level detected, the fluorescence level of these mobile packets was, on average, $28.01 \pm 0.036\%$ of that found in the stationary punctae ($n=45$, $n=45$, Student's *t*-test, $p < 0.0002$) (Fig.6.1.B).

The next step was to establish the rate of vesicle transport between synapses. This was achieved by measuring the distance travelled by the fluorescent packets during the imaging period in order to gain an estimate of the speed of movement. Rates were calculated from 30 mobile vesicle packets taken from 3 cultures, from 2 animals. The average rate recorded was $0.375 \pm 0.028 \mu\text{m/s}$ ($n=30$ from 3 coverslips). This rate is broadly consistent with the value typically reported for fast axonal transport, of 0.5-5

$\mu\text{m/s}$ (Brown, 2003) (Fig.6.1.C). This value for the recorded rate is lower than that indicated in Brown (2003), which may be due to these punctae representing not only vesicles which move laterally along microtubules, but also vesicles with a ‘diffusive’ movement pattern, as reported previously in Westphal et al. (2008).

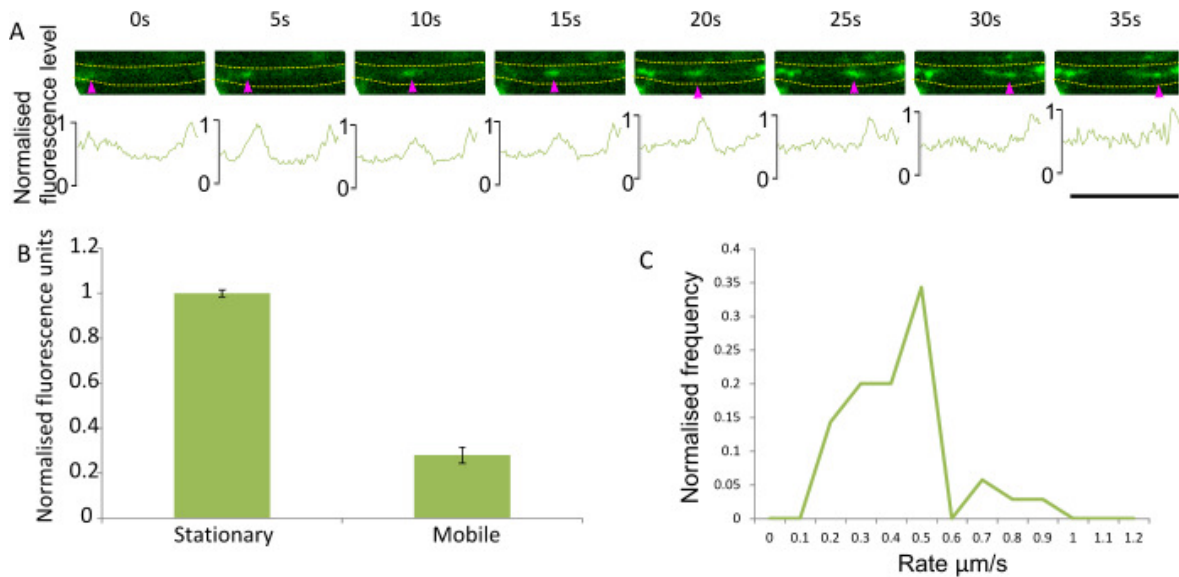


Figure 6.1 Lateral movement of FM 1-43 labelled vesicles in cultured neurons

A) An example of fluorescent punctae moving horizontally along a process over time. Scale bar indicates $2 \mu\text{m}$. B) Mobile fluorescent packets exhibit $28.01 \pm 3.6\%$ of the fluorescence of stable fluorescent punctae ($n=45$, $n=45$, Student's *t*-test for unequal variance, $p < 0.0002$). C) Distribution of the rates of packet movement along processes. The mean rate was $0.375 \pm 0.0277 \mu\text{m/s}$ ($n=30$ from 3 coverslips).

6.2.2 Using FM 1-43 to observe mobile vesicles in acute hippocampal slice preparations

In cultured neurons it is relatively easy to identify moving packets of synaptic vesicles. The monolayer of neurons on an astrocytic feeder layer provides a sparse lattice of processes with very little background fluorescence. The 3D structure of native tissue, even with confocal imaging methods to limit background fluorescence, makes it difficult to identify vesicles moving laterally through processes.

Previous work using an FM dye loaded slice revealed some evidence for the movement of packets of fluorescence between punctae (Staras et al., 2010). However, these experiments were based on relatively crude labelling protocols based on high potassium activation. An objective here was to repeat these experiments using controlled electrical stimulation (1200 AP/10 Hz) to label recycling vesicles with FM dye. Slices were then imaged using confocal microscopy at a rate of 0.5 Hz. Results are taken from three brain slices obtained from three animals.

The high level of background fluorescence and the relatively low intensity of the fluorescent signal make extrasynaptic vesicles much harder to identify than in cultures, and in many samples only synapses were clearly visible. A likely part of the problem is the absolute requirement for axons to run perfectly in parallel with the sectioning plane to permit unequivocal evidence for mobile fluorescence trafficking. However, clear examples of moving punctae were obtained, providing clear support for the idea that the superpool is a feature of native tissue (Fig.6.2.A).

For these packets, we found that the mean vesicle transport rate of $0.58 \pm 0.035 \mu\text{m/s}$ ($n=35$ from 4 slices) was again broadly consistent with fast axonal transport (Brown, 2003) (Fig.6.2.C).

As before, in order to establish the relative numbers of recycling vesicles in these moving packets compared to those in synaptic locations, in three preparations which demonstrated sufficient fluorescence to background ratio to allow differentiation of punctae, we selected an equal number of stationary responsive punctae in regions next to punctae which showed lateral movement. In native tissue, we found that the fluorescence of the mobile packets compared to the stationary punctae was $56.12 \pm 0.016\%$ (Fig.6.2.B), a value significantly higher than that found in cultured neurons ($n=45$, $n=45$). Of course, one likely reason for the higher value is that the elevated levels of background obscure the identification of smaller packets and introduce a selection bias, such that only the largest moving packets can be readily identified.

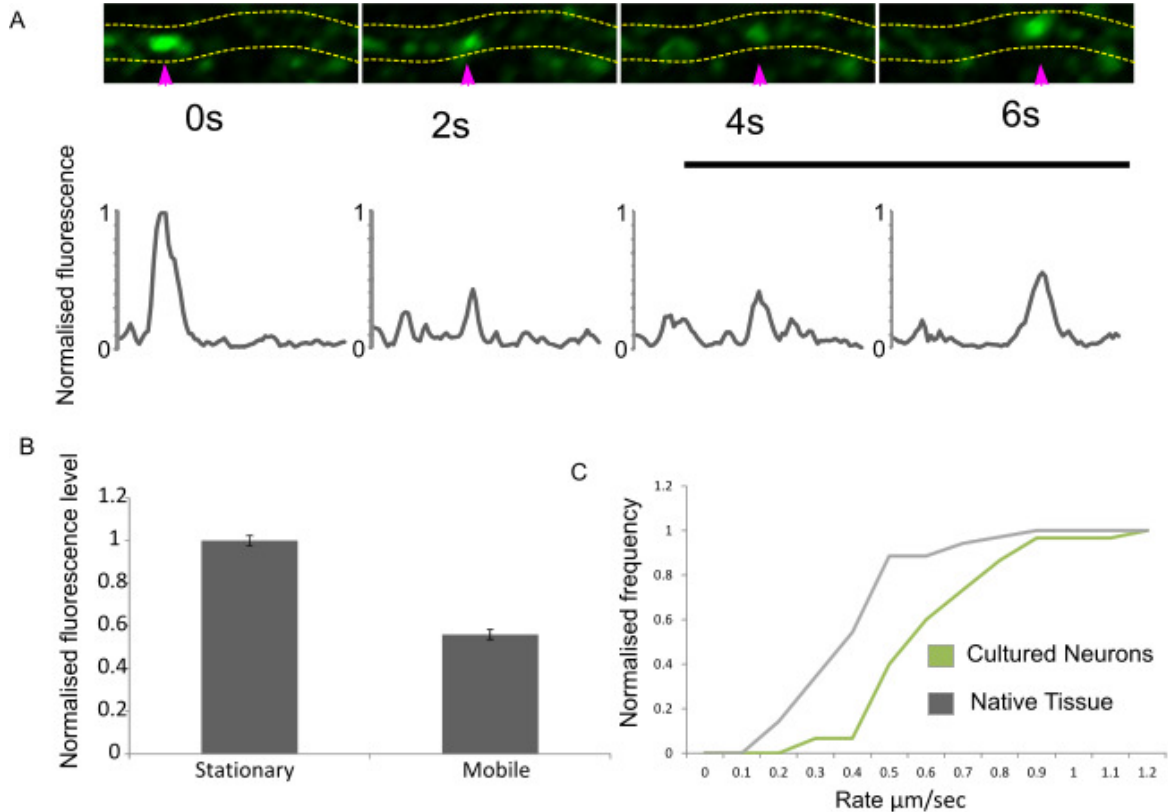


Figure 6.2 Lateral movement of FM 1-43 labelled vesicles in native tissue

A) An example of fluorescent punctae moving horizontally along a process over time. Scale bar indicates 5 μm . B) Mobile fluorescent packets exhibit $56.12 \pm 1.63\%$ of the fluorescence of stable fluorescent punctae ($n=15$, $n=15$, Student's t -test for unequal variance, $p < 0.0002$). C) Distribution of the rates of punctae movement along processes. The mean rate was $0.582 \pm 0.0345 \mu\text{m/s}$. This was significantly higher than the value found in cultured neurons (slice $n=35$ from 4 slices, culture $n=30$ from 3 coverslips, Student's t -test for unequal variance, $p < 0.0002$).

6.2.3 Using antibodies to observe extrasynaptic functional vesicles

As described in previous chapters, FM dye labelled synapses appeared as discrete punctae, and mobile vesicle packets could be seen moving between them. FM dyes are clearly useful tools for these investigations, but they do have a few limitations. One of these is the low levels of specificity of binding, and another is their susceptibility to photobleaching. As discussed in previous chapters, we considered the use of an

alternative to styryl dyes, an antibody raised against synaptotagmin-1. It has the additional benefit of exhibiting a lower level of photobleaching, and a high affinity for long-term binding to its epitope. These latter two properties are especially beneficial when it comes to looking at vesicle transport rather than vesicle release.

Similarly to FM dye labelling, slices were injected with a 1:100 solution of syOyster550 in ACSF for 7 min. After the first 3 min, a 1200 AP/10 Hz stimulation was applied to give the antibody access to the luminal domain of the vesicles. Following the application of syOyster550, the slice was washed with ACSF at 3 ml/min for 20 min and then imaged using confocal microscopy at a rate of 2 fps.

In slices labelled by syOyster550, there were fewer laterally mobile punctae visible, despite lower background levels of labelling. One possibility is that this is because synaptotagmin1 selectively labels a restricted subset of vesicles; for example, only those participating in full collapse fusion, or due to a lower affinity of the probe. However, packet movement was visible in some slices (Fig.6.3.A).

These mobile fluorescently labelled vesicle clusters had $49.51 \pm 0.02\%$ of the fluorescence of the stationary responsive punctae (Fig.6.3.B). Though significantly different from that found in FM dye-labelled slices (FM 1-43 $n=15$ from 3 slices, Oyster 550 $n=15$ from 3 slices, Student's *t*-test for unequal variance, $p < 0.002$), this is a broadly similar figure to that found in FM dye-labelled synapses, and also those found in cultured neurons (syOyster550 $n=15$ from 3 slices, FM 1-43 in culture $n=30$ from 3 coverslips, Student's *t*-test, $p < 0.002$).

As described above, the rate of vesicle transfer was calculated by measuring the distance that these laterally moving punctae could be traced and the time over which it was imaged. Mobile vesicles labelled with syOyster550 are functional vesicles. These functional vesicles were observed to move through the processes with a mean rate of $0.632 \pm 0.045 \mu\text{m/s}$ (Fig.6.3.C). This rate was not significantly different from the values obtained when measuring the rate of intersynaptic vesicle transport of FM 1-43 labelled vesicles (FM 1-43 $n=34$ from 4 slices, syOyster550 $n=29$ from 3 slices, Student's *t*-test for unequal variance, not significant, $p=0.47$)

This shows we were successfully able to use an alternate labelling method to observe mobile vesicles in the hippocampal slice system, providing significant confirmatory

evidence for our findings. Though the Oyster550-labelled mobile vesicles pose the same challenge for measuring as those in FM 1-43 labelled slices, which might explain the higher rates of movement observed compared to mobile vesicle packets in cultured neurons, the lack of difference in the rates suggests that that we are labelling the same population of vesicles with the anti-synaptotagmin Oyster550 antibody, and that the presence of the probe does not alter the function of these vesicles compared to FM 1-43.

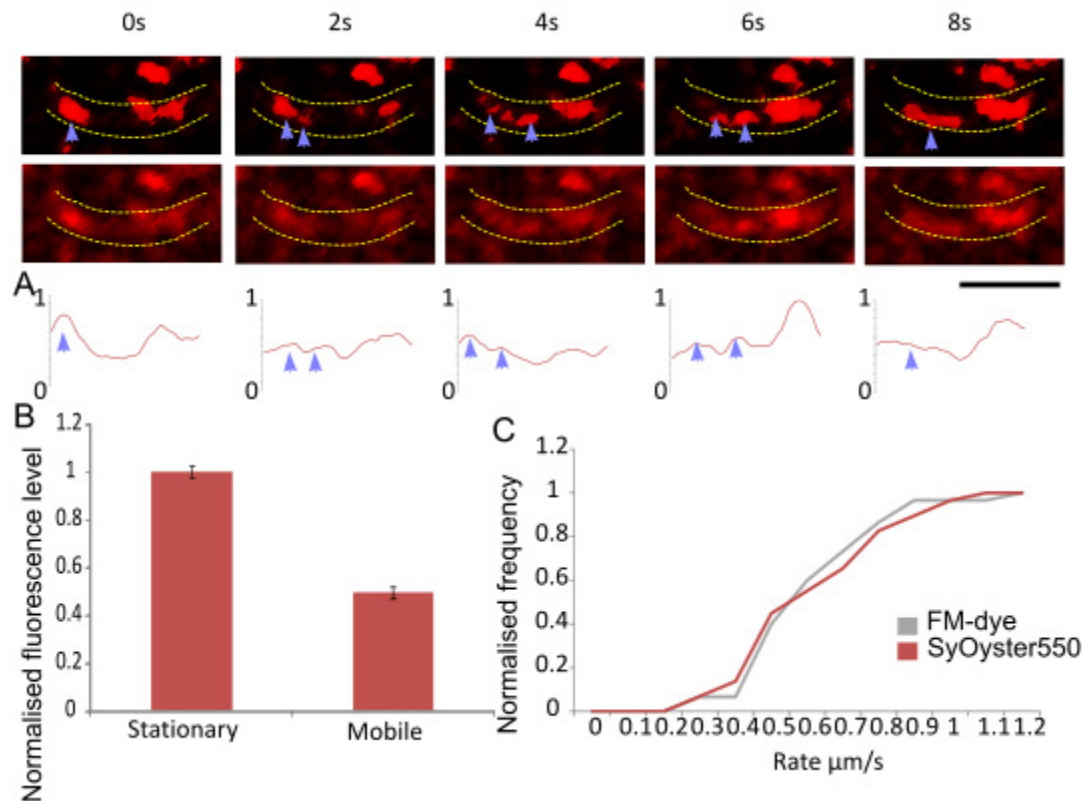


Figure 6.3 Using syOyster550 to label mobile vesicles

A) An example of fluorescent punctae moving horizontally along a process over time. Scale bar indicates 2 μm . B) Mobile fluorescent packets display $49.51 \pm 0.0235\%$ of the fluorescence of stable fluorescent punctae ($n=15$, $n=15$, Student's t -test for unequal variance, $p < 0.0002$). C) Distribution of the rates of punctae movement along processes. The mean rate was $0.582 \pm 0.0345 \mu\text{m/s}$. This was significantly higher than the value found in cultured neurons (FM 1-43 $n=35$ from 4 slices, syOyster550 $n=29$ from 3 slices, Student's t -test for unequal variance, $p=0.47$).

6.3 Ultrastructural studies of extrasynaptic functional vesicles

6.3.1 Using conventional electron microscopy to study functional extrasynaptic vesicles

In the above sections, we demonstrated that functional vesicles do experience lateral movement along processes in native tissue neurons, although they appear to do so in larger numbers than in cultured neurons. This makes ultrastructural study of recycling vesicles in processes all the more relevant, as it becomes important to establish whether these higher fluorescence levels point to a fundamental difference between neurons in native tissue and those in culture, or whether it is an artefact of the interaction between fluorescent probes and the environment that a brain slice presents. Establishing how the composition of these mobile packets with regards to recycling vesicles compared to synapses in tissue slices, and the values established for these measurements in tissue culture, might provide insights into synapse organisation, novel signalling pathways, and possible substrates for plasticity in slice.

Though a lot of valuable information can be gathered even from single sections of synaptic vesicle clusters, the density of vesicles in axons and processes is however much lower. In order to sample sufficient numbers of vesicles to acquire any sort of complete picture of the vesicle composition of these areas, 3D reconstructions based on serial section information are required.

In order to produce a 3D reconstruction, a hippocampal slice was loaded as previously described, with a 1200 AP/10 Hz stimulus in the presence of 20 μ M FM 1-43FX and allowed to wash for 20 min, fixed using rapid microwave fixation, bathed in 1 mg/ml DAB solution, photoconverted, and prepared for electron microscopy. Serial sections of 70 nm depth were prepared by Dr JJ Burden and mounted as ribbons on formvar-coated slot grids for viewing under an electron microscope. A region of interest was located on a section, imaged, and then located on each subsequent section (Fig.6.4.A). Regions of interest were synapses which appeared as cross-sections that attached to a process which continued along the plane of sectioning. Synapses containing photoconverted vesicles and one visible active zone were selected. Vesicles were then identified and classified as either photoconversion positive (functional) or photoconversion negative (non-functional vesicles) and marked accordingly (Fig.6.4.C).

Serial sections of these processes and synapses were aligned (Fig.6.4.B, D) and imported into Reconstruct software (Fiala, 2005), where the key features were reconstructed and from which measurements could be taken (Fig.6.4.E).

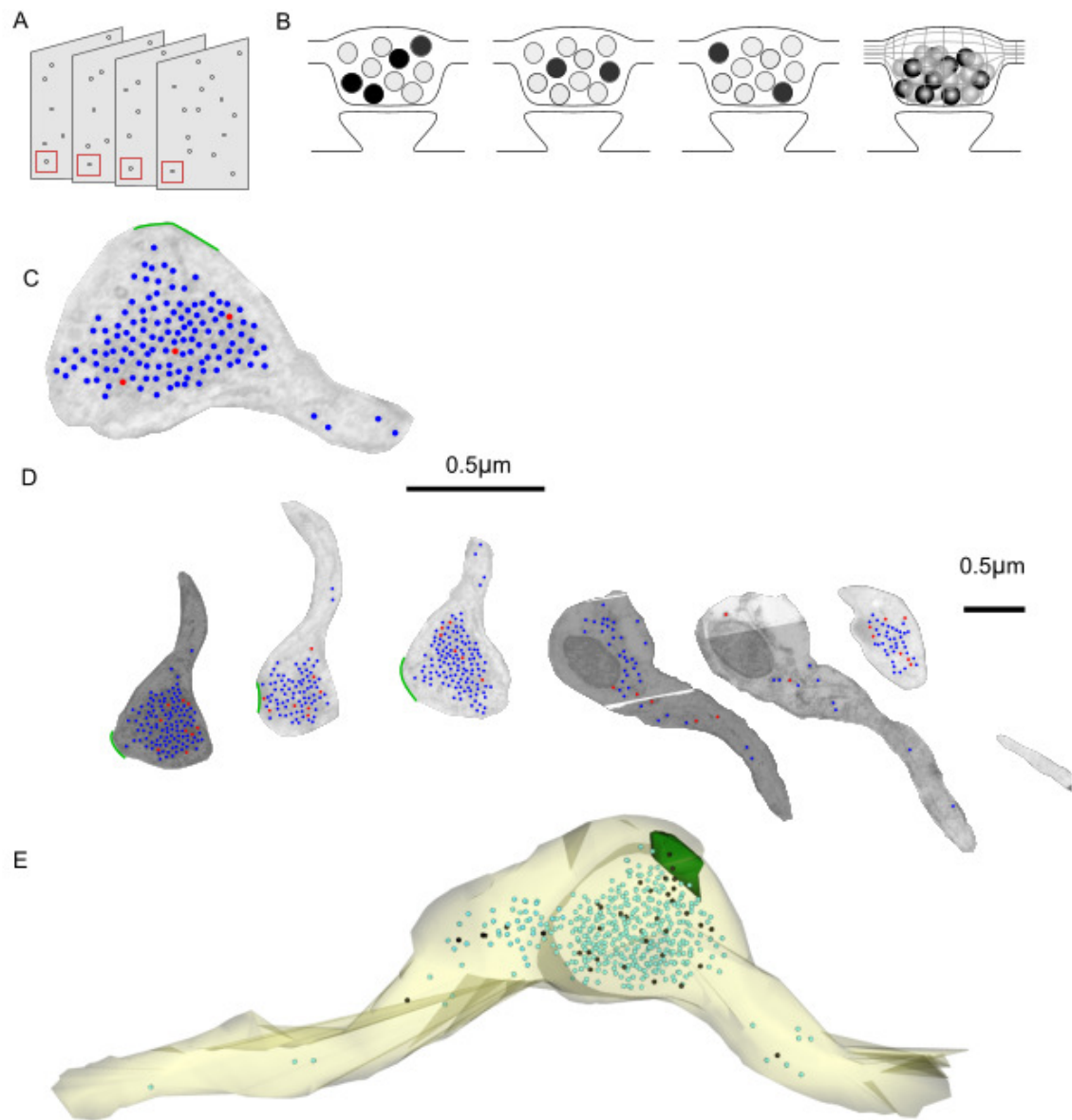


Figure 6.4 Producing 3D reconstructions of processes containing recycling vesicles

A) A region of interest is located. It must be relocated on every section to produce the reconstruction. B) The synapse sections are then aligned in the same orientation and converted into 3D reconstructions. C) Vesicles in synapses and attached processes were labelled as either recycling or non-recycling. D) This was done to the region of interest in all sections. The sections were then aligned. E) A 3D reconstruction of a synapse, produced in Reconstruct.

There were several technical challenges in collecting this dataset. Due to selection constraints, it was difficult to find synapses which met a variety of key requirements: with a process running parallel to the plane in which the sections were made; with a single clearly-defined active zone; with unequivocal photoconverted vesicles; and finally, fully described in the span of the available serial sections. Relocating regions on subsequent sections was also no insignificant challenge, as sections contained a large amount of dense tissue, a problem which is not encountered when reconstructing cultured neurons. Because of these technical difficulties, all reconstructions were taken from two samples and a limited number of processes (8) were able to be reconstructed.

We identified synapses that contained photoconverted vesicles which had a process attached. These processes also contained photoconverted vesicles (e.g. Fig.6.5.A). As before, these could be identified by the shape of a linear profile across each vesicle's diameter (Fig.6.5.B). Vesicles were labelled as functional within the synapses and marked accordingly, and a reconstruction was generated using Reconstruct software. Vesicles were classified as being part of the synaptic cluster or as being extrasynaptic. Clustered vesicles were those in a dense group in the synaptic terminal, close to an active zone, and not within the process. Extrasynaptic vesicles were defined as those within a process and not in contact with the cluster. In the case of vesicles which could not easily be classified, a rule was applied stating that vesicles within 100 nm (two vesicle widths) from the nearest cluster vesicles were considered to be intrasynaptic, and those which were further away than this were determined to be extrasynaptic (Fig.6.5.C).

6.3.2 Properties of extrasynaptic recycling vesicle populations

Vesicles within clusters were a maximum of $0.6 \pm 0.10 \mu\text{m}$ (average between synapses) from the active zone, while vesicles outside clusters had an average maximum of $3.36 \pm 0.62 \mu\text{m}$ from the active zone. In these samples the length of processes was on average 5.6 times longer than the attached synapse.

For these experiments, intrasynaptic vesicles were found to be composed of $20.7 \pm 0.03\%$ functional vesicles, which is broadly consistent with the recycling vesicle fractions found in reconstructed synapses in the previous study conducted by Marra et al. (2012) (18-20%). The extrasynaptic, non-cluster vesicles were composed of $31.1 \pm 4.6\%$ photoconverted, functional vesicles (synapses $n=8$, processes $n=8$, paired

Student's *t*-test for unequal variance, $p=0.117$) (Fig.6.5.D). This fraction is similar to, but lower than, the value of $36\pm 7\%$ noted by Darcy et al. (2006), although their experiments were conducted at physiological temperatures which elevated the recycling fraction. Though not a significant increase, it hints that perhaps recycling vesicles are preferentially selected for movement into the superpool.

We looked at the absolute number of recycling vesicles in the processes to see if we could explain the results given by the fluorescence data. These values, showing that on average extrasynaptic vesicles have 66.5% (Fig.6.5.E) of the level of fluorescent labelling of synaptic vesicle clusters, are roughly in line with the value found for fluorescence levels of punctae versus mobile vesicle packets ($56.12\pm 1.63\%$), suggesting that these correspond to the same phenomenon.

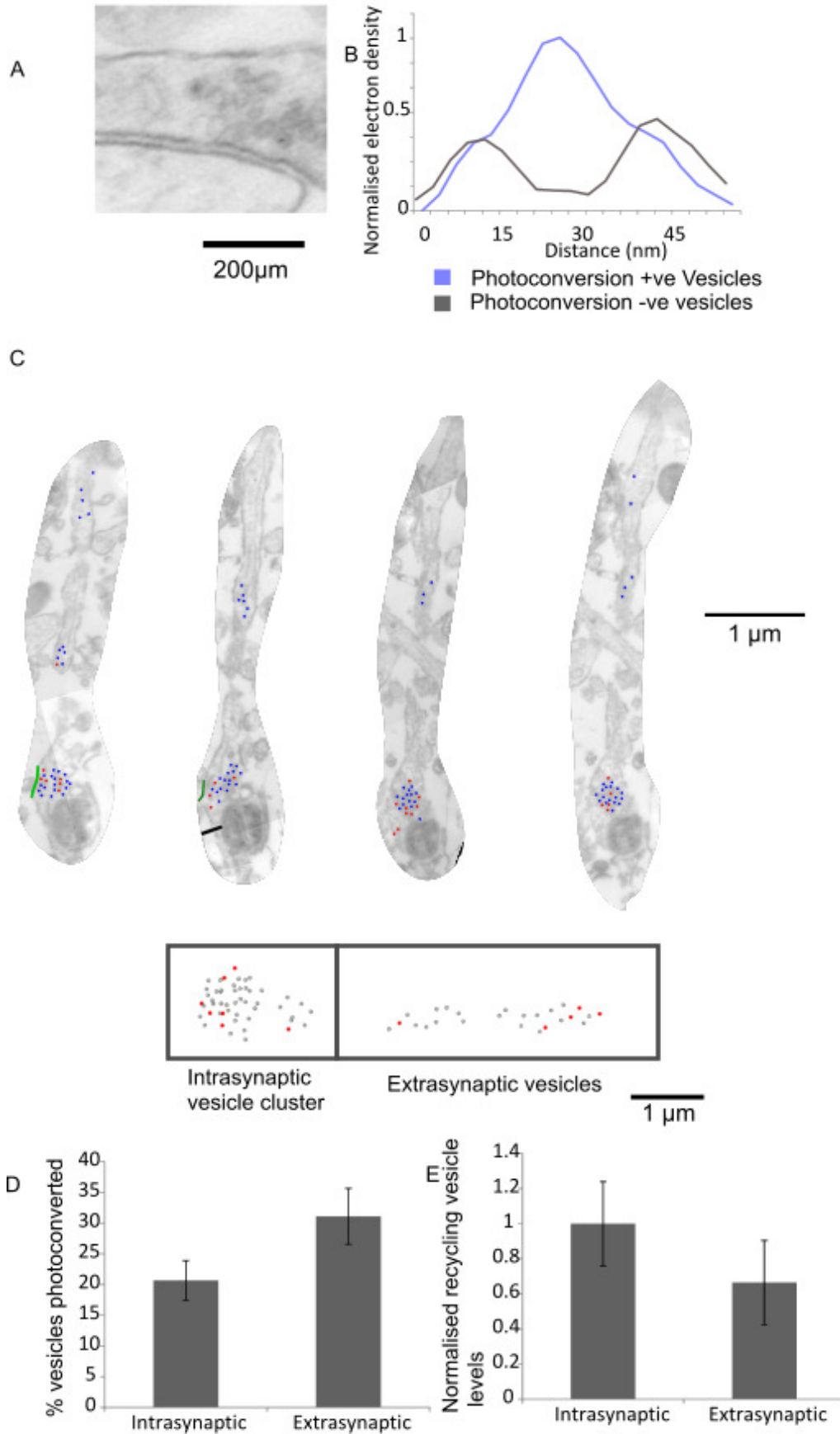


Figure 6.5 Identifying and quantifying intrasynaptic and extrasynaptic vesicles in native tissue

A) Photoconverted vesicles were identified in the processes of neurons, indicating that recycling vesicles are being transported between terminals in the slice system. B) These photoconverted vesicles could be identified by the distinctive profile: showing an increase in electron density in the lumen, as opposed to the decrease shown by non-photoconverted vesicles. C) Terminals containing photoconverted vesicles, seen attached to a length of axon, were aligned, and vesicles were classified as either photoconverted or not based on the criteria described in B). Vesicles were also classified as intrasynaptic or extrasynaptic. Extrasynaptic vesicles were classified as those more than two vesicle widths from the nearest cluster vesicle. D) Photoconverted vesicles made up $20.7 \pm 3.2\%$ of the total population of intrasynaptic vesicles, and $31.1 \pm 4.6\%$ of the total population of extrasynaptic vesicles (synapses $n=8$, processes $n=8$, Student's t -test, $p=0.173$). E) When comparing the numbers of recycling vesicles found in extrasynaptic locations to those in intrasynaptic locations, the extrasynaptic vesicle population was on average $66.5 \pm 14.9\%$ of those in found in the synaptic terminals.

This demonstrated that, like in cultured neurons, recycling vesicles leave the synapse following reuptake and are transferred through the processes. This posed the question as to how recycling vesicles were positioned within the processes. If recycling vesicles are constantly being released from the intrasynaptic cluster, then it follows that there will be a larger number of them at sites just outside the terminal, but if recycling vesicles leave primarily during a single event, such as during large scale vesicle turnover, it should be expected that we might see recycling vesicles appear more prominently further from the active zone. Vesicle recycling at extrasynaptic sites could also contribute to this finding (Ratnayaka et al., 2011).

To examine this, we used Reconstruct software to obtain 3D measurements of the distance between the centre of each vesicle and the centre of the active zone. These measurements show a small distance (approx. $1 \mu\text{m}$) around the active zone of extremely densely arranged non-recycling vesicles, followed by vesicles spread more sparsely over greater distances ($\sim 2\text{-}6 \mu\text{m}$). Recycling vesicles show a similar pattern, except in smaller numbers (Fig.6.6.B).

In order to allow comparisons between different processes and vesicle arrangements, vesicles were once again characterised as intra- or extrasynaptic, and their distances from the active zone were normalised against the maximum distance in each category. These normalised distances of recycling vesicles vs non-recycling vesicles were then compared.

There were no statistically significant differences between the distributions of recycling and non-recycling vesicles. However, as described in Marra et al. (2012), in 3D reconstructions of synaptic terminals, recycling vesicles were closer to the active zone (Fig.6.6.C). This effect is less pronounced than in data collected for 2D sections. This is likely due to having to select sections from the centre of the terminal in order to meet selection criteria, leading to the periphery being under-represented. Conversely, extrasynaptic recycling vesicles were typically further away from the active zone than non-recycling vesicles.

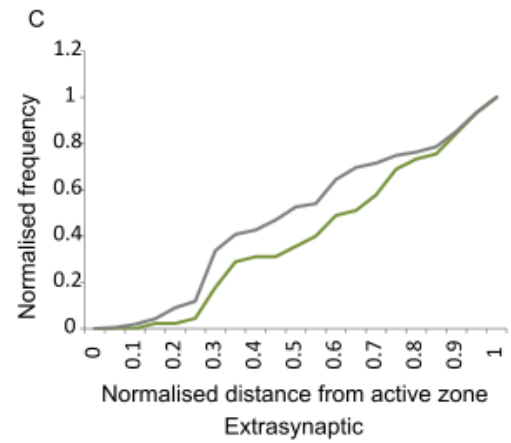
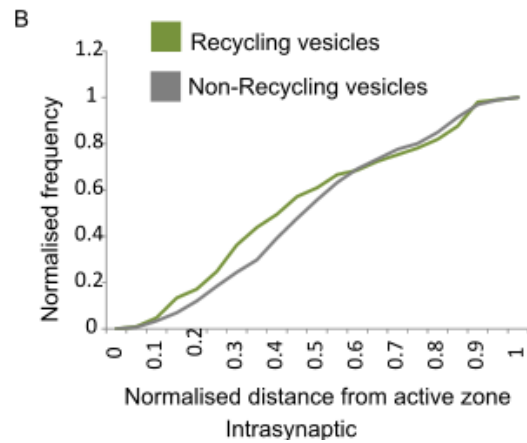
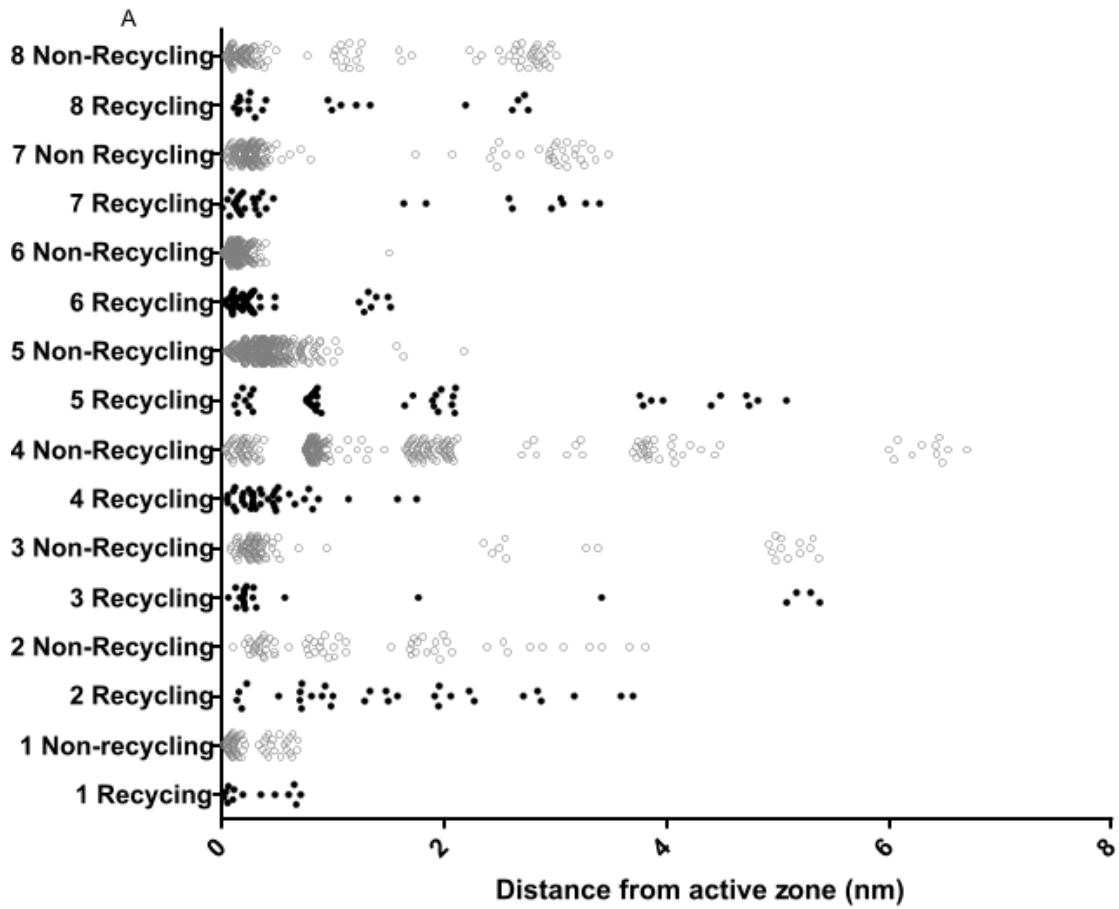


Figure 6.6 Distribution of intra- and extrasynaptic vesicles relative to the active zone

A) Distribution of vesicles within terminals in absolute distance from the active zone in all processes used for analysis in this section. B) When distance from the active zone was normalised to allow comparison between the reconstructed processes, we found that recycling vesicles were distributed slightly closer to the active zone, but this effect was not significant (synapses $n=8$, paired Student's t -test for unequal variance, $p=0.295$). C) Recycling vesicles at extrasynaptic locations were significantly further away from the active zone (processes $n=8$, paired Student's t -test for unequal variance, $p<0.05$).

Using the maximum distance of each vesicle from the active zone, we were able to calculate the number of vesicles per micrometre within the synaptic terminals. As expected, extrasynaptic vesicles occurred at a significantly lower density than intrasynaptic vesicles. This was the case for both recycling and non-recycling vesicles ($n=8$, statistically significant, Student's t -test, $p<0.002$, $p<0.002$) (Fig.6.7.A).

Within the synaptic terminal, recycling vesicles occurred at a density of 38.9 ± 5 vesicles/ μm , with non-recycling vesicles, which make up the majority of the pool, occurring at 207.9 ± 43.7 vesicles/ μm ($n=8$, statistically significant, Student's t -test, $p<0.002$). At extrasynaptic locations there were 13.7 ± 3 recycling vesicles/ μm , and 39.6 ± 9 non-recycling vesicles/ μm ($n=8$, statistically significant, Student's t -test, $p<0.05$).

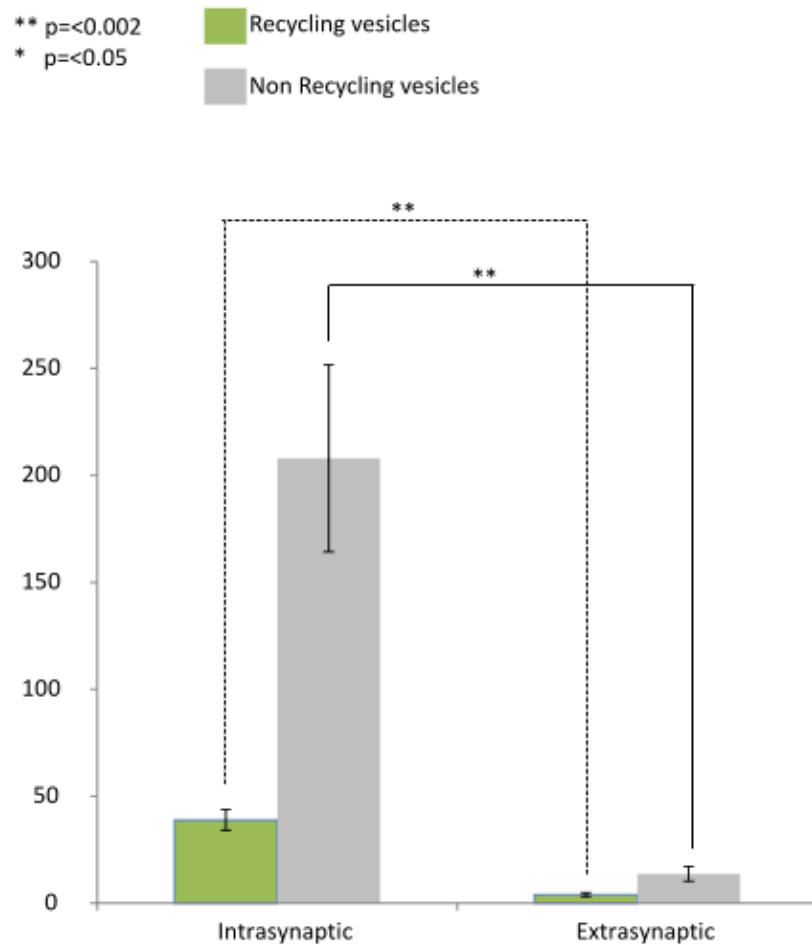


Figure 6.7 Vesicle density within synapses and processes

The density of both recycling and non-recycling vesicles was significantly lower at extrasynaptic locations ($n=8$, $n=8$, Student's t -test for unequal variance, $p<0.002$ for intrasyntaptic, $p<0.002$ for extrasynaptic locations). At extrasynaptic locations there were 13.7 ± 3 recycling vesicles/ μm , and 3.9 ± 1 non-recycling vesicles/ μm ($n=8$, statistically significant, Student's t -test, $p<0.05$). Within the synaptic terminal, recycling vesicles occurred at a density of 38.9 ± 5 vesicles/ μm , compared to non-recycling vesicles at 207.9 ± 43.7 vesicles/ μm ($n=8$, statistically significant, Student t -test, $p<0.002$).

The indications that extrasynaptic recycling vesicles occur further from the active zone than non-recycling vesicles suggested that perhaps these vesicles had been transferred to the processes during activity, and this was the distance they had moved during the 20 min wash-out period, and perhaps activity causes increased recycling vesicle transfer to the superpool. Alternatively, this could be caused by recycling vesicles having an ability to travel more quickly through neuronal processes. In order to determine further which of these was the case and to point to a possible mechanism of transport, it was important to examine the extent to which extrasynaptic recycling vesicles clustered together. If, as suggested, recycling vesicles were found in clusters within the synapses, this could be further evidence in favour of the first hypothesis.

Intrinsynaptically, both recycling and non-recycling vesicles form a sharp peak, indicating that large numbers of vesicles have very small distances between them, and that there is not a wide variety in the distances between vesicles. This profile is indicative of tight clustering. Extrasynaptic vesicles demonstrate a profile consisting of a small peak and then a long and shallow tail off. This is indicative of very few vesicles being within close proximity of each other, and there being a very wide distribution of synaptic vesicles (Fig.6.8.A).

Within terminals, recycling vesicles showed no greater tendency to cluster together than non-recycling vesicles. There was a slight, but not significant, trend towards clustering in the recycling vesicles, but this was thought to be representative of the preferential positioning of recycling vesicles towards the active zone ($n=8$, Student's t -test for unequal variance, not significant, $p=0.241$) (Fig.6.8.B). In extrasynaptic terminals, however, there was evidence that recycling vesicles were less clustered together than non-recycling vesicles ($n=8$, Student's t -test for unequal variance, $p<0.02$) (Fig.6.8.C).

This result suggests that recycling vesicles at extrasynaptic locations are usually isolated. This evidence suggests that recycling vesicles are not further from synapses as a result of a single event, such as the stimulus, occurring. This suggests that movement of vesicles from the recycling pool within terminals to the superpool is continuous and occurs at rest.

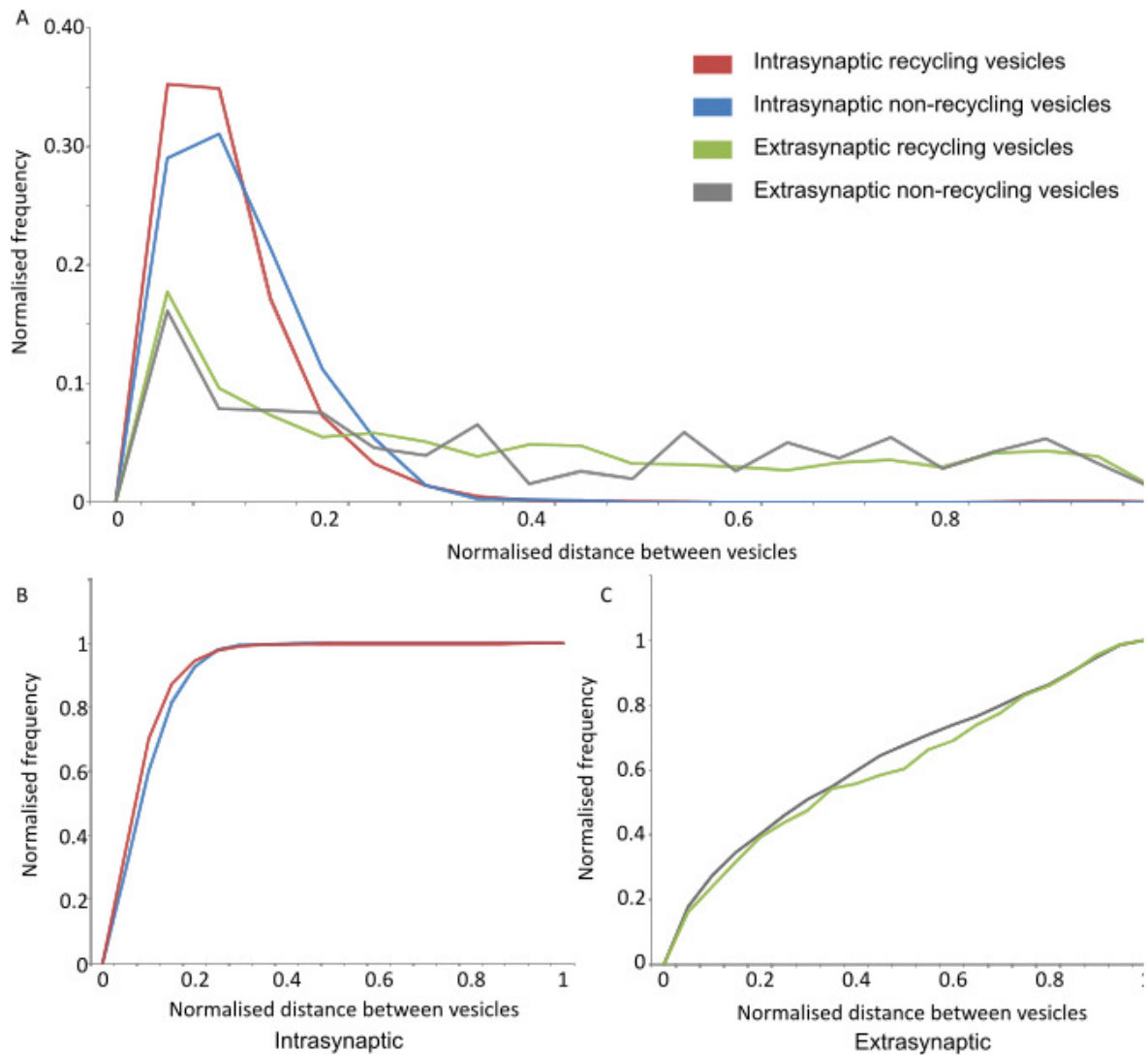


Figure 6.8 Clustering analysis of synaptic vesicles

A) Intrasynaptic vesicles demonstrate tight clustering, indicated by the steep peaks shown. The small peak and shallow drop off of the profile of the graph of distances between extrasynaptic vesicles indicates a wide distribution with little clustering of vesicles. B) Frequency distribution of the distances between recycling and non-recycling vesicles within synaptic terminals ($n=8$, no significant difference, Student's t -test for unequal variance, $p=0.241$). C) Frequency distribution of the distances between non-recycling vesicles at extrasynaptic locations ($n=8$, Student's t -test for unequal variance, $p<0.02$).

6.4 Using Focused Ion Beam Scanning Electron Microscopy to study extrasynaptic vesicles

Reconstructing processes using conventional electron microscopy is a prohibitively difficult process. Once a suitable region of interest is identified, it must then be found on subsequent and preceding sections. Synapses are relatively easy to identify within sections, as are in sections of processes which are cut lengthways, but in certain orientations they can be very difficult to identify and track. Producing thin serial sections, locating the region of interest in multiple sections, and imaging the region and aligning the photos, all before any work can be done on reconstructing features of the synapse, is a very time-consuming process. To do this over the several microns required to image large sections of processes in native tissue is prohibitively difficult.

A potential answer to some of these technical challenges is offered by the exciting new breed of semi-automated EM machines, broadly referred to as block-face EM systems. One of the most exciting systems to emerge is focused ion beam scanning electron microscopy (FIBSEM). This is a new method for ultrastructurally imaging blocks of tissue, which offers the ability to obtain aligned serial images of relatively large volumes of tissue over the course of a few hours. This operation of this microscope involves uses an ion beam to mill away the surface of a sample which has been placed inside a microscope, and measures the backscatter of those ions to generate a picture of what the surface looked like (Burkhardt et al., 2005). This is particularly useful for investigations of processes, which can travel long distances through tissue, where challenges of gathering the many consecutive serial sections required to reconstruct whole volumes becomes very limiting. FIBSEM addresses these challenges, making it very attractive for such work. To date, the combination of functional vesicle readout and FIBSEM has not been trialled.

Through a lab collaboration with Prof M Hausser, it was possible to gain access to FIBSEM technology for the purposes of collecting a series sample which could go some way to addressing a number of the limitations of axon analysis imposed by conventional EM technology. Samples were prepared using 1200 AP/10 Hz FM dye loading, and were fixed and photoconverted as described in previous chapters. Samples were then prepared for FIBSEM as described in section 2.5.7. Access to the FIBSEM system was limited. Although I carried out a number of sample preps for FIBSEM work, the sample

eventually selected and used for the FIBSEM data run presented here was prepared by Dr V Marra. The dataset features 250 sections and a resolution of 1 pixel = 6.3 nm, with only 9.3 nm between sections (Fig.6.9.A and example image demonstrated in Fig.6.9.B). Following a number of rounds of optimisation of this process (Hausser and Roth), the achievable resolution was sufficient for us to identify synaptic process and synapses. Using appropriate software (FIJI with Trak2EM) (Cardona et al., 2012), these could be traced through the tissue (Fig.6.9.C). This software could also be used to produce reconstructions of both the synapses and the processes, which allowed us to recreate long sections of neuronal processes (Fig.6.9.D).

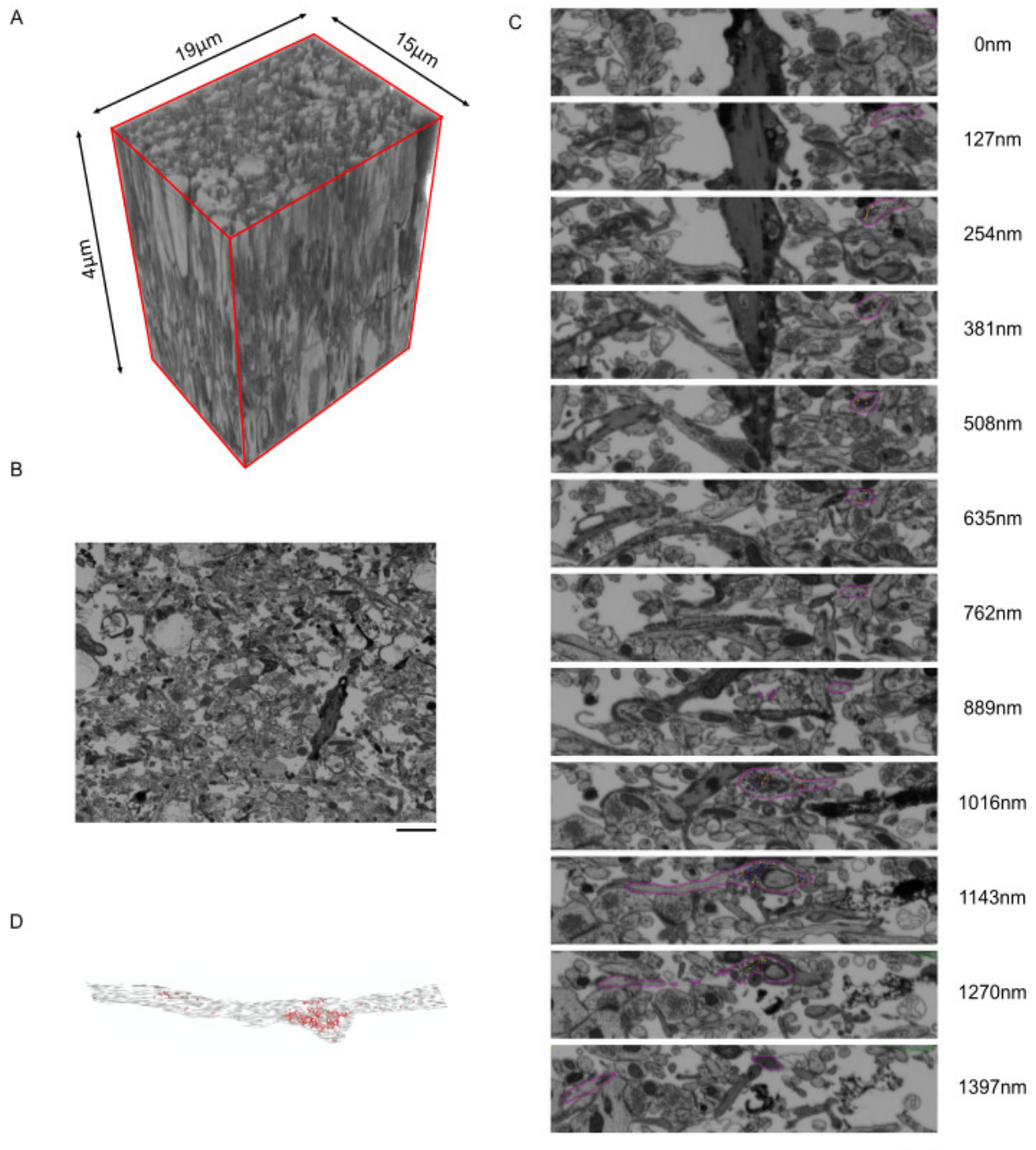
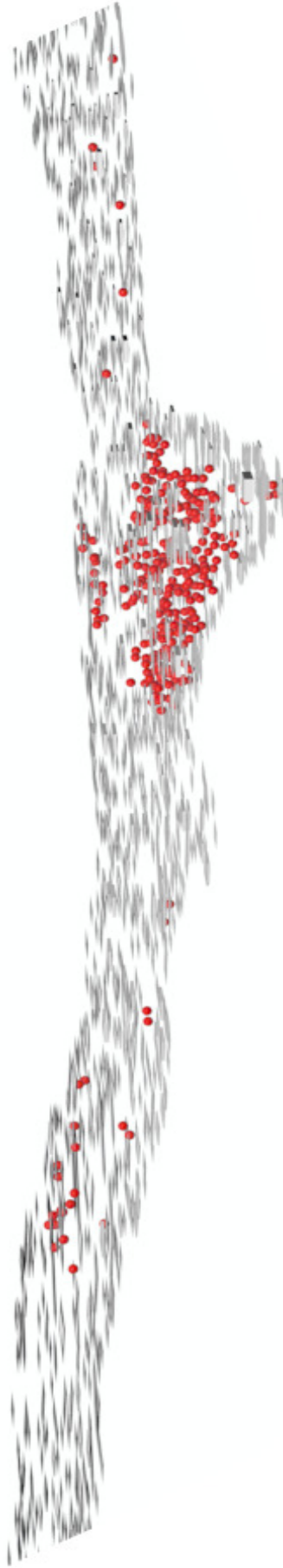


Figure 6.9 FIBSEM images are suitable for tracing synapses over large distances

A) The FIBSEM system is able to image serial sections of a block of dimensions 19 μm x 14 μm x 4 μm . B) These blocks consist of 450 images of the block face with a voxel depth of 9.3 nm. Scale bar indicates 1 μm . C) Processes stemming from synapses can be followed through these regions. A sample synapse is outlined in pink. Scale bar represents 500 nm. D) A reconstruction of the synapse pictured in C (enlarged view on next page).



Enlarged view of Figure 6.9.D

6.4.1 Identifying recycling vesicles in FIBSEM images

Though FIBSEM images provide access to large regions of the tissue in aligned stacks of images, these images do not have the resolution of those obtained through conventional transmission electron microscopy. In our case, the size of each pixel was 6.3 nm x 6.3 nm. Given that a synaptic vesicle has a diameter of 40-60 nm (Palay, 1956), they will be represented by spots of only 6-9 pixel diameters. The first step was establishing whether this resolution was sufficient for us to identify photoconverted vesicles within synapses.

Major structures such as postsynaptic densities could easily be identified, and these were used to aid in the identification of synapses. Vesicle clusters were also visible and were the primary determinant of synaptic identity. Within some synapses, black punctae were visible, darker than the surrounding vesicle cluster (Fig.6.10.A). These were identified as photoconverted recycling vesicles. These were not present in every synapse, providing supporting evidence to show that these were due to photoconversion of FM dye rather than artefacts of the fixation and imaging process (Fig.6.10.B).

The next step was to determine whether we could reliably identify recycling vesicles within synaptic terminals and processes. To do this, we measured the electron density profile across the diameter of both photoconverted and non-photoconverted vesicles. The low resolution of the images used meant that both photoconverted and non-photoconverted vesicles exhibit a single peaked electron density profile (Fig.6.10.D), rather than non-photoconverted vesicles displaying their distinctive two peak profile (see Fig.6.5.A).

Though the horizontal profiles of photoconverted and non-photoconverted vesicles have a similar shape, the electron density of the lumen in photoconverted vesicles was significantly higher (photoconverted $n=50$ vesicles from 5 synapses, non-photoconverted $n=50$ vesicles from 5 synapses, Student's t -test for unequal variance, $p<0.02$) (Fig.6.10.D).

As mentioned above, synaptic vesicles have a diameter of 40-60 nm. As the FIBSEM system produces serial sections 9.3 nm apart, this means that each vesicle appears in several sections. Using a fixed size region of interest, we measured the electron intensity of the centre of regions containing photoconverted and non-photoconverted

vesicles over the course of 10 sections. When going vertically through the tissue, at central sections of the synapse, the lumen is significantly darker than that found in non-photoconverted vesicles (photoconverted $n=50$ vesicles from 5 synapses, non-photoconverted $n=50$ vesicles from 5 synapses, Student's t -test for unequal variance, $p < 0.02$) (Fig.6.10.E).

From this we were able to conclude that the centre point of recycling vesicles can be identified with confidence. As a single vesicle appeared over many sections, we used the 'color cues' function of Trak2EM, which provided an outline of each labelled vesicle for 4 sections before and after the centre labelled point. This prevented double counting of vesicles.

The sheer numbers of non-photoconverted vesicles and their uniform electron density made it impossible to identify individual non-recycling vesicles within the cluster. As such, using this method we were unable to take numbers of non-recycling vesicles into account.

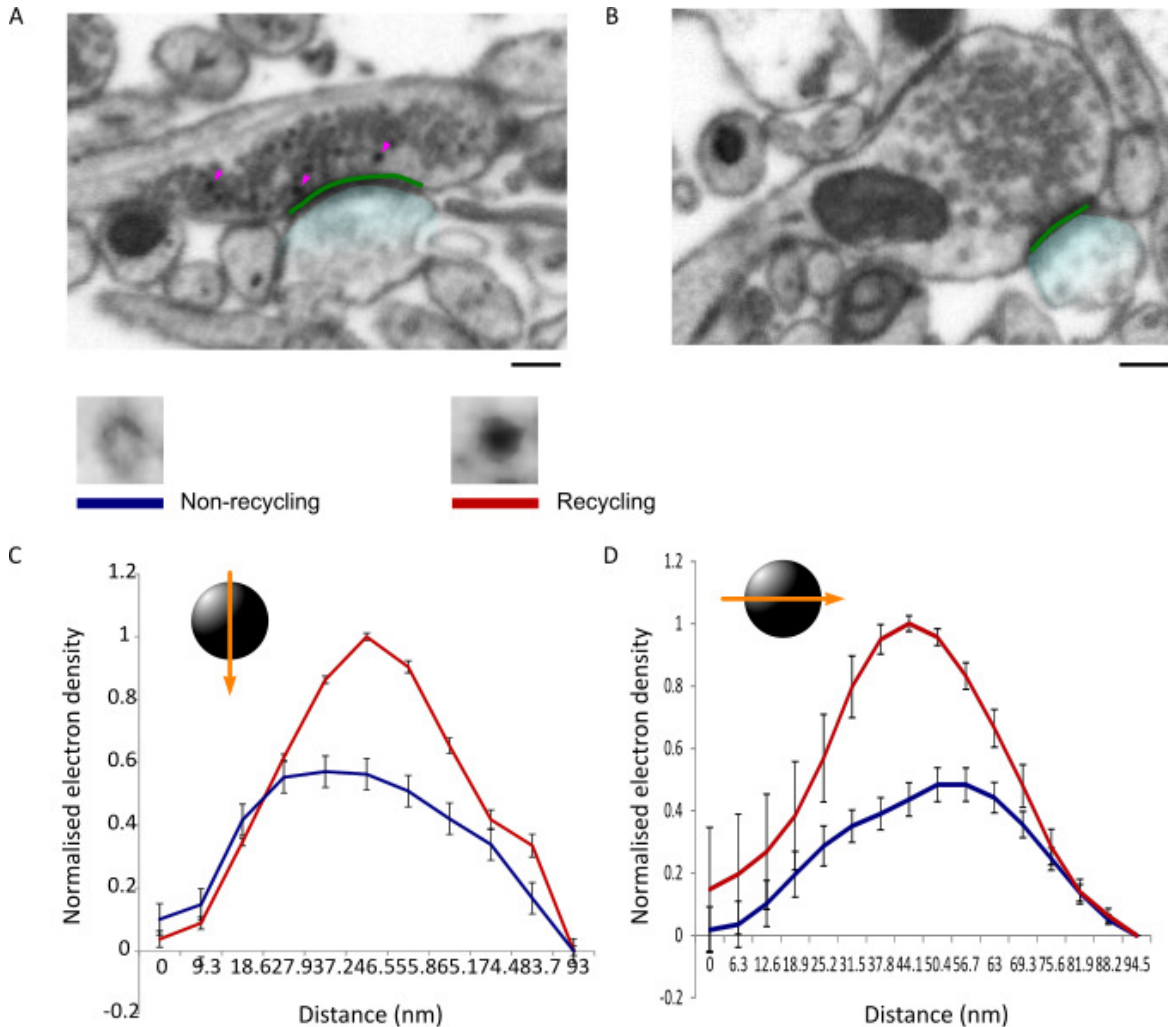


Figure 6.10 Identifying recycling vesicles in FIBSEM sections

A) Photoconverted vesicles visible within a terminal. Recycling vesicles indicated by pink arrows. Green – active zone, blue – postsynaptic region. Scale bar indicates 200 nm. B) Synapse not containing recycling vesicles. Green – active zone, blue – postsynaptic region. C) When going vertically through the tissue, at central sections of the synapse, the lumen is significantly darker than that found in non-photoconverted vesicles (photoconverted, $n=50$ vesicles from 5 synapses, non-photoconverted, $n=50$ vesicles from 5 synapses, Student's t -test for unequal variance, $p<0.02$). D) Horizontal profiles in single layers also demonstrated a significantly darker lumen in photoconverted vesicles (photoconverted $n=50$ vesicles from 5 synapses, non-photoconverted $n=50$ vesicles from 5 synapses, Student's t -test for unequal variance, $p<0.02$).

6.4.2 Investigating distribution of recycling vesicles using FIBSEM

The ability to identify recycling vesicles in complete image sets of processes presented an exciting opportunity to provide more detailed information about the properties of extrasynaptic recycling vesicles in native terminals. In order to exploit this data, processes were selected according to the following criteria: first, the presence of photoconverted vesicles; second, the presence of two synapses with active zones; which, third, was joined by a complete section of process which does not branch. Five processes matching these criteria were selected and reconstructions of the arrangements of recycling vesicles were produced (Fig.6.11.A).

Using the x,y,z coordinates produced by Trak2EM, which provided the location of recycling vesicles and active zones of analysed processes, we used the distance equation,

$d = \sqrt{(x_1 - x_2)^2 + (y_1 - y_2)^2 + (z_1 - z_2)^2}$, a variation of Pythagoras' theorem expanded for three dimensions, on the spatial arrangement of both recycling vesicles and the active zones present at both synapses.

Vesicles within two vesicle diameters of the main vesicle cluster were defined as intrasynaptic, and those within the processes or outside of 2 vesicle distance from the main cluster were classified as extrasynaptic. Using this classification, the distance from the each vesicle to the center of the nearest active zone was measured. The results are displayed in Fig.6.11.B. As expected, intrasynaptic vesicles are very close to the active zone, with a mean distance of $0.31 \pm 0.006 \mu\text{m}$ from the active zone, with extrasynaptic vesicles being on average $2.38 \pm 0.08 \mu\text{m}$ from the active zone (n=974 vesicles from 10 synapses, n=200 vesicles from 5 processes, Student's *t*-test for unequal variance, p=0.002).

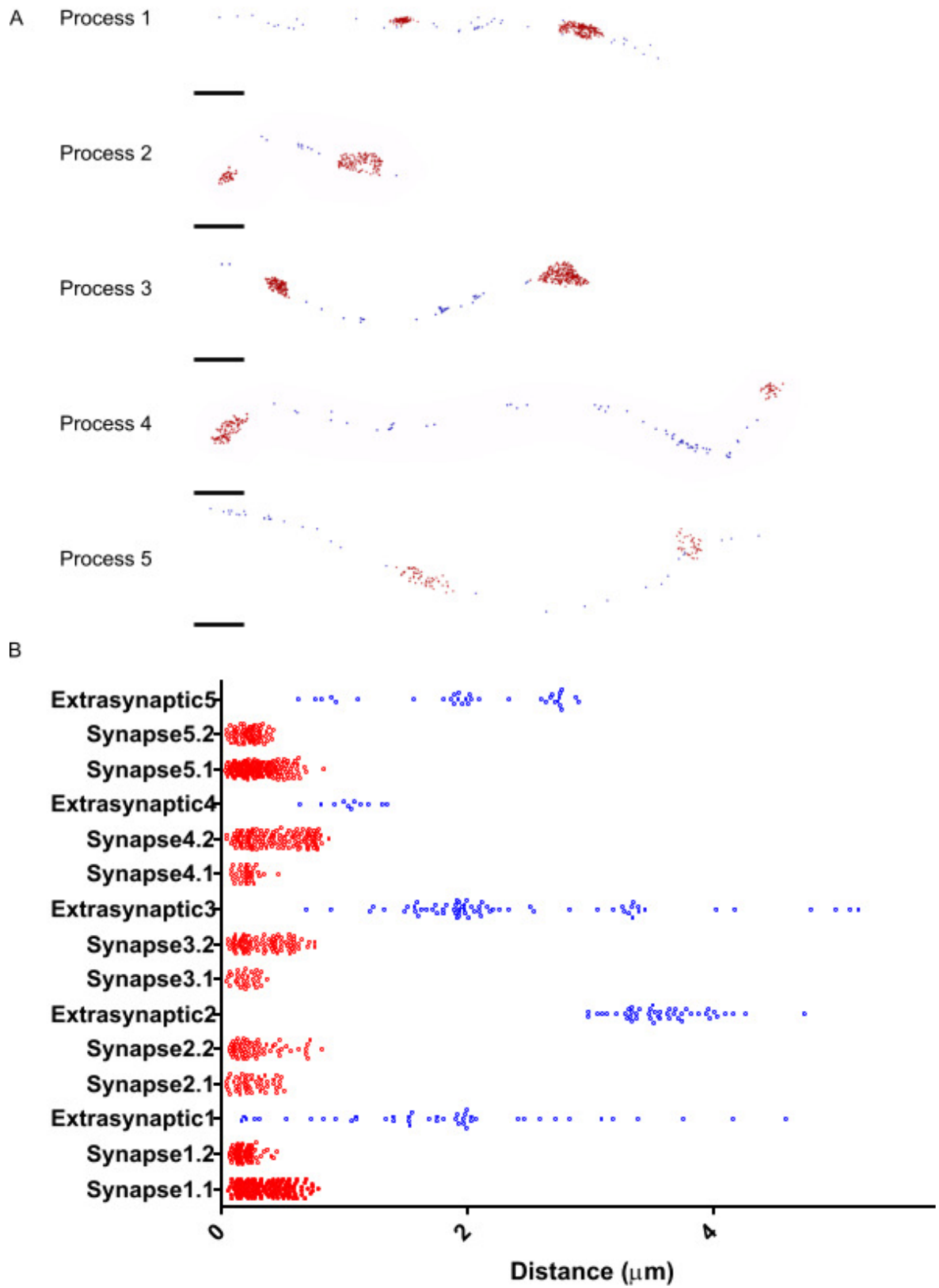


Figure 6.11 Extracting distance data from FIBSEM images

A) Processes were reconstructed with vesicles in intrasynaptic vesicles in each cluster and extrasynaptic vesicles being categorised separately. Red – intrasynaptic vesicles, blue – extrasynaptic vesicles. Scale bar represents 1 μm . B) The distance of each vesicle from the nearest active zone was calculated and is plotted here.

To examine further the positioning of recycling vesicles in terminals reconstructed in FIBSEM compared to the active zone, we normalised these values against the maximum distance from the active zone of any vesicle measured in a process, and plotted a cumulative frequency curve. Extrasynaptic vesicles are significantly further from the active zone than cluster vesicles (intrasynaptic vesicles $n=974$ vesicles from 10 synapses, extrasynaptic vesicles $n=200$ vesicles from 5 processes, Student's *t*-test for unequal variance, $p<0.0002$) (Fig.6.12.A).

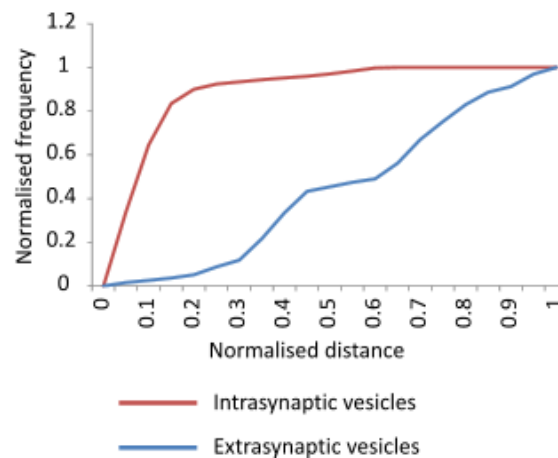


Figure 6.12 Recycling vesicle distribution relative to the active zone within synapses and processes

Cumulative frequency distribution of normalised distance from the active zone. Intrasynaptic vesicles are significantly more frequent at positions closer to the active zone than extrasynaptic vesicles (intrasynaptic vesicles $n=974$ vesicles from 10 synapses, extrasynaptic vesicles $n=200$ vesicles from 5 processes, Student's *t*-test for unequal variance, $p<0.0002$).

The density of recycling vesicles in synapses and processes is a parameter that we already established earlier in this chapter (see section 6.3.2). In order to verify that this method was suitable for characterising the recycling pool, we calculated the density of recycling vesicles both within terminals and in processes.

In intrasynaptic terminals from the image set collected using FIBSEM, recycling vesicles occurred at a density of 161.6 ± 27 vesicles/ μm . Extrasynaptic vesicles were significantly less frequently occurring, with a density of only 10.3 ± 0.8 vesicles/ μm . This value was significantly higher than that found in samples imaged with serial sectioning and conventional transmission electron microscopy (38.9 ± 4 vesicles/ μm) (FIBSEM $n=10$ synapses, TEM $n=8$ synapses, Student's t -test for unequal variance, $p < 0.002$).

We compared the density of recycling vesicles within the synaptic cluster that was calculated from data generated through conventional TEM, and that generated using FIBSEM. In samples imaged with serial sectioning and conventional transmission electron microscopy, intrasynaptic vesicles occur at a significantly lower density of 38.9 ± 4 vesicles/ μm (FIBSEM $n=10$ synapses, TEM $n=8$ synapses, Student's t -test for unequal variance, $p < 0.002$) (Fig.6.13.A). Likewise, extrasynaptic vesicles imaged using FIBSEM occurred at a density of 10.3 ± 1 vesicles/ μm , significantly higher than the density of 3.9 ± 1 vesicles/ μm found in processes imaged using conventional TEM (FIBSEM $n=5$ processes, TEM $n=8$ processes, Student's t -test for unequal variance, $p < 0.002$) (Fig.6.13.B).

In order to explain this difference, we calculated the ratios of intrasynaptic recycling vesicles and extrasynaptic recycling vesicles imaged using both methods of electron microscopy. We found no significant difference between the ratios of the two (conventional TEM $n=8$, FIBSEM $n=5$, Student's t -test for unequal variance, $p=0.286$) (Fig.6.13.C).

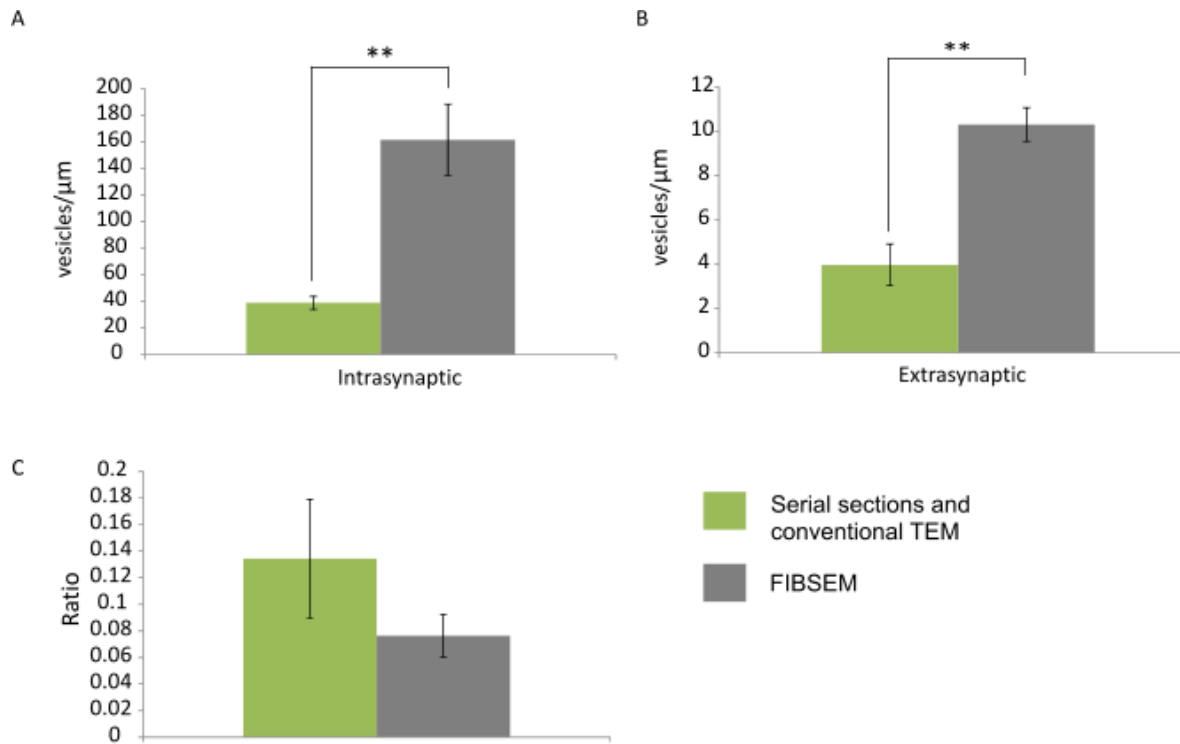


Figure 6.13 Intrasynaptic and extrasynaptic vesicle distribution

A) In intrasynaptic terminals, using FIBSEM, recycling vesicles occurred at a density of 116.6 ± 27 vesicles/ μm , a value significantly higher than that found in samples imaged with serial sectioning and conventional transmission electron microscopy (38.9 ± 4 vesicles/ μm) (FIBSEM $n=10$ synapses, TEM $n=8$ synapses, Student's t -test for unequal variance, $p < 0.002$). B) Extrasynaptic vesicles imaged using FIBSEM occurred at a density of 10.3 ± 1 vesicles/ μm , a significantly higher figure than that found in processes imaged using conventional TEM (3.9 ± 1 vesicles/ μm) (FIBSEM $n=5$ processes, TEM $n=8$ processes, Student's t -test for unequal variance, $p < 0.002$). C) Ratio of extrasynaptic vesicles to intrasynaptic vesicles compared for the samples imaged using these two different processes: FIBSEM 0.076 ± 0.01 , conventional TEM 0.134 ± 0.045 . These are not significantly different (FIBSEM $n=5$ processes, TEM $n=8$ processes, Student's t -test for unequal variance, $p = 0.287$).

The next step was to use this more complete record of recycling vesicles to determine whether they exhibited any clustering within terminals, which might have implications for their function. To do this, we measured the distances between each recycling vesicle in the synapse and those around it, and the same for each recycling vesicle within the cluster. We collected the same measurements between extrasynaptic vesicles and compared the distribution of distances between these two categories of vesicles. The

distribution of recycling vesicles showed that, in intrasynaptic vesicles, the distances between vesicles were very small and there were very few large distances between vesicles. In extrasynaptic vesicles, there were significantly fewer vesicles with another recycling vesicle in close proximity, as indicated by the small peak seen in Fig.6.14.A. Extrasynaptic vesicles exhibited a wide array of distances between vesicles with very little discernable clustering (intrasynaptic n=10 synapses, extrasynaptic n=5 processes, Student *t*-test for unequal variance, $p < 0.005$).

We compared this to the vesicle clustering data gathered using conventional TEM. We found there to be no significant difference in the distribution of distances between recycling vesicles within synaptic terminals (FIBSEM n=10 synapses, TEM n=8 synapses, Student's *t*-test for unequal variance, not significant, $p=0.747$). The same was true with extrasynaptic vesicles: we found no significant difference in the distribution of the distances between extrasynaptic vesicles between samples imaged using conventional TEM and those imaged using FIBSEM (FIBSEM n=5 processes, TEM n=8 processes, Student's *t*-test for unequal variance, not significant, $p=0.462$). The similarities show that FIBSEM is able to produce results comparable to those of serial sectioning and electron microscopy, and as it is able to do so to large regions of tissue over a shorter period of time, it opens up many exciting new avenues of research, particularly ones which look at changes in the size of synaptic features such as the active zone or vesicle cluster size in response to plasticity.

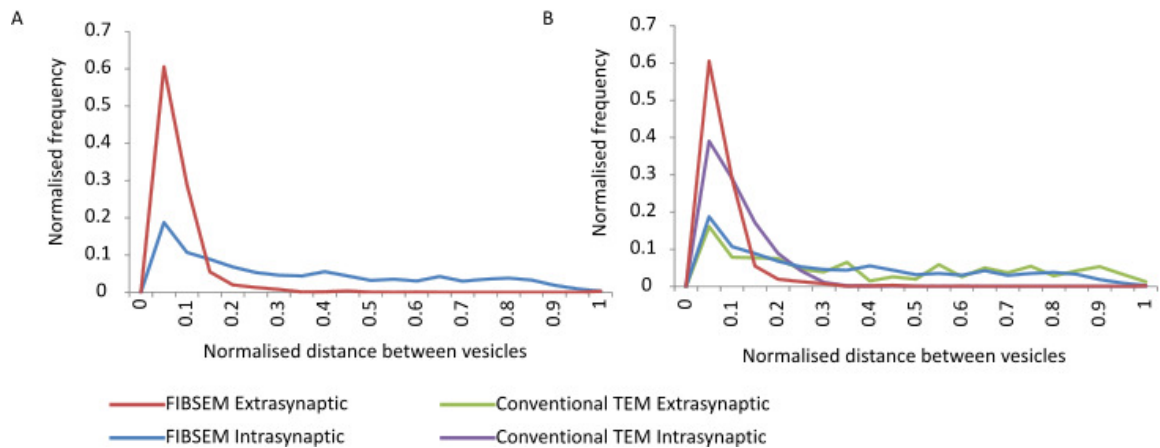


Figure 6.14 Recycling vesicle clustering at intra and extrasynaptic locations.

A) Normalised distribution of the distance between intrasynaptic vesicles and the distance between extrasynaptic vesicles. The distance between vesicles is significantly smaller between intrasynaptic vesicles than between extrasynaptic vesicles (intrasynaptic $n=10$ synapses, extrasynaptic $n=5$ processes, Student's t -test for unequal variance, $p<0.005$). B) Comparing recorded clustering in samples imaged using conventional TEM to those measured using FIBSEM. There was no significant difference between the distribution of distances between the intrasynaptic vesicles (FIBSEM $n=10$ synapses, TEM $n=8$ synapses, Student's t -test for unequal variance, not significant, $p=0.747$), and no significant difference between the distribution of distances between extrasynaptic vesicles (FIBSEM $n=5$ processes, TEM $n=8$ processes, Student's t -test for unequal variance, not significant, $p=0.462$).

6.5 Discussion

In this chapter, we establish that functionally labelled recycling vesicles undergo lateral movement between synapses in the hippocampal slice system, and that their movement can be observed over short distances. Hints of this behaviour were observed in previous papers (Ratnayaka et al., 2011, Staras et al., 2010), but this chapter provides a closer look at the properties of mobile vesicles within hippocampal slices at a fluorescence level.

The existence of a population of vesicles which move from established synapses, and move between them within synaptic processes, challenges the conventional view of synapses as isolated structures. The discovery that these mobile vesicles can integrate

into any synapse and join the recycling pool has important implications for function (Staras et al., 2010). There is evidence that vesicles can be drawn from this superpool in order to create new synapses at sites within processes (Staras et al., 2010, Darcy et al., 2006a). Another possible function is that the additional vesicles to support the increase in total pool size which has been observed in synapses which have undergone LTP (Bell et al., 2014) might be provided by the superpool, and consequently it may have other roles in synaptic plasticity.

In slices labelled with FM 1-43 and, novel to this work, with syOyster550, we found that we could consistently measure the rate of vesicle transfer over short distances. When we measured and compared the rates of fluorescence packet movement using both these probes, we found no significant difference between them. When we compared the rate of puncta movement to that observed in hippocampal cultured neurons, the values seen were significantly lower.

The rates of vesicle transfer in processes recorded by this chapter are towards the lower end of the 0.5-5 $\mu\text{m/s}$ range stated by the literature (Brown, 2003). If a full and further study were to be made of this property, acquisition rates should be increased: the verification of syOyster550 as a probe for the successful monitoring of laterally moving vesicles helps in this regard, as it undergoes less fluorescence loss due to photobleaching than FM 1-43. A major barrier to identifying the higher rates is the lack of ability to follow processes with any confidence through the tissue. Future work on this property would require the filling of a neuron using a fluorescent solution (e.g. Branco et al. (2008) in cultured neurons). The use of a red fluorescent probe such as syOyster550 would also be useful as it would allow the brighter, more easily identified, green dyes to be used as for anatomical tracing. Filling a target neuron with a fluorescent probe would also allow loading at specific points rather than through generalised applications of FM 1-43 dye and would provide an interesting field for further study.

We next moved on to a study of these vesicles at an ultrastructural level. This was the first observation of labelled recycling vesicles in native hippocampal tissue at an ultrastructural level, and allowed us to look at how this pool is organised in a physiologically relevant environment. In fluorescence studies, we found that mobile punctae had 50-60% of the fluorescence of the stable fluorescent punctae. This value was consistent with values for recycling vesicle fraction found in our ultrastructural

study. This confirmed that extrasynaptic vesicles are the mobile vesicles seen in fluorescence studies.

By definition, extrasynaptic recycling vesicles were bound to be further from the active zone than intrasynaptic vesicles; an interesting finding was that, within the pool of extrasynaptic recycling vesicles, the recycling vesicles were significantly further from the active zone than non-recycling vesicles. This shows a difference between a functional pool and vesicles which have not undergone recycling recently. In addition, recycling vesicles demonstrate significantly less clustering than non-recycling vesicles. These two findings may be linked: potentially whatever makes recycling vesicles less likely to cluster together in processes also allows them to travel further through the terminal following recycling.

Synapsin is a vesicle membrane protein which binds the vesicle to the actin cytoskeleton (Greengard et al., 1993). Docked pool vesicles do not appear to have synapsin attached (Bloom et al., 2003), and synapsin knock-out mice do not appear to affect mobilisation of the docked pool (Orenbuch et al., 2012, Gaffield and Betz, 2007). The greater clustering of non-recycling vesicles within the terminals is likely due to the increased likelihood of the presence of synapsin on these vesicles. Experiments in knock-out mice revealed increased vesicle numbers in neuronal process, but did not look at the distance between vesicles. It is likely that this distance would increase without synapsin (Orenbuch et al., 2012).

Synapsin knock-out models do not have an effect on the mobility of the recycling pool (Gaffield and Betz, 2007). Recycling vesicles lose synapsin from their membrane during exocytosis, and do not regain it for some time afterwards (Bloom et al., 2003). Recycling vesicles have been observed to have a greater degree of mobility than non-recycling vesicles (Kamin et al., 2010). CDK5 inhibition has been shown to both increase the mobilisation of recycling pool (Orenbuch et al., 2012) and increase the recycling fraction (Kim and Ryan, 2010, Marra et al., 2012), pointing to a further link between membership of the recycling pool and increased mobility. The result in this chapter, that extrasynaptic recycling vesicles are further from the active zone in processes than non-recycling extrasynaptic vesicles, further points to this idea of increased mobility in the recycling pool; the above studies suggest that this may be mediated by CDK5. In the dynamic environment of a synapse undergoing activation, these factors could contribute towards recycling vesicles leaving the active zone and

travelling through the processes. Future work could include carrying out this experiment in the presence of the CDK5 inhibitor Roscovitine. If this hypothesis is correct, this would increase the recycling fraction at extrasynaptic processes and increase the distance between vesicles.

In this chapter we present the first look at a block of native hippocampal tissue with photoconverted FM dye-labelled neurons in a hippocampal slice. We were successfully able to identify photoconverted vesicles within terminals and processes, and produce results comparable to those seen using conventional electron microscopy.

Using FIBSEM, perfectly aligned serial images of the entire volume could be obtained in a matter of hours. The ability to look at large volumes of tissue is incredibly useful for future studies. The ability to look at populations of synapses rather than individual samples, and the ability to link synapses together with confidence, allows us to ask questions that would be prohibitively difficult to answer using conventional TEM. Combining FIBSEM and our novel hippocampal slice system would be particularly helpful in plasticity studies, as unlike in cultured neurons, not all synapses in the imaged region of the slice system receive a stimulus from the Schaffer collaterals. This means stimulated synapses could be identified by the presence of photoconverted vesicles and unstimulated synapses in the same region, allowing a more direct comparison of properties to be made.

The low resolution and resulting inability to identify individual non-recycling vesicles within synapses limit the usefulness of this technique at present, although doubtless resolution will increase as this technique matures. FIBSEM is an exciting opportunity to carry out large scale investigations of 3D reconstructions of synapses, as well as on synaptic processes. It provides context on each synapse within a process and allows pre- and postsynaptic targets to be linked. The potential for future work could include looking at how the superpool interacts over time, looking at how other pools interact with the superpool, and looking at how plasticity affects extrasynaptic vesicles, all questions which would benefit from the application of this technique.

6.6 Acknowledgements

FIBSEM sample provided by Dr V Marra, and processed by Dr JJ Burden, Dr A Roth and Prof M Hausser.

Chapter 7: General discussion

7.1 Functional studies in the acute hippocampal slice preparation

7.1.1 A method for studying function in slice

The aim of this thesis was to link the function of recycling vesicles with their ultrastructural position, and to use this to determine the fundamental properties of vesicle recycling within synapses and within cells as a whole. To do this, the work in this thesis exploited novel approaches based on functional and ultrastructural readouts to reveal new characteristics of presynaptic vesicle pools in small central synapses. Using an established technique of labelling recycling vesicles in cultured neurons (Ryan and Smith, 1995, Harata et al., 2001, Ratnayaka et al., 2011, Darcy et al., 2006a) offered us a baseline of comparison for investigating the properties of recycling vesicles in native hippocampal slices (Marra et al., 2014).

The starting point for this work was to establish an approach that allows for ultrastructural readout of functional vesicle pools. As I described in chapter 3, FM dye offers an excellent approach to address such an issue, since it allows the labelling of vesicles which previously made up a stimulus defined pool, and then permits us to see how that vesicle population responds to further stimulation. In addition, a fixable analogue of FM-143 can be used to photoconvert DAB to produce an electron-dense product, visible only in synapses which had previously undergone recycling. Previously, this work has been conducted largely in cultured neurons and frog NMJ systems (Ariel and Ryan, 2010, Betz and Bewick, 1992, Betz et al., 1992, Darcy et al., 2006b, Darcy et al., 2006a, Ratnayaka et al., 2011, Ryan and Smith, 1995, Pyle et al., 1999), which has the advantage of ease of imaging due to the neurons being arranged in a monolayer and the sparsity of synaptic contacts. However, in this system the variety of cells and the complexity of connections does not match that in the normal physiological environment. In this thesis, I use a novel method of labelling recycling vesicles with FM 1-43 in the hippocampal slice system, and then producing photoconverted vesicles.

7.1.2 Physiological temperature and functionality

Carrying out experiments at room temperature, rather than physiological temperature, increases the longevity and stability of hippocampal slices, making them easier to use for experiments (Aitken et al., 1995); consequently, many labs have conducted experiments in this system at room temperature, including Zakharenko et al. (2002). As the vast majority of experiments into synaptic vesicle recycling have been conducted at room temperature, we elected to do the same for the experiments described in this thesis. Attempting to image vesicle activity in hippocampal slices at physiological temperature led to movement of the slice in response to the stimulus, causing z-drift and preventing individual synapses from being tracked. However, in order to provide a more physiologically relevant environment, it is vital that these technical issues are overcome.

The rate of endocytosis increases at physiological temperature (Pyott and Rosenmund, 2002, Fernandez-Alfonso and Ryan, 2004), and the rate of exocytosis may either increase (Pyott and Rosenmund, 2002, Micheva and Smith, 2005), decrease (Fernandez-Alfonso and Ryan, 2004), or exhibit no change (Kushmerick et al., 2006, Bui and Glavinovic, 2014). Another key property that alters at physiological temperature is the rate at which docking sites are refilled at the active zone following release, which shows an increase (Bui and Glavinovic, 2014). This is particularly important for the work discussed here, although it does suggest that even faster fixation times would be required in order for re-entry to be properly charted at physiological temperature.

Another concern is that, at physiological temperature, there is a completely different method of vesicle retrieval which is not present in room temperature experiments. Watanabe et al. (2014) demonstrated an ultrafast mode of endocytosis which occurs at physiological temperatures, but is absent in recycling at room temperature. Ultrafast endocytosis involves the uptake of large synaptic vesicles, 80-100 nm in diameter, which then fuse into endosomes within the cell and undergo budding in a clathrin-dependent manner. In electron microscopy studies, synapses stimulated at physiological temperature showed an increased number of large endocytic structures (Micheva and Smith, 2005), and Renden and von Gersdorff (2007) found that in addition to a mode of endocytosis which occurred at a rate identical to conventional, 'slow' endocytosis, there was an additional faster process also occurring. Future

experiments, particularly those looking at endocytosis, will need to take this into account in order to ensure they are seeing the complete picture of vesicle interactions.

7.1.3 Ultrastructural properties of synaptic vesicles in hippocampal slice

Precursors to the slice-based systems of FM dye labelling have previously been introduced with varying success. Using systems featuring dye immersion requires two photon microscopy to ensure that the signal to noise ratio is sufficiently low to provide useful data (Stanton et al., 2005, Pyle et al., 1999, W et al., 2010), and methods involving the pressure injection of dye had not previously been developed sufficiently to be used independently of two photon microscopy (Zakharenko et al., 2001), even with the use of FM dye chelators to remove background fluorescence (Kay et al., 1999). The method described in this thesis, and in Marra et al. (2014), refined this method to allow the use of confocal microscopy to image functional terminals in the acute hippocampal slice preparation and, for the first time, provide successful photoconversion of recycling vesicles to allow for ultrastructural studies.

7.2 Synaptic vesicle pools and the fate of retrieved vesicles

In recent years, there has been substantial focus on the concept that vesicles fall into different pools, which might be explained by molecular markers of identity (Ramirez and Kavalali, 2011). Orenbuch et al. (2012) suggested that vesicles in the recycling pool interact differently with the cytoarchitecture than the vesicles in the resting pool, suggesting that membership of a pool is a part of an individual vesicle's identity. Denker et al. (2011) also suggests synapsin as a molecular marker of resting pool vesicles. It has been found that the t-SNARE protein Syntaxin 1a is located in the luminal domain of synaptic vesicles following endocytosis, and that these vesicles do not undergo recycling (Mitchell and Ryan, 2004). Work by Hua et al. (2011) showed that the vesicle protein VAMP7 is a molecular marker of the spontaneous pool.

There have also been studies linking the spontaneous pool and the recycling pool to two separate populations through the presence of VAMP7 and Vti1a (Ramirez and Kavalali, 2011). These are alternate v-SNARE proteins. Vti1 has intensely helical structure compared to synaptobrevin and SNAP25, which only obtain a helical structure when in contact with the t-SNARE proteins. This might be why these vesicles are able

to undergo non-calcium dependent fusion, but preferentially move when the synapse is at rest (Tishgarten et al., 1999). All these studies provide evidence that membership of a particular pool is predetermined, and is retained permanently or over long time periods. However, there is another possibility: that membership of a given pool is based on the positioning of a vesicle at a specific moment in time. To differentiate between these possibilities, we looked at the fate of recycling vesicles following re-entry into the terminal after recycling.

In order to address the question of the fate of recycling vesicles, we first chose to look at the RRP, a group of vesicles which respond quickly to either a short train of action potentials (40 AP/20 Hz) or hypertonic sucrose (Rosenmund and Stevens, 1996). Using ultrastructural information gathered when slices were fixed 1, 5, and 20 min following FM dye loading, photoconverted and prepared for electron microscopy, we looked at the spatial organisation of this pool over time. The RRP corresponded to $5.5 \pm 2.8\%$ of the total pool of synaptic vesicles and, importantly, was consistent over all time periods, confirming that we were successfully labelling this pool even immediately after loading. Notably, this value is well aligned with previous values reported in cultured neurons where 4-6% has been estimated (Moulder and Mennerick, 2005, Rosenmund and Stevens, 1996, Schikorski and Stevens, 2001), giving us further confidence in our effective labelling of this pool.

In samples fixed at 1 min following stimulation, the retrieved vesicles were predominantly positioned towards the active zone. A significantly higher fraction of FM 1-43 labelled vesicles were present at active zone sites. This effect is less pronounced at the 5 min time point, and by 20 min following stimulation, this effect was entirely eliminated and the recycling vesicles showed no preferential distribution compared to the vesicles which had not undergone recycling.

Regarding the experiment looking at the fate of vesicles retrieved following RRP stimulation, we hypothesised one of three likely outcomes 20 min following FM dye reloading: 1) that newly retrieved vesicles would be positioned near the active zone, thus more available for reuse (Fig.7.1.A); 2) that recycling vesicles would show no preferential positioning and would be intermingled with the non-recycling vesicles (Fig.7.1.B); or 3) that recycling vesicles might be located at a specific location within the terminal in which they are least likely to be used for reuse (Fig.7.1.C).

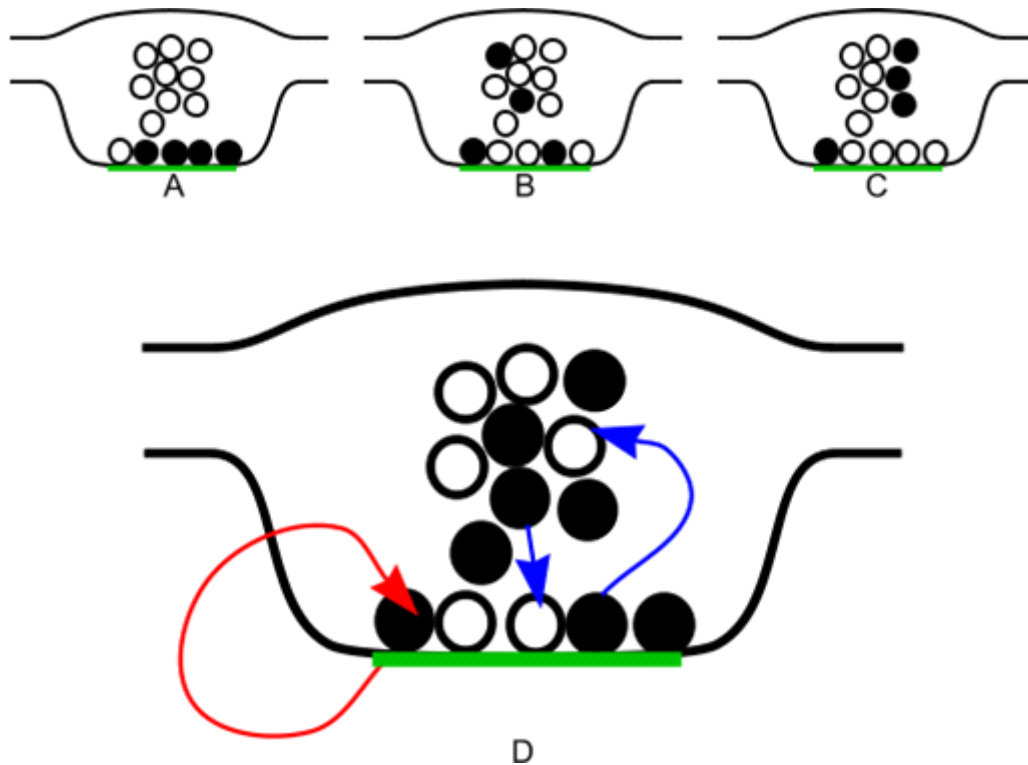


Figure 7.1 Cartoon of RRP vesicle positioning on re-entry into the synapse

A,B,C) Hypotheses for RRP vesicle positioning following recycling. A) Recycling vesicles might be positioned preferentially towards the active zone. B) RRP vesicles might be integrated into the vesicle cluster with no preferential positioning. C) Recycling vesicles might be positioned preferentially within the synapse at a location away from the active zone. Black vesicles represent RRP vesicles, and white vesicles represent other vesicles. D) The results in this thesis suggest that RRP vesicles are actually drawn from two pools: the reserve pool, and a small pool of vesicles which are preferentially releasable. These vesicles stay at or around the active zone following reuptake, ready to be occupied at the next stimulus (indicated by black vesicles and red arrow). The rest of the RRP is taken from the reserve pool, and is returned to the active zone as those which are in preferential positions undergo exocytosis.

This outcome suggested that membership of the RRP was not a feature of individual vesicles, but of vesicles which were closest to the active zone at any given point.

7.3 Plasticity-induced changes in synaptic properties

7.3.1 Recycling pool scaling in response to plasticity protocols

A saturating stimulus only labels a small fraction of vesicles (Betz and Bewick, 1992, Harata et al., 2001, Marra et al., 2012, Darcy et al., 2006b). This fraction can be changed through plasticity protocols (Ratnayaka et al., 2012) and through CDK5 regulation (Marra et al., 2012). The size of the total recycling pool is an important property in determining synaptic strength (Murthy et al., 1997).

As mentioned above, in synapses where LTD has been induced, there is a reduced total recycling pool, roughly half the size of that in control synapses. The size of the TRP in the control samples is concordant with that seen in other studies (Marra et al., 2012, Harata et al., 2001, Darcy et al., 2006b, Denker et al., 2011), so the system can presume to label the TRP in a comparative manner, and therefore the changes are likely due to LTD. Zakharenko et al. (2002) saw a reduction in the fluorescence levels of synapses which also suggests that a smaller fraction of the recycling pool is labelled with FM dye following LTD induction.

As mentioned above, the work by Orenbuch et al. (2012) using synapsin triple knock-out mice demonstrated that recycling vesicles interact with the actin cytoskeleton differently from resting pool vesicles. Previous work has shown that CDK5 can alter the size of the releasable pool (Marra et al., 2012, Orenbuch et al., 2012), so it seems likely that this would be a mechanism through which LTD would act.

These pieces of evidence indicate that there is a fundamental difference between recycling and non-recycling vesicles. Based on the ideas raised here, recent experiments carried out in the lab by Dr S Rey have confirmed the broad principle. They point to interactions between vesicle proteins and the cytoskeletal structures within terminals being crucial to determining the function of a vesicle, rather than the fundamental properties of any given vesicle.

7.3.2 Docking sites as a mechanism of synaptic plasticity

Previous work suggested that the entire population of docked vesicles is not released in response to an RRP labelling stimulus, suggesting that there are vesicles at the active zone which are not primed or ready to undergo release (Moulder and Mennerick, 2005). We proposed that one possible explanation for these 'reluctant' vesicles at docking

sites is that the number of release sites available is a way of regulating the rate of vesicle recycling and neurotransmitter release, and vesicles may sit and block sites to prevent recycling (Fig.7.2). There are many advantages to this mechanism, in particular that it allows a rapid and highly reactive response to plasticity as it uses molecular machinery that is already in place, without new docking sites needing to be created. It also explains the presence of docked vesicles not accessed by stimulation.

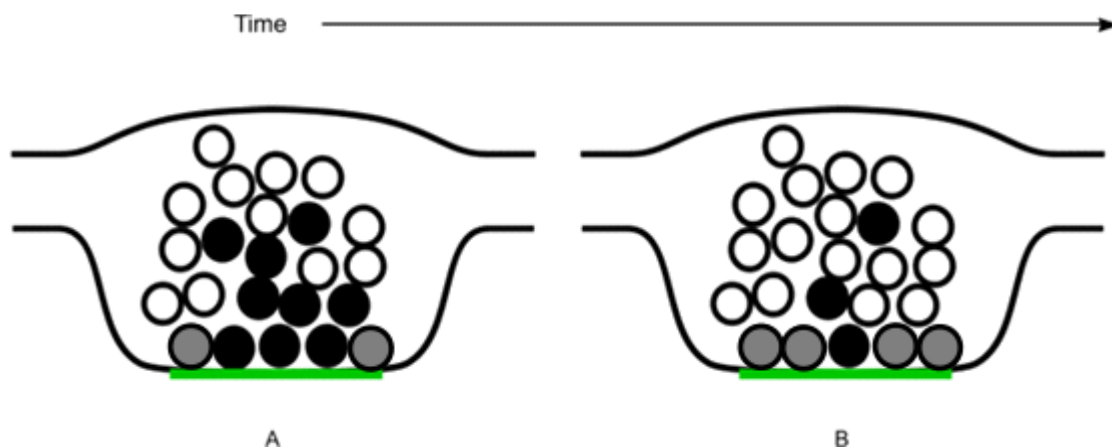


Figure 7.2 Hypothesis of docking sites as a mechanism of synaptic vesicle recycling

A) A number of docking sites at the active zone could potentially be deactivated during normal use. During stimulation vesicle turnover might only be occurring at only the active docking sites. B) Following LTD, there is an increase in the number of deactivated docking sites, and a decrease in the number of vesicles which can undergo recycling in a given time. Green – active zone, white – non-recycling vesicles, black – recycling vesicles, grey – inactive docked vesicles.

In order to determine this, we looked at the composition of the docked pool in LTD and control synapses. In LTD synapses, there was no significant difference in the fraction of the total pool of vesicles which was at docking sites. In LTP synapses there has been evidence that the size of the active zone and the number of docking sites increases (Bell et al., 2014), and that the size of the total pool of vesicles increases in potentiated synapses (Bourne et al., 2013). The results obtained by Marra et al. (2012) point to a loosely proportional relationship between these two properties. If this is the case in LTD

synapses, both active zone shrinkage and reduction in the size of the total pool of vesicles must occur, in order to preserve the relationship between these two properties.

If this is the case, what is the molecular underpinning of docking site regulation? One possible mechanism is through CAST and ELK, proteins associated with the maintenance of the active zone that are amongst the first to be dismantled from the synapse following silencing (Lazarevic et al., 2011). These proteins are linked to RIM1 and Munc13 (Hida and Ohtsuka, 2010), which in turn have roles in priming vesicles in docking sites at the active zone (Betz et al., 2001). Recently, a study on *Drosophila* noted activity-dependent changes to the level of a homologue of ELK/CAST within terminals (Sugie et al., 2015). Decreases in this protein dispersed RIM1 and decreased the density of calcium channels. This supports the idea that docking sites may be being deactivated following sustained low frequency stimulation.

7.4 Activity-dependent arrangement of recycling vesicles within terminals

The distribution of synaptic vesicles at 20 min following labelling with FM dye within terminals is not significantly different from the arrangement of non-recycling vesicles. By contrast, at the same point, Marra et al. (2012) found that recycling vesicles were preferentially positioned towards the active zone. One possible explanation for this is that recycling vesicles are taken up at the active zone and then delivered further back into the synapse, and vesicles are recruited from the front of the synapse to refill the RRP. In this hypothesis, during continuous stimulation, like that used to label the TRP, all vesicles that are able to undergo recycling from around the active zone are used and returned to the total pool, and then trafficked towards the active zone as vesicles in front of them are used (Fig.7.3). This process would likely be related to the interaction of vesicles with actin within the terminals, as this protein has been shown to be essential for preserving the preferential positioning of recycling vesicles (Marra et al., 2012).

This idea supports the results seen in LTD synapses, where recycling vesicles are seen clustered around the active zone and towards the sides of the cluster, but not preferentially clustered towards the front of the synapse. The TRP in LTD synapses is significantly smaller than in control synapses ($12\pm 1\%$ in LTD synapses vs $23\pm 4\%$ in

control synapses), meaning that fewer vesicles are used during recycling, so fewer vesicles are cleared from the front of the synapse and replaced with vesicles which have previously undergone recycling.

In order to verify this, in further experiments, using either probes which are less likely to be removed from vesicles following a second round of exocytosis (e.g. Oyster550), or using very low levels of stimulation which would not release the entire recycling pool, a hippocampal slice with the RRP labelled with FM dye should be exposed to a second round of stimulation prior to fixation, photoconversion, and preparation for electron microscopy. If spatial positioning is activity-dependent, the trend towards the active zone should be restored to some degree.

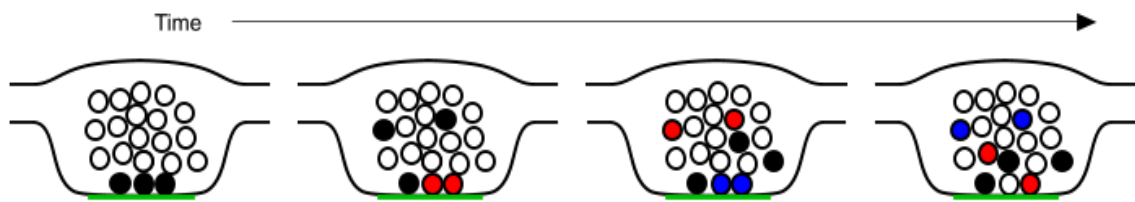


Figure 7.3 Hypothesis of activity dependent preferential positioning of recycling vesicles at active zones

When a stimulus is applied, the vesicles at the docking sites are released and are taken up back into the terminal (black vesicles) where they eventually integrate into the cluster, and vesicles close to the active zone are brought in to refill the active zone sites (red vesicles). This cycle continues with each subsequent set of docked vesicles undergoing recycling and return to the cluster, and the docking sites are refilled with vesicles proximate to the active zone (blue vesicles). This refilling of the RRP from vesicles near the front of the cluster leads to the preferential positioning of recycling vesicles near the front of the cluster over time. Lower stimulus results in less clearing from recycling vesicles from the front, so this preferential positioning is less evident.

7.5 Evidence for a preferentially-accessed pool of vesicles near the active zone

Another key question is whether the structural arrangement of these vesicles has any effect on their functional properties. The work in this thesis demonstrates that a labelled RRP pool loses its fluorescence at a more rapid rate than a labelled TRP pool; however, the RRP is a subset of the TRP, and thus would relate to the initial phase of

destaining. This fraction can be isolated, suggesting that RRP vesicles do have a degree of preferential recycling over those recruited from the reserve pool, and that they do not become less recyclable following endocytosis. The recycling vesicles which can be seen near the active zone at all time points might be responsible for this. In order to investigate whether the former RRP vesicles are preferentially rereleased, future experiments could look at the representation of these vesicles in the next group released by an RRP-releasing stimulus. If these vesicles are preferentially released, there should be a large fluorescence loss following the application of this stimulus, compared to a minimal one if they are simply reintegrated into the pool. These experiments were attempted using the hippocampal slice system, but the signal to noise ratio was insufficient to allow such small changes in fluorescence to be reliably measured. The tissue culture system, though less physiologically relevant, would be useful in answering questions involving very low numbers of vesicles.

Even at later time points, when recycling vesicles do not display any preferential positioning, there are some recycling vesicles at and around the active zone. Functional data also shows that there are FM-dye vesicles amongst those which first respond to the destaining stimulus. This suggests that there are actually two components to the RRP labelling using a 40 AP/10 Hz stimulus, one which is taken from a preferentially releasable pool and one drawn from the recycling pool, based on their position next to the active zone. The preferentially releasable pool is returned to positions close to the active zone, and those drawn from the reserve pool are reintegrated into the cluster (Fig.7.1.D).

This theory goes some way to explaining the contradiction between our findings and those of Park et al. (2012), and the observations of Marra et al. (2012) of the distribution of the total pool of recycling vesicles. Though this thesis and Park et al. discuss the movement and ultimate location of RRP vesicles following reuptake, we may potentially be discussing different pools. Park et al. used a 10 AP/10 Hz RRP labelling protocol, which is much lower than the 40 AP/20 Hz selected for our experiments. The conflicting results suggest that those vesicles which are released by a 10 AP stimulus might have different properties from those released by the additional 30 AP used by us. In other words, there may be some heterogeneity across the RRP in terms of the properties of individual vesicles. Such an idea is also suggested by Alabi and Tsien (2012) in an important recent review. Even at later time points, some recycling vesicles remain at or

near the active zone. It may be that these vesicles which retain their preferential position form a sort of 'RRP+' pool which supports transmission. This theory is in line with a previous study by Vanden Berghe and Klingauf (2006), who found that at low frequencies, a small population of vesicles drives recycling. Current work in the lab is providing evidence to support this conclusion (Dr S Rey and Prof K Staras, personal communication).

This theory may also explain the differences between the results found by Xu et al. (2013) and those in the data presented here. Xu et al. biotinylated synaptic proteins in an activity-dependent manner, lysed the cells and then used Western blotting to quantify the levels of labelling and to compare properties. They observed an increase in the rate of vesicle recycling, and supposed this to be a homeostatic response to postsynaptic receptor internalisation. This is a novel and interesting technique, but it is difficult to compare these results to those of other studies in the field. Using more established indicators of vesicle turnover, particularly visual ones such as iGluSnFR, would be required to verify their results (Marvin et al., 2013). If vesicles are able to be labelled multiple times by the immunological probes, then there may be a small number of vesicles undergoing intense recycling, and a smaller pool of vesicles from the TRP which are only occasionally recruited.

7.6 Activity-dependent properties of the superpool

Synaptic vesicles are able to travel between synapses and engage with functional processes, such as recycling, in their destination synapses (Darcy et al., 2006a). Recently discovered and relatively unexplored, the superpool plays a part in the interactions of synapses both with their postsynaptic targets and their presynaptic environment. The need to examine this pool further becomes more important following compelling evidence that the superpool is a modulator in disease conditions (Scott and Roy, 2012). Using 3D reconstructions of hippocampal neuronal processes, we were able to look at the arrangement of recycling vesicles within processes, compared with the arrangement of non-recycling vesicles.

We found that recycling vesicles tended to be further away from the nearest active zone and vesicle cluster than their non-recycling counterparts. The finding that synapsin primarily controls the movement of resting pool vesicles, and the finding that a lack of synapsin causes an increase in the number of extrasynaptic vesicles (Orenbuch et al.,

2012), does suggest that recycling vesicles have altered synapsin properties which allow them to travel more easily through the processes. Future experiments, using the method outlined in this paper, carried out on Synapsin triple knock-out mice, would give an interesting look at the ways in which the superpool moves through processes.

The ability to study recycling vesicles in the superpool in a physiologically-relevant system like native hippocampal slices using the method described in this thesis, twinned with the development and wider availability of FIBSEM (Knott et al., 2008), allowing large sections of processes to be imaged in a relatively rapid manner, means that the possibilities for future experiments are huge. A key first step would be to look at the effect of vesicles labelled immediately after the induction of LTP or LTD, and those at later time periods after the plasticity protocol, and to see how this affects the movement of vesicles within a process. In these experiments, one would be looking at the interaction of the RRP with the superpool and seeing whether these interactions differ from those of the reserve pool, and looking to see whether the pool labelled by Park et al. (2012) a 'very readily releasable pool' is confined to terminals, whether it can be induced to leave the terminal, and what the impact on function is if it does.

In this thesis, the idea of vesicle pools is explored through ultrastructural and functional studies, and the results paint a picture of a population in which vesicles may have molecularly and spatially defined roles, but these roles are flexible and can change over time and in response to stimuli. The fate of a recycling vesicle depends on the initial activity of the synapse that triggers exocytosis and reuptake, any subsequent activity that follows, and most likely other factors such as unique and preserved characteristics of specific vesicles that differentiate them from the pool as a whole. Our introduction of a slice-based system allows these questions to be addressed in synapses where they are able to experience relevant physiological activity and plasticity protocols. This provides an exciting basis for future research and a better understanding of the properties affecting synaptic transmission.

7.7 Conclusions and future work

Taken together, these results suggest that the activity to which a synapse is exposed has a huge influence on the way that synaptic vesicles within them are organised and behave, but that there are vesicles which have specific recycling properties. The synapse is revealed as being highly dynamic, with a relatively small pool of vesicles

being disproportionately active in exocytosis, similar to the findings of Denker et al. (2011). These vesicles are kept close to the active zone and readily accessible, and the rest of the recycling vesicles form a reserve pool, which is scalable to meet the recycling demands of the synapse (Ratnayaka et al., 2012).

Through gaining a better understanding of the ways that synaptic vesicle activity can be adjusted in response to the activity in the synapse, and of how synapses interact with each other, we gain more information as to how cellular properties translate to behavioural ones. Because of this, a key target for future work is the relationship between learning, memory, and synaptic vesicle function. Studies *in vivo* have shown that changes in synaptic properties, such as those seen in long-term plasticity, require not only a stimulation protocol, but also a learning task. In LTP formation, this involves learning and recognition of a space or environment (Goh and Manahan-Vaughan, 2013b), whereas LTD formation occurs when an animal engages in learning and recognising more subtle clues within an environment, such as objects being changed or moved (Goh and Manahan-Vaughan, 2013a). Firing patterns in the hippocampus can be used to create memories in behaving rats (Liu et al., 2012), providing a direct link between plasticity protocols in CA1 and learning and memory.

The work in this thesis also makes it clear that increasing the physiological relevance of the models used to study synaptic properties is highly important, as deviations from physiological conditions can hugely alter the results and capabilities of systems and neurons. Conducting experiments at room temperature rather than physiological temperature means not only that the rates of endocytosis and exocytosis are altered, but the number of vesicles which are available for recycling (Renden and von Gersdorff, 2007) and the modes of endocytosis which are engaged (Watanabe et al., 2014) are also affected. Induction of plasticity in cultured neurons is difficult to achieve through electrical stimulation protocols (Molnar, 2011), yet this is readily achievable in the slice system; meanwhile, in the living organism, achieving long-term plasticity requires a behavioural protocol in addition to an electrical stimulation protocol to achieve the same synaptic aims (Goh and Manahan-Vaughan, 2013b, Goh and Manahan-Vaughan, 2013a). Meanwhile, the ability for these synaptic changes to occur can also be affected by the animal's experience, with behavioural stress limiting the ability of LTP to be induced and facilitating LTD (Artola et al., 2006). Pilot experiments by Marra et al. (2012) demonstrated the possibility of labelling vesicles in the visual cortex with FM

dye, *in vivo*, by providing a visual stimulus. This, teamed with the new ability to study large volumes of tissue at an ultrastructural level afforded by FIBSEM, could provide direct link between cellular and behavioural studies, providing functional connectomics and revolutionising our understanding of how synaptic vesicles behave. It would be certainly interesting to compare behavioral methods of inducing long-term plasticity with the results seen when they are induced in the slice system.

Another key target for future work is the superpool. The work in this thesis demonstrated that vesicles can move between pools in an activity-dependent fashion and as a result of their arrangement within terminals, but also hinted that the movement between synapses is activity-dependent. The functions of the superpool have been speculated but not yet determined, and gaining more information as to how it behaves over time and during the course of plasticity may provide clues as to how it affects the properties of a neuron. Being able to look at the superpool in hippocampal slice following LTP and LTD would help determine whether proposed changes in pool size (Bourne et al., 2013) are caused by the superpool. Using FIBSEM microscopy could also allow us to look at many synapses along a process, allowing us to determine whether vesicles are removed from synapses specifically to enhance another. Is it a pool to store vesicles until they are called upon, a pool specifically to transfer vesicles between synapses, or simply an accident when the cytoskeletons keeping vesicles within the synapse fail? How this pool behaves could have dramatic implications for our understanding of the flexibility and capabilities of neurons.

The ultrastructural properties of functional vesicles provide us with important clues to determine how neuronal activity can be delivered and shaped. The work in this thesis provides a new technique to study these questions and demonstrates the activity dependence of vesicle arrangement within a synapse, and suggests mechanisms through which the functional properties of a synapse may be controlled.

References

- ADIE, E. J., KALINKA, S., SMITH, L., FRANCIS, M. J., MARENGHI, A., COOPER, M. E., BRIGGS, M., MICHAEL, N. P., MILLIGAN, G. & GAME, S. 2002. A pH-sensitive fluor, CypHer 5, used to monitor agonist-induced G protein-coupled receptor internalization in live cells. *Biotechniques*, 33, 1152-4, 1156-7.
- AHMARI, S. E., BUCHANAN, J. & SMITH, S. J. 2000. Assembly of presynaptic active zones from cytoplasmic transport packets. *Nat Neurosci*, 3, 445-51.
- AIBA, A., KANO, M., CHEN, C., STANTON, M. E., FOX, G. D., HERRUP, K., ZWINGMAN, T. A. & TONEGAWA, S. 1994. Deficient cerebellar long-term depression and impaired motor learning in mGluR1 mutant mice. *Cell*, 79, 377-88.
- AITKEN, P. G., BREESE, G. R., DUDEK, F. F., EDWARDS, F., ESPANOL, M. T., LARKMAN, P. M., LIPTON, P., NEWMAN, G. C., NOWAK, T. S., JR., PANIZZON, K. L. & ET AL. 1995. Preparative methods for brain slices: a discussion. *J Neurosci Methods*, 59, 139-49.
- AKERBOOM, J., CHEN, T. W., WARDILL, T. J., TIAN, L., MARVIN, J. S., MUTLU, S., CALDERON, N. C., ESPOSTI, F., BORGHUIS, B. G., SUN, X. R., GORDUS, A., ORGER, M. B., PORTUGUES, R., ENGERT, F., MACKLIN, J. J., FILOSA, A., AGGARWAL, A., KERR, R. A., TAKAGI, R., KRACUN, S., SHIGETOMI, E., KHAKH, B. S., BAIER, H., LAGNADO, L., WANG, S. S., BARGMANN, C. I., KIMMEL, B. E., JAYARAMAN, V., SVOBODA, K., KIM, D. S., SCHREITER, E. R. & LOOGER, L. L. 2012. Optimization of a GCaMP calcium indicator for neural activity imaging. *J Neurosci*, 32, 13819-40.
- ALABI, A. A. & TSIEN, R. W. 2012. Synaptic vesicle pools and dynamics. *Cold Spring Harb Perspect Biol*, 4, a013680.
- ARAVANIS, A. M., PYLE, J. L. & TSIEN, R. W. 2003. Single synaptic vesicles fusing transiently and successively without loss of identity. *Nature*, 423, 643-7.
- ARIEL, P. & RYAN, T. A. 2010. Optical mapping of release properties in synapses. *Front Neural Circuits*, 4.
- ARTOLA, A., VON FRIJTAG, J. C., FERMONTE, P. C., GISPEN, W. H., SCHRAMA, L. H., KAMAL, A. & SPRUIJT, B. M. 2006. Long-lasting modulation of the induction of LTD and LTP in rat hippocampal CA1 by behavioural stress and environmental enrichment. *Eur J Neurosci*, 23, 261-72.
- ATLURI, P. P. & RYAN, T. A. 2006. The kinetics of synaptic vesicle reacidification at hippocampal nerve terminals. *J Neurosci*, 26, 2313-20.
- ATWOOD, B. K., LOVINGER, D. M. & MATHUR, B. N. 2014. Presynaptic long-term depression mediated by Gi/o-coupled receptors. *Trends Neurosci*, 37, 663-73.
- AUTRY, A. E., ADACHI, M., NOSYREVA, E., NA, E. S., LOS, M. F., CHENG, P. F., KAVALALI, E. T. & MONTEGGIA, L. M. 2011. NMDA receptor blockade at rest triggers rapid behavioural antidepressant responses. *Nature*, 475, 91-5.
- AWAPARA, J., LANDUA, A. J., FUERST, R. & SEALE, B. 1950. Free gamma-aminobutyric acid in brain. *J Biol Chem*, 187, 35-9.
- BAKER, K. D., EDWARDS, T. M. & RICKARD, N. S. 2013. The role of intracellular calcium stores in synaptic plasticity and memory consolidation. *Neurosci Biobehav Rev*, 37, 1211-39.
- BANKER, G. A. & COWAN, W. M. 1977. Rat hippocampal neurons in dispersed cell culture. *Brain Res*, 126, 397-42.

- BATES, M., BLOSSER, T. R. & ZHUANG, X. 2005. Short-range spectroscopic ruler based on a single-molecule optical switch. *Phys Rev Lett*, 94, 108101.
- BEAR, M. F. & LINDEN, D. J. 2001. The Mechanisms and Meaning of Long-Term Synaptic Depression in the Mammalian Brain. In: COWAN, W. M., SUDHOF, T. C. & STEVENS, C. F. (eds.) *Synapses*. Johns Hopkins University Press
- BEATTIE, E. C., CARROLL, R. C., YU, X., MORISHITA, W., YASUDA, H., VON ZASTROW, M. & MALENKA, R. C. 2000. Regulation of AMPA receptor endocytosis by a signaling mechanism shared with LTD. *Nat Neurosci*, 3, 1291-300.
- BEKKERS, J. M. & STEVENS, C. F. 1990. Presynaptic mechanism for long-term potentiation in the hippocampus. *Nature*, 346, 724-9.
- BELL, M. E., BOURNE, J. N., CHIRILLO, M. A., MENDENHALL, J. M., KUWAJIMA, M. & HARRIS, K. M. 2014. Dynamics of nascent and active zone ultrastructure as synapses enlarge during long-term potentiation in mature hippocampus. *J Comp Neurol*.
- BENARROCH, E. E. 2013. Synaptic vesicle exocytosis: molecular mechanisms and clinical implications. *Neurology*, 80, 1981-8.
- BENNETT, M. R. 1999. The early history of the synapse: from Plato to Sherrington. *Brain Res Bull*, 50, 95-118.
- BERLUCCHI, G. & BUCHTEL, H. A. 2009. Neuronal plasticity: historical roots and evolution of meaning. *Exp Brain Res*, 192, 307-19.
- BETZ, A., THAKUR, P., JUNGE, H. J., ASHERY, U., RHEE, J. S., SCHEUSS, V., ROSENMUND, C., RETTIG, J. & BROSE, N. 2001. Functional interaction of the active zone proteins Munc13-1 and RIM1 in synaptic vesicle priming. *Neuron*, 30, 183-96.
- BETZ, W. J. & BEWICK, G. S. 1992. 'Optical Analysis of Synaptic Vesicle Recycling at the Frog Neuromuscular Junction'. *Science*, 255, 200-203.
- BETZ, W. J., BEWICK, G. S. & RIDGE, R. M. 1992a. Intracellular movements of fluorescently labeled synaptic vesicles in frog motor nerve terminals during nerve stimulation. *Neuron*, 9, 805-13.
- BETZ, W. J., MAO, F. & BEWICK, G. S. 1992b. Activity-dependent fluorescent staining and destaining of living vertebrate motor nerve terminals. *J Neurosci*, 12, 363-75.
- BETZ, W. J., MAO, F. & SMITH, C. B. 1996. 'Imaging endocytosis and endocytosis'. *Curr Opin Neurobiol*, 6, 365-371.
- BETZIG, E., PATTERSON, G. H., SOUGRAT, R., LINDWASSER, O. W., OLENYCH, S., BONIFACINO, J. S., DAVIDSON, M. W., LIPPINCOTT-SCHWARTZ, J. & HESS, H. F. 2006. Imaging intracellular fluorescent proteins at nanometer resolution. *Science*, 313, 1642-5.
- BISCHOFBERGER, J., ENGEL, D., LI, L., GEIGER, J. R. & JONAS, P. 2006. Patch-clamp recording from mossy fiber terminals in hippocampal slices. *Nat Protoc*, 1, 2075-81.
- BITTNER, G. D. & KENNEDY, D. 1970. Quantitative aspects of transmitter release. *J Cell Biol*, 47, 585-92.
- BLISS, T. V. & COLLINGRIDGE, G. L. 1993. A synaptic model of memory: long-term potentiation in the hippocampus. *Nature*, 361, 31-9.
- BLISS, T. V. & LOMO, T. 1973. Long-lasting potentiation of synaptic transmission in the dentate area of the anaesthetized rabbit following stimulation of the perforant path. *J Physiol*, 232, 331-56.

- BLOOM, O., EVERGREN, E., TOMILIN, N., KJAERULFF, O., LOW, P., BRODIN, L., PIERIBONE, V. A., GREENGARD, P. & SHUPLIAKOV, O. 2003. Colocalization of synapsin and actin during synaptic vesicle recycling. *J Cell Biol*, 161, 737-47.
- BOLSHAKOV, V. Y. & SIEGELBAUM, S. A. 1994. Postsynaptic induction and presynaptic expression of hippocampal long-term depression. *Science*, 264, 1148-52.
- BOLSHAKOV, V. Y. & SIEGELBAUM, S. A. 1995. Hippocampal long-term depression: arachidonic acid as a potential retrograde messenger. *Neuropharmacology*, 34, 1581-7.
- BORTOLOTTO, Z. A., ANDERSON, W. W., ISAAC, J. T. R. & COLLINGRIDGE, G. L. 2001. 'Synaptic Plasticity in the Hippocampal Slice Preparation'. *Curr Protoc Neurosci*, 6, 1-23.
- BOURNE, J. N., CHIRILLO, M. A. & HARRIS, K. M. 2013. Presynaptic ultrastructural plasticity along CA3→CA1 axons during long-term potentiation in mature hippocampus. *J Comp Neurol*, 521, 3898-912.
- BOYKEN, J., GRONBORG, M., RIEDEL, D., URLAUB, H., JAHN, R. & CHUA, J. J. 2013. Molecular profiling of synaptic vesicle docking sites reveals novel proteins but few differences between glutamatergic and GABAergic synapses. *Neuron*, 78, 285-97.
- BOZZA, T., MCGANN, J. P., MOMBAERTS, P. & WACHOWIAK, M. 2004. In vivo imaging of neuronal activity by targeted expression of a genetically encoded probe in the mouse. *Neuron*, 42, 9-21.
- BRANCO, T., MARRA, V. & STARAS, K. 2010. Examining size–strength relationships at hippocampal synapses using an ultrastructural measurement of synaptic release probability. *J Struct Biol*, 172, 203-210.
- BRANCO, T., STARAS, K., DARCY, K. J. & GODA, Y. 2008. Local Dendritic Activity Sets Release Probability at Hippocampal Synapses. *Neuron*, 59, 475-485.
- BRIGGS, M. S., BURNS, D. D., COOPER, M. E. & GREGORY, S. J. 2000. A pH sensitive fluorescent cyanine dye for biological applications. *Chem Commun (Camb)*, 2323-2324.
- BROSE, N., PETRENKO, A. G., SUDHOF, T. C. & JAHN, R. 1992. Synaptotagmin: a calcium sensor on the synaptic vesicle surface. *Science*, 256, 1021-5.
- BROWN, A. 2003. Axonal transport of membranous and nonmembranous cargoes: a unified perspective. *J Cell Biol*, 160, 817-21.
- BRUCHEZ, M. P. 2011. Quantum dots find their stride in single molecule tracking. *Curr Opin Chem Biol*, 15, 775-80.
- BRUMBACK, A. C., LIEBER, J. L., ANGLESON, J. K. & BETZ, W. J. 2004. Using FM1-43 to study neuropeptide granule dynamics and exocytosis. *Methods*, 33, 287-94.
- BUI, L. & GLAVINOVIC, M. I. 2014. Temperature dependence of vesicular dynamics at excitatory synapses of rat hippocampus. *Cogn Neurodyn*, 8, 277-86.
- BURKHARDT, C., GNAUCK, P., WOLBURG, H. & NISCH, W. 2005. Serial block-face sectioning and high resolution imaging of biological samples with a crossbeam FIB/FESEM microscope. *Proceedings of the microscopy conference*, 106.
- BURRE, J., BECKHAUS, T., SCHAGGER, H., CORVEY, C., HOFMANN, S., KARAS, M., ZIMMERMANN, H. & VOLKNANDT, W. 2006. Analysis of the synaptic vesicle proteome using three gel-based protein separation techniques. *Proteomics*, 6, 6250-62.
- BYKHOVSKAIA, M. 2011. Synapsin regulation of vesicle organization and functional pools. *Semin Cell Dev Biol*, 22, 387-92.

- CAHALAN, M. & NEHER, E. 1992. Patch clamp techniques: an overview. *Methods Enzymol*, 207, 3-14.
- CARDONA, A., SAALFELD, S., SCHINDELIN, J., ARGANDA-CARRERAS, I., PREIBISCH, S., LONGAIR, M., TOMANCAK, P., HARTENSTEIN, V. & DOUGLAS, R. J. 2012. TrakEM2 software for neural circuit reconstruction. *PLoS One*, 7, e38011.
- CASTILLO, P. E., WEISSKOPF, M. G. & NICOLL, R. A. 1994. The role of Ca²⁺ channels in hippocampal mossy fiber synaptic transmission and long-term potentiation. *Neuron*, 12, 261-9.
- CECCARELLI, B. & HURLBUT, W. P. 1980. Ca²⁺-dependent recycling of synaptic vesicles at the frog neuromuscular junction. *J Cell Biol*, 87, 297-303.
- CECCARELLI, B., HURLBUT, W. P. & MAURO, A. 1973. Turnover of transmitter and synaptic vesicles at the frog neuromuscular junction. *J Cell Biol*, 57, 499-524.
- CHANG, D. T., HONICK, A. S. & REYNOLDS, I. J. 2006. Mitochondrial trafficking to synapses in cultured primary cortical neurons. *J Neurosci*, 26, 7035-45.
- CHANG, Y. P., PINAUD, F., ANTELMAN, J. & WEISS, S. 2008. Tracking bio-molecules in live cells using quantum dots. *J Biophotonics*, 1, 287-98.
- CHAPMAN, E. R. 2008. How does synaptotagmin trigger neurotransmitter release? *Annu Rev Biochem*, 77, 615-41.
- CHEN, X., BARG, S. & ALMERS, W. 2008. Release of the styryl dyes from single synaptic vesicles in hippocampal neurons. *J Neurosci*, 28, 1894-903.
- CHEUNG, G. & COUSIN, M. A. 2013. Synaptic vesicle generation from activity-dependent bulk endosomes requires calcium and calcineurin. *J Neurosci*, 33, 3370-9.
- CLAYTON, E. L., EVANS, G. J. & COUSIN, M. A. 2008. Bulk synaptic vesicle endocytosis is rapidly triggered during strong stimulation. *J Neurosci*, 28, 6627-32.
- CONTRIBUTORS", M. I. 2013. *The Key Steps in Clathrin-Mediated Endocytosis* [Online]. MBIInfo Wiki. Available: <http://www.mechanobio.info/figure/1384925268515.jpg.html> [Accessed 3/26/2014 2014].
- COOPER, S. J. 2005. Donald O. Hebb's synapse and learning rule: a history and commentary. *Neurosci Biobehav Rev*, 28, 851-74.
- COUSIN, M. A. 2014. Synaptic Vesicle Endocytosis and Endosomal Recycling in Central Nerve Terminals: Discrete Trafficking Routes? *Neuroscientist*.
- COUSIN, M. A. & ROBINSON, P. J. 2001. The dephosphins: dephosphorylation by calcineurin triggers synaptic vesicle endocytosis. *Trends Neurosci*, 24, 659-65.
- COUTEAUX, R. & PECOT-DECHAVASSINE, M. 1970. [Synaptic vesicles and pouches at the level of "active zones" of the neuromuscular junction]. *C R Acad Sci Hebd Seances Acad Sci D*, 271, 2346-9.
- COWAN, W. M. & KANDEL, E. R. 2001. Brief History of Synapses and Synaptic Transmission. In: COWAN, W. M. (ed.) *Synapses*. Baltimore: Johns Hopkins Press.
- COWAN, W. M., SÜDHOF, T. C., STEVENS, C. F. & INSTITUTE, H. H. M. 2001. *Synapses*, Johns Hopkins University Press.
- CUMMINGS, J. A., MULKEY, R. M., NICOLL, R. A. & MALENKA, R. C. 1996. Ca²⁺ signaling requirements for long-term depression in the hippocampus. *Neuron*, 16, 825-33.
- CUPAIOLI, F. A., ZUCCA, F. A., BORASCHI, D. & ZECCA, L. 2014. Engineered nanoparticles. How brain friendly is this new guest? *Prog Neurobiol*, 119-120C, 20-38.

- CURTIS, D. R., PHILLIS, J. W. & WATKINS, J. C. 1959a. Chemical excitation of spinal neurones. *Nature*, 183, 611-2.
- CURTIS, D. R., PHILLIS, J. W. & WATKINS, J. C. 1959b. The depression of spinal neurones by gamma-amino-n-butyric acid and beta-alanine. *J Physiol*, 146, 185-203.
- CURTIS, D. R. & WATKINS, J. C. 1963. Acidic amino acids with strong excitatory actions on mammalian neurones. *J Physiol*, 166, 1-14.
- DARCY, K. J., STARAS, K., COLLINSON, L. M. & GODA, Y. 2006a. Constitutive sharing of recycling synaptic vesicles between presynaptic boutons. *Nat Neurosci*, 9, 315-21.
- DARCY, K. J., STARAS, K., COLLINSON, L. M. & GODA, Y. 2006b. An ultrastructural readout of fluorescence recovery after photobleaching using correlative light and electron microscopy. *Nat Protoc*, 1, 988-994.
- DE BLASI, A., CONN, P. J., PIN, J. & NICOLETTI, F. 2001. Molecular determinants of metabotropic glutamate receptor signaling. *Trends Pharmacol Sci*, 22, 114-20.
- DE CAMILLI, P., HAUKE, V., TAKEI, K. & MUGNAINI, E. 2001. The Structure of Synapses. In: COWAN, W. M., SUDHOF, T. C. & STEVENS, C. F. (eds.) *Synapses*. Baltimore, Maryland: Johns Hopkins University Press.
- DE JONG, A. P. & VERHAGE, M. 2009. Presynaptic signal transduction pathways that modulate synaptic transmission. *Curr Opin Neurobiol*, 19, 245-53.
- DE ROBERTIS, E. D. & BENNETT, H. S. 1954. A submicroscopic vesicular component of Schwann cells and nerve satellite cells. *Exp Cell Res*, 6, 543-5.
- DE ROBERTIS, E. D. & BENNETT, H. S. 1955. Some features of the submicroscopic morphology of synapses in frog and earthworm. *J Biophys Biochem Cytol*, 1, 47-58.
- DEERINCK, T. J., BUSHONG, E. A., THOR, A. & ELLISMAN, M. H. 2010. NCMIR methods for 3D EM: a new protocol for preparation of biological specimens for serial block face scanning electron microscopy.
- DEMPSEY, G. T., BATES, M., KOWTONIUK, W. E., LIU, D. R., TSIEN, R. Y. & ZHUANG, X. 2009. Photoswitching mechanism of cyanine dyes. *J Am Chem Soc*, 131, 18192-3.
- DENKER, A., BETHANI, I., KROHNERT, K., KORBER, C., HORSTMANN, H., WILHELM, B. G., BARYSCH, S. V., KUNER, T., NEHER, E. & RIZZOLI, S. O. 2011. A small pool of vesicles maintains synaptic activity in vivo. *Proc Natl Acad Sci U S A*, 108, 17177-82.
- DENKER, A. & RIZZOLI, S. O. 2010. Synaptic vesicle pools: an update. *Front Synaptic Neurosci*, 2, 135.
- DITTMAN, J. S., KREITZER, A. C. & REGEHR, W. G. 2000. Interplay between facilitation, depression, and residual calcium at three presynaptic terminals. *J Neurosci*, 20, 1374-85.
- DOBRUNZ, L. E. 2002. Release probability is regulated by the size of the readily releasable vesicle pool at excitatory synapses in hippocampus. *Int J Dev Neurosci*, 20, 225-36.
- DOBRUNZ, L. E. & STEVENS, C. F. 1999. Response of hippocampal synapses to natural stimulation patterns. *Neuron*, 22, 157-66.
- DOUSSAU, F. & AUGUSTINE, G. J. 2000. The actin cytoskeleton and neurotransmitter release: an overview. *Biochimie*, 82, 353-63.
- DUDEK, S. M. & BEAR, M. F. 1992. Homosynaptic long-term depression in area CA1 of hippocampus and effects of N-methyl-D-aspartate receptor blockade. *Proc Natl Acad Sci U S A*, 89, 4363-7.

- EDWARDS, F. A. & KONNERTH, A. 1992. Patch-clamping cells in sliced tissue preparations. *Methods Enzymol*, 207, 208-22.
- EHLERS, M. D. 2000. Reinsertion or degradation of AMPA receptors determined by activity-dependent endocytic sorting. *Neuron*, 28, 511-25.
- EVANS, G. J. & COUSIN, M. A. 2007. Activity-dependent control of slow synaptic vesicle endocytosis by cyclin-dependent kinase 5. *J Neurosci*, 27, 401-11.
- FATT, P. & KATZ, B. 1951. An analysis of the end-plate potential recorded with an intracellular electrode. *J Physiol*, 115, 320-70.
- FATT, P. & KATZ, B. 1952. Spontaneous subthreshold activity at motor nerve endings. *J Physiol*, 117, 109-28.
- FEJTOVA, A. & GUNDELFINGER, E. D. 2006. Molecular organization and assembly of the presynaptic active zone of neurotransmitter release. *Results Probl Cell Differ*, 43, 49-68.
- FERNANDEZ-ALFONSO, T., KWAN, R. & RYAN, T. A. 2006. Synaptic vesicles interchange their membrane proteins with a large surface reservoir during recycling. *Neuron*, 51, 179-86.
- FERNANDEZ-ALFONSO, T. & RYAN, T. 2008. A heterogeneous "resting" pool of synaptic vesicles that is dynamically interchanged across boutons in mammalian CNS synapses. *Brain Cell Biol*, 36, 87-100.
- FERNANDEZ-ALFONSO, T. & RYAN, T. A. 2004. The kinetics of synaptic vesicle pool depletion at CNS synaptic terminals. *Neuron*, 41, 943-53.
- FIALA, J. C. 2005. Reconstruct: a free editor for serial section microscopy. *J Microsc*, 218, 52-61.
- FIFKOVA, E., MARKHAM, J. A. & DELAY, R. J. 1983. Calcium in the spine apparatus of dendritic spines in the dentate molecular layer. *Brain Res*, 266, 163-8.
- FIORAVANTE, D., CHU, Y., DE JONG, A. P., LEITGES, M., KAESER, P. S. & REGEHR, W. G. 2014. Protein kinase C is a calcium sensor for presynaptic short-term plasticity. *Elife*, 3, e03011.
- FREDJ, N. B. & BURRONE, J. 2009. A resting pool of vesicles is responsible for spontaneous vesicle fusion at the synapse. *Nat Neurosci*, 12, 751-8.
- FUJINO, I., YAMADA, N., MIYAWAKI, A., HASEGAWA, M., FURUICHI, T. & MIKOSHIBA, K. 1995. Differential expression of type 2 and type 3 inositol 1,4,5-trisphosphate receptor mRNAs in various mouse tissues: in situ hybridization study. *Cell Tissue Res*, 280, 201-10.
- GAD, H., LOW, P., ZOTOVA, E., BRODIN, L. & SHUPLIAKOV, O. 1998. Dissociation between Ca²⁺-triggered synaptic vesicle exocytosis and clathrin-mediated endocytosis at a central synapse. *Neuron*, 21, 607-16.
- GAFFIELD, M. A. & BETZ, W. J. 2007. Synaptic vesicle mobility in mouse motor nerve terminals with and without synapsin. *J Neurosci*, 27, 13691-700.
- GARTHWAITE, J. 2010. New insight into the functioning of nitric oxide-receptive guanylyl cyclase: physiological and pharmacological implications. *Mol Cell Biochem*, 334, 221-32.
- GARTNER, A. & STAIGER, V. 2002. Neurotrophin secretion from hippocampal neurons evoked by long-term-potential-inducing electrical stimulation patterns. *Proc Natl Acad Sci U S A*, 99, 6386-91.
- GE-HEALTHCARE 2006. CypHer5E 25-8010-12UM pH sensitive cyanine dye based technology for receptor internalization studies. *In: HEALTHCARE, G. (ed.)*. www.gelifesciences.com.

- GIBB, A. J. & EDWARDS, F. A. 1994. 'Patch clamp recording from cells in sliced tissues'. In: OGDEN, D. (ed.) *"Microelectrode Techniques: The Plymouth Workshop Handbook"*. Second Edition ed.: The Company of Biologists Ltd.
- GOH, J. J. & MANAHAN-VAUGHAN, D. 2013a. Hippocampal long-term depression in freely behaving mice requires the activation of beta-adrenergic receptors. *Hippocampus*, 23, 1299-308.
- GOH, J. J. & MANAHAN-VAUGHAN, D. 2013b. Spatial object recognition enables endogenous LTD that curtails LTP in the mouse hippocampus. *Cereb Cortex*, 23, 1118-25.
- GONON, F., MSGHINA, M. & STJARNE, L. 1993. Kinetics of noradrenaline released by sympathetic nerves. *Neuroscience*, 56, 535-8.
- GRABRUCKER, A., VAIDA, B., BOCKMANN, J. & BOECKERS, T. M. 2009. Synaptogenesis of hippocampal neurons in primary cell culture. *Cell Tissue Res*, 338, 333-41.
- GRANSETH, B. & LAGNADO, L. 2008. The role of endocytosis in regulating the strength of hippocampal synapses. *J Physiol*, 586, 5969-82.
- GRAY, E. G. 1959. Axo-somatic and axo-dendritic synapses of the cerebral cortex: an electron microscope study. *J Anat*, 93, 420-33.
- GREENGARD, P., VALTORTA, F., CZERNIK, A. J. & BENFENATI, F. 1993. Synaptic vesicle phosphoproteins and regulation of synaptic function. *Science*, 259, 780-5.
- GUNDELFINGER, E. D., KESSELS, M. M. & QUALMANN, B. 2003. Temporal and spatial coordination of exocytosis and endocytosis. *Nat Rev Mol Cell Biol*, 4, 127-39.
- HALFF, A. W., GOMEZ-VARELA, D., JOHN, D. & BERG, D. K. 2014. A novel mechanism for nicotinic potentiation of glutamatergic synapses. *J Neurosci*, 34, 2051-64.
- HANLEY, J. G. & HENLEY, J. M. 2005. PICK1 is a calcium-sensor for NMDA-induced AMPA receptor trafficking. *EMBO J*, 24, 3266-78.
- HARATA, N., RYAN, T. A., SMITH, S. J., BUCHANAN, J. & TSIEN, R. W. 2001. Visualizing recycling synaptic vesicles in hippocampal neurons by FM 1-43 photoconversion. *Proc Natl Acad Sci U S A*, 98, 12748-53.
- HARDINGHAM, N., DACHTLER, J. & FOX, K. 2013. The role of nitric oxide in pre-synaptic plasticity and homeostasis. *Front Cell Neurosci*, 7, 190.
- HARRIS, K. M. & SULTAN, P. 1995. Nonuniform Probability of Release at Hippocampal CA1 Synapses. *Neuropharmacology*, 34, 1387-1395.
- HARRIS, K. M. & WEINBERG, R. J. 2012. Ultrastructure of synapses in the mammalian brain. *Cold Spring Harb Perspect Biol*, 4.
- HARTMANN, M., HEUMANN, R. & LESSMANN, V. 2001. Synaptic secretion of BDNF after high-frequency stimulation of glutamatergic synapses. *EMBO J*, 20, 5887-97.
- HAYASHI, T. 1954. Effects of sodium glutamate on the nervous system. *Keio J Med*, 3, 183-192.
- HE, L. & WU, L. G. 2007. The debate on the kiss-and-run fusion at synapses. *Trends Neurosci*, 30, 447-55.
- HEBB, D. O. 1949. *Organization of behavior.*, New York, Wiley Subscription Services, Inc., A Wiley Company.
- HELL, S. W. & WICHMANN, J. 1994. Breaking the diffraction resolution limit by stimulated emission: stimulated-emission-depletion fluorescence microscopy. *Opt Lett*, 19, 780-2.

- HERZOG, E., NADRIGNY, F., SILM, K., BIESEMANN, C., HELLING, I., BERSOT, T., STEFFENS, H., SCHWARTZMANN, R., NAGERL, U. V., EL MESTIKAWY, S., RHEE, J., KIRCHHOFF, F. & BROSE, N. 2011. In vivo imaging of intersynaptic vesicle exchange using VGLUT1 Venus knock-in mice. *J Neurosci*, 31, 15544-59.
- HEUSER, J. E. & REESE, T. S. 1973. Evidence for recycling of synaptic vesicle membrane during transmitter release at the frog neuromuscular junction. *J Cell Biol*, 57, 315-44.
- HIDA, Y. & OHTSUKA, T. 2010. CAST and ELKS proteins: structural and functional determinants of the presynaptic active zone. *J Biochem*, 148, 131-7.
- HILFIKER, S., PIERIBONE, V. A., CZERNIK, A. J., KAO, H. T., AUGUSTINE, G. J. & GREENGARD, P. 1999. Synapsins as regulators of neurotransmitter release. *Philos Trans R Soc Lond B Biol Sci*, 354, 269-79.
- HIRES, S. A., ZHU, Y. & TSIEN, R. Y. 2008. Optical measurement of synaptic glutamate spillover and reuptake by linker optimized glutamate-sensitive fluorescent reporters. *Proc Natl Acad Sci U S A*, 105, 4411-6.
- HONORE, T., LAURIDSEN, J. & KROGSGAARD-LARSEN, P. 1982. The binding of [3H]AMPA, a structural analogue of glutamic acid, to rat brain membranes. *J Neurochem*, 38, 173-8.
- HOPF, F. W., WATERS, J., MEHTA, S. & SMITH, S. J. 2002. Stability and plasticity of developing synapses in hippocampal neuronal cultures. *J Neurosci*, 22, 775-81.
- HRABETOVA, S. & SACKTOR, T. C. 1996. Bidirectional regulation of protein kinase M zeta in the maintenance of long-term potentiation and long-term depression. *J Neurosci*, 16, 5324-33.
- HRABETOVA, S., SERRANO, P., BLACE, N., TSE, H. W., SKIFTER, D. A., JANE, D. E., MONAGHAN, D. T. & SACKTOR, T. C. 2000. Distinct NMDA receptor subpopulations contribute to long-term potentiation and long-term depression induction. *J Neurosci*, 20, RC81.
- HUA, Y., SINHA, R., MARTINEAU, M., KAHMS, M. & KLINGAUF, J. 2010. A common origin of synaptic vesicles undergoing evoked and spontaneous fusion. *Nat Neurosci*, 13, 1451-3.
- HUA, Z., LEAL-ORTIZ, S., FOSS, SARAH M., WAITES, CLARISSA L., GARNER, CRAIG C., VOGLMAIER, SUSAN M. & EDWARDS, ROBERT H. 2011. v-SNARE Composition Distinguishes Synaptic Vesicle Pools. *Neuron*, 71, 474-487.
- IKEDA, K. & BEKKERS, J. M. 2009. Counting the number of releasable synaptic vesicles in a presynaptic terminal. *Proc Natl Acad Sci U S A*, 106, 2945-50.
- INGEBRITSEN, T. S. & COHEN, P. 1983. The protein phosphatases involved in cellular regulation. 1. Classification and substrate specificities. *Eur J Biochem*, 132, 255-61.
- JAMES, W. 1890. *Principles of Psychology*, London, MacMillan.
- JOHNSTON, G. A., DE GROAT, W. C. & CURTIS, D. R. 1969. Tetanus toxin and amino acid levels in cat spinal cord. *J Neurochem*, 16, 797-800.
- KAMIN, D., LAUTERBACH, M. A., WESTPHAL, V., KELLER, J., SCHONLE, A., HELL, S. W. & RIZZOLI, S. O. 2010. High- and low-mobility stages in the synaptic vesicle cycle. *Biophys J*, 99, 675-84.
- KAMIYAMA, D. & HUANG, B. 2012. Development in the STORM. *Dev Cell*, 23, 1103-10.
- KANDEL, E. R. 1976. *Cellular basis of behavior : an introduction to behavioral neurobiology* / Eric R. Kandel, San Francisco, W.H. Freeman.

- KASHIWABUCHI, N., IKEDA, K., ARAKI, K., HIRANO, T., SHIBUKI, K., TAKAYAMA, C., INOUE, Y., KUTSUWADA, T., YAGI, T., KANG, Y. & ET AL. 1995. Impairment of motor coordination, Purkinje cell synapse formation, and cerebellar long-term depression in GluR delta 2 mutant mice. *Cell*, 81, 245-52.
- KAVALALI, E. T. & JORGENSEN, E. M. 2014. Visualizing presynaptic function. *Nat Neurosci*, 17, 10-6.
- KAY, A. R., ALFONSO, A., ALFORD, S., CLINE, H. T., HOLGADO, A. M., SAKMANN, B., SNITSAREV, V. A., STRICKER, T. P., TAKAHASHI, M. & WU, L. G. 1999. Imaging synaptic activity in intact brain and slices with FM1-43 in *C. elegans*, lamprey, and rat. *Neuron*, 24, 809-17.
- KHLAIFIA, A., FARAH, H., GACKIERE, F. & TELL, F. 2013. Anandamide, cannabinoid type 1 receptor, and NMDA receptor activation mediate non-Hebbian presynaptically expressed long-term depression at the first central synapse for visceral afferent fibers. *J Neurosci*, 33, 12627-37.
- KIM, S. H. & RYAN, T. A. 2010. CDK5 serves as a major control point in neurotransmitter release. *Neuron*, 67, 797-809.
- KIM, Y. J. & SERPE, M. 2013. Building a synapse: a complex matter. *Fly (Austin)*, 7, 146-52.
- KLINGAUF, J., KAVALALI, E. T. & TSIEN, R. W. 1998. Kinetics and regulation of fast endocytosis at hippocampal synapses. *Nature*, 394, 581-5.
- KNOTT, G., MARCHMAN, H., WALL, D. & LICH, B. 2008. Serial section scanning electron microscopy of adult brain tissue using focused ion beam milling. *J Neurosci*, 28, 2959-64.
- KOBAYASHI, K., MANABE, T. & TAKAHASHI, T. 1999. Calcium-dependent mechanisms involved in presynaptic long-term depression at the hippocampal mossy fibre-CA3 synapse. *Eur J Neurosci*, 11, 1633-8.
- KOHARA, K., KITAMURA, A., MORISHIMA, M. & TSUMOTO, T. 2001. Activity-dependent transfer of brain-derived neurotrophic factor to postsynaptic neurons. *Science*, 291, 2419-23.
- KOJIMA, M., TAKEI, N., NUMAKAWA, T., ISHIKAWA, Y., SUZUKI, S., MATSUMOTO, T., KATOH-SEMBA, R., NAWA, H. & HATANAKA, H. 2001. Biological characterization and optical imaging of brain-derived neurotrophic factor-green fluorescent protein suggest an activity-dependent local release of brain-derived neurotrophic factor in neurites of cultured hippocampal neurons. *J Neurosci Res*, 64, 1-10.
- KONONENKO, N. L., DIRIL, M. K., PUCHKOV, D., KINTSCHER, M., KOO, S. J., PFUHL, G., WINTER, Y., WIENISCH, M., KLINGAUF, J., BREUSTEDT, J., SCHMITZ, D., MARITZEN, T. & HAUCKE, V. 2013. Compromised fidelity of endocytic synaptic vesicle protein sorting in the absence of stonin 2. *Proc Natl Acad Sci U S A*, 110, E526-35.
- KORKOTIAN, E. & SEGAL, M. 1996. Lasting effects of glutamate on nuclear calcium concentration in cultured rat hippocampal neurons: regulation by calcium stores. *J Physiol*, 496 (Pt 1), 39-48.
- KOUSHIKA, S. P., RICHMOND, J. E., HADWIGER, G., WEIMER, R. M., JORGENSEN, E. M. & NONET, M. L. 2001. A post-docking role for active zone protein Rim. *Nat Neurosci*, 4, 997-1005.
- KREBS, H. A., EGGLESTON, L. V. & HEMS, R. 1949. Distribution of glutamine and glutamic acid in animal tissues. *Biochem J*, 44, 159-63.
- KRNJEVIC, K. 2004. How does a little acronym become a big transmitter? *Biochem Pharmacol*, 68, 1549-55.

- KRNJEVIC, K. & PHILLIS, J. W. 1963. Actions of certain amines on cerebral cortical neurones. *Br J Pharmacol Chemother*, 20, 471-90.
- KRUEGER, S. R., KOLAR, A. & FITZSIMONDS, R. M. 2003. The presynaptic release apparatus is functional in the absence of dendritic contact and highly mobile within isolated axons. *Neuron*, 40, 945-57.
- KUSHMERICK, C., RENDEN, R. & VON GERSDORFF, H. 2006. Physiological temperatures reduce the rate of vesicle pool depletion and short-term depression via an acceleration of vesicle recruitment. *J Neurosci*, 26, 1366-77.
- LAI, M. M., HONG, J. J., RUGGIERO, A. M., BURNETT, P. E., SLEPNEV, V. I., DE CAMILLI, P. & SNYDER, S. H. 1999. The calcineurin-dynamitin 1 complex as a calcium sensor for synaptic vesicle endocytosis. *J Biol Chem*, 274, 25963-6.
- LANDISMAN, C. E. & CONNORS, B. W. 2005. Long-term modulation of electrical synapses in the mammalian thalamus. *Science*, 310, 1809-13.
- LANGLEY, J. N. 1905. On the reaction of cells and of nerve-endings to certain poisons, chiefly as regards the reaction of striated muscle to nicotine and to curari. *J Physiol*, 33, 374-413.
- LANGLEY, J. N. 1906. Croonian Lecture, 1906: On Nerve Endings and on Special Excitable Substances in Cells. *Proc R Soc Lond B Biol Sci*, 78, 170-194.
- LANORE, F., REBOLA, N. & CARTA, M. 2009. Spike-timing-dependent plasticity induces presynaptic changes at immature hippocampal mossy fiber synapses. *J Neurosci*, 29, 8299-301.
- LAZAREVIC, V., SCHONE, C., HEINE, M., GUNDELFINGER, E. D. & FEJTOVA, A. 2011. Extensive remodeling of the presynaptic cytomatrix upon homeostatic adaptation to network activity silencing. *J Neurosci*, 31, 10189-200.
- LEAO, R. M. & VON GERSDORFF, H. 2009. Synaptic vesicle pool size, release probability and synaptic depression are sensitive to Ca²⁺ buffering capacity in the developing rat calyx of Held. *Braz J Med Biol Res*, 42, 94-104.
- LEE, H. K., KAMEYAMA, K., HUGANIR, R. L. & BEAR, M. F. 1998. NMDA induces long-term synaptic depression and dephosphorylation of the GluR1 subunit of AMPA receptors in hippocampus. *Neuron*, 21, 1151-62.
- LESSMANN, V. 1998. Neurotrophin-dependent modulation of glutamatergic synaptic transmission in the mammalian CNS. *Gen Pharmacol*, 31, 667-74.
- LI, Q., GORDON, M., CAO, C., UGEN, K. E. & MORGAN, D. 2007. Improvement of a low pH antigen-antibody dissociation procedure for ELISA measurement of circulating anti-A β antibodies. *BMC Neurosci*, 8, 22.
- LIM, N. F., NOWYCKY, M. C. & BOOKMAN, R. J. 1990. Direct measurement of exocytosis and calcium currents in single vertebrate nerve terminals. *Nature*, 344, 449-51.
- LINDEN, D. J. 1994. Long-term synaptic depression in the mammalian brain. *Neuron*, 12, 457-72.
- LISMAN, J. 1989. A mechanism for the Hebb and the anti-Hebb processes underlying learning and memory. *Proc Natl Acad Sci U S A*, 86, 9574-8.
- LISMAN, J., YASUDA, R. & RAGHAVACHARI, S. 2012. Mechanisms of CaMKII action in long-term potentiation. *Nat Rev Neurosci*, 13, 169-82.
- LIU, X., RAMIREZ, S., PANG, P. T., PURYEAR, C. B., GOVINDARAJAN, A., DEISSEROTH, K. & TONEGAWA, S. 2012. Optogenetic stimulation of a hippocampal engram activates fear memory recall. *Nature*, 484, 381-5.
- LOGIN, G. R., LEONARD, J. B. & DVORAK, A. M. 1998. Calibration and standardization of microwave ovens for fixation of brain and peripheral nerve tissue. *Methods*, 15, 107-17.

- LOPEZ-MUNOZ, F., BOYA, J. & ALAMO, C. 2006. Neuron theory, the cornerstone of neuroscience, on the centenary of the Nobel Prize award to Santiago Ramon y Cajal. *Brain Res Bull*, 70, 391-405.
- LU, B. & GOTTSCHALK, W. 2000. Modulation of hippocampal synaptic transmission and plasticity by neurotrophins. *Prog Brain Res*, 128, 231-41.
- LU, H. E., MACGILLAVRY, H. D., FROST, N. A. & BLANPIED, T. A. 2014. Multiple spatial and kinetic subpopulations of CaMKII in spines and dendrites as resolved by single-molecule tracking PALM. *J Neurosci*, 34, 7600-10.
- LUMINARTIS. 2011. *Oyster550 Fact Sheet* [Online]. www.luminartis.com. Available: <http://www.luminartis.com/> [Accessed 10/07/2015].
- MACDOUGALL, M. J. & FINE, A. 2014. The expression of long-term potentiation: reconciling the preists and the postivists. *Philos Trans R Soc Lond B Biol Sci*, 369, 20130135.
- MACGILLAVRY, H. D., KERR, J. M. & BLANPIED, T. A. 2011. Lateral organization of the postsynaptic density. *Mol Cell Neurosci*, 48, 321-31.
- MACGILLAVRY, H. D., SONG, Y., RAGHAVACHARI, S. & BLANPIED, T. A. 2013. Nanoscale scaffolding domains within the postsynaptic density concentrate synaptic AMPA receptors. *Neuron*, 78, 615-22.
- MAGBY, J. P., BI, C., CHEN, Z. Y., LEE, F. S. & PLUMMER, M. R. 2006. Single-cell characterization of retrograde signaling by brain-derived neurotrophic factor. *J Neurosci*, 26, 13531-6.
- MALENKA, R. C. & BEAR, M. F. 2004. LTP and LTD: an embarrassment of riches. *Neuron*, 44, 5-21.
- MALENKA, R. C. & SIEGELBAUM, S. A. 2001. Synaptic Plasticity and Efficacy. In: COWAN, W. M., SUDHOF, T. C. & STEVENS, C. F. (eds.) *Synapses*. Baltimore, Maryland: Johns Hopkins University Press.
- MARRA, V., BURDEN, J. J., CRAWFORD, F. & STARAS, K. 2014. Ultrastructural readout of functional synaptic vesicle pools in hippocampal slices based on FM dye labeling and photoconversion. *Nat Protoc*, 9, 1337-47.
- MARRA, V., BURDEN, J. J., THORPE, J. R., SMITH, I. T., SMITH, S. L., HAUSSER, M., BRANCO, T. & STARAS, K. 2012. A preferentially segregated recycling vesicle pool of limited size supports neurotransmission in native central synapses. *Neuron*, 76, 579-89.
- MARTENS, H., WESTON, M. C., BOULLAND, J. L., GRONBORG, M., GROSCHE, J., KACZA, J., HOFFMANN, A., MATTEOLI, M., TAKAMORI, S., HARKANY, T., CHAUDHRY, F. A., ROSENMUND, C., ERCK, C., JAHN, R. & HARTIG, W. 2008. Unique luminal localization of VGAT-C terminus allows for selective labeling of active cortical GABAergic synapses. *J Neurosci*, 28, 13125-31.
- MARVIN, J. S., BORGHUIS, B. G., TIAN, L., CICHON, J., HARNETT, M. T., AKERBOOM, J., GORDUS, A., RENNINGER, S. L., CHEN, T. W., BARGMANN, C. I., ORGER, M. B., SCHREITER, E. R., DEMB, J. B., GAN, W. B., HIRES, S. A. & LOOGER, L. L. 2013. An optimized fluorescent probe for visualizing glutamate neurotransmission. *Nat Methods*, 10, 162-70.
- MATTHEWS, G. 1996. Synaptic exocytosis and endocytosis: capacitance measurements. *Curr Opin Neurobiol*, 6, 358-64.
- MAZZARELLO, P. 1999. A unifying concept: the history of cell theory. *Nat Cell Biol*, 1, E13-5.
- MCNEIL, B. D. & WU, L. G. 2009. Location matters: synaptotagmin helps place vesicles near calcium channels. *Neuron*, 63, 419-21.

- MEINRENKEN, C. J., BORST, J. G. & SAKMANN, B. 2002. Calcium secretion coupling at calyx of Held governed by nonuniform channel-vesicle topography. *J Neurosci*, 22, 1648-67.
- MERINEY, S. D., UMBACH, J. A. & GUNDERSEN, C. B. 2014. Fast, Ca²⁺-dependent exocytosis at nerve terminals: shortcomings of SNARE-based models. *Prog Neurobiol*, 121, 55-90.
- MICHALSKI, P. J. 2013. The delicate bistability of CaMKII. *Biophys J*, 105, 794-806.
- MICHEVA, K. D. & SMITH, S. J. 2005. Strong effects of subphysiological temperature on the function and plasticity of mammalian presynaptic terminals. *J Neurosci*, 25, 7481-8.
- MIESENBOCK, G., DE ANGELIS, D. A. & ROTHMAN, J. E. 1998. Visualizing secretion and synaptic transmission with pH-sensitive green fluorescent proteins. *Nature*, 394, 192-5.
- MISNER, D. L. & SULLIVAN, J. M. 1999. Mechanism of cannabinoid effects on long-term potentiation and depression in hippocampal CA1 neurons. *J Neurosci*, 19, 6795-805.
- MITCHELL, S. J. & RYAN, T. A. 2004. Syntaxin-1A is excluded from recycling synaptic vesicles at nerve terminals. *J Neurosci*, 24, 4884-8.
- MOLNAR, E. 2011. Long-term potentiation in cultured hippocampal neurons. *Semin Cell Dev Biol*, 22, 506-13.
- MOULDER, K. L., JIANG, X., TAYLOR, A. A., OLNEY, J. W. & MENNERICK, S. 2006. Physiological activity depresses synaptic function through an effect on vesicle priming. *J Neurosci*, 26, 6618-26.
- MOULDER, K. L. & MENNERICK, S. 2005. Reluctant vesicles contribute to the total readily releasable pool in glutamatergic hippocampal neurons. *J Neurosci*, 25, 3842-50.
- MOULDER, K. L. & MENNERICK, S. 2006. Synaptic vesicles: turning reluctance into action. *Neuroscientist*, 12, 11-5.
- MUKHERJEE, S. & MANAHAN-VAUGHAN, D. 2013. Role of metabotropic glutamate receptors in persistent forms of hippocampal plasticity and learning. *Neuropharmacology*, 66, 65-81.
- MULKEY, R. M., ENDO, S., SHENOLIKAR, S. & MALENKA, R. C. 1994. Involvement of a calcineurin/inhibitor-1 phosphatase cascade in hippocampal long-term depression. *Nature*, 369, 486-8.
- MULKEY, R. M., HERRON, C. E. & MALENKA, R. C. 1993. An essential role for protein phosphatases in hippocampal long-term depression. *Science*, 261, 1051-5.
- MULKEY, R. M. & MALENKA, R. C. 1992. Mechanisms underlying induction of homosynaptic long-term depression in area CA1 of the hippocampus. *Neuron*, 9, 967-75.
- MURTHY, V. N., SCHIKORSKI, T., STEVENS, C. F. & ZHU, Y. 2001. Inactivity produces increases in neurotransmitter release and synapse size. *Neuron*, 32, 673-82.
- MURTHY, V. N., SEJNOWSKI, T. J. & STEVENS, C. F. 1997. Heterogeneous release properties of visualized individual hippocampal synapses. *Neuron*, 18, 599-612.
- MURTHY, V. N. & STEVENS, C. F. 1998. Synaptic vesicles retain their identity through the endocytic cycle. *Nature*, 392, 497-501.
- MUTCH, S. A., KENSEL-HAMMES, P., GADD, J. C., FUJIMOTO, B. S., ALLEN, R. W., SCHIRO, P. G., LORENZ, R. M., KUYPER, C. L., KUO, J. S., BAJJALIEH, S. M. & CHIU, D. T. 2011. Protein quantification at the single vesicle level reveals that a subset of synaptic vesicle proteins are trafficked with high precision. *J Neurosci*, 31, 1461-70.

- NAGERL, U. V. & BONHOEFFER, T. 2010. Imaging living synapses at the nanoscale by STED microscopy. *J Neurosci*, 30, 9341-6.
- NAKANO, T., DOI, T., YOSHIMOTO, J. & DOYA, K. 2010. A kinetic model of dopamine- and calcium-dependent striatal synaptic plasticity. *PLoS Comput Biol*, 6, e1000670.
- NEHER, E., SAKMANN, B. & STEINBACH, J. H. 1978. The extracellular patch clamp: a method for resolving currents through individual open channels in biological membranes. *Pflugers Arch*, 375, 219-28.
- NEVES, G. & LAGNADO, L. 1999. The kinetics of exocytosis and endocytosis in the synaptic terminal of goldfish retinal bipolar cells. *J Physiol*, 515 (Pt 1), 181-202.
- NEWSHOLME, P., PROCOPIO, J., LIMA, M. M., PITHON-CURI, T. C. & CURI, R. 2003. Glutamine and glutamate--their central role in cell metabolism and function. *Cell Biochem Funct*, 21, 1-9.
- NEYMAN, S. & MANAHAN-VAUGHAN, D. 2008. Metabotropic glutamate receptor 1 (mGluR1) and 5 (mGluR5) regulate late phases of LTP and LTD in the hippocampal CA1 region in vitro. *Eur J Neurosci*, 27, 1345-52.
- NICHOLSON-TOMISHIMA, K. & RYAN, T. A. 2004. Kinetic efficiency of endocytosis at mammalian CNS synapses requires synaptotagmin I. *Proc Natl Acad Sci U S A*, 101, 16648-52.
- OORSCHOT, D. E. & JONES, D. G. 1986. Non-neuronal cell proliferation in tissue culture: implications for axonal regeneration in the central nervous system. *Brain Res*, 368, 49-61.
- ORENBUCH, A., SHALEV, L., MARRA, V., SINAI, I., LAVY, Y., KAHN, J., BURDEN, J. J., STARAS, K. & GITLER, D. 2012. Synapsin selectively controls the mobility of resting pool vesicles at hippocampal terminals. *J Neurosci*, 32, 3969-80.
- PALAY, S. L. 1956. Synapses in the central nervous system. *J Biophys Biochem Cytol*, 2, 193-202.
- PALAY, S. L. & PALADE, G. E. 1955. The fine structure of neurons. *J Biophys Biochem Cytol*, 1, 69-88.
- PAREDES, R. M., ETZLER, J. C., WATTS, L. T., ZHENG, W. & LECHLEITER, J. D. 2008. Chemical calcium indicators. *Methods*, 46, 143-51.
- PARK, H., LI, Y. & TSIEN, R. W. 2012. Influence of synaptic vesicle position on release probability and exocytotic fusion mode. *Science*, 335, 1362-6.
- PEARCE, J. M. 2004. Sir Charles Scott Sherrington (1857-1952) and the synapse. *J Neurol Neurosurg Psychiatry*, 75, 544.
- PEREZ-ASO, M., SEGURA, V., MONTO, F., BARETTINO, D., NOGUERA, M. A., MILLIGAN, G. & D'OCÓN, P. 2013. The three alpha1-adrenoceptor subtypes show different spatio-temporal mechanisms of internalization and ERK1/2 phosphorylation. *Biochim Biophys Acta*, 1833, 2322-33.
- PETTIT, D. L., PERLMAN, S. & MALINOW, R. 1994. Potentiated transmission and prevention of further LTP by increased CaMKII activity in postsynaptic hippocampal slice neurons. *Science*, 266, 1881-5.
- POPOVA, N. V., DEYEV, I. E. & PETRENKO, A. G. 2013. Clathrin-mediated endocytosis and adaptor proteins. *Acta Naturae*, 5, 62-73.
- POSCHEL, B. & STANTON, P. K. 2007. Comparison of cellular mechanisms of long-term depression of synaptic strength at perforant path-granule cell and Schaffer collateral-CA1 synapses. *Prog Brain Res*, 163, 473-500.
- PYLE, J. L., KAVALALI, E. T., CHOI, S. & TSIEN, R. W. 1999. Visualization of synaptic activity in hippocampal slices with FM1-43 enabled by fluorescence quenching. *Neuron*, 24, 803-8.

- PYLE, J. L., KAVALALI, E. T., PIEDRAS-RENTERIA, E. S. & TSIEN, R. W. 2000. Rapid reuse of readily releasable pool vesicles at hippocampal synapses. *Neuron*, 28, 221-31.
- PYOTT, S. J. & ROSENEMUND, C. 2002. The effects of temperature on vesicular supply and release in autaptic cultures of rat and mouse hippocampal neurons. *J Physiol*, 539, 523-35.
- RAJU, T. N. 1999. The Nobel chronicles. 1936: Henry Hallett Dale (1875-1968) and Otto Loewi (1873-1961). *Lancet*, 353, 416.
- RAMIREZ, D. M. & KAVALALI, E. T. 2011. Differential regulation of spontaneous and evoked neurotransmitter release at central synapses. *Curr Opin Neurol*, 21, 275-82.
- RATNAYAKA, A., MARRA, V., BRANCO, T. & STARAS, K. 2011. Extrasynaptic vesicle recycling in mature hippocampal neurons. *Nature Commun*, 2, 531.
- RATNAYAKA, A., MARRA, V., BUSH, D., BURDEN, J. J., BRANCO, T. & STARAS, K. 2012. Recruitment of resting vesicles into recycling pools supports NMDA-receptor dependent synaptic potentiation in cultured hippocampal neurons. *J Physiol*.
- RAVIOLA, E. & MAZZARELLO, P. 2011. The diffuse nervous network of Camillo Golgi: facts and fiction. *Brain Res Rev*, 66, 75-82.
- RENDEN, R. & VON GERSDORFF, H. 2007. Synaptic vesicle endocytosis at a CNS nerve terminal: faster kinetics at physiological temperatures and increased endocytotic capacity during maturation. *J Neurophysiol*, 98, 3349-59.
- REQUEJO-ISIDRO, J. 2013. Fluorescence nanoscopy. Methods and applications. *J Chem Biol*, 6, 97-120.
- RIZZOLI, S. O. & BETZ, W. J. 2004. The structural organization of the readily releasable pool of synaptic vesicles. *Science*, 303, 2037-9.
- RIZZUTO, R., DE STEFANI, D., RAFFAELLO, A. & MAMMUCARI, C. 2012. Mitochondria as sensors and regulators of calcium signalling. *Nat Rev Mol Cell Biol*, 13, 566-78.
- ROBERTS, E. & FRANKEL, S. 1950. gamma-Aminobutyric acid in brain: its formation from glutamic acid. *J Biol Chem*, 187, 55-63.
- ROSE, T., SCHOENENBERGER, P., JEZEK, K. & OERTNER, T. G. 2013. Developmental refinement of vesicle cycling at Schaffer collateral synapses. *Neuron*, 77, 1109-21.
- ROSENEMUND, C. & STEVENS, C. F. 1996. Definition of the readily releasable pool of vesicles at hippocampal synapses. *Neuron*, 16, 1197-207.
- ROYLE, S. J., GRANSETH, B., ODERMATT, B., DEREVIER, A. & LAGNADO, L. 2008. Imaging phluorin-based probes at hippocampal synapses. *Methods Mol Biol*, 457, 293-303.
- RUST, M. J., BATES, M. & ZHUANG, X. 2006. Sub-diffraction-limit imaging by stochastic optical reconstruction microscopy (STORM). *Nat Methods*, 3, 793-5.
- RYAN, T. A., REUTER, H., WENDLAND, B., SCHWEIZER, F. E., TSIEN, R. W. & SMITH, S. J. 1993. The kinetics of synaptic vesicle recycling measured at single presynaptic boutons. *Neuron*, 11, 713-24.
- RYAN, T. A. & SMITH, S. J. 1995. Vesicle Pool Mobilization during Action Potential Firing at Hippocampal Synapses. *Neuron*, 14, 983-989.
- RYAN, T. A., SMITH, S. J. & REUTER, H. 1996. The timing of synaptic vesicle endocytosis. *Proc Natl Acad Sci U S A*, 93, 5567-71.
- SABATINI, B. L. & REGEHR, W. G. 1999. Timing of synaptic transmission. *Annu Rev Physiol*, 61, 521-42.

- SAHEKI, Y. & DE CAMILLI, P. 2012. Synaptic vesicle endocytosis. *Cold Spring Harb Perspect Biol*, 4, a005645.
- SANDELL, J. H. & MASLAND, R. H. 1988. Photoconversion of some fluorescent markers to a diaminobenzidine product. *J Histochem Cytochem*, 36, 555-9.
- SARA, Y., VIRMANI, T., DEÁK, F., LIU, X. & KAVALALI, E. T. 2005. An Isolated Pool of Vesicles Recycles at Rest and Drives Spontaneous Neurotransmission. *Neuron*, 45, 563-573.
- SCHIESS, A. R., SCULLIN, C. & PARTRIDGE, L. D. 2010. Maturation of Schaffer collateral synapses generates a phenotype of unreliable basal evoked release and very reliable facilitated release. *Eur J Neurosci*, 31, 1377-87.
- SCHIKORSKI, T. & STEVENS, C. 1997. Quantitative Ultrastructural Analysis of Hippocampal Excitatory Synapses. *J Neurosci*, 17, 5858-5867.
- SCHIKORSKI, T. & STEVENS, C. F. 2001. Morphological correlates of functionally defined synaptic vesicle populations. *Nat Neurosci*, 4, 391-5.
- SCOTT, D. & ROY, S. 2012. alpha-Synuclein inhibits intersynaptic vesicle mobility and maintains recycling-pool homeostasis. *J Neurosci*, 32, 10129-35.
- SHAPIRA, M., ZHAI, R. G., DRESBACH, T., BRESLER, T., TORRES, V. I., GUNDELFINGER, E. D., ZIV, N. E. & GARNER, C. C. 2003. Unitary assembly of presynaptic active zones from Piccolo-Bassoon transport vesicles. *Neuron*, 38, 237-52.
- SHEPHERD, G. M. & HARRIS, K. M. 1998. Three-dimensional structure and composition of CA3-->CA1 axons in rat hippocampal slices: implications for presynaptic connectivity and compartmentalization. *J Neurosci*, 18, 8300-10.
- SIGWORTH, F. J. & NEHER, E. 1980. Single Na⁺ channel currents observed in cultured rat muscle cells. *Nature*, 287, 447-9.
- SILVEIRA, P. E., LIMA, R. F., GUIMAR, A. J., MOLGO, J., NAVES, L. A. & KUSHMERICK, C. 2015. Ryanodine and inositol triphosphate receptors modulate facilitation and tetanic depression at the frog neuromuscular junction. *Muscle Nerve*.
- SMITH, S. M., RENDEN, R. & VON GERSDORFF, H. 2008. Synaptic vesicle endocytosis: fast and slow modes of membrane retrieval. *Trends Neurosci*, 31, 559-68.
- SOLLNER, T., BENNETT, M. K., WHITEHEART, S. W., SCHELLER, R. H. & ROTHMAN, J. E. 1993. A protein assembly-disassembly pathway in vitro that may correspond to sequential steps of synaptic vesicle docking, activation, and fusion. *Cell*, 75, 409-18.
- SORRA, K. E., MISHRA, A., KIROV, S. A. & HARRIS, K. M. 2006. Dense core vesicles resemble active-zone transport vesicles and are diminished following synaptogenesis in mature hippocampal slices. *Neuroscience*, 141, 2097-106.
- SPACEK, J. & HARRIS, K. M. 1997. Three-dimensional organization of smooth endoplasmic reticulum in hippocampal CA1 dendrites and dendritic spines of the immature and mature rat. *J Neurosci*, 17, 190-203.
- STADLER, H. & TSUKITA, S. 1984. Synaptic vesicles contain an ATP-dependent proton pump and show 'knob-like' protrusions on their surface. *EMBO J*, 3, 3333-7.
- STANDAERT, F. G. & DRETCHEN, K. L. 1979. Cyclic nucleotides and neuromuscular transmission. *Fed Proc*, 38, 2183-92.
- STANTON, P. K., WINTERER, J., BAILEY, C. P., KYROZIS, A., RAGINOV, I., LAUBE, G., VEH, R. W., NGUYEN, C. Q. & MULLER, W. 2003. Long-term depression of presynaptic release from the readily releasable vesicle pool induced by NMDA receptor-dependent retrograde nitric oxide. *J Neurosci*, 23, 5936-44.

- STANTON, P. K., WINTERER, J., ZHANG, X. L. & MULLER, W. 2005. Imaging LTP of presynaptic release of FM1-43 from the rapidly recycling vesicle pool of Schaffer collateral-CA1 synapses in rat hippocampal slices. *Eur J Neurosci*, 22, 2451-61.
- STARAS, K. 2007. Share and share alike: trading of presynaptic elements between central synapses. *Trends Neurosci*, 30, 292-8.
- STARAS, K. & BRANCO, T. 2010. Sharing vesicles between central presynaptic terminals: implications for synaptic function. *Front Synaptic Neurosci*, 2, 20.
- STARAS, K., BRANCO, T., BURDEN, J. J., POZO, K., DARCY, K., MARRA, V., RATNAYAKA, A. & GODA, Y. 2010. A vesicle superpool spans multiple presynaptic terminals in hippocampal neurons. *Neuron*, 66, 37-44.
- STEVENS, C. F. & TSUJIMOTO, T. 1995. Estimates for the pool size of releasable quanta at a single central synapse and for the time required to refill the pool. *Proc Natl Acad Sci U S A*, 92, 846-9.
- STRIEGEL, A. R., BIELA, L. M., EVANS, C. S., WANG, Z., DELEHOY, J. B., SUTTON, R. B., CHAPMAN, E. R. & REIST, N. E. 2012. Calcium binding by synaptotagmin's C2A domain is an essential element of the electrostatic switch that triggers synchronous synaptic transmission. *J Neurosci*, 32, 1253-60.
- SUDHOF, T. C. 2006. Synaptic vesicles: an organelle comes of age. *Cell*, 127, 671-3.
- SUDHOF, T. C. 2012. The presynaptic active zone. *Neuron*, 75, 11-25.
- SUDHOF, T. C. 2013. Neurotransmitter release: the last millisecond in the life of a synaptic vesicle. *Neuron*, 80, 675-90.
- SUDHOF, T. C. & RIZO, J. 1996. Synaptotagmins: C2-domain proteins that regulate membrane traffic. *Neuron*, 17, 379-88.
- SUDHOF, T. C. & SCHELLER, R. H. 2001a. Mechanism and Regulation of Neurotransmitter Release. In: COWAN, W. M. (ed.) *Synapses*. Johns Hopkins University Press: Johns Hopkins University Press.
- SUDHOF, T. C. & SCHELLER, R. H. 2001b. Mechanism and Regulation of Neurotransmitter Release. In: COWAN, W. M., STEVENS, C. F. & SUDHOF, T. C. (eds.) *Synapses*. Baltimore, Maryland: Johns Hopkins University Press.
- SUETSUGU, S., TOYOOKA, K. & SENJU, Y. 2010. Subcellular membrane curvature mediated by the BAR domain superfamily proteins. *Semin Cell Dev Biol*, 21, 340-9.
- SUGIE, A., HAKEDA-SUZUKI, S., SUZUKI, E., SILIES, M., SHIMOZONO, M., MOHL, C., SUZUKI, T. & TAVOSANIS, G. 2015. Molecular Remodeling of the Presynaptic Active Zone of Drosophila Photoreceptors via Activity-Dependent Feedback. *Neuron*, 86, 711-25.
- SUVARNA, Y., MAITY, N. & SHIVAMURTHY, M. C. 2015. Emerging Trends in Retrograde Signaling. *Mol Neurobiol*.
- SZIRMAI, I., BUZSAKI, G. & KAMONDI, A. 2012. 120 years of hippocampal Schaffer collaterals. *Hippocampus*.
- TAKAMORI, S., HOLT, M., STENIUS, K., LEMKE, E. A., GRONBORG, M., RIEDEL, D., URLAUB, H., SCHENCK, S., BRUGGER, B., RINGLER, P., MULLER, S. A., RAMMNER, B., GRATER, F., HUB, J. S., DE GROOT, B. L., MIESKES, G., MORIYAMA, Y., KLINGAUF, J., GRUBMULLER, H., HEUSER, J., WIELAND, F. & JAHN, R. 2006. Molecular anatomy of a trafficking organelle. *Cell*, 127, 831-46.
- TAMAGNINI, F., BARKER, G., WARBURTON, E. C., BURATTINI, C., AICARDI, G. & BASHIR, Z. I. 2013. Nitric oxide-dependent long-term depression but not endocannabinoid-mediated long-term potentiation is crucial for visual recognition memory. *J Physiol*, 591, 3963-79.

- TANSEY, E. M. 1997. Not committing barbarisms: Sherrington and the synapse, 1897. *Brain Res Bull*, 44, 211-2.
- THIAGARAJAN, T. C., LINDSKOG, M. & TSIEN, R. W. 2005. Adaptation to synaptic inactivity in hippocampal neurons. *Neuron*, 47, 725-37.
- TISHGARTEN, T., YIN, F. F., FAUCHER, K. M., DLUHY, R. A., GRANT, T. R., FISCHER VON MOLLARD, G., STEVENS, T. H. & LIPSCOMB, L. A. 1999. Structures of yeast vesicle trafficking proteins. *Protein Sci*, 8, 2465-73.
- TONNESEN, J., NADRIGNY, F., WILLIG, K. I., WEDLICH-SOLDNER, R. & NAGERL, U. V. 2011. Two-color STED microscopy of living synapses using a single laser-beam pair. *Biophys J*, 101, 2545-52.
- UDENFRIEND, S. 1950. Identification of gamma-aminobutyric acid in brain by the isotope derivative method. *J Biol Chem*, 187, 65-9.
- UPRETI, C., ZHANG, X. L., ALFORD, S. & STANTON, P. K. 2013. Role of presynaptic metabotropic glutamate receptors in the induction of long-term synaptic plasticity of vesicular release. *Neuropharmacology*, 66, 31-9.
- VALENSTEIN, E. S. 2002. The discovery of chemical neurotransmitters. *Brain Cogn*, 49, 73-95.
- VANDEN BERGHE, P. & KLINGAUF, J. 2006. Synaptic vesicles in rat hippocampal boutons recycle to different pools in a use-dependent fashion. *J Physiol*, 572, 707-20.
- VON GERSDORFF, H. & MATTHEWS, G. 1999. Electrophysiology of synaptic vesicle cycling. *Annu Rev Physiol*, 61, 725-52.
- WAGH, D. A., RASSE, T. M., ASAN, E., HOFBAUER, A., SCHWENKERT, I., DURRBECK, H., BUCHNER, S., DABAUVALLE, M. C., SCHMIDT, M., QIN, G., WICHMANN, C., KITTEL, R., SIGRIST, S. J. & BUCHNER, E. 2006. Bruchpilot, a protein with homology to ELKS/CAST, is required for structural integrity and function of synaptic active zones in *Drosophila*. *Neuron*, 49, 833-44.
- WATANABE, S., ROST, B. R., CAMACHO-PEREZ, M., DAVIS, M. W., SOHL-KIELCZYNSKI, B., ROSENMUND, C. & JORGENSEN, E. M. 2013. Ultrafast endocytosis at mouse hippocampal synapses. *Nature*, 504, 242-7.
- WATANABE, S., TRIMBUCH, T., CAMACHO-PEREZ, M., ROST, B. R., BROKOWSKI, B., SOHL-KIELCZYNSKI, B., FELIES, A., DAVIS, M. W., ROSENMUND, C. & JORGENSEN, E. M. 2014. Clathrin regenerates synaptic vesicles from endosomes. *Nature*, 515, 228-33.
- WATKINS, J. C. 2000. l-glutamate as a central neurotransmitter: looking back. *Biochem Soc Trans*, 28, 297-309.
- WATKINS, J. C. & JANE, D. E. 2006. The glutamate story. *Br J Pharmacol*, 147 Suppl 1, S100-8.
- WELZEL, O., HENKEL, A. W., STROEBEL, A. M., JUNG, J., TISCHBIREK, C. H., EBERT, K., KORNHUBER, J., RIZZOLI, S. O. & GROEMER, T. W. 2011. Systematic heterogeneity of fractional vesicle pool sizes and release rates of hippocampal synapses. *Biophys J*, 100, 593-601.
- WELZEL, O., LOY, K., TISCHBIREK, C. H., TABOR, A., GMEINER, P., KORNHUBER, J. & GROEMER, T. W. 2013. The pH probe CypHer5E is effectively quenched by FM dyes. *J Fluoresc*, 23, 487-94.
- WESTPHAL, V., RIZZOLI, S. O., LAUTERBACH, M. A., KAMIN, D., JAHN, R. & HELL, S. W. 2008. Video-rate far-field optical nanoscopy dissects synaptic vesicle movement. *Science*, 320, 246-9.
- WHITTAKER, V. P. 1968. The storage of transmitters in the central nervous system. *Biochem J*, 109, 20P-21P.

- WU, Y., YEH, F. L., MAO, F. & CHAPMAN, E. R. 2009. Biophysical characterization of styryl dye-membrane interactions. *Biophys J*, 97, 101-9.
- XU, J. Y., CHEN, R., ZHANG, J. & CHEN, C. 2010. Endocannabinoids differentially modulate synaptic plasticity in rat hippocampal CA1 pyramidal neurons. *PLoS One*, 5, e10306.
- XU, W., TSE, Y. C., DOBIE, F. A., BAUDRY, M., CRAIG, A. M., WONG, T. P. & WANG, Y. T. 2013. Simultaneous monitoring of presynaptic transmitter release and postsynaptic receptor trafficking reveals an enhancement of presynaptic activity in metabotropic glutamate receptor-mediated long-term depression. *J Neurosci*, 33, 5867-77.
- YE, Z. C. & SONTHEIMER, H. 1998. Astrocytes protect neurons from neurotoxic injury by serum glutamate. *Glia*, 22, 237-48.
- ZAKHARENKO, S. S., PATTERSON, S. L., DRAGATIS, I., ZEITLIN, S. O., SIEGELBAUM, S. A., KANDEL, E. R. & MOROZOV, A. 2003. Presynaptic BDNF required for a presynaptic but not postsynaptic component of LTP at hippocampal CA1-CA3 synapses. *Neuron*, 39, 975-90.
- ZAKHARENKO, S. S., ZABLOW, L. & SIEGELBAUM, S. A. 2001. Visualization of changes in presynaptic function during long-term synaptic plasticity. *Nat Neurosci*, 4, 711-7.
- ZAKHARENKO, S. S., ZABLOW, L. & SIEGELBAUM, S. A. 2002. Altered presynaptic vesicle release and cycling during mGluR-dependent LTD. *Neuron*, 35, 1099-110.
- ZIFF, E. B. 1997. Enlightening the postsynaptic density. *Neuron*, 19, 1163-74.
- ZORUMSKI, C. F. & IZUMI, Y. 2012. NMDA receptors and metaplasticity: mechanisms and possible roles in neuropsychiatric disorders. *Neurosci Biobehav Rev*, 36, 989-1000.